The design of a cost-effective mechanical prosthetic knee

JS Malan

orcid.org/ 0000-0002-5321-1739

Dissertation accepted in fulfilment of the requirements for the degree
Master of Engineering in Mechanical Engineering
at the North-West University

Supervisor:	Dr J Kruger
Co-supervisor:	Prof AJ Grobler
Graduation:	May 2026

Abstract

The limited functionality of a typical low-cost knee prosthesis results in poor gait performance and subsequently leads to reduced quality of life due to adverse health outcomes. Several concepts and methods are used in premium knees to improve functional performance (e.g., stance-phase locking and swing-phase damping), but due to high costs and specialised maintenance from international suppliers, few patients can be helped with these devices. Therefore, the problem in South Africa is restricted access to cost-effective prosthetic knees with functional gait performance, exacerbated by the lack of expertise in the local design and manufacture of these prostheses.

This study involved the design, manufacture, and testing of a cost-effective mechanical prosthetic knee. A narrative review of the literature on prosthetic knee types, control mechanisms, materials, design tools, design frameworks, and testing methodologies informed the design approach. A voluntary control four-bar mechanism knee was selected as a suitable candidate for the purposes of this study. A MATLAB based link-segment mathematical model was created to evaluate candidate geometry for stability, range of motion, and ground clearance. The geometry was then used as a base to design a functional prototype that can be used for gait analysis. Modular components, standard fasteners, and readily available materials were used to fabricate the prototype. It was manufactured using a CNC machine and a precision lathe.

The prototype performance was evaluated through a controlled human gait trial using 3D motion-capture analysis. The participant completed walking trials with the mechanical prototype and with a microprocessor-controlled knee, which served as a performance baseline. Gait symmetry was assessed using cross-correlation (r) for waveform parameters such as joint kinematics and ground reaction force, while the Symmetry Index was used to indicate quality when comparing spatio-temporal parameters such as cadence, swing time, and stance time. The average maximum r for the prototype was 0.948 with a signed lag of -4%, while the corresponding values for the microprocessor knee was 0.964 and -5%, respectively. The SIs for crucial metrics were evaluated for the prototype and the microprocessor knee respectively: stride time (1.34% and 1.83%), speed (1.68% and 2.19%), step length (10.14% and 10.85%), step time (14.94% and 17.82%), steps/minute (15.08% and 17.8%), stride length (0.32% and 0.34%), stance time (18.1% and 16.28%) and swing time (26.36% and 21.87%).

The prototype demonstrated consistent and physiologically appropriate gait parameters and gait symmetry metrics that closely match those of the microprocessor knee. Although the microprocessor knee still performed better overall, the prototype demonstrated comparable functional outcomes at radically lower cost($\approx$ R22 000 vs $>$ R500 000).

However, the scope of the testing was limited to level ground walking at self-selected speeds with one participant. Therefore, more research is required to investigate the operational limitations of the prototype. Nevertheless, this study achieved it's aim to design, manufacture and evaluate a cost effective mechanical knee. The results were encouraging and contributed to the local knowledge base for the design of transfemoral prosthetic solutions for lower resource settings.

Keywords: Mechanical prosthetic knee, gait trial, four-bar mechanism knee, cost-effective

Declaration

I, **J.S. Malan** hereby declare that

1. I understand what plagiarism is and am aware of the University's policy in this regard.
2. I know that "plagiarism" means using another person's work and ideas without acknowledgement, and pretending that it is one's own. I know that plagiarism not only includes verbatim copying, but also the extensive (albeit paraphrased) use of another person's ideas without acknowledgement. I know that plagiarism covers this sort of use of material found in textbooks, journal articles, theses AND on the internet.
3. "The design of a cost-effective mechanical prosthetic knee" submitted in the fulfilment in the requirement for the Master's degree in Mechanical Engineering (M-Eng) is my own original work.
4. Where other people's work has been used (either from a printed source, Internet or any other source), this has been properly acknowledged and referenced in accordance with departmental requirements.
5. I have not used work previously produced by another student or any other person to hand in as my own.
6. I have not allowed, and will not allow, anyone to copy my work with the intention of passing it off as his or her own work.

2026/02/23

_ _

STUDENT DATE

Acknowledgements

I want to thank the following:

Our Heavenly Father, for it is only through Him and His grace that I was able to complete this degree.

My parents, Joël and Linda Malan, for their unwavering love, support and advice.

My study leaders, Dr Jan-Hendrik Kruger and Prof André Grobler, for their advice, insights and being willing to undertake this journey with me.

My friends, for keeping my spirits high and to laugh with me at my frustrations, and be exited with me in my victories.

The instrument makers, Mr Thys Taljaard and Mr Trevor van Niekerk for their advice as well as fabricating the prototype.

Prof. Mark Kramer and Dr. Clement Gambelli for assisting with the data collection.

The participant, for his willingness to help with data collection.

Contents

List of Figures viii

List of Tables x

Nomenclature xi

1. Introduction 1
- 1.1. Background . . . 1
  - 1.1.1. Functional Challenges and Prosthetic Access . . . 1
  - 1.1.2. Design Parameters Associated with Knee Design . . . 1
  - 1.1.3. Impact of Cost of Prosthetic Knees . . . 2
- 1.2. Problem Statement, Aim and Objectives . . . 2
  - 1.2.1. Problem Statement . . . 2
  - 1.2.2. Aim . . . 3
  - 1.2.3. Objectives . . . 3
- 1.3. Research Design . . . 3
  - 1.3.1. Quality Research Management . . . 3
  - 1.3.2. Research Validation Matrix . . . 4
  - 1.3.3. Research Challenges and the RVM . . . 4
- 1.4. Testing Methodology . . . 6
  - 1.4.1. Ethical considerations . . . 6
- 1.5. Delineations and Limitations . . . 7
  - 1.5.1. Significance of study . . . 7
- 1.6. Chapter Overview . . . 7

2. Literature Review 9
- 2.1. Introduction . . . 9
- 2.2. Prosthetic Function . . . 9
  - 2.2.1. Structural Support and Basic Functionality . . . 9
  - 2.2.2. Mechanical Enhancement and Functional Replication . . . 10
  - 2.2.3. Gait Optimisation and Energy Efficiency . . . 10
  - 2.2.4. Normal Gait . . . 10
  - 2.2.5. Amputee Gait . . . 11
- 2.3. Types of Prosthetic Knees . . . 12
  - 2.3.1. Appropriate Technology . . . 12
  - 2.3.2. Passive Mechanical Knees . . . 12
  - 2.3.3. Microprocessor-Controlled Prosthetic Knees . . . 13
  - 2.3.4. Active Prosthetic Knees . . . 13
- 2.4. Prosthetic Knee Control . . . 14
  - 2.4.1. Ground Reaction Force Vector and Passive Stability . . . 14
  - 2.4.2. Stance Phase Control . . . 15
  - 2.4.3. Types of polycentric four-bar mechanisms . . . 16
  - 2.4.4. Swing Phase Control . . . 16
  - 2.4.5. Comparison of Knee Mechanism Characteristics . . . 18

2.5. Materials . . . 18
2.5.1. **Summary of materials and their uses** . . . 18
2.5.2. **Metals** . . . 20
2.5.3. Carbon fibre reinforced polymer . . . 20
2.5.4. **Engineering Plastics** . . . 20
2.6. Comparative Cost Analysis . . . 21
2.7. Simulation Tools and Approaches . . . 21
2.7.1. Mathematical Models . . . 21
2.7.2. Finite Element Analysis . . . 22
2.8. Testing Methods and Parameters . . . 22
2.8.1. Gait Analysis . . . 23
2.8.2. Spatio-temporal Parameters . . . 23
2.8.3. Gait Symmetry . . . 24
2.9. Design Frameworks for Cost-Effective Prosthetic Knees . . . 25
2.9.1. Biomechanical Modelling: Kinematics and Kinetics . . . 25
2.9.2. User-Centred Needs Assessment . . . 25
2.9.3. Prototyping and Feedback Loops . . . 25
2.9.4. Optimisation Methods for Geometry . . . 25
2.10. Final Choice of Concept Solutions . . . 25
2.10.1. RC1: Type of knee and required functionality . . . 26
2.10.2. RC2: Design considerations . . . 26
2.10.3. RC3: Outcome measures . . . 26
2.10.4. RC4: Design tools . . . 26
2.10.5. RC5: Testing methods . . . 26

3. Mathematical Modelling and Design **27**
3.1. Introduction . . . 27
3.2. Research Design . . . 27
3.2.1. Approach and Framework . . . 27
3.2.2. Methodological Structure . . . 28
3.2.3. Data Collection and Analysis Plan . . . 28
3.3. Design Methodology . . . 28
3.3.1. Functional Requirements Definition . . . 29
3.3.2. Verification Matrix . . . 31
3.4. Mathematical Modelling of 4BM Polycentric Knee . . . 31
3.4.1. Biomechanics Equations . . . 31
3.5. Proposed link geometry . . . 35
3.6. MATLAB implementation of 4BM Design Tool . . . 35
3.6.1. Instantaneous Centre of Rotation . . . 36
3.6.2. Flexion Factor . . . 37
3.6.3. Toe clearance . . . 38
3.6.4. Range of Motion . . . 42
3.6.5. Relationship between design parameters and performance . . . 43
3.7. Final parameters from the 4BM Design Tool . . . 44

4. Prototype Development **45**
4.1. Introduction . . . 45
4.2. Design cycle . . . 45
4.3. Forces acting on links and joints . . . 47
4.4. General design considerations . . . 49
4.5. Final Design Description . . . 50
4.5.1. Components . . . 50

4.5.2. Damping mechanism . . . 53
4.5.3. Manufacturing Tolerances . . . 54
4.5.4. Materials . . . 54
4.6. Shear force on shafts . . . 55
4.7. Finite Element Analysis (FEA) . . . 55
4.7.1. Simulation Setup . . . 56
4.7.2. FEA Results . . . 56
4.7.3. Results and Interpretation . . . 56
4.8. Manufacturing Methods . . . 59
4.8.1. Alternative Manufacturing Techniques . . . 59
4.9. Prototyping and Manufacturing Outcomes . . . 60
4.10. Prototype Scope and Limitations . . . 61
4.11. In summary . . . 61

5. Experimental Methodology and Results **62**
5.1. Introduction . . . 62
5.2. Experimental Protocol and Ethical Compliance . . . 62
5.3. Experimental Equipment Setup . . . 63
5.4. Data Processing Pipeline . . . 67
5.4.1. Data gathering . . . 67
5.4.2. Filtering and sorting . . . 67
5.4.3. Normalisation . . . 67
5.5. Outcome measures . . . 67
5.5.1. Kinetic and Kinematic Outcome Measures . . . 67
5.5.2. Spatio-temporal Outcome Measures . . . 68
5.5.3. Evaluation criteria . . . 68
5.6. Results . . . 68
5.6.1. Kinetic and Kinematic Plots . . . 68
5.6.2. Cross correlation results . . . 71
5.7. Spatio-temporal Results . . . 72
5.8. Discussion . . . 73
5.8.1. Kinematic and Kinetic Results . . . 73
5.8.2. Cross-correlation Results . . . 74
5.8.3. Spatio-temporal results . . . 74
5.8.4. Cost-effectiveness Argument . . . 74
5.8.5. Limitations . . . 74
5.9. In summary . . . 75

6. Conclusion and Recommendations **76**
6.1. Introduction . . . 76
6.2. Restatement of problem, aim and objectives . . . 76
6.2.1. Problem Statement . . . 76
6.2.2. Aim . . . 76
6.2.3. Objectives . . . 76
6.3. How each objective was achieved . . . 77
6.3.1. Completed Research Verification Matrix . . . 77
6.3.2. Objective 1: Literature Review . . . 77
6.3.3. Objective 2: Design and Manufacturing . . . 77
6.3.4. Objective 3: Test and Evaluation . . . 80
6.3.5. Objective 4 . . . 80
6.4. Contribution to Knowledge and Practice . . . 80
6.5. Limitations . . . 81

6.6. Recommendations for Future Work 81
6.7. Conclusion 82

Bibliography **83**

A. Four-bar Mechanism Design Tool Scripts **88**

B. Gait Trial Results — 4BM Prototype **99**

C. Gait Trial Results — Ottobock Genium X3 **134**

List of Figures

1.1. Simplified House of Quality [19] . . . 5
1.2. Top of the RVM showing the definition of research challenges . . . 5

2.1. Research challenges and Literature topics . . . 9
2.2. Human gait cycle progressing through stance phase to swing phase [23] . . . 10
2.3. Illustration of how GRFV changes with applied hip moment, adapted from [4] . . . 15
2.4. Comparison of the three four-bar mechanism types. . . . 17

3.1. Implementation aspects in Chapter 3 that contributed to RC1, RC2 and RC4 . . . 27
3.2. Illustration of the forces and moments acting on the prosthetic knee during stance phase adapted from [39] . . . 32
3.3. Coordinate system that will be used for vector loop equations . . . 34
3.4. Standard Prosthesis Dimensions [1] . . . 36
3.5. Instantaneous centre of rotation centrode plots for full range of knee motion. . . . 37
3.6. Validation of MATLAB ICR calculation and Siemens NX reconstruction. . . . 37
3.7. Flexion factor vs Knee Flexion angle over 5° . . . 38
3.8. Evaluation of toe clearance and socket centrode motion during knee flexion. . . . 40
3.9. Calculating the minimum toe clearance. . . . 41
3.10. Range of motion determined by the maximum knee flexion. . . . 42

4.1. Implementation aspects in Chapter 4 that contributed to RC1, RC2 and RC4 . . . 45
4.2. Design process flow diagram . . . 46
4.3. NX Motion Simulation Setup showing link layout and socket connector at the top. 48
4.4. Vector force of 4130N applied downward on the top link. . . . 48
4.5. NX Motion results: Force responses for joints 1-4 shows a maximum force of ≈2300N for the anterior joints and ≈1900N for the posterior joints . . . 49
4.6. CAD model of knee overlaid with the mathematical links . . . 51
4.7. Final version of the four-bar knee mechanism. . . . 52
4.8. Anterior link showing brake pad cutout and damping mechanism. . . . 54
4.9. FEM setup of critical components. . . . 57
4.10. FEM Von Mises stress results for critical components. . . . 58
4.11. 3D printed concepts showing different design choices. . . . 59
4.12. The functional prototype 4BM knee showing full extension and full flexion positions. 60

5.1. Concept solution implementation in Chapter 5 . . . 62
5.2. IOR lower body marker set definition used in Qualysis . . . 64
5.3. Gait-trial setup: (a) Marker placement on both legs, (b) Infrared marker with mount, (c) Qualisys camera, (d) Walking track with force plates. . . . 65
5.4. Participant walking with the prototype four-bar mechanism knee (4BM). . . . 66
5.5. Participant walking with the Ottobock Genium X3. . . . 66
5.6. Human gait cycle showing percentage completion. . . . 68
5.7. Knee flexion angle over the gait cycle for the prototype mechanical knee and the Genium X3 at self-selected walking speed. . . . 69
5.8. Hip flexion angle over the gait cycle for the prototype mechanical knee and the Genium X3 at self-selected walking speed. . . . 69

5.9. Toe height over the gait cycle for the prototype mechanical knee and the Genium X3 at self-selected walking speed. 70
5.10. Vertical ground reaction force (normalised to body weight) over the gait cycle for the prototype mechanical knee and the Genium X3. 70
5.11. Hip angular velocity over the gait cycle for the prototype mechanical knee and the Genium X3. 71
5.12. Cross correlation of Knee Flexion across gait cycle with 4BM knee prototype . . 71

6.1. Completed Research Verification Matrix for 4BM prosthetic knee development. . 78

List of Tables

2.1. Summary of knee function during the gait cycle (adapted from [24]) 11
2.2. Comparison of prosthetic knee control mechanisms. 18
2.3. Comparative Summary of Materials Used in Knee Prosthesis Components 19

3.1. Functional requirements for prosthetic knee design 29
3.2. Verification Matrix 30
3.3. Summary of symbols and descriptions 31
3.4. Proposed link geometry obtained from the 4BM Design Tool 35
3.5. Final knee parameters calculated with the 4BM Design Tool 44

4.1. Materials used for components of prototype 55

5.1. Cross-correlation results for the mechanical prototype and Genium X3 72
5.2. Spatio-temporal results for the 4BM prototype mechanical knee 72
5.3. Spatio-temporal results for the Genium X3 73
5.4. Comparison of kinematic parameters for the prototype and Genium X3 knees. . . 73

6.1. Research Challenges and Corresponding Solutions for Objective 1 79

B.1. Overview of 4BM gait-trial plots included in this appendix. Each variable includes both group-average and left–right cross-correlation plots. 99

C.1. Overview of Genium X3 gait-trial plots included in this appendix. Each variable includes both group-average and left–right cross-correlation plots. 134

Nomenclature

Acronyms and Abbreviations

4BM	Four-bar Mechanism
ARL	Alignment reference line: vertical line that connects hip and ankle
CAD	Computer Aided Design
CSV	Comma Separated Value
ESAR	Energy Storage and Return
FEA	Finite Element Analysis
HoQ	House of Quality
HS	Heel Strike
ICR	Instantaneous Centre of Rotation
IOR	Istituti Ortopedici Rizzoli
MPK	Micro-processor knee
RC	Research Challenge
ROM	Range of Motion
RVM	Research Validation Matrix
SI	Symmetry Index
TO	Toe Off
WHO	World Health Organisation

List of Symbols

π	Pi	–
τ_{allow}	Allowable shear stress	MPa
τ_{ave}	Average shear stress	MPa
θ_1	Angle of link OC with respect to horizontal	$^\circ$
θ_2	Angle of link OA with respect to horizontal	$^\circ$

θ_3	Angle of link AB with respect to horizontal	$^\circ$
θ_4	Angle of link CB with respect to horizontal	$^\circ$
F_s	Shear force	N
L	Distance between hip joint and heel contact	m
M_h	Extension moment about hip joint	Nm
M_k	Break moment supplied by knee prosthesis	Nm
P	Axial load force along hip-heel direction	N
r	Pearson Correlation Coefficient	$-$
$r_{\min}$	Minimum radius	m
S	Shear force at heel contact in hip moment equation	N
x	Perpendicular distance between load line and centre of rotation	m
y	distance between centre of rotation and heel contact	m
A	Cross-sectional area	m^2
a	Length of link OA	m
b	Length of link AB	m
c	Length of link BC	m
d	Length of link OC	m

Definitions

Anterior Refers to the frontal part of the body

Flexion Factor Parameter derived from hip moment equation to evaluate stability

Gait Cycle Refers to the sequence of events that describe walking

Heel strike Event in the gait cycle where the heel makes contact with the floor and the stance phase is initiated

Hip moment equation Equation used to estimate the moment required by the amputee's hip to control the prosthetic knee through the flexion range

Instantaneous Centre of Rotarian (ICR) Intersection of the lines that are perpendicular to the tangential velocity vectors of the links OA and BC

Posterior Refers to the rear part of the body

Spatio-Temporal Relating to time and distance parameters

Stance phase section of the gait cycle where the foot is in contact with the floor

Swing phase section of the gait cycle where the foot is not in contact with the floor

Toe clearance The distance between the toe and the floor during the swing phase of the gait cycle

Toe off Event in the gait cycle where the toe leaves the floor and the swing phase is initiated

Vector Loop Equations Equantions that are used to analytically describe the positions of the 4BM links in relation to each other

1. Introduction

1.1. Background

This section provides an overview of the prevalence and causes of transfemoral amputations, the availability of knee prosthetics, the difficulty in designing and testing prosthetic knee prototypes, and the impact of cost on prosthetic knees.

1.1.1. Functional Challenges and Prosthetic Access

Transfemoral (above knee) amputation is a life-changing event that affects the mobility, gait, quality of life, and independence of people around the world[1][2]. The gait cycle is the series of events that describes walking and is discussed in detail in Chapter 2. Amputees face several challenges in regaining independence and mobility after a transfemoral amputation. Although several options (ranging from rudimentary crutches to complex microprocessor controlled prosthetics) are available to help amputees regain mobility, access to advanced prosthetic knees is limited due to their high cost. As a result, many amputees opt for inexpensive prosthetic knees that do not provide the same level of functionality and quality of life benefits [3]

1.1.2. Design Parameters Associated with Knee Design

The design of a prosthetic knee is inherently complex due to the number of interrelated parameters that must be considered and the various methods available to address them. The primary objective is to replicate, as closely as possible, the natural function of the human knee [2], [4]. Achieving this goal requires attention to several critical factors, including the ability to support the user's body weight during the stance phase, allow efficient control of the swing phase, and accommodate a range of walking speeds and surface conditions [5]–[8].

An effective prosthetic knee must offer both durability and a lightweight structure, minimising the metabolic cost of walking while enduring repeated load cycles without mechanical failure [2], [9]–[11]. It must also provide sufficient ground clearance during swing to prevent tripping, reduce the hip moment required for operation, and enable voluntary user control where possible[1]. Many of these factors are interdependent; for example, improving structural durability may add weight, which can increase energy demands.

It is crucial to have customisable features that can be tailored to meet the specific preferences or requirements of individual users. The usability of the knee, defined by the degree to which the user can engage and adapt to the system, remains a central consideration for long-term function and user satisfaction [1], [12].

Understanding user mobility classifications helps guide prosthetic knee selection and highlights the trade-offs between cost and functionality. Functional classification systems are often used to guide the prescription of prostheses. Medicare K levels (K0 to K4) define the mobility potential of the user, each level corresponding to an increase in functional capacity [13]. For example, individuals at the K1 level often receive simple single-axis or constant-friction knees, typically

with a manual locking mechanism suitable for movement primarily in and around the house. K2 users may benefit from multi-axis designs with extension assist, enabling limited outdoor ambulation on level surfaces. In contrast, K3 and K4 individuals can walk with variable cadence and can perform more demanding tasks. These users are candidates for hydraulic, pneumatic, or microprocessor-controlled knees, which offer greater adaptability throughout the gait cycle [12], [14].

Each of these mechanisms and the design trade-offs they involve are discussed in detail in Chapter 2. There, the mechanical, functional, and clinical implications of specific prosthetic knee technologies are examined in more depth. Suffice to say, here is that functional use of such a knee (for example, returning to work) requires a device level comparable to K2 or higher.

1.1.3. Impact of Cost of Prosthetic Knees

Cost is a major barrier to accessing advanced prosthetic knee technologies. Premium devices from international suppliers are typically associated with improved functionality, improved gait symmetry, and greater mobility, all of which significantly improve the quality of life of amputees [3], [12], [15]. In contrast, low-cost prosthetic knees often offer limited adaptability and reduced biomechanical efficiency, which can hinder daily function and long-term health [5], [8], [11], [14], [16]. The link between prosthesis cost and functionality is important in the local South African context and is further explored in Chapter 2.

Low-cost prostheses and gait performance. Budget constraints often result in the use of single-axis or constant-friction knees that lack stance-phase control and adaptive swing damping. These limitations lead to irregular gait patterns, asymmetric limb loading, and increased reliance on compensatory movements such as hip hiking and other gait abnormalities[8]. Gait deviations are also linked to fall risk and can be a useful metric for overall health[17]. Furthermore, low cost knees demonstrated reduced clinical mobility performance, reported lower balance confidence, and experienced less comfort when compared with individuals using more advanced prosthetic knees[18]. Studies have shown that basic mechanical knee users expend more energy during walking compared to those who use more advanced designs [8], [15].

These issues are particularly pronounced in low-resource settings, where economic constraints often require the use of simplified prosthetic designs. The resulting mismatch between user needs and device performance is a central challenge in the field of prosthetic knee design. This study aims to address this challenge by identifying mechanical design strategies that balance functionality, cost, and accessibility. These relationships, as well as the engineering principles underlying different control mechanisms, are explored in more detail in the literature review chapter.

1.2. Problem Statement, Aim and Objectives

1.2.1. Problem Statement

The limited functionality of a typical low-cost knee prosthesis results in poor gait performance and subsequently leads to reduced quality of life due to adverse health outcomes. Several concepts and methods are used in premium knees to improve functional performance (e.g. stance-phase locking and swing-phase damping), but due to high costs and specialised maintenance from international suppliers, few patients can be helped with these devices. Therefore, the problem in South Africa is restricted access to cost-effective prosthetic knees with functional

gait performance, exacerbated by the lack of expertise in the local design and manufacture of these prostheses.

1.2.2. Aim

This study aims to expand the local knowledge base by designing, manufacturing, and functional testing of a cost-effective mechanical prosthetic knee with swing-phase damping and stance-phase locking that facilitates functional gait performance.

1.2.3. Objectives

Specific objectives that support the aim of this study are as follows.

1. **Review** the relevant literature on prosthetic knees to identify key design challenges, potential solutions, and to select a suitable knee concept.
2. **Design and manufacture** a cost-effective mechanical prosthetic knee prototype using appropriate modelling, simulation, and engineering tools.
3. **Test** the prototype through a controlled case study, using 3D motion capture technology to analyse lower-limb gait kinematics.
4. **Validate** the performance of the prototype against functional outcome measures and compare it with an existing commercial device.

1.3. Research Design

The overall research design of this study follows a structured engineering cycle of problem formulation, prototype development, testing, and reflection. To ensure that this process remained systematic and traceable, the study adopted the Quality Research Management (QRM) framework, supported by the use of a Research Validation Matrix (RVM) to link research challenges, literature findings, and conceptual solutions. These frameworks are described below.

1.3.1. Quality Research Management

To ensure traceability and systematic progress, this study is guided by the Quality Research Management (QRM) framework developed by Holm and van der Merwe [19]. QRM integrates tools from quality management, engineering management, and research methodology into six iterative phases: inception/definition, analysis, synthesis, testing and evaluation, communication, and close-out. Within this study, the QRM framework was not applied in its full formal detail but served as a guiding structure to align objectives with the findings of the literature, to systematically document decisions and to ensure that the results could be traced back to the research challenges.

1.3.2. Research Validation Matrix

The Research Validation Matrix (RVM), an integral component of the QRM framework, serves as a structural and visual tool to organise research efforts in a matrix format. Its primary objective is to collect relevant research to optimise resource allocation. This is achieved by connecting research challenges, literature topics, and conceptual solutions, ensuring traceability, and providing a clear link from research needs to solutions.

Research Challenges One way of conceptualising research challenges (RCs) is to identify the problems the study aims to solve by addressing the research need. RCs should be as independent as possible to ensure minimal overlap and reduce possible duplication of effort and possible confusion.

Concept Solutions During the analysis phase, a robust review of the existing literature allows the identification of evidence that substantiates the authenticity of the research challenges. In addition to this, it also reveals potential strategies that can be employed to address these challenges effectively. The conceptual solutions derived from this process serve as a crucial foundation for the subsequent synthesis phase, where they are integrated and refined to formulate a unified solution that addresses the specific research requirements.

Validation of Concept solutions Various approaches can be used to validate conceptual solutions. These encompass methodologies such as conducting experiments, conducting detailed case studies, and direct implementation, among others.

Implementation of the RVM One of the core tools in this framework is the House of Quality (HoQ), a simplified version of which can be seen in Fig. 1.1. The HoQ uses a graded representation of the relationship between various Customer Requirements and Solution Characteristics as basis and culminates with a weighted correlation between the different solution options, to identify the most appropriate selections.

1.3.3. Research Challenges and the RVM

The research validation matrix (RVM) is a custom version of the HoQ that allows for visual traceability of the progress of the study. It relates the research need, resulting research challenges, concept solutions and validation of these solutions. Downward arrows indicate the synthesis side, while upward arrows indicate the analysis side. At the beginning of each subsequent chapter, its part of the RVM will be indicated. In Chapter 6, the completed RVM shows how the study progressed.

The research need is identified in the problem statement, and to address this need, several research challenges (RCs) were defined. The top of the RVM, shown in Fig. 1.2 shows how the RCs were informed by previous literature. The next section describes the five RCs listed in more detail.

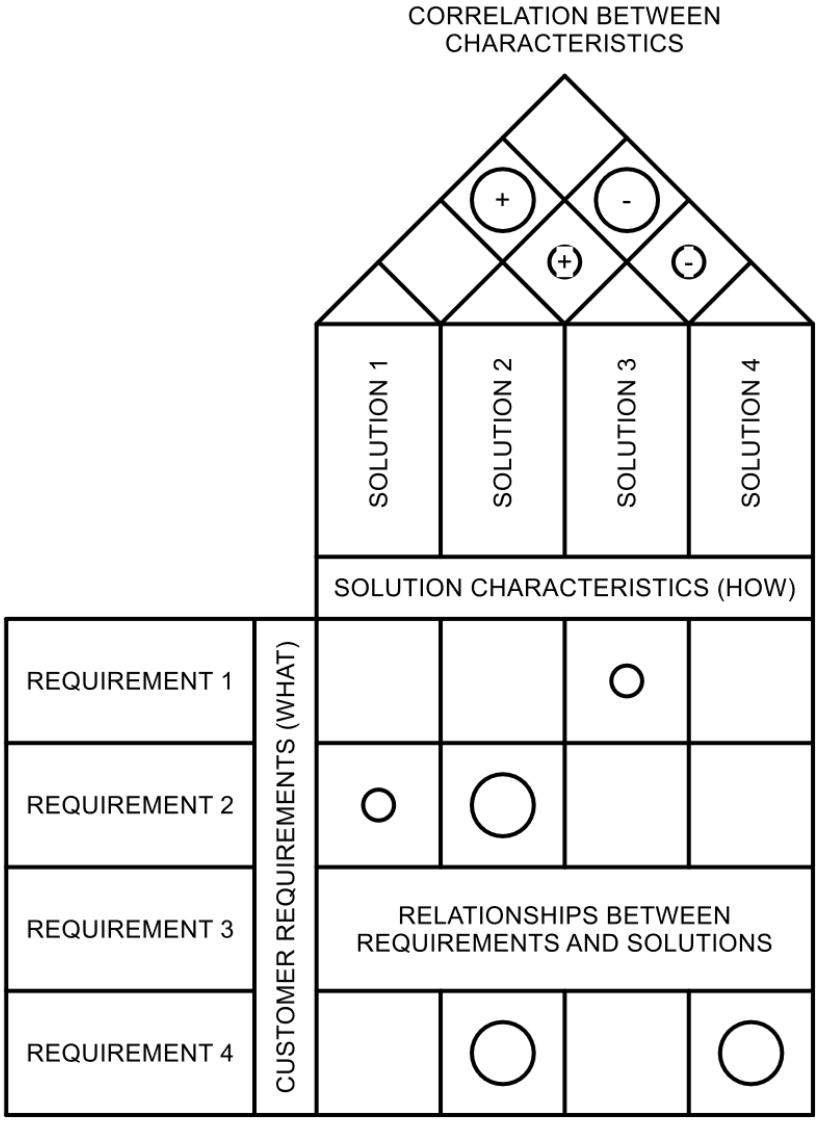

Figure 1.1. Simplified House of Quality [19]

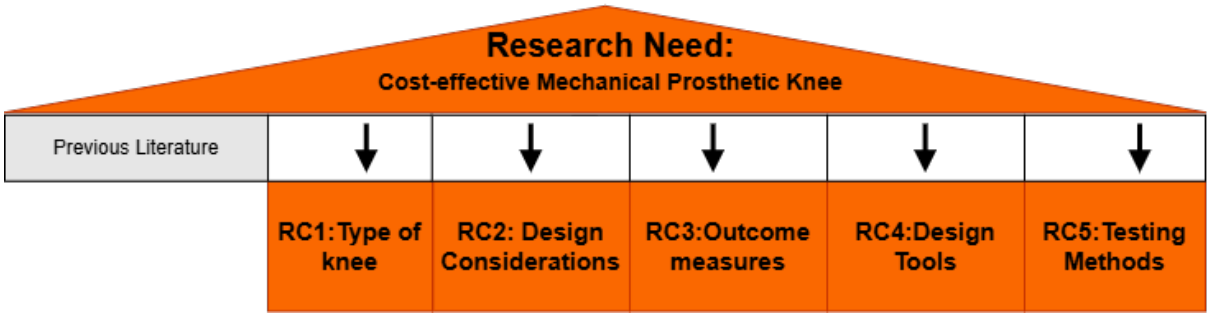

Figure 1.2. Top of the RVM shows how previous literature informed the research challenges.

Description of Research Challenges RCs frame the key decisions that must be addressed through literature review, design work, and testing.

- **RC 1: Type of Knee.** Determine which category of prosthetic knee is most appropriate for the context of this study (e.g. single-axis, polycentric/four-bar, hydraulic/pneumatic, microprocessor-controlled), given trade-offs between functionality, complexity, cost, and suitability for low-resource settings. This RC identifies the family of baseline mechanisms for prototype development.
- **RC 2: Design Considerations.** Define the critical parameters at the mechanism and system level that govern the function and feasibility. These include stability/locking features, allowable range of knee flexion, toe-clearance target, and adjustability features, among others. The parameters must be bounded by manufacturability, material availability, tolerance capability, maintenance simplicity, and safety constraints.
- **RC 3: Outcome Measures.** Select a concise, clinically significant, and feasible set of performance metrics to evaluate the prototype. Candidate measures include kinematic (e.g. knee angle profile, toe clearance), kinetic (e.g. ground reaction forces), and spatio-temporal (e.g., cadence, step length) parameters.
- **RC 4: Design Tools.** Identify modelling, simulation, and design systems that can predict performance within time and resource constraints (e.g., link-segment modelling, optimisation workflows, CAD/FEA) and that support design-for-manufacture and traceability.
- **RC 5: Testing Methods.** Determine an evidence-generating test strategy (e.g. mechanical test bench, gait emulator, human gait trials), balancing cost, data quality, ethical considerations, and applicability. Define how the chosen methods will validate the RC2 parameters against the RC3 outcome measures.

1.4. Testing Methodology

To evaluate the functional performance of the prototype, a human gait trial case study is anticipated to be used as one of the testing methods. Specific testing protocols and outcome measures will be defined during the literature review in Chapter 2 as part of the identified Research Challenges. Outcome measures include knee angle, ground reaction force, and toe clearance, among others.

1.4.1. Ethical considerations

The ethics number for this study is NWU-00473-24-S3. When dealing with human participants in a study, the methods used must adhere to strict ethical guidelines. To ensure that the research is done ethically and responsibly and that the dignity of the participant is protected, the following measures were implemented.

- **Informed consent:** The participant will be fully informed about what the study entails.
- **Voluntary Participation:** The participant will not be forced to participate and can decline to continue at any time.
- **Minimisation of risk:** A controlled environment, under the supervision of experienced researchers, only basic ambulation, self-selected walking speeds, mandatory rest periods, among others, ensure minimal to no risk.

- **Personal information and data collection:** No unnecessary information will be recorded and the collected data will be stored responsibly.

1.5. Delineations and Limitations

This study is subject to several typical limitations that define the scope and influence the interpretation of the results. These limitations are standard for a master's-level research project and have to be acknowledged to give context to the findings.

Time limitations The research was conducted within the three-year time frame for a Master's dissertation. This limited the number of design iterations, precluded long-term testing and clinical trials. Therefore, the focus of this study was to develop and evaluate a single prototype that would serve as a proof of concept instead of pursuing endless design improvements.

Financial resources The available funds for this study are approximately R50000. This restricts material choice, manufacturing processes, and testing equipment. This financial constraint allows one to develop and evaluate a prototype, but priority was given to cost-effective solutions rather than expensive approaches, such as composites or large-scale production methods.

Sample size The experimental evaluation was limited to a single participant in a controlled case study. The case study is a performance comparison between the prototype prosthesis and an existing product with one participant to demonstrate the proof of concept. Although this approach provided valuable information about functional performance, the small sample size limits the generalisability of the findings. More research with a larger cohort is required to validate the study results.

Focus of design The study focused on developing a cost-effective mechanical prosthesis with swing phase damping and locking in the stance phase. Other concepts like microprocessor-controlled knees or active (motorised) knees were excluded. This delineation is in line with the overall objective of accessibility in low-resource environments.

1.5.1. Significance of study

The contribution of this study lies in bridging the gap between functionality and affordability in prosthetic knee design. Current high-end prosthetic knees are prohibitively expensive and, therefore, inaccessible in lower resource settings, while low-cost devices mostly do not have essential features like stance-phase locking and swing-phase damping required for active work. By demonstrating that a cost-effective prosthetic knee can be designed without sacrificing core functionality, this research has the potential to support mobility, independence, and improved quality of life for amputees in low-resource contexts.

1.6. Chapter Overview

This section provides an overview of the structure and content of subsequent chapters in the dissertation.

- **Chapter 2: Literature review:** Focusses on addressing the research challenges identified in Chapter 1 and identifies concept solutions.

- **Chapter 3: Methods and Analytical Modelling** describes the research design, as well as the analytical and computer methodologies used for the current study.
- **Chapter 4: Prototype Development**: Details the implementation of the design process and how the physical prototype was manufactured.
- **Chapter 5: Experimental Methodology and Results:** Describes the procedure for the case study, data analysis methods, and reports the results of the experimental evaluation.
- **Chapter 6: Conclusion and recommendations** Critically evaluate the study and recommend future work.

2. Literature Review

2.1. Introduction

This chapter reviews previous contributions from the literature related to the design of mechanical prosthetic knees. To address the research challenges identified in Chapter 1, the topics of the literature shown in Fig. 2.1 were investigated.

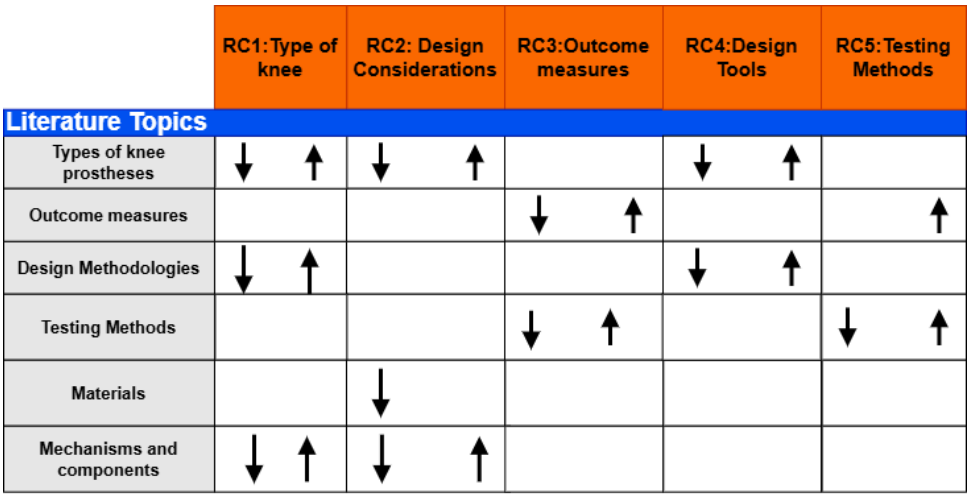

Figure 2.1. Research challenges and Literature topics

2.2. Prosthetic Function

Lower limb prostheses aim to restore structural integrity and mimic the biomechanics of a natural joint, with varying functionality depending on the complexity of the design and integration of components[14]. Understanding the functions required of the knee is crucial to designing a prosthetic that meets fundamental requirements.

2.2.1. Structural Support and Basic Functionality

At their most fundamental level, prosthetic devices provide structural support to compensate for loss of skeletal segments due to amputation [16]. These systems enable users to perform essential tasks, such as standing and basic ambulation. Simpler prostheses, often single-axis designs, are more cost-effective and easier to maintain, but offer limited control over joint behaviour and are less effective in accommodating complex movements; therefore, more advanced options were considered for the current study [4], [11].

2.2.2. Mechanical Enhancement and Functional Replication

More advanced prosthetic designs integrate mechanical components that aim to replicate specific biomechanical functions of the musculoskeletal system. These include features such as improved joint stability, variable damping for smoother motion, and mechanisms for energy storage and return (ESAR)[4], [5], [9], [10], [20].

Polycentric designs and adjustable damping systems help achieve more natural movement and lessen compensatory requirements. These features are particularly beneficial for active users or those navigating uneven terrain. Functional replication is associated with improved gait symmetry, stability, and joint loading patterns [4].

2.2.3. Gait Optimisation and Energy Efficiency

Beyond structural and mechanical considerations, the ultimate goal of lower limb prostheses is to facilitate safe, efficient, and natural movement. A well-designed prosthesis can greatly improve the participation of an amputee in daily and recreational activities, improving quality of life [12].

During level walking, the prosthetic knee must support the user's body weight while managing energy dissipation and facilitating a smooth transition through the gait cycle [4]. Optimal gait requires minimising asymmetry and reducing the metabolic cost of walking. Studies have shown that prosthetic systems that better approximate natural joint mechanics result in lower energy expenditure and improved walking economy [6], [14], [21], [22]. Therefore, a candidate prosthesis design should aim to facilitate a gait that is as symmetric between the left and right legs as possible.

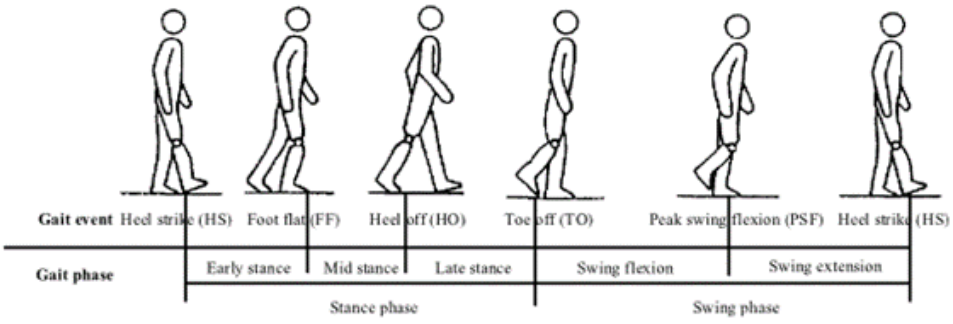

Figure 2.2. Human gait cycle progressing through stance phase to swing phase [23]

2.2.4. Normal Gait

To design an effective prosthetic knee, a thorough understanding of the normal gait cycle (shown in Fig. 2.2) is essential, especially regarding the role of the knee in each phase of this cycle. Outlined in Table 2.1 are the phases and sub-phases of the gait cycle, highlighting the functions of the knee in each sub-phase. Ideally, a prosthetic knee should replicate all required functions, from initial contact to terminal swing phase.

Table 2.1. Summary of knee function during the gait cycle (adapted from [24])

Phase / Sub-phase	Gait Cycle (%)	Knee Action	Knee Function
Stance Phase (60%)			
Initial Contact	0–3%	∼5° flexion, shock absorption	Stabilises limb, absorbs impact forces
Loading Response	3–10%	Slight flexion	Supports body weight, dissipates impact, facilitates weight transfer
Mid-Stance	10–30%	Extended	Provides stability and support for body weight
Terminal Stance	30–50%	Slight flexion	Prepares for forward propulsion
Pre-Swing	50–60%	Considerable flexion	Enables toe off and transition to swing
Swing Phase (40%)			
Initial Swing	60–75%	Further flexion	Ensures foot clearance during forward swing
Mid-Swing	75–87%	Begins extension	Propels limb forward under torso
Terminal Swing	87–100%	Fully extended	Prepares for heel strike and initial contact

2.2.5. Amputee Gait

Gait patterns in individuals with lower limb amputations frequently deviate from the typical gait observed in non-amputees[25]. These deviations arise from two primary sources: patient-related factors and prosthetic-related factors [26].

Patient-related causes include muscle weakness, joint contractures, pain, and reduced confidence in either the prosthesis or the residual limb. However, prosthetic-related causes often stem from poor socket fit or misalignment of prosthetic components, both of which can change gait mechanics and stability.

Amputee gait is not only distinct from that of non-amputees, but also varies considerably depending on the level of amputation. Transfemoral amputees typically show greater gait asymmetry than transtibial amputees, whose knee joint is preserved. This difference comes from the additional biomechanical challenges associated with replicating knee function. The type of prosthesis used also plays a critical role. For transfemoral amputees in particular, prosthetic design, especially the knee mechanism and socket configuration, can significantly influence gait performance and the user's ability to adapt [25]. A proposed prosthesis mechanism that facilitates stance-phase locking and increased toe clearance may thus mitigate some gait deviations (such as hip-hiking [1]) due to an increased trust in the prosthesis.

In summary, amputee gait is shaped by a complex interplay of biomechanical, physiological, psychological, and prosthetic factors. Understanding these influences is essential for designing effective prosthetic systems that support long-term mobility and health.

[1] Hip-hiking is the act of one hip lifting higher than the other.

2.3. Types of Prosthetic Knees

Prosthetic knees can be classified into three main categories: passive knees, microprocessor controlled knees, and powered knees, as noted by Grant & McGimpsey, and Keerthana et al. [3], [12]. These categories encompass various methods to accommodate the needs of the individual patient. However, it is important to view these types of knee through the lens of "Appropriate Technology".

2.3.1. Appropriate Technology

Within the field of rehabilitation for lower limb amputations, the World Health Organisation [27] has defined the term "appropriate technology" as:

"A system providing proper fit and alignment based on sound biomechanical principles that suits the needs of the individual and can be sustained by the country at the most economical and affordable price."

This definition highlights devices that consider the specific context, placing emphasis on:

1. **Technical Reliability:** Prosthetic devices should be able to withstand thousands of cycles of use under various circumstances without mechanical failure or severe degradation.
2. **Biomechanical Fit**: Prosthetic devices should emulate natural movement and properly align with the user's residual limb, thus reducing the risk of complications such as joint strain, muscle imbalances, or skin irritation.
3. **Customisation and Usability:** Prostheses need to address the individual requirements of each user, ensuring that they are customisable for comfort, mobility, and ease of use across different terrains and physical activities.
4. **Economic Viability and Sustainability:** High-tech interventions qualify as "appropriate" only when they are accessible, maintainable, and reproducible according to the regulations in the healthcare system and the economic conditions of the country.
5. **Enhancement of local skills and resources:** Developing local manufacturing and technician training enhances resilience and encourages wider adoption.
6. **Responsible Technology Transfer:** This approach counters the negative practice of "technology dumping" where excessively expensive (or inferiorly cheap) but still unsuitable devices are provided without plans for sustainable uptake or acceptance by the receiving community.

2.3.2. Passive Mechanical Knees

Passive mechanical knees are relying on mechanical components to generate resistance during both the stance and swing phases. These systems are generally more affordable and require less maintenance than active or electronic alternatives [4]. However, their simplicity comes at a cost: they offer limited adaptability during dynamic tasks and often increase the energy expenditure of the user [4], [11], [16].

Among passive options, single-axis knees represent the most basic design. They operate as hinge joints, allowing flexion and extension in a single plane. Their straightforward construction makes them cost-effective and easy to maintain, but this simplicity also limits their ability to accommodate complex movement patterns, often resulting in less fluid gait mechanics.

A more advanced passive option is the polycentric knee, which uses multiple axes of rotation to shift the instantaneous centre of rotation during ambulation. This design improves anatomical alignment and provides greater stability than single-axis models [1], [5], [28]–[30]. The most common variant is the four-bar mechanism (4BM), although configurations with five [31] or six bars also exist. These knees offer better resistance to anterior displacement during the swing phase and improved stability during the stance phase, but tend to be bulkier and more expensive. Two notable advantages of a 4BM knee are that with the appropriate geometric configuration they offer inherent stance-phase stability, and during the swinging movement the mechanism naturally shortens with increased flexion, thus facilitating greater toe clearance.

Friction brakes are sometimes incorporated into polycentric or single-axis designs to further stabilise the knee and to add swing-phase damping. Another refinement involves hydraulic damping systems, which use hydraulic fluid to provide resistance during stance and absorb shock during swing. Compared to purely mechanical systems, hydraulic knees offer smoother gait transitions and reduced energy demands. They are available in models with either manually adjustable valves or integrated microprocessors. Although effective, these knees are heavier and require regular maintenance of their hydraulic components.

Together, these passive mechanical systems provide a range of control options that are suited to different user needs. When properly selected, they can substantially improve mobility and safety for transfemoral amputees.

2.3.3. Microprocessor-Controlled Prosthetic Knees

Microprocessor-controlled prosthetic knees (MPKs) represent the most advanced category of passive prostheses currently on the market[3]. These systems integrate sensors and adaptive control algorithms that continuously monitor gait parameters such as joint angle, load, and cadence. In response, the microprocessor changes resistance to optimise knee behaviour during the stance and swing phases [14]. This adaptive functionality enables smoother transitions, improved stability on variable terrain, and gait patterns that more closely resemble natural human locomotion.

MPKs have been shown to reduce energy expenditure during ambulation compared to traditional passive designs [12]. They also enhance user safety by minimising the risk of stumbling or knee collapse, particularly during irregular gait conditions. Most MPKs incorporate hydraulic or pneumatic damping elements controlled by the microprocessor to dynamically adjust the resistance throughout the gait cycle. Subcategories of MPKs include variable-damping or semi-active systems, which offer intermediate levels of adaptability while remaining within the broader class of passive prostheses.

Despite their advantages, MPKs remain the most expensive category of prosthetic knees[3]. Their cost, combined with maintenance and power requirements, limits their accessibility in low-resource settings. For this reason, the current study will not consider MPKs, as their production and use in developing contexts pose significant challenges in terms of affordability, infrastructure, and local technical support [12].

2.3.4. Active Prosthetic Knees

Active prosthetic knees extend beyond the passive and semi-active categories by incorporating actuators that generate net positive mechanical work[2]. These powered systems actively assist with knee flexion and extension, rather than simply modulating resistance to user-generated

motion. As a result, they offer the potential to more closely replicate the biomechanical function of a biological knee.

Designs vary widely but commonly employ electric motors, series elastic actuators, or pneumatic artificial muscles to deliver torque during the gait cycle [6], [9], [20]. These actuators are typically controlled by embedded microcontrollers or real-time systems that use inertial and load sensors to detect gait phase and user intent[2], [22]. Several studies have shown that active knees can improve swing dynamics, ascent and descent of stairs, and walking in inclines by providing additional joint torque during flexion or extension [10], [14].

Innovative approaches include the use of a transmission clutch, which can rapidly switch between passive and powered modes to optimise energy use and performance[32]. Others emphasise lightweight structures and efficient actuators to enhance battery life without compromising functionality[31].

Despite their promise, active knees also present significant technical and practical challenges. These include high power consumption, actuator complexity, heat dissipation, and the need for advanced control systems to ensure safety and responsiveness. Combined with high production costs and limited accessibility, these factors currently restrict their use to research contexts and specialised clinical settings.

As with microprocessor-controlled knees, the cost, infrastructure demands, and maintenance requirements of active systems make them unsuitable for widespread deployment in low-resource environments. For these reasons, the current study will also not consider active prosthetic knees.

However, active prostheses remain a critical area of innovation in lower limb prosthetics. Their ability to generate positive mechanical work, rather than simply modulate motion, offers transformative potential to restore mobility for transfemoral amputees.

2.4. Prosthetic Knee Control

Control mechanisms in prosthetic knees are essential for restoring functionality after limb loss. They are typically divided according to their role in the stance and swing phases of the gait cycle. The ability of these mechanisms to offer stability, adaptability, and energy efficiency directly impacts user safety and mobility.

2.4.1. Ground Reaction Force Vector and Passive Stability

The stability of a prosthetic knee is predominantly influenced by several key factors, including mechanical design (inherent passive stability), alignment, and interaction with the residual musculature of the user (active stability) [4]. Passive mechanical stability is typically related to the direction of the Ground Reaction Force Vector (GRFV), which can activate a locking mechanism or produce an extension moment at the knee joint[33].

In gait analysis, the GRFV is often used as it combines the mass and acceleration impacts of the body into one vector. This load line, originating at the foot's centre of pressure, acts upward according to the load conditions. A force plate can accurately identify the orientation of the GRFV, as was used in [7]. The orientation of the GRFV is crucial for assessing the stability of the prosthesis during the stance phase. To evaluate gait symmetry, one can compare the ground reaction force profiles of the healthy limb and the prosthetic limb.

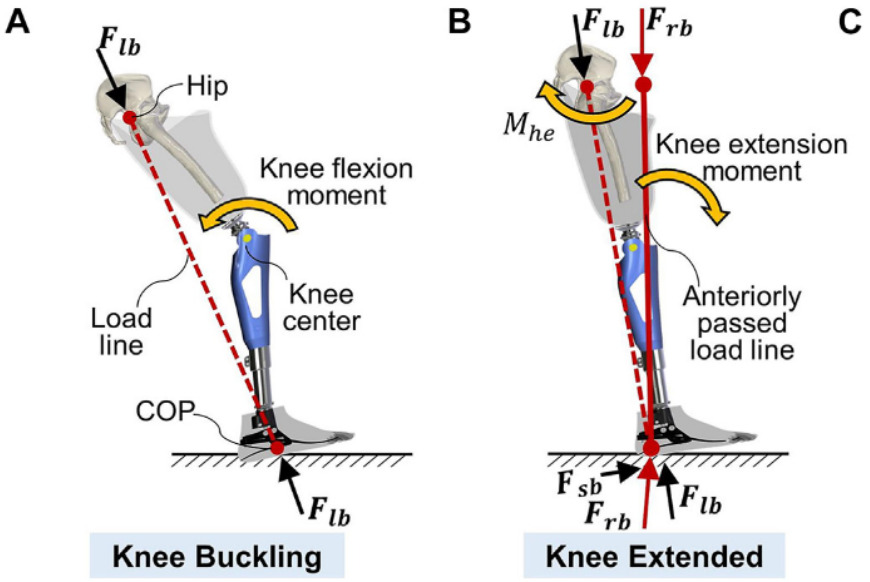

Figure 2.3. Illustration of how GRFV (red dotted line) with applied hip moment moves forward to solid red line and thus a stable position, adapted from [4]

Figure 2.3 shows the forward shift of the ground reaction force vector (GRFV), also known as the load line F_{lb}, when a hip moment is applied. The foot exerts a shear force F_{sb} for traction with the resultant force vector given by F_{rb}. This forward shift of the load line results in the knee joint being positioned posteriorly to the load line, allowing a stable extension of the leg in stance phase, by maintaining its alignment and balance under these biomechanical conditions.

2.4.2. Stance Phase Control

During stance, the prosthetic knee must resist flexion to support body weight and prevent collapse or buckling. Several distinct mechanisms address this requirement:

Mechanical Friction Systems These provide constant resistance to knee flexion using simple mechanical elements. They are cost-effective and widely used in low-resource settings, but lack adaptability to different walking speeds or terrains [4], [34].

Weight-Activated Locking Mechanisms In this design, the knee locks under axial load and unlocks when the weight is removed. Although highly stable, these systems can produce less natural gait patterns and increase energy demands [21], [33], [35].

Hydraulic Systems Hydraulic systems dynamically adjust the resistance based on the gait phase and walking speed. They improve both comfort and energy efficiency and offer smoother transitions during ambulation [4], [36]–[38].

Polycentric Designs Polycentric knees use multiple pivot points, allowing the instantaneous centre of rotation to shift during movement. In the stance phase, the geometry of certain configurations allows for inherent stability, while other configurations require a hip moment to remain stable. This geometry improves ground reaction force alignment and increases toe clearance during the swing phase, which is beneficial for users walking on uneven terrain [1], [28], [39].

Microprocessor-Controlled Knees (MPKs). MPKs use real-time sensor input to automatically adjust knee resistance. Compared to passive knees, MPKs improve gait symmetry, reduce metabolic cost, and significantly lower the risk of falls [7], [23], [40].

2.4.3. Types of polycentric four-bar mechanisms

There are three broad types of polycentric four-bar mechanism, differentiated by geometry and function [28] and by how stance phase control is achieved. Fig. 2.4 shows the ICR curves for the different mechanisms overlaid with the zone of voluntary stability (red).

The **hyper-stable configuration** is characterised by an instantaneous centre of rotation that is located behind and above the knee axis at heel strike . This geometry allows the load line to pass anteriorly to the ICR for most of the stance phase, thereby creating an inherently stable configuration that resists knee flexion during the stance phase [1], [4], [28]. It is used predominantly in cases where the patient lacks the required strength in the stump/ hip to safely keep the knee in a locked position. Although this design is used when user safety is paramount (low-activity or older users), increased difficulty when initiating the swing phase can lead to gait abnormalities, such as hip-hiking [39].

The **elevated ICR mechanism** moves the ICR upward and closer to the load line compared to the hyper-stable configuration. This reduces the hip moment required to initiate flexion, enabling smoother transitions from stance to swing. However, the ICR of these mechanisms decreases rapidly after initial flexion, thereby increasing the hip moment required to stabilise the knee. As such, elevated ICR mechanisms are used in cases where the amputee is more active. The resulting gait with these mechanisms is more dynamic and symmetrical.

The ICR of **voluntary control mechanisms** is located near the load line for most of the flexion range. This allows for relatively easy control of knee flexion and extension. Furthermore, the ICR of these types of mechanisms is fairly concentrated for the first few degrees of flexion, allowing for minimal hip moment to control flexion and extension. As such, this type of knee is most suitable for active and experienced amputees who require a knee that performs better[4].

2.4.4. Swing Phase Control

The swing phase mechanisms regulate the forward swinging movement of the limb when leaving the ground after toe off, ensuring proper foot clearance and timed extension for the next heel strike.

Frictional Damping. These components offer constant or adjustable damping during swing. Although simple, they do not adapt well to variable cadence and can result in irregular gait patterns [4], [16].

Pneumatic Systems. The pneumatic knees are dependent on compressed air to provide resistance, allowing some adaptation to the speed of movement. They are lighter than the hydraulic versions, but may not offer the same precision. An example is where Waycaster, Wu, and Shen [41] employed pneumatics for knee actuation and control.

Hydraulic Swing Control. Hydraulic swing-phase control enables fine-tuned resistance adjustment, resulting in smoother and more natural motion over a range of walking speeds [23], [42], [43].

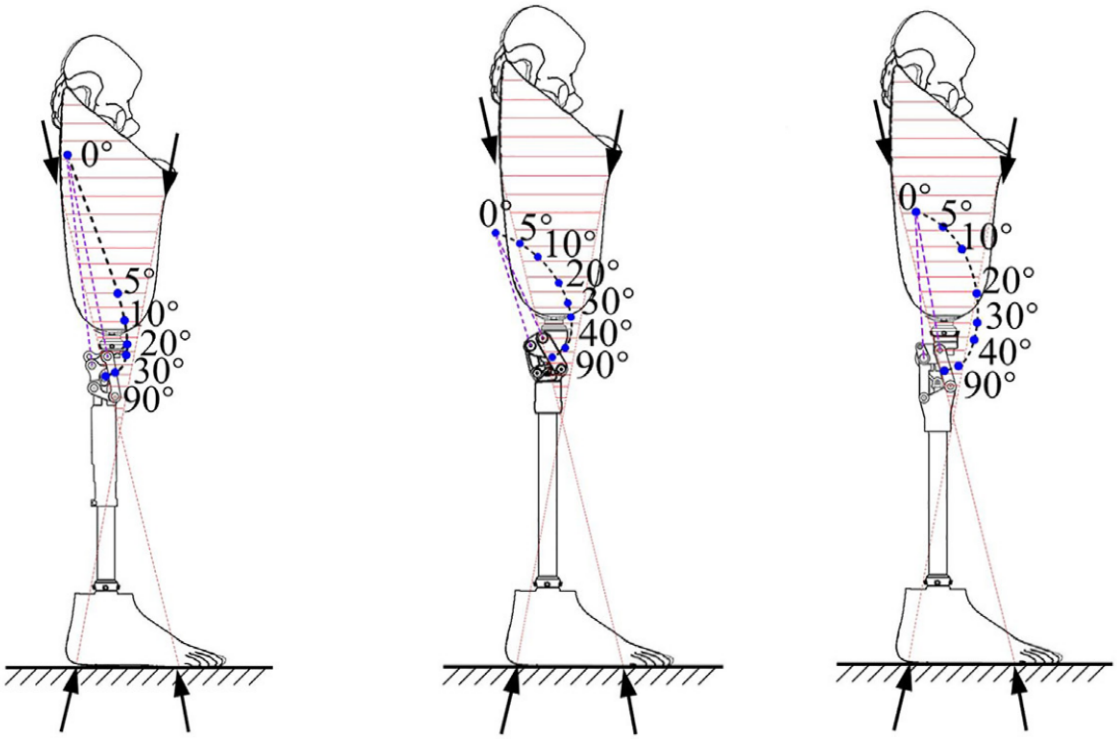

(a) Elevated ICR mechanism **(b)** Hyper-stable mechanism **(c)** Voluntary-control mechanism

Figure 2.4. Comparison of the three four-bar mechanism types showing different instantaneous-centre-of-rotation (ICR) configurations overlaid with zone of voluntary stability adapted from [4].

2.4.5. Comparison of Knee Mechanism Characteristics

Table 2.2 compares common prosthetic knee control mechanisms across several key criteria, including adaptability, stance-phase stability, cost, and typical use cases. In general, it can be seen that as the desired functionality increases, the cost and complexity also increase.

Table 2.2. Comparison of prosthetic knee control mechanisms.

Mechanism	Adaptability	Stability (Stance)	Cost	Typical Use Case
Friction-based	Low	Moderate	Low	Basic mobility in low-resource settings
Weight-activated lock	Moderate	High	Medium	New users or individuals with poor balance
Hydraulic (stance/swing)	High	High	High	Active users with variable walking speeds
Pneumatic (swing)	Moderate	N/A	Medium	Lightweight gait solutions with moderate adaptability
Polycentric	Moderate	High	Medium	Is dependant on link configuration
Microprocessor-controlled	Very High	Very High	Very High	Advanced prosthetics for high-functioning users

2.5. Materials

The selection of materials for prosthetic knees requires careful consideration of mechanical properties, weight, durability, cost, and manufacturability. These devices undergo substantial dynamic loads and environmental exposure. The principles of foundational materials science, such as strength-to-weight ratio, fatigue resistance, corrosion behaviour, and formability, play a decisive role in determining suitability. A range of materials is used in the production of prosthetic knees for transfemoral amputees, most commonly aluminium, titanium, and various fibre-reinforced composite materials, each selected for its specific mechanical properties and performance characteristics [15].

2.5.1. Summary of materials and their uses

The combination of materials used in mechanical knee prostheses must satisfy a complex set of often conflicting criteria. Table 2.3 gives a summary of the materials commonly used in prosthetic knees by comparing their strength and fatigue, wear resistance, weight, cost, and ease of manufacturing with each other, as well as noting the typical use case for each material. More information on the choice of metals is available in Section 2.5.2 and regarding engineering plastics in Section 2.5.4.

Table 2.3. Comparative Summary of Materials Used in Knee Prosthesis Components

Material	**Strength & Fatigue**	**Frictional Wear Resistance**	**Weight**	**Cost**	**Manufacturing**	**Typical Use Case / Notes**
Aluminium Alloy (7075-T6)	Moderate strength; limited fatigue resistance	Moderate; anodising improves lifespan	Light (2.8 g/cm^3)	Low	Excellent machinability	Frame structures, linkage arms; good for lightweight designs with moderate fatigue loads
Titanium Alloy (Ti-6Al-4V)	High strength; excellent fatigue resistance	Excellent; corrosion and wear resistant	Medium (4.4 g/cm^3)	High	Poor machinability; suitable for additive manufacturing	High-stress structural components in premium or advanced prostheses
Stainless Steel (304)	High strength; moderate fatigue life	High	Heavy (8.0 g/cm^3)	Moderate	Good machinability and weldability	Used in budget prostheses or prototypes; strong but heavy
Carbon Fibre Composite	Very high fatigue strength; excellent stiffness-to-weight ratio	Excellent	Ultra-light	Very high	Complex fabrication; not easily repairable	High-performance pylons or knee housings; used in sports or advanced prostheses
Vesconite	High compressive strength; low creep under load	Excellent in dry/wet environments	Light (1.4 g/cm^3)	Moderate	Easily machined; stable in humid environments	Bushings and bearings in outdoor or mixed environments
Iglidur J3 (igus®)	Moderate strength; fatigue-optimised polymer	Very low wear rate in dry running	Light (1.46 g/cm^3)	Moderate	Injection moulded; dimensionally stable	Friction pads, sliding guides; quiet, low-maintenance dry operation

2.5.2. Metals

Aluminium alloys, particularly 7075-T6, are commonly used in prosthetic components due to their high strength-to-weight ratio and good machinability. According to [44], certain aluminium alloys exhibit a relatively high strength to weight ratio, making them especially useful in reducing the inertial mass of prosthetic limbs during the gait swing phase. Certain alloys also offer acceptable corrosion resistance, though their fatigue performance is more limited compared to titanium alloys. These characteristics make it suitable for components such as linkages, connectors, and knee frames where high strength and lightness are required [45].

In contrast, titanium alloys such as Ti-6Al-4V provide exceptional mechanical performance, including high tensile strength (approximately 900 MPa) and excellent fatigue resistance, paired with a relatively low density of about 4.4 g/cm^3. As described by Ashby [46], the superior resistance of titanium to corrosion and wear also contributes to its long service life, making it ideal for high-stress applications such as the central joint axis or load-bearing rotary elements. However, titanium is more difficult to machine because of its hardness, and its cost remains significantly higher than that of aluminium. Therefore, it is reserved primarily for premium or microprocessor-controlled prosthetic knees where performance and durability outweigh economic constraints.

Stainless steel (e.g., AISI 304) is also a suitable material for use in prosthetic devices. It offers excellent strength and corrosion resistance, but its high density ($\tilde{8}.0$ g/cm^3) makes it less suitable for weight-sensitive applications. However, its affordability, ease of fabrication, and mechanical robustness make it particularly suitable for low-cost or test-phase prosthetic devices.

2.5.3. Carbon fibre reinforced polymer

Carbon fibre reinforced polymer is also a suitable material for certain prosthetic knee components due to it's stiffness and high strength to weight ratio[15]. However, the fabrication process is complex and expensive, and it is not easily reparable.

2.5.4. Engineering Plastics

Engineering plastics are commonly used in frictional components of external knee prostheses, such as bushings, sliding pads, and articulating surfaces. These components experience repeated movement under load and often operate in dry conditions, without lubrication. The materials used in these interfaces must combine low friction and high wear resistance with dimensional stability, mechanical strength, and environmental durability.

The friction components of prosthetic knees experience a variety of loading conditions. They are subjected to cyclic compression and shear forces, especially during gait transitions, and they must maintain functional integrity in the presence of moisture, temperature fluctuations, and dust. Materials for these applications are chosen not only for their strength, but also for their ability to resist creep, deformation, and surface wear over thousands of movement cycles.

Two engineered materials that can work particularly well in prosthetic bushings and frictional interfaces are Vesconite and Iglidur J3.

Vesconite is a proprietary, internally lubricated thermopolymer developed for high-load, low-friction bearing applications. It offers excellent dimensional stability in humid conditions and resists swelling, making it especially suitable for prosthetic bushings exposed to sweat or outdoor

environments. Its compressive strength and wear resistance under dry-running conditions allow it to perform well in certain load-bearing roles [47].

Iglidur J3, developed by igus®, is an advanced polymer composite designed for long-lasting, dry applications[48]. It offers a lower wear rate and extended service life compared to earlier Iglidur formulations, particularly in pivoting or rotational movements under moderate loads. The material maintains a very low coefficient of friction across a broad range of shaft materials, including aluminium and stainless steel, and performs well even at higher cycle counts. Its low density and corrosion resistance make it especially suitable for use in prosthetic knee components such as sliding pads or articulating bushings, where both weight savings and low maintenance are critical. The quiet performance of the material combined with its resistance to moisture absorbing makes it a particularly suitable choice for prosthetic systems that are sensitive to friction and designed for direct user interaction.

Despite their utility, engineering plastics must be carefully matched to their intended function. Variables such as moisture sensitivity, temperature range, and long-term creep must be managed through appropriate material selection and design tolerances. However, when integrated into hybrid assemblies, these materials offer an effective and durable solution for key wear components in prosthetic knees.

2.6. Comparative Cost Analysis

A white paper published in 2017 found that a basic below-the-knee prosthesis costs between $5,000 and $7,000 and enables the user to stand and walk on level ground. However, a $10,000 device can allow for more complex activities, such as climbing stairs and ambulation in the community. In the $12,000 to $15,000 range, users often gain access to polycentric mechanical knees with swing and stance control, allowing gait patterns that closely resemble those of non-amputees. Microprocessor-controlled knees, which provide dynamic adjustment to terrain and walking speed, generally fall in the $20,000 to $30,000 range, but can be as expensive as $70,000 [3].

2.7. Simulation Tools and Approaches

Simulation tools play a critical role in prosthetic knee design by providing a controlled environment to explore parameter ranges, predict behaviour, and reduce the reliance on costly trial-and-error prototyping. These tools also allow researchers to test whether the design parameters meet functional and safety requirements before committing to physical manufacture. The main approaches relevant to this study are mathematical models and finite element analysis (FEA).

2.7.1. Mathematical Models

Mathematical and computational models are widely used to approximate the kinematics and kinetics of prosthetic mechanisms. Link-segment models, for example, provide a means of predicting joint angles, moments, and ground reaction force interactions at critical points in the gait cycle (heel strike and toe off). Such models can be implemented in environments like MATLAB/Simulink, allowing the rapid evaluation of proposed link geometries, range of motion, and instantaneous centre of rotation paths [1], [31], [33]. These models are particularly useful in early design stages because they allow systematic variation of linkage lengths and

pivot locations to test whether the mechanism achieves critical performance targets such as stance stability or toe clearance. Although mathematical models simplify reality, their strength lies in speed, adaptability, and ability to support optimisation methods before moving to more complex tools.

2.7.2. Finite Element Analysis

Once a feasible mechanism has been identified, finite element analysis (FEA) provides higher-resolution insight into the structural performance of individual components. FEA is especially relevant for the evaluation of design parameters such as material choice and stress concentrations. Using commercial software platforms, prosthetic knee components can be subjected virtually to representative gait-cycle loading conditions, allowing the designer to predict structural validity and deformation and calculate the safety factor [5], [26], [45], [49]. This approach supports design-for-manufacture decisions by highlighting whether low-cost materials (e.g., aluminium alloys, engineering polymers) can meet safety margins under cyclic loading or whether higher-performance alternatives are necessary. In cost-sensitive contexts, FEA also helps justify simplifications in geometry or reductions in part count by quantifying their mechanical impact. FEA complements the mathematical model by validating that the proposed mechanisms are not only kinematically functional but structurally robust.

Together, mathematical modelling and finite element analysis provide a sound simulation approach: the first narrows down feasible configurations, and the second confirms durability and manufacturability. This layered approach is central to addressing the design and testing challenges of cost-effective prosthetic knees.

2.8. Testing Methods and Parameters

This section addresses RC3 and RC5. A recent scoping review by Kooiman, van Staveren, Leijendekkers, *et al.* [50] surveyed and categorised the outcome measures and research protocols of 48 articles related to the development and testing of transfemoral prostheses prototypes. The main finding of the study is that there is a large variability in methodology and currently no standardised methods on how to evaluate the performance and functionality of a pre-commercial prosthesis prototype or prosthetic parts during walking. Of these 48 studies, kinetic/kinematic gait parameters were most often reported, followed by the spatio-temporal gait parameters. The outcome measure most frequently reported overall was the angle of the knee (degrees) displayed during the gait cycle, mainly corresponding to the aim of mobility [50]. Therefore, the literature review of the current study focused on these methodologies.

Human gait trials All studies reviewed by [50] included human gait trials. An advantage of human gait trials is that they provide data on how the prosthesis performs during actual walking. It also gives insight into user-specific compensations, variability, and adaptations that cannot be captured from gait emulators or simulations. Human gait trials also offer direct measurement of key parameters such as joint angles, ground reaction forces, cadence, and step length, among others. This allows researchers to characterise the gait and evaluate symmetry, gait coordination, and energy expenditure. Users can also give feedback, which can aid in the iterative design process.

However, they involve ethical considerations, logistical complexity, and variability between participants, which can limit the comparability between studies. Safety protocols and the burden on amputee participants further constrain the scope of experiments in the prototype stage.

Gait Emulators Gait emulators provide an alternative to direct human subject testing by reproducing the mechanical dynamics of walking in a controlled laboratory environment. These devices, often constructed as robotic rigs or programmable test benches, can replicate joint motions and ground reaction forces with high repeatability [23], [51]. Compared to human gait trials, emulators allow systematic variation of parameters such as cadence, stride length, and loading conditions without the variability of individual participants. This makes them particularly useful for early-stage prototype evaluation, where stability thresholds, swing-phase damping behaviour, or failure modes need to be quantified under reproducible conditions.

By contrast, human gait trials are still the standard for assessing functional outcomes and user experience. Trials provide insight into factors such as comfort, compensatory movements, and overall gait symmetry, which cannot be fully replicated in mechanical emulators [50].

In practice, gait emulators and human trials are complementary rather than mutually exclusive. Emulators enable accelerated iteration and pre-screening of design concepts, while human trials validate clinical relevance and real-world usability.

2.8.1. Gait Analysis

Gait analysis is a widely used biomechanical technique for quantifying human walking patterns. It involves capturing motion and force data during walking to assess joint angles, timing parameters, and kinetic forces[50]. The most common method in clinical and research settings involves a combination of 3D motion capture systems and force plates to measure kinematics and ground reaction forces (GRFs), respectively. However, alternative sensing technologies, such as inertial measurement units (IMUs), have also been used for their portability and ease of use in non-laboratory environments, as demonstrated in studies by Seel, Raisch, and Schauer [52] and Manz, Seifert, Altenburg, *et al.* [53].

The parameters are typically plotted against the percentage of the gait cycle, with 0% marking the initial heel strike of the reference limb. A wide range of biomechanical variables can be analysed, but joint kinematics, particularly knee angle, are among the most reported outcomes [50]. In addition to kinematic waveforms, spatio-temporal parameters and kinetic data such as GRF profiles are commonly extracted to provide a more comprehensive understanding of gait mechanics.

2.8.2. Spatio-temporal Parameters

The spatio-temporal parameters offer a different perspective on gait by describing the timing and distance-based characteristics of each walking cycle[14], [17], [50]. These include, but is not limited to:

- **Cadence**: the number of steps taken per minute.
- **Step length**: the distance between successive foot contacts of opposite limbs.
- **Stride length**: the distance between two successive contacts of the same foot.
- **Speed**: the overall walking velocity, typically in metres per second.
- **Swing time**: the time the foot is in the air during the gait cycle.
- **Stance time**: the duration for which the foot remains in contact with the ground.

These parameters are especially useful for identifying compensatory strategies, instability, or asymmetries in people using prosthetic devices.

2.8.3. Gait Symmetry

Gait symmetry is a fundamental measure in the assessment of gait performance, particularly in people with prosthetic limbs. It refers to the degree of similarity between the left and right limbs during walking[17], [54]. High symmetry is often associated with efficient, balanced and coordinated gait, while asymmetry can indicate compensatory movements, discomfort, or misalignment of the prosthesis.

There are multiple ways to characterise symmetry, depending on whether the data are scalar (e.g., step length) or time-series (e.g., joint angles over time). Two commonly used methods are the *Symmetry Index (SI)* for scalar variables and *cross-correlation* for waveform-based comparisons.

Symmetry Index (SI) Symmetry Index (SI) is a quantitative metric used to express the percentage difference between a corresponding parameter X of the left and right limbs. One commonly used formulation is as follows:

$$\text{SI} = \left| \frac{X_{left} - X_{right}}{0.5 \times (X_{left} + X_{right})} \right| \times 100$$

An SI value of 0% indicates perfect symmetry, while higher values reflect increasing asymmetry. This method has been extensively used in the literature to evaluate spatio-temporal gait parameters in prosthetic users [54]–[56].

Cross-correlation Cross-correlation is a mathematical method used to quantify the similarity between two time-series signals, making it particularly suitable for analysing gait waveforms such as joint angles, ground reaction forces (GRFs), or toe trajectories across the gait cycle[17], [57]. Cross-correlation captures the dynamic similarity between signals over time.

Given two discrete signals $x[n]$ and $y[n]$, representing, for example, the left and right limb trajectories, the normalised Pearson correlation coefficient r is defined as:

$$r = \frac{\sum_{n=1}^{N}(x[n] - \bar{x})(y[n] - \bar{y})}{\sqrt{\sum_{n=1}^{N}(x[n] - \bar{x})^2} \cdot \sqrt{\sum_{n=1}^{N}(y[n] - \bar{y})^2}}$$

where N is the number of samples in the gait cycle and $\bar{x}$ and $\bar{y}$ are the mean values of the respective signals.

This correlation coefficient r ranges from -1 to 1:

- $r = 1$: perfect positive correlation (identical waveform shape and timing),
- $r = 0$: no correlation,
- $r = -1$: perfect negative correlation (inverted waveforms).

One signal (e.g. the left parameter) is used as a reference while the other signal is swept across it. The correlation coefficient is calculated at each increment to determine at which offset the value of r is the highest. This offset is called the phase lag.

In gait analysis, high values of r, typically close to 1, will indicate a high degree of symmetry in the shape and timing of the waveforms.

Together, Symmetry Index and cross-correlation offer complementary perspectives: the former quantifies static asymmetry in scalar gait parameters, while the latter evaluates dynamic pattern similarity, improving the overall assessment of gait symmetry and prosthetic performance.

2.9. Design Frameworks for Cost-Effective Prosthetic Knees

This section outlines the design frameworks and considerations that guide the development of cost-effective prosthetic knees. The emphasis is on methods that allow for a clear evaluation of trade-offs between functionality, manufacturability, and affordability.

2.9.1. Biomechanical Modelling: Kinematics and Kinetics

Mathematical and computational models are used to estimate joint angles, moments, and loads during ambulation. Link-segment models help translate gait requirements into design targets, for example, range of motion and toe clearance. These models allow for the first feasibility screening for possible mechanisms and guide parameter ranges prior to physical prototyping, thus reducing the time and cost of iteration [1], [31], [33].

2.9.2. User-Centred Needs Assessment

Engaging end-users and clinicians (interviews, structured questionnaires) clarifies context-specific requirements such as stability expectations, terrain use and maintenance demands. These inputs inform design requirements and help resolve trade-offs (e.g. weight vs durability) to ensure the concept selected for prototyping aligns with real-world use [7], [8].

2.9.3. Prototyping and Feedback Loops

Early, low-cost prototypes (e.g. using 3D-printing methods) are used to verify fit, range of motion, and adjustability. Controlled user test-runs provide qualitative and quantitative feedback that refines the mechanism settings (e.g., locking threshold in the stance-phase, swing-phase damping level) before formal evaluation [7], [8].

2.9.4. Optimisation Methods for Geometry

Where appropriate, numerical optimisation is used to adjust geometric variables against multi-objective criteria (e.g., maximise toe clearance and stance stability, minimise stabilising hip moment). Optimisation reduces the iteration time to a feasible concept. [1].

2.10. Final Choice of Concept Solutions

The literature review focuses on the research challenges described in Chapter 1. The functionality and different types of prosthetic knees are discussed, together with design frameworks, appropriate material selection, and construction options. The modelling, simulation, and validation tools conclude.

The final choice of concept solutions for these RCs is laid out and discussed in the following subsections.

2.10.1. RC1: Type of knee and required functionality

It is evident that the knee mechanism has to facilitate stance phase-locking and swing-phase damping. In addition to this functionality, a mechanism that allows for increased ground clearance of the toes is also favourable. When the appropriate technology lens is applied, microprocessor knees are not applicable due to their high cost and maintenance complexity.

Concept solution: Therefore, this study focused on the design of a four-bar mechanism knee with a frictional damping component. With the correct geometry, this class of knees satisfied all the requirements as they were laid out. There are broadly three types of 4BM knees, namely: voluntary control, elevated ICR, and hyper-stable. Each has its own unique use case, and for the purposes of this study, a voluntary control variation was implemented due to its wide applicability.

2.10.2. RC2: Design considerations

The second research challenge overlapped somewhat with RC1. As stated previously, stance phase locking, swing phase damping, and ground clearance in the swing phase were all important factors. In addition, material selection was also crucial to balance cost, performance, and manufacturability. Other considerations included adjustable alignment and damping features, easily manufacturable and maintainable designs (simple geometry, standardised fasteners, etc.), low mass envelope and maximal range of motion.

2.10.3. RC3: Outcome measures

Gait symmetry is the core outcome measure that needs to be characterised in order to evaluate the prototype. To that end, the symmetry index and cross-correlation were used. The former was used to evaluate spatio-temporal metrics and the latter to evaluate wave form similarity. The spatio-temporal metrics that were evaluated are stride time, speed, cadence, stance time, swing time, and step length. The wave forms that were evaluated included the progression of the joint angle, as well as the hip angular velocity, the vertical ground reaction force, and the height of the toe.

2.10.4. RC4: Design tools

A link segment model was developed in MATLAB [58] and used to quickly evaluate prospective geometries in order to reduce the overall design iteration time, similar to the one used by Anand and Sujatha [1]. Furthermore, Siemens NX 2312[59] was used to model and simulate the mechanism with FEA used to ensure the structural validity of the design.

2.10.5. RC5: Testing methods

A gait trial case study with a single participant was used to gather data and evaluate the prototype. The participant conducted two separate gait trials: first with his current prosthetic knee (a microprocessor-controlled device) and second with the new mechanical prototype in which the microprocessor knee served as a baseline for comparison. The comparison between these two gave insight into the performance of the prototype, as well as highlighted possible improvements that could be made in future work.

3. Mathematical Modelling and Design

3.1. Introduction

This chapter provides an explanation of the research design, modelling framework, and verification plan used to develop and evaluate a voluntary-control four-bar mechanism prosthetic knee. Detailed component design and manufacturing are presented in Chapter 4, and the human case study protocol and analysis are presented in Chapter 5.

Fig. 3.1 shows the implementation aspects in Chapter 3 that contributed to the various concept solutions for the research challenges RC1, RC2 and RC4 (see Section 2.10).

Concept solutions	Four bar Knee	Defined design considerations	Symmetry of Kinematic and Spatio-temporal parameters	Link segment model, CAD,FEA	Gait trial
Chapter 3					
Defined Design requirements	↑	↑			
Link segment model				↑	

Figure 3.1. Implementation aspects in Chapter 3 that contributed to RC1, RC2 and RC4

3.2. Research Design

The research design adopted in this study follows an approach which integrates mathematical modelling, iterative prototyping, and empirical testing. The general objective is to design, manufacture and evaluate a cost-effective mechanical prosthetic knee that provides voluntary control, stability of stance, and adequate swing-phase behaviour. Therefore, this section outlines the systematic process through which the prototype was conceived, modelled, and verified.

3.2.1. Approach and Framework

The research approach is rooted in the principles of *Design Science Research* (DSR), supported by the *Quality Research Management* (QRM) framework introduced in Chapter 1. This framework ensures traceability between the research challenges (RCs), the design requirements, and the verification and validation methods used. The process was iterative: insights gained from simulations and prototype testing informed subsequent design refinements and additional rounds of testing.

3.2.2. Methodological Structure

The research was structured into three interrelated phases:

1. **Modelling and simulation phase:** Development of mathematical and kinematic models of the four-bar mechanism, including derivation of the hip-moment equation, vector loop equations, and flexion-factor analysis. MATLAB was used to simulate the kinematic behaviour and verify the results against a CAD motion model in Siemens NX 2312. The output of this phase was a MATLAB based design tool that allows the user to quickly iterate on link geometry and evaluate key features such as the ICR centrode and flexion factor profile.
2. **Prototype development phase:** The final geometry was selected on the basis of ICR and design metrics derived from the MATLAB model and prioritised voluntary control and mechanical simplicity. Following this, a prototype of the final design was built using locally accessible materials and processes. The deliverables of this phase were the functional prototype and the documentation of material selection, part drawings, and the manufacturing procedure.
3. **Evaluation phase:** Verification and validation of design performance through human gait testing. The gait trial compared kinematic and spatio-temporal parameters, such as knee flexion angles, swing-phase duration, and toe clearance, between the prototype and a microprocessor reference knee. The deliverables of this phase were the gait analysis data and a functional performance evaluation report for the prototype.

3.2.3. Data Collection and Analysis Plan

Data were obtained from both simulation output and human gait trials. Simulation data included ICR trajectories, flexion factors, toe clearance, and joint force estimates. The experimental data consisted of joint-angle profiles, stride parameters, and derived symmetry metrics. The results of both sources were comparatively analysed to determine whether the design met the defined functional requirements. Quantitative metrics, including the Symmetry Index (SI) and waveform cross-correlation, were used to evaluate gait similarity between prosthetic and sound limbs.

3.3. Design Methodology

The design methodology used was as follows:

1. **Requirements Definition:** Defined the design parameters identified in Chapter 2 and described the primary design lever for each requirement.
2. **Mathematical modelling:** Described the modelling approach and equations related to the modelling of the knee mechanism.
3. **Force simulations:** Siemens NX motion simulations were used to determine the forces acting on the joints and links.
4. **Dimensioning and Component Sizing:** The geometry of components, materials, fasteners, and tolerances was determined through the lens of design for manufacturability. This involved the sub-loop of the following steps:

- **Iterative design and review:** Consulted with the supervisors and workshop technicians on design choices and made changes accordingly.
- **Rapid prototyping:** 3D printing technology was used to verify fit, form, and function of the components and mechanism.
- **Detail design / Finite Element Analysis:** Ensure that the detail design configuration as it was developed was structurally sound.

3.3.1. Functional Requirements Definition

Table 3.1 lists the requirements related to the design of a prosthetic knee. These requirements were adapted from [1], [7], [12], as well as from an engineer who personally uses a prosthetic limb[60]. This process provided a combination of both technical and user-centred perspectives.

Table 3.1. Functional requirements for prosthetic knee design

ID	Requirement Name
1	Stance-phase stability
2	Swing-phase toe clearance
3	Physiological range of motion
4	Gait symmetry
5	Mass of prosthesis
6	Structural strength to support specified user mass
7	Adjustability and alignment
8	Manufacturability and cost
9	Serviceability and maintainability

1. **Stance-phase stability:** The knee must maintain mechanical stability when the ground reaction force vector passes anteriorly relative to the knee joint. This ensures safe weight bearing during stance without unintended flexion or collapse. The primary design lever used to achieve this is the link geometry.
   Acceptance criterion: No uncontrolled flexion during stance phase under bodyweight at self selected walking speed.
2. **Swing-phase toe clearance:** Adequate shortening of the shank during flexion is required to prevent toe scuffing or hip hiking. The geometry of the linkage will be the primary design lever to increase ground clearance while maintaining smooth motion.
   Acceptance criteria: No visible toe scuffing during gait trials. Average minimum toe height during swing-phase is greater than healthy limb. Greater or equal minimum toe clearance than comparable commercial 4BM knee.
3. **Physiological range of motion:** The mechanism must provide sufficient flexion and extension to allow normal gait while preventing hyperextension. The device must also have minimum flexion of 90° . Range of motion limits will be verified in simulation and physical testing.
   Acceptance criterion: Range of motion must not be limited by the knee mechanism itself, but rather by interference with the socket.
4. **Gait symmetry:** The prosthetic should promote balanced motion between limbs, reducing compensatory movements and energy expenditure.
   Acceptance criterion: Gait symmetry will be evaluated using symmetry index and cross-correlation metrics and should be within acceptable limits.

5. **Mass of prosthesis:** The total weight of the knee should be less than 2.27 kg to minimise metabolic cost and improve comfort[7]. The use of lightweight materials and compact geometry will be prioritised to achieve this goal.
   Acceptance criterion: Weighing the prototype should indicate a mass below 2.27 kg.
6. **Structural strength to support specified user mass:** Must be able to support an individual weighing 150 kg (similar to the Ottobock Genium X3[61]). All components must withstand expected loads during walking with an adequate safety factor.
   Acceptance criterion: Finite element analysis (FEA) to confirm structural strength.
7. **Adjustability and alignment:** The design must allow for easy adjustment of damping, alignment, and fit using simple tools.
   Acceptance criterion: Adjustment ranges should accommodate user variability and alignment tuning during fitment.
8. **Manufacturability and cost:** All components must be manufacturable with locally available materials and standard processes to reduce cost. Design for Manufacture and Assembly (DfMA) principles will guide simplification.
   Acceptance criterion: The cost of materials and manufacturing should not exceed R25 000 during prototyping.
9. **Serviceability and maintainability:** Key parts should be easily accessible and replaceable to extend product life and facilitate local repair.
   Acceptance criterion: Confirm use of modular components and standardised fasteners incorporated in the design to support long-term maintainability.

Table 3.2. Verification Matrix

ID Requirement	Simulation Check	Case Study
1. Stance-phase stability	Flexion factor < 0 at heel strike	No buckling during tests
2. Swing-phase toe clearance	Minimum toe clearance $\geq$ commercial 4BM	Average minimum toe height during swing-phase $\geq$ healthy leg
3. Physiological range of motion	Design tool measurement $> 90°$	Physical prototype ROM testing $> 90°$
4. Gait symmetry	NA	Symmetry index / cross-correlation for key parameters
5. Mass of prosthesis	CAD assembly calculation of mass	Mass of prototype $< 2.27kg$
6. Structural strength	FEA analysis shows safety factor > 3	No structural failure during tests
7. Adjustability and alignment	NA	Participant can modify damping/ adaptor location/alignment
8. Manufacturability and cost	NA	Cost $<$ R25000
9. Serviceability and maintainability	NA	Reflective evaluation of design components used

3.3.2. Verification Matrix

The design requirements listed in Table 3.1 need to be verified once the physical design has been completed. Table 3.2 summarises the acceptance strategies described in Section 3.3.1 to verify that the prototype meets the design requirements before functional testing and validation can begin with the human gait trail case study.

3.4. Mathematical Modelling of 4BM Polycentric Knee

This section details how the hip moment and the vector loop equations were derived and used to describe the geometry of a 4BM polycentric knee. These equations formed the basis on which the design tool was built.

3.4.1. Biomechanics Equations

Kinematics

Understanding biomechanic kinematics is crucial to designing an effective knee prosthesis. This section is divided into two main parts: the hip moment equation and the vector loop equations. The hip moment equation forms an integral part of the knee prosthesis design process, allowing the designer to accurately estimate the moment required by the amputee's hip to voluntarily control the prosthesis throughout the flexion range. Vector loop equations, on the other hand, are used to solve the positions of the links of the four-bar mechanism. Together, these two sets of equations determine the critical functional character of the knee, as reflected in the functional requirements ID1, ID2, and ID3 from Table 3.2.

Derivation of the hip moment equation

The hip moment equation is fundamental for estimating the moment required by the amputee's hip to control the prosthesis throughout the flexion range accurately. This enables the designer to ensure the stability and functionality of the prosthesis. Fig. 3.2 illustrates the forces and moments acting on a prosthetic knee, along with Table 3.3 that summarises the symbols used in the equations, with their descriptions.

Table 3.3. Summary of symbols and descriptions

Symbol	Description
P	Axial load force along the hip-heel direction.
M_h	Extension moment about hip joint on the amputated side. The anticlockwise direction is positive.
M_k	Brake moment supplied by the knee mechanism. Anticlockwise direction is positive.
S	Shear force at heel contact.
L	Distance between hip joint and heel contact.
y	Distance between centre of rotation and heel contact.
x	Perpendicular distance between load line and centre of rotation.

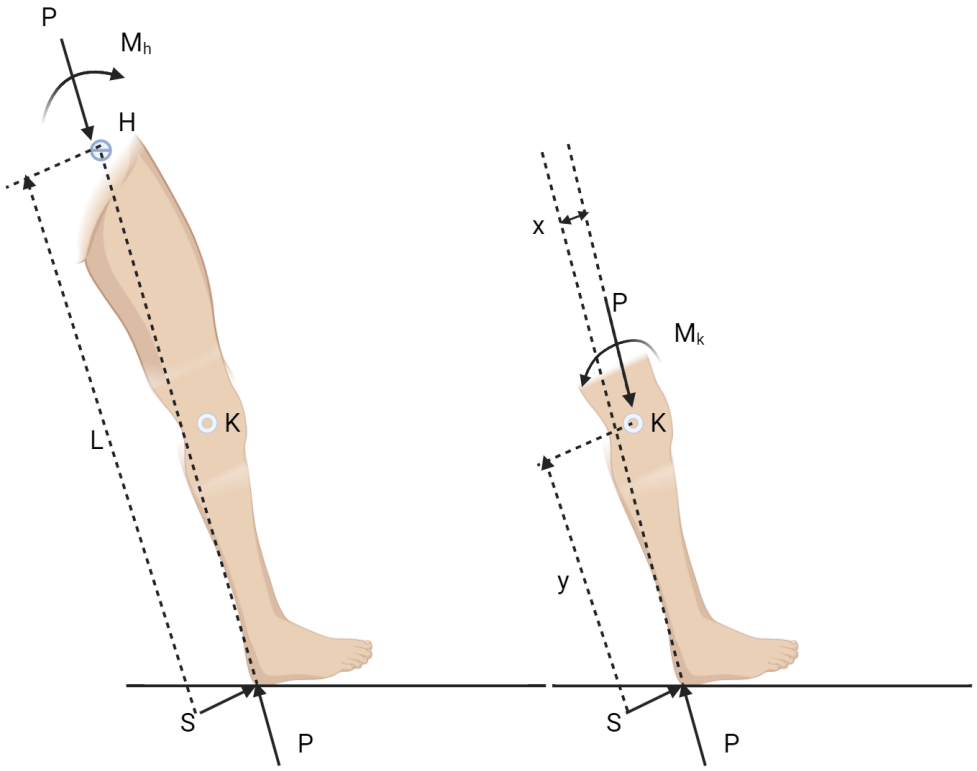

Figure 3.2. Illustration of the forces and moments acting on the prosthetic knee during stance phase adapted from [39]

1. Sum of moments around the hip:

$$-M_h + SL = 0 \tag{3.1}$$

2. Solve (3.1) for the heel shear force:

$$S = \frac{M_h}{L} \tag{3.2}$$

3. Sum of moments around the knee:

$$Sy - Px + M_k = 0 \tag{3.3}$$

4. Substitute (3.2) into (3.3) :

$$\left(\frac{M_h}{L}\right) y - Px + M_k = 0 \tag{3.4}$$

5. Solve for the hip moment M_h required to maintain a stable knee in full extension:

$$M_h = \left(\frac{L}{y}\right)(Px - M_k) \tag{3.5}$$

6. For most four-bar mechanisms there is no knee braking moment ($M_k = 0$), therefore (3.5) reduces to:

$$M_h = (PL)\left(\frac{x}{y}\right) \tag{3.6}$$

where $\frac{x}{y}$ is called the *Flexion Factor* [39].

Vector loop equations

The vector loop method is used to analytically describe the positions of the 4BM links in relation to each other. In order to use this method, all the link lengths as well as two out of the four angles need to be known. (As part of a design routine, the lengths of the links are initially estimated together with the starting angles. The mechanism's locus of motion is then evaluated against the acceptance criteria and geometric parameters adjusted if needed.)

Fig. 3.3 illustrates the coordinate system and the naming convention that will be used throughout this section. It also shows the position of the ICR (see 3.6.1).

OC with length d acts as a ground link and forms an angle θ_1 with the horizontal. The shank (ankle and foot) will be attached to the link OC at some location along its length. The link OA with length a is the floating link and is at an angle θ_2 with horizontal. AB with length b is connected to the bottom of the prosthetic socket and forms the input link, sometimes referred to as the crank, and has an angle θ_3 with horizontal. BC is the fourth link and connects the socket link to the shank link. It is at an angle θ_4 to the horizontal and has a length of c.

As stated previously, in order to resolve the vector loop equations, the link lengths and two of the four angles need to be known. In this case, the specified angles are θ_1 and θ_3. These angles can be taken as known values since they are initially determined by the posture of the leg and knee and the fit of the prosthetic.

To resolve the unknown angles θ_2 and θ_4 in Fig. 3.3, the vector loop equations are used as follows, considering fundamental geometric relationships.

$$\overrightarrow{OA} + \overrightarrow{AB} = \overrightarrow{OC} + \overrightarrow{CB} \tag{3.7}$$

The components of the vector distances on the x-axis must sum to zero for the vector loop:

$$-a\cos\theta_2 - b\cos\theta_3 + d\cos\theta_1 + c\cos\theta_4 = 0 \tag{3.8}$$

Similarly, for the components on the y-axis:

$$-a\sin\theta_2 - b\sin\theta_3 + d\sin\theta_1 + c\sin\theta_4 = 0 \tag{3.9}$$

Rearranging the vector loop equations gives the following equations to solve for θ_2 [5]:

$$\theta_2 = 2\tan^{-1}\left(\frac{-B \pm \sqrt{B^2 - 4AC}}{2A}\right) \tag{3.10}$$

Where A, B and C are given by:

$$A = \frac{a^2 + b^2 - c^2 + d^2}{2ab} - \frac{d(\cos(\theta_1)\cos(\theta_3) + \sin(\theta_1)\sin(\theta_3))}{a} - \cos(\theta_3) + \frac{d\cos(\theta_1)}{b} \tag{3.11}$$

$$B = 2\left(\sin(\theta_3) - \frac{d\sin(\theta_1)}{b}\right) \tag{3.12}$$

$$C = \frac{a^2 + b^2 - c^2 + d^2}{2ab} - \frac{d(\cos(\theta_1)\cos(\theta_3) + \sin(\theta_1)\sin(\theta_3))}{a} + \cos(\theta_3) - \frac{d\cos(\theta_1)}{b} \tag{3.13}$$

Similarly, the following equations to solve for θ_4 can be defined [5]:

$$\theta_4 = 2\tan^{-1}\left(\frac{-E \pm \sqrt{E^2 - 4DF}}{2D}\right) \tag{3.14}$$

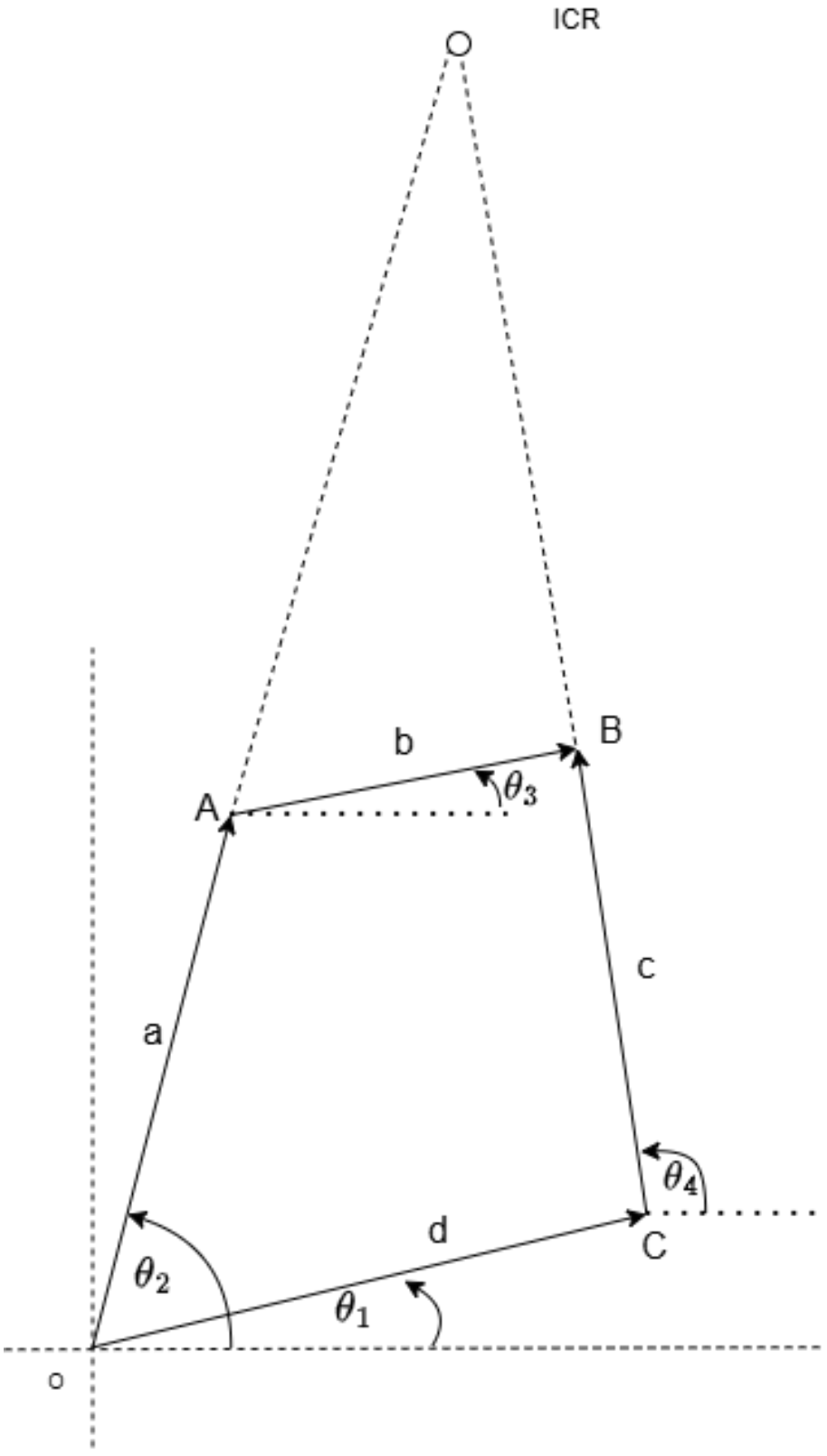

Figure 3.3. Coordinate system that will be used for vector loop equations

Where:

$$D = \frac{b^2 - a^2 + c^2 + d^2}{2bc} - \frac{d(\cos(\theta_1)\cos(\theta_3) + \sin(\theta_1)\sin(\theta_3))}{c} - d\cos(\theta_1) + b\cos(\theta_3) \tag{3.15}$$

$$E = 2\left(\frac{d\sin(\theta_1)}{b} - \sin(\theta_3)\right) \tag{3.16}$$

$$F = \frac{b^2 - a^2 + c^2 + d^2}{2bc} - \frac{d(\cos(\theta_1)\cos(\theta_3) + \sin(\theta_1)\sin(\theta_3))}{c} + \frac{d\cos(\theta_1)}{b} - \cos(\theta_3) \tag{3.17}$$

Note that the radical $\pm$ in the equations for θ_2 and θ_4 means that there are two solutions and that they can be of three types: real and equal, real and unequal or complex and conjugate. The numerical solution procedure therefore needs to make provision so that only real solutions are considered (other solutions will give unphysical results).

In the following sections, the iterative numerical design process using a MATLAB implementation is explained in more detail, where it will be shown how the link geometry and design requirements come together in order to evaluate the practicality of design parameters.

3.5. Proposed link geometry

The MATLAB code developed in the current study is called "4BM Design Tool", and an extensive design investigation resulted in the link lengths and initial angles listed in Table 3.4. These values were selected because they meet the criteria for a voluntary control knee. They were adapted from a study by Vintimilla Leon, Ferrandiz Bou, Cobos Maldonado, *et al.* [5] and are close to the requirements for a voluntary control four-bar mechanism as laid out by [28].

The original specification suggested by [5] was that the initial position of the ICR is approximately 6 mm behind the alignment reference line (ARL; the vertical line that connects the hip and ankle, see Fig. 3.4) and about 100 mm above the cosmetic centre of the knee. In this case, the coordinates are $X = -7.56$ mm and $Y = 137.34$ mm. Note that the dimensions were simplified to facilitate the manufacturing process.

Table 3.4. Proposed link geometry obtained from the 4BM Design Tool

Parameter	Value
OA [mm]	66
AB [mm]	30
BC [mm]	56
OC [mm]	45
θ_1 [°]	26
θ_3[°]	18

3.6. MATLAB implementation of 4BM Design Tool

The complete MATLAB implementation of the 4BM Design Tool is provided in Appendix A (see listings A.1 and A.2).

In order to design a four-bar mechanism knee prosthesis, certain characteristics and dimensions must be defined and standardised. Fig. 3.4 shows these dimensions and is the same as is used

by Radcliffe [28] and Anand and Sujatha [1]. The cosmetic knee centre (point B, Fig. 3.3) is on the horizontal axis 500 mm above the ankle. The hip is located 450 mm above the centre of the knee and vertically above the ankle. The heel is 50 mm behind the alignment reference line and the toe is located 200 mm in front of the ARL.

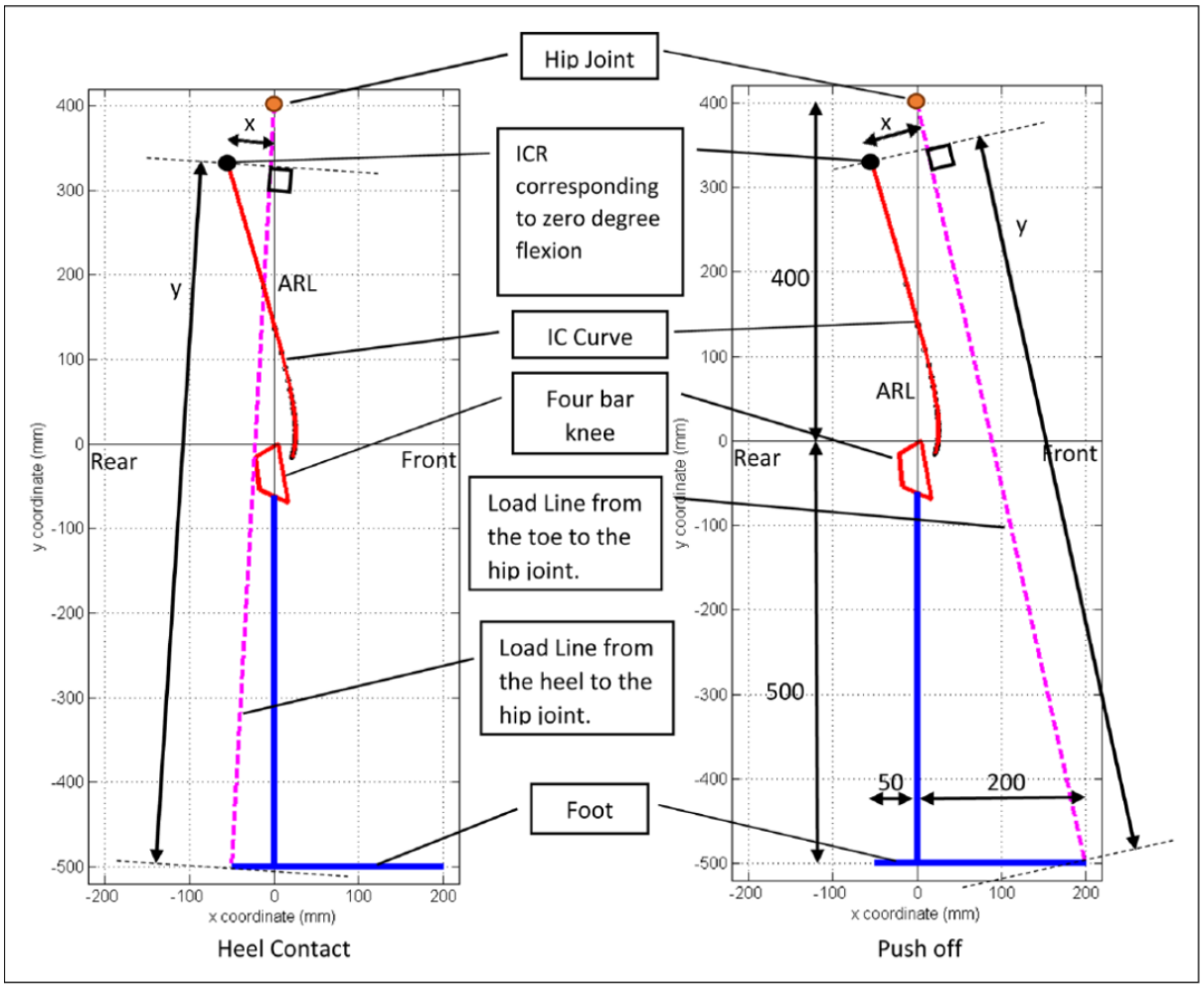

Figure 3.4. Standard Prosthesis Dimensions [1]

3.6.1. Instantaneous Centre of Rotation

The Instantaneous Centre of Rotation (ICR) is located at the intersection of the lines that are perpendicular to the tangential velocity vectors of the links OA and BC (Fig. 3.3). This is equivalent to extending the direction vectors of these links and determining their point of intersection. Perform this calculation through the flexion range to determine the centrode[1] of the four-bar mechanism, which for this configuration of link lengths and angles can be seen in Fig. 3.5a. The ICR centrode is one of the key functional design features of a 4BM knee and is used to determine various important factors such as the hip moment, the flexion factor, and it also governs the stability of the knee in the stance phase (see Fig. 3.5b). The different link lengths and initial angles greatly affect the shape of the centrode and therefore ultimately how the knee functions during use [28].

To verify the accuracy of the MATLAB implementation and ICR calculation, the four-bar mechanism was also recreated in the Siemens NX 2312 assembly environment and the centrodes

[1]The centrode is the path traced by the instantaneous centre of rotation as it moves in the plane of the knee.

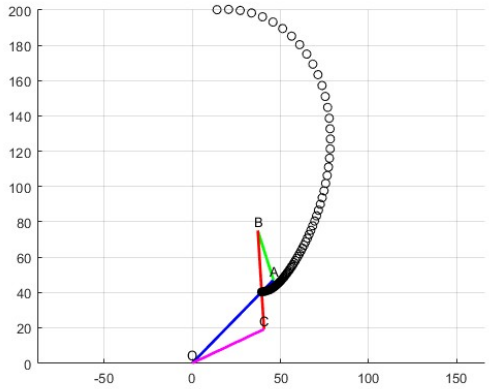

(a) Plot of Instantaneous Centre of Rotation centrode

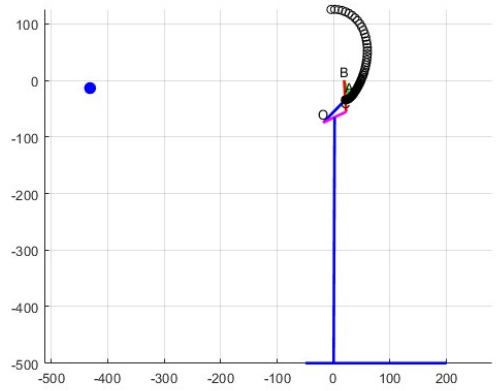

(b) Plot of Instantaneous Centre of Rotation centrode in relation to the rest of the leg

Figure 3.5. Instantaneous centre of rotation centrode plots for full range of knee motion.

of the two methods were compared. The NX geometry and ICR centrode can be seen in Fig. 3.6a and the comparative plots between NX and MATLAB in Fig. 3.6b. It can be seen that the shape of the centrodes are virtually indistinguishable and therefore the the accuracy of the MATLAB implementation is verified.

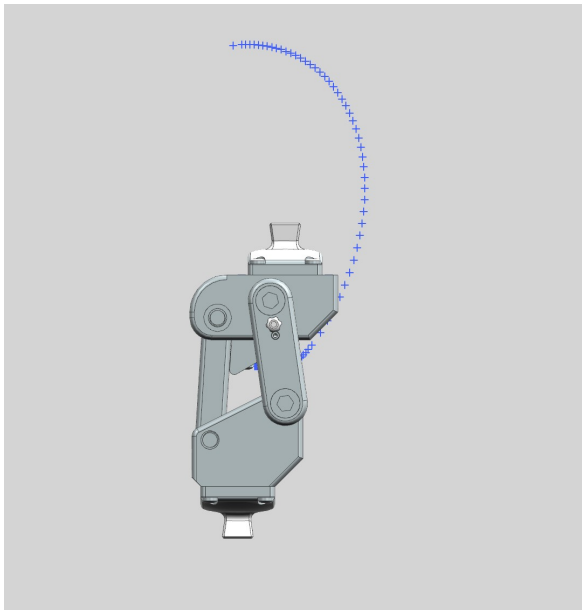

(a) Shank centrode in Siemens NX

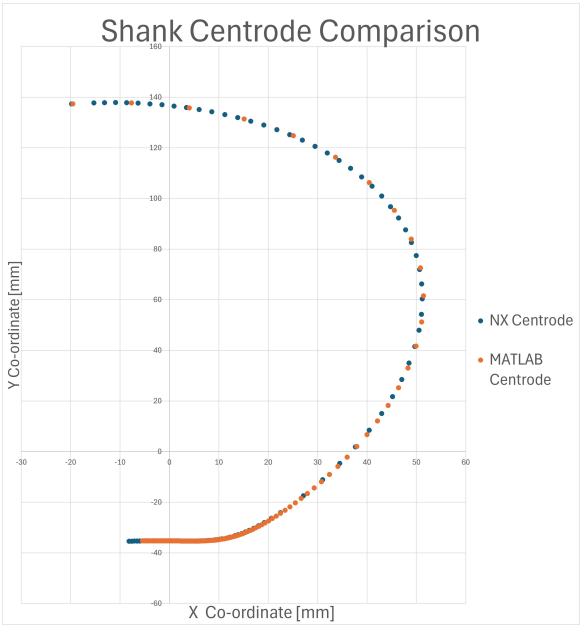

(b) Shank centrode verification

Figure 3.6. Validation of MATLAB ICR calculation and Siemens NX reconstruction. The MATLAB implementation was verified by comparing ICR coordinates to a Siemens NX assembly reconstruction.

3.6.2. Flexion Factor

The flexion factor is a metric that is used as a proxy to determine the hip moment required to stabilise the knee or flex the knee voluntarily through the knee flexion range. It is the ratio x/y where x is the perpendicular distance between the load line, L, and the ICR and y is the distance between ICR and the centre of pressure (CP).

The flexion factor therefore depends on the location of the centre of pressure (either heels strike or toe off). To achieve stability at heel strike (thus zero Knee Flexion angle), the flexion factor must be negative, while to initiate the swing phase with minimal hip moment, it should approach zero at toe off. For the current geometric configuration, the flexion factor was -0.02, which is an acceptable value for both heel strike and toe off (refer to the coordinate at zero flexion angle in Fig. 3.7).

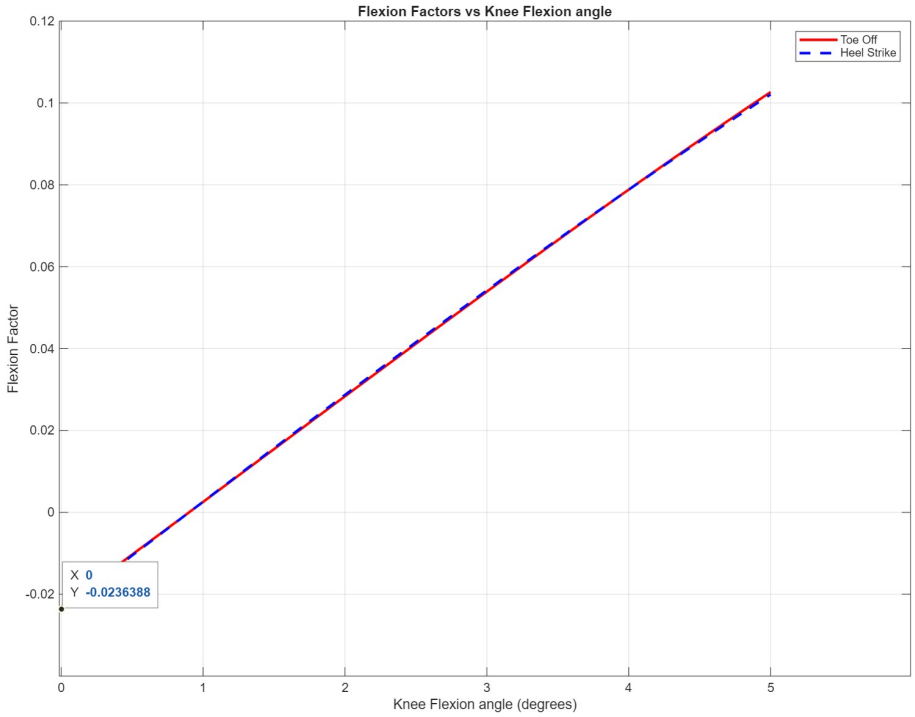

Figure 3.7. Flexion factor vs Knee Flexion angle over 5°

3.6.3. Toe clearance

Due to the nature of a four-bar mechanism (4BM), the overall length of the prosthetic knee shortens and lengthens as the knee flexes and extends, respectively. This is advantageous as it reduces the likelihood of tripping or stumbling over small obstacles or uneven terrain. According to [39], the socket centrode provides a more informative insight into swing-phase behaviour and can thus be used to calculate certain design metrics.

The socket centrode is calculated by keeping the hip stationary while the knee flexes, and the shank centrode is determined by keeping the foot stationary while the knee flexes. Fig. 3.8a shows the configuration for the socket centrode. The red dot indicates the toe, while the blue dot indicates the hip. In Fig. 3.8b the socket centrode can be seen in full flexion.

The minimum clearance during walking of the toe occurs when the hip is flexed at 23° and the knee is flexed at 49° [1]. Figure 3.9a shows the setup to calculate the minimum clearance for the toe. The ground line is rotated 23° about the hip to simulate the appropriate hip flexion, and the knee is flexed 49°. The perpendicular distance between the toe and the ground line is 2.87 mm above the ground line for this configuration (see Fig. 3.9b).

It can be seen that in 3.9b there are values lower than 2.78 mm during the simulated motion. This is because the motion produced in the model is not of a full gait cycle but simply a flexion of the knee while the hip remains stationary. In normal walking, the hip and knee flex at the same time, leading to a different foot trajectory and therefore a different global minimum

toe clearance value. The hip and knee angles that produce the minimum toe clearance in the literature are for walking, while the model isolates the effect of the knee mechanism.

This is an improvement compared to both the Ottobock 3R36 (2.4 mm below ground line), the Ottobock 3R70 (2.8 mm below ground line), and the Provetal knee (2.2 mm above ground line) but not compared to the Ottobock 3R55 (19.4 mm above ground line) [1]. The IITM knee developed by Anand and Sujatha [1] also performed better with 11 mm above the ground line.

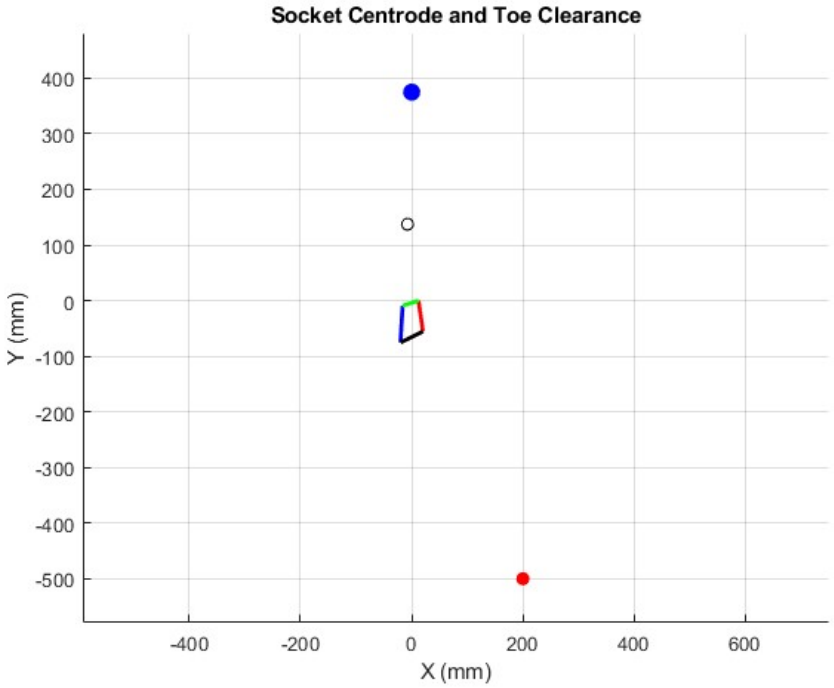

(a) Socket centrode setup

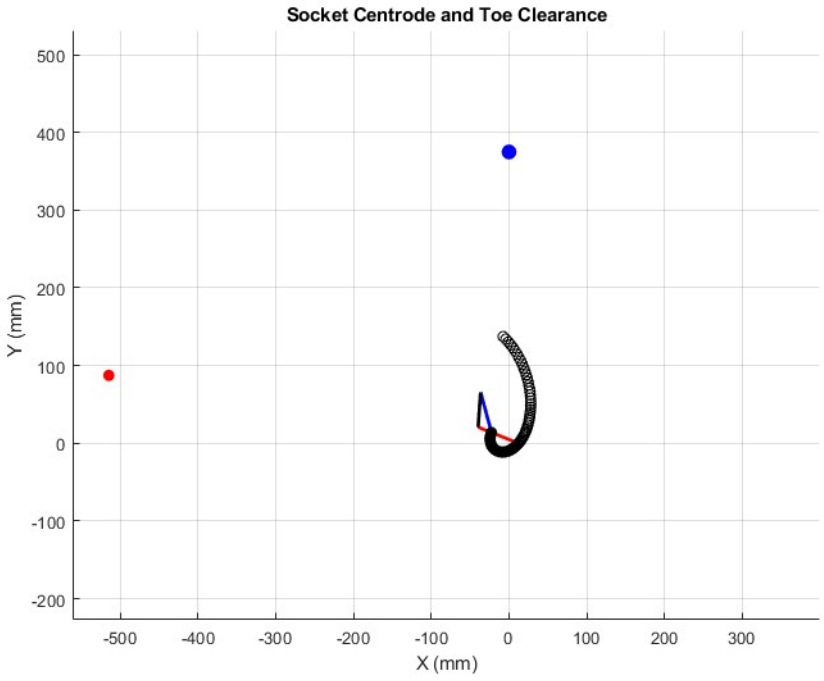

(b) Socket centrode at full flexion (120°)

Figure 3.8. Evaluation of toe clearance and socket centrode motion during knee flexion. (a) shows the socket centrode setup, (b) is the centrode at full flexion. The red dot indicates the toe, while the blue dot indicates the hip.

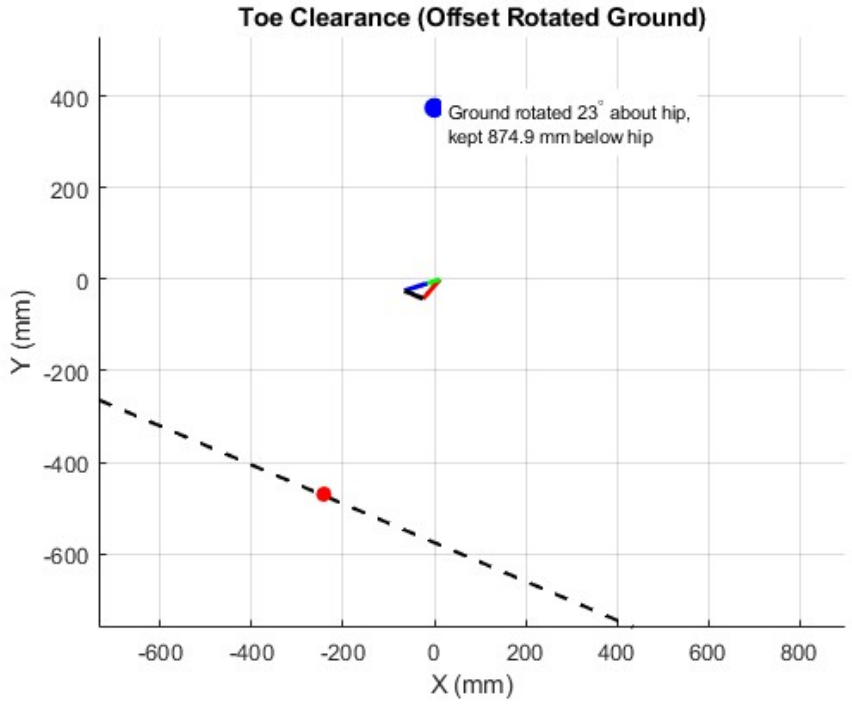

(a) Minimum toe clearance

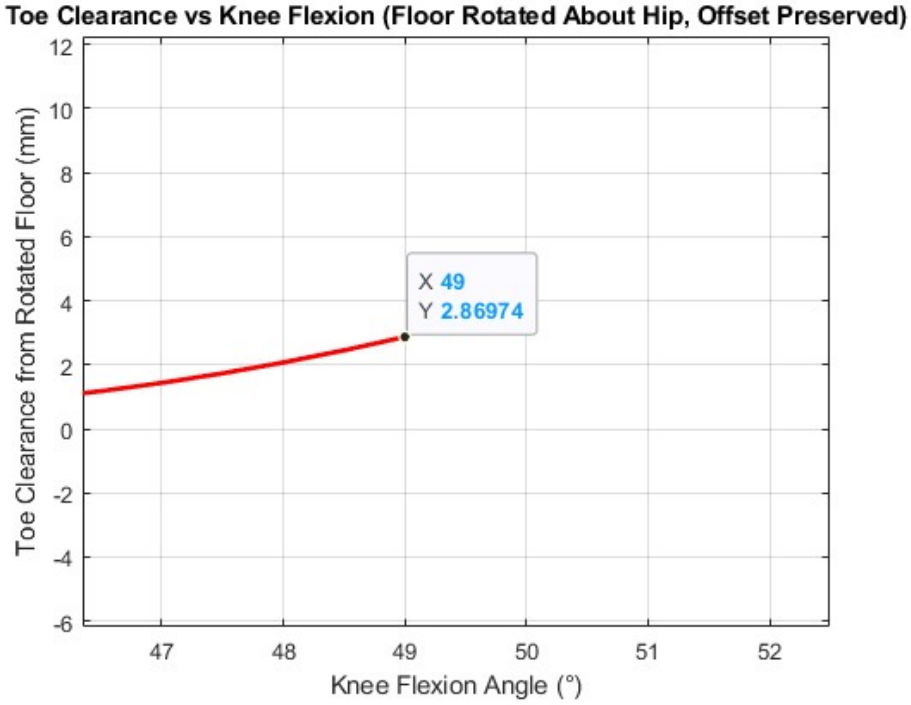

(b) Minimum toe clearance plot

Figure 3.9. Calculating the minimum toe clearance. The red dot indicates the toe, while the blue dot indicates the hip.

3.6.4. Range of Motion

The range of motion (ROM) of the knee is another key characteristic of the design. Sufficient ROM is necessary to facilitate any motion, for example, kneeling, entering and exiting vehicles, and sitting down, among other activities. Maximum possible knee flexion is the angle at which the pylon on the shank or the mechanism itself comes into contact with the socket. To incorporate this effect in the numerical model, a reference socket was added to the 4BM model as a circle with radius 60 mm with its centre 20 mm in front and 80 mm above point B (the cosmetic centre of the knee) [1]. The resultant plots for this setup are shown in Fig. 3.10. The maximum knee flexion achieved with the current link geometry was 127.8°, which was more than satisfactory for performing the activities listed above.

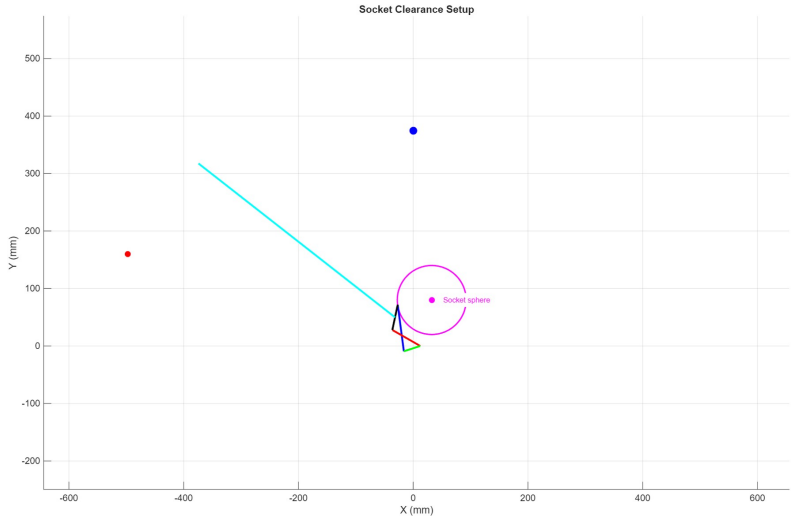

(a) Socket Clearance Setup

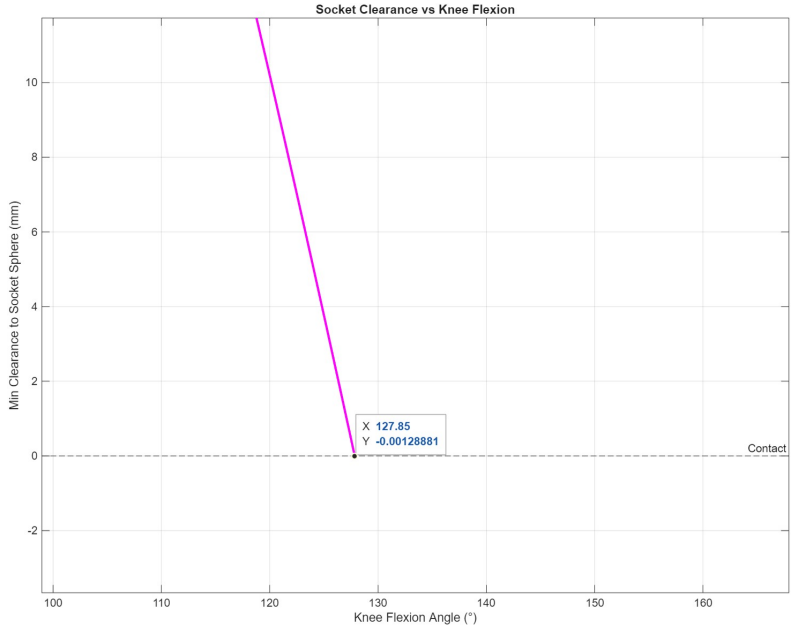

(b) Socket Clearance Plot

Figure 3.10. Range of motion determined by the maximum knee flexion. (a) shows the setup for determining the maximum Knee Flexion of this mechanism with a reference socket. (b) shows that the four bar mechanism contacts the reference socket at about 127.8 degrees of flexion

3.6.5. Relationship between design parameters and performance

All of the parameters stated thus far are a function of the link lengths and angles and are therefore derived metrics to assess the proposed geometry for suitability. As discussed in2.4.3, different geometry can have significant impact on the type of 4BM knee, and subsequently the use case and performance of the device. A longer anterior link, in this case it is link BC, will tend to move the ICR posteriorly. This is typical of hyper stable configurations and will increase stance phase stability by promoting extension under load but can also increase the required hip-moment to initiate the swing phase, which in turn can lead to gait deviations. In contrast, if the ICR is positioned more anteriorly, the transition to swing phase will be smoother but at the cost of early stance phase stability. Since the ICR path and flexion factor are defined by the link geometry, any changes in link lengths or pivot locations directly modify them. Similarly, changing the geometry also necessarily alters the flexion path of the knee, and therefore, also alters the ground clearance and range of motion. The design process becomes a multi-variable optimisation problem where link dimensions must be selected to find the right balance between competing performance metrics. This being the case, thoughtful designers will need to alter the geometry for the specific use case as specified in 2.4.3.

3.7. Final parameters from the 4BM Design Tool

Table 3.5 summarises the final design parameters that were calculated for the knee mechanism, as well as the derived parameters that were determined from the final geometry.

These parameters were used in the prototype development phase discussed in Chapter 4.

Table 3.5. Final knee parameters calculated with the 4BM Design Tool

Parameter	Unit	Value
Link OA	[mm]	66
Link AB	[mm]	30
Link BC	[mm]	56
Link OC	[mm]	45
θ_1	°	26
θ_2	°	86.6
θ_3	°	18
θ_4	°	104.5
Flexion Factor at Heelstrike	Ratio	-0.02
Flexion Factor at Toe -off	Ratio	-0.02
ICR Co-ordinates at full extension	[mm]	[-7.56,137.34]
Min toe clearance	[mm]	2.87
Maximum Knee flexion	°	127.8

4. Prototype Development

4.1. Introduction

This chapter focusses on the development process of the prototype knee prosthesis. Geometry design, component design trade-offs, material selection, FEA analysis, manufacturing, and assembly are all discussed here.

Fig. 4.1 shows the implementation aspects in Chapter 4 that contributed to the various concept solutions for the research challenges RC1, RC2 and RC4 (see Section 2.10).

Concept solutions	Four bar Knee	Defined design considerations	Symmetry of Kinematic and Spatio-temporal parameters	Link segment model, CAD,FEA	Gait trial
Chapter 4					
Prototype design	↑			↑	
Strength analysis		↑		↑	
Feature implementation		↑			
Manufacturing	↑	↑			

Figure 4.1. Implementation aspects in Chapter 4 that contributed to RC1, RC2 and RC4

Scope and Intent of Prototype Development Phase

The main objective of this phase was to confirm the validity of the design process and assess the functional performance of the four-bar knee prototype, but without aiming at complete mechanical optimisation. With this in mind, the design choices were centred on practicality, ease of manufacturing, and verification of motion behaviour, rather than focusing on detailed shape and mass optimisation. As a result, finite element analysis and static load evaluations focused on the failure assessment of critical structural components. This approach was sufficient to ensure safe operation during the controlled case study testing, but did not extend to demonstrate compliance with the full structural and fatigue assessments of ISO10328.

4.2. Design cycle

The design cycle was iterative and its implementation process can be seen in Fig. 4.2. As soon as the design met the fit, form and function requirements, the continuation of design iterations was stopped.

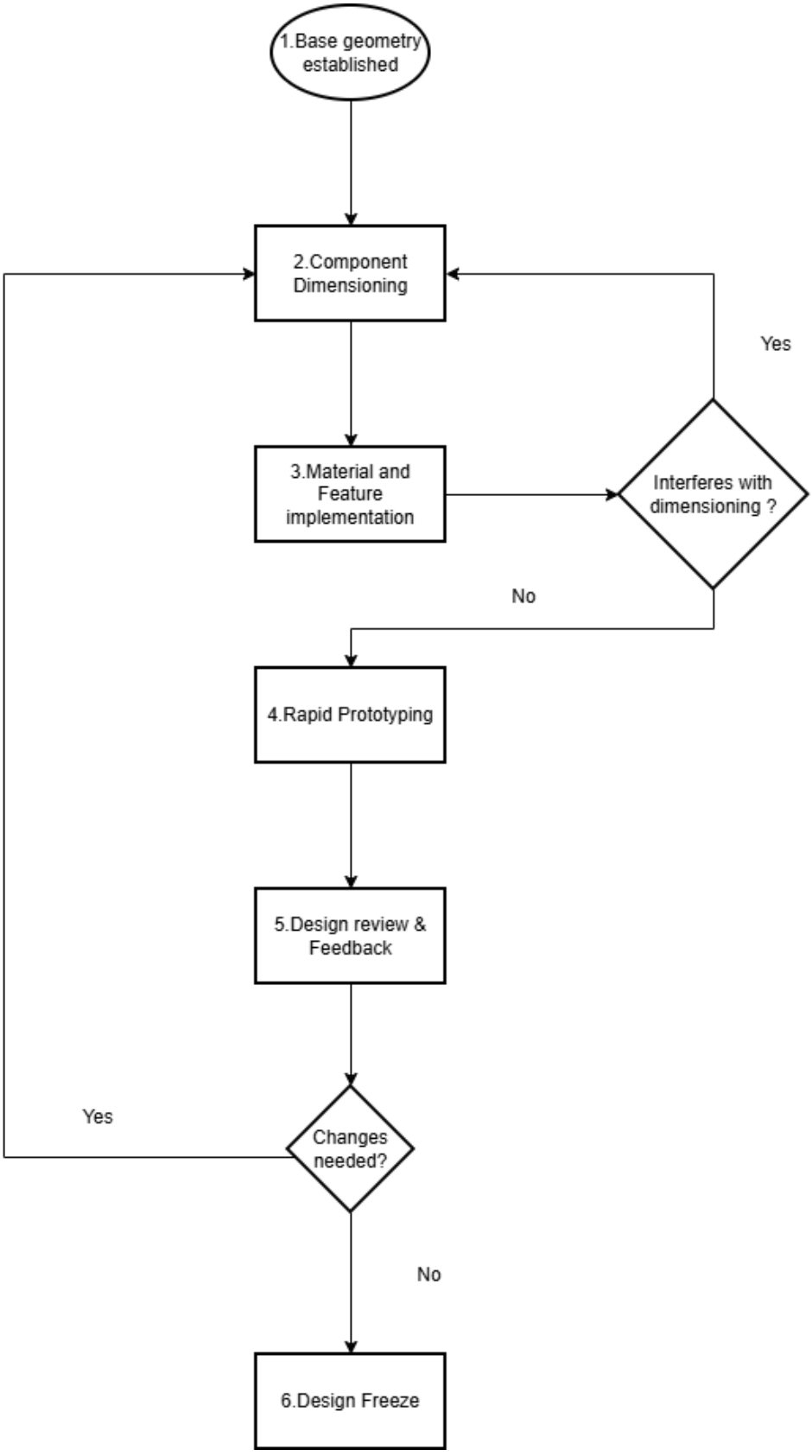

Figure 4.2. Design process flow diagram

1. **Baseline geometry established:** The base geometry of the link lengths and angles was defined in Chapter 3 served as a starting point for the design.
2. **Component Dimensioning:** Estimate/ calculate/ simulate forces and define and refine link thicknesses, joint diameters, fastener types and tolerances. Do hand calculations/ FEA to verify stresses and deflections. Adjust for manufacturability and available materials.
3. **Material and feature implementation:** Select the appropriate materials for the component and implement features such as the friction damping mechanism and adjustable mounting interfaces. If features interfere with step 2, revise the dimensioning.
4. **Rapid Prototyping:** Fabricate prototypes using an Raise 3D Pro3+ FDM 3D printer [62] to assess fit, form, and function. This includes tolerances at shafts/bushings, range of motion, and interfaces with the shank and socket.
5. **Design review and feedback:** Consult with peers about design decisions and implement changes by repeating steps 2 to 5 if necessary.
6. **Design Freeze:** Once the design satisfies the criteria of fit, form, and function, the iterative process is terminated. This decision is grounded in the necessity to prevent an endless cycle of modifications. Given the inherent time limitations of the study, it is not practical to allocate more time than necessary to further refine the design. While more iterations could have refined component geometries or mass distributions further, the design cycle was stopped once the design was deemed adequate for functional evaluation. The intent of this study was to demonstrate viability and validate the design process for a cost-effective prosthetic knee, not to optimise the mechanical design. That optimisation will be appropriate in future work or in a commercialisation phase.

4.3. Forces acting on links and joints

According to ISO Standard 10328:2016, a prosthetic should withstand a maximum static load of 4130N without the maximum stress exceeding the material yield stress [45], [63].

To determine the forces that act on the joints, an NX Motion simulation was developed. The revolute joints were placed in pivot locations on the left and right side of the knee (eight in total). FEA was then used to evaluate the stress and deformation of the components under this force. Fig. 4.3 shows the setup of the links and joints in the NX Motion environment, and Fig. 4.4 shows where the downward vector force was applied.

The maximum load case considered for static safety was that when the full static load of 4130N, as outlined in ISO 10328, was applied directly downward with the knee in a locked position (thus the full stance phase). During the swing phase, when the knee is open, the only weight acting on the joint is that of the prothetic and shank, which is much less than the maximum static load, even accounting for changes in the moment arms and force vector components.

Fig. 4.5 shows the joint forces resulting from the applied static force, with a result of 2300N for the anterior and 1900N for the posterior joints.

The goal of prototype development was to provide controlled functional validation, not full certification testing. As a result, it was sufficient that only these joint loadings were used for subsequent FEA simulations, while other tests, such as the cyclic loading and torsional tests, were omitted.

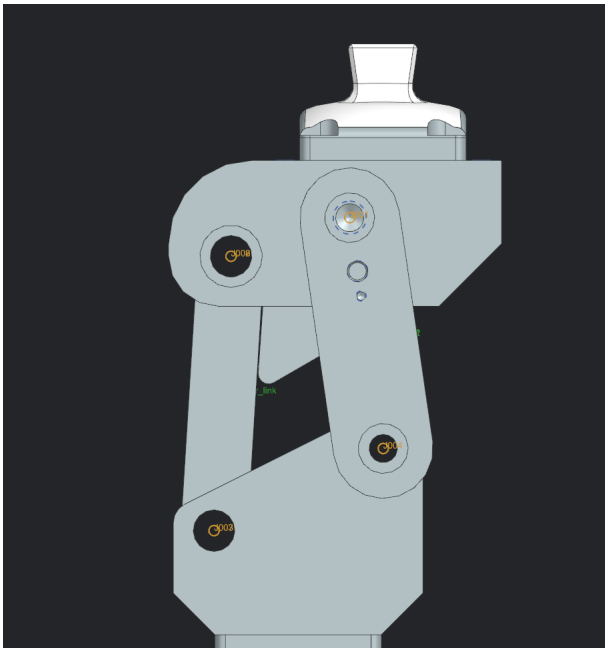

Figure 4.3. NX Motion Simulation Setup showing link layout and socket connector at the top.

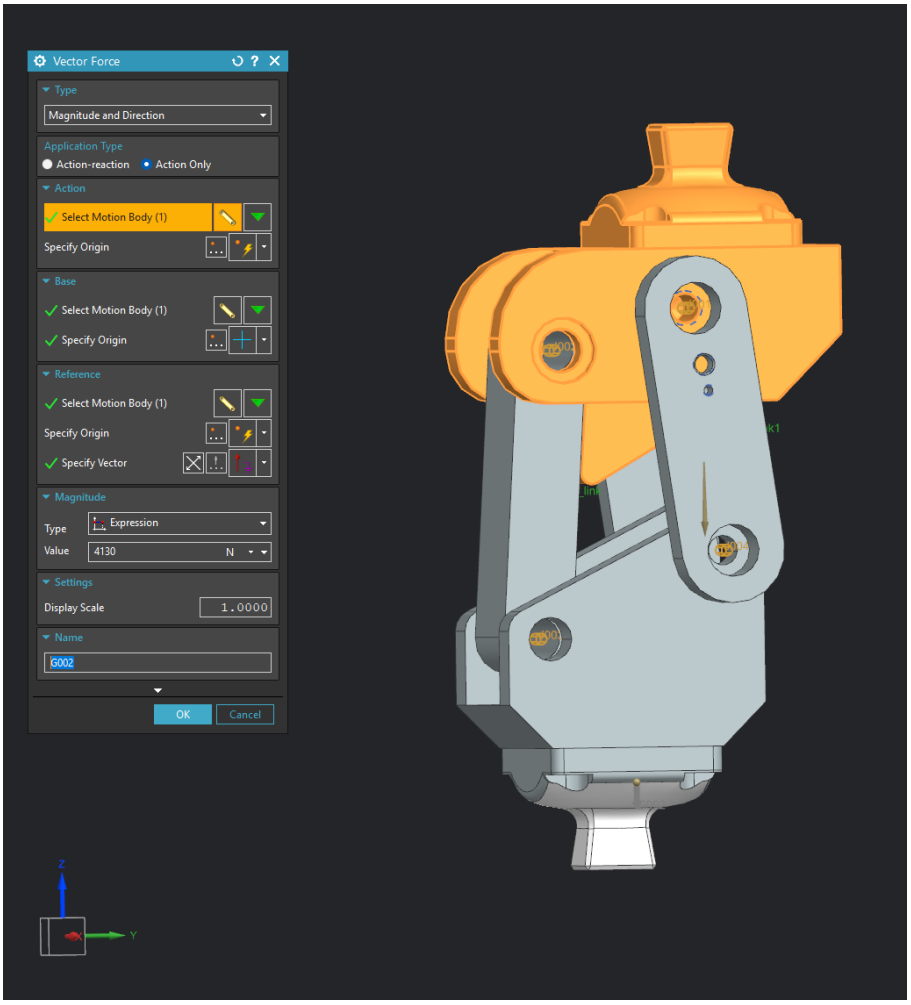

Figure 4.4. Vector force of 4130N applied downward on the top link (motion body shown highlighted) where the bottom link is formed by the base body and also acts as reference body.

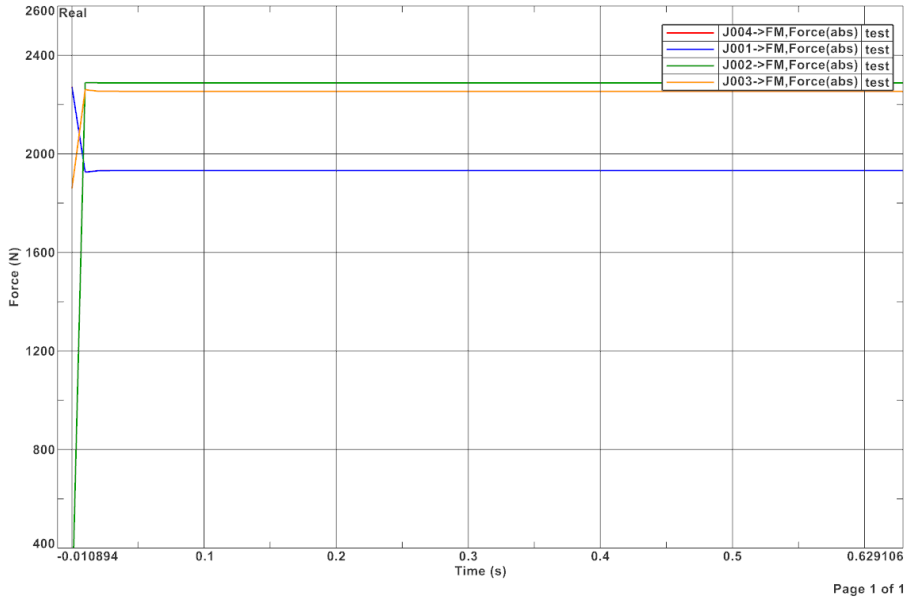

Figure 4.5. NX Motion results: Force responses for joints 1-4 shows a maximum force of ≈2300N for the anterior joints and ≈1900N for the posterior joints

4.4. General design considerations

Manufacturability During the design process, the principles of fit, form and function predominantly influenced the decision-making process. The concept of "fit" describes the interface and interaction between various components, ensuring that they connect and operate efficiently together. The concept of "form" involves consideration of both the geometry and the visual aesthetics of these components, reflecting their physical attributes and appearance. "Function", on the other hand, identifies the specific role or purpose each component is intended to fulfil within the overall system.

In particular, while each component has unique interfaces and purposes, the primary consideration guiding the geometry and aesthetics of all components was simplicity. The emphasis on simple geometric designs is crucial, as such configurations are more straightforward to manufacture, which, in turn, leads to a reduction in the associated manufacturing costs. By prioritising simplicity in design, manufacturers can achieve cost-effectiveness without compromising on the essential aspects of fit, form, and function.

Standardised Components The use of mass-produced components contributes to cost reduction. Specifically, for the knee mechanism, standard M5 bolts were used to secure the pyramid adapters to the upper and lower linkages and to attach the extension stop to the upper linkage. This configuration not only facilitates the straightforward replacement of these components in the event of failure but also allows the adjustment of the upper pyramid adapter position when the knee is fitted to a user.

In addition to the M5 bolts, M8 shoulder bolts were used to connect the anterior links to the top and bottom linkages. Consequently, the shoulder bolts fulfil dual functions, acting both as fasteners and as shafts. The design allows for the removal of these fasteners using basic Allen keys, which simplifies the processes of disassembly and maintenance. In addition, circlips were used to keep the upper and lower shafts of the posterior link in place. This method highlights practical, efficient serviceability and adjustment, in line with engineering principles favouring simple, modular designs.

Standard Dimensions In an effort to minimise the costs associated with the machining processes, the use of standard geometric angles such as $30°, 45°, 60°,$ and $90°$, along with specific radii, was maximised for the creation of chamfers and fillets. This methodology was adopted in order to optimise manufacturing processes by simplifying production, thereby improving cost-effectiveness. This was achieved by reducing the complexity and variability inherent in machining specifications, which can often lead to increased costs and inefficiencies.

Machinist Input During the design process, consultations with machinists were integral in ensuring the manufacturability of the design[64]. Based on the expert recommendations of the machinists, several modifications were implemented. These changes aimed to decrease the number of components that required machining, minimised the complexity of the parts, and consequently, reduced both the machining time and overall manufacturing expenses.

Material considerations This study delivered a prototype intended to establish functional viability and performance parameters and was not developed as a market ready product. As such, material selection prioritised availability and ease of machining over long term performance characteristics. The selected materials represent practical substitutes for cost effective prototyping and therefore not the optimal choices or commercial manufacturing. Most of the main components were made from 6061 Aluminium. The pyramid adaptors were made of 304 stainless steel, as the grub screws used to secure the knee to the socket and the shank would significantly damage the adaptors if they were made of aluminium. Vesconite [47] was used for the bushings and washers while Igludur J3 [48] was used for the friction pads.

4.5. Final Design Description

In this section, the knee mechanism that resulted from the design process is presented. Fig. 4.6 shows the 3D CAD model overlaid with the mathematical geometry calculated with the link segment model of the 4BM Design Tool. From this, the progression from the mathematical model to its physical implementation can be clearly seen.

Fig. 4.7 illustrates the outcome of the prototype development process, where Fig. 4.7a shows the knee in heel strike position, Fig. 4.7b shows the knee in full flexion and Fig. 4.7c is an exploded view of all components. The colour indices of the parts link to the following description of the components and their respective functions. This is followed by an explanation of the damping mechanism, an overview of the materials used, and a discussion of the manufacturing tolerances.

4.5.1. Components

The important functional components and their interaction are described in the following, where the colour indices match those used in Fig. 4.6 and Fig. 4.7.

Pyramid adaptors (Yellow):

- The structural interfaces between the knee mechanism and the socket above and the shank below.
- Provide an adjustable connection point and allow proper alignment of the mechanism in relation to the rest of the prosthetic leg.

Top link (Dark Blue):

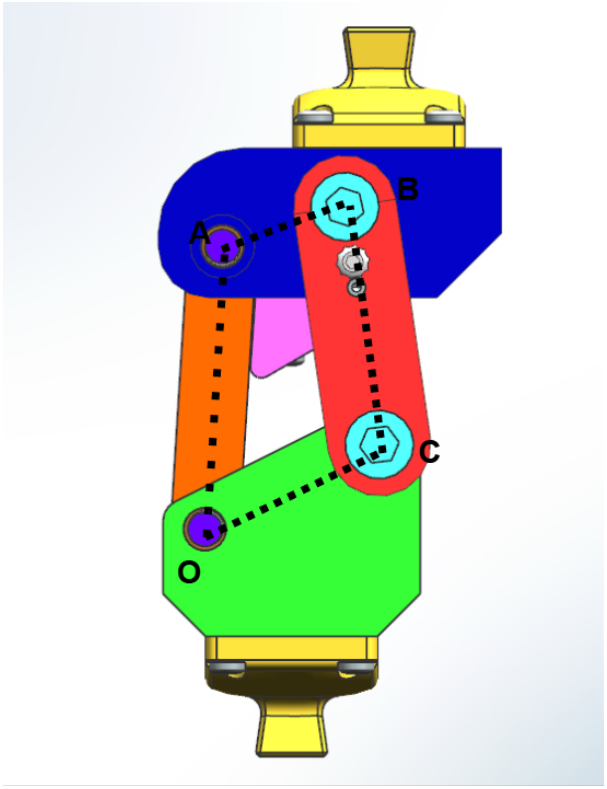

Figure 4.6. CAD model of knee overlaid with the mathematical links

- Input link (crank) that drives the four-bar knee mechanism.
- Provides a mounting location for pyramid adapters that is adjustable to suit the stability preferences of any individual user.
- Provides mounting locations for the anterior and posterior links, as well as for the extension stop.
- Forms part of the frictional damping mechanism by acting as an integrated brake surface. See 4.5.2 for more details.

Anterior links (Red):

- Floating link that connects the crank and ground links in the four-bar knee mechanism.
- Supports weight of the user.
- Forms part of the damping mechanism. (See 4.5.2.)

Posterior link (Orange):

- Floating link that connects the crank and ground links in the four-bar knee mechanism.
- Supports the weight of the user.
- Presses against the extension stop during heel strike, preventing over extension of the knee.

Bottom link (Green):

- Bottom (ground) link for the four-bar mechanism, driven by the floating links.
- Provides a mounting location for the bottom pyramid adaptor.

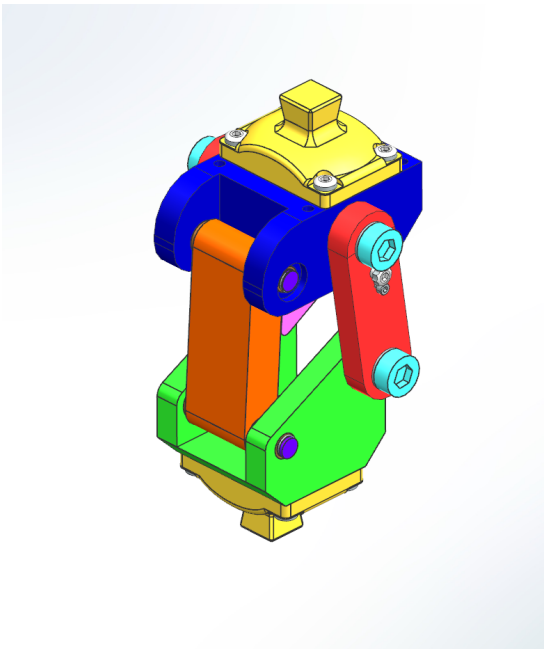

(a) Isometric view of knee in heel strike position.

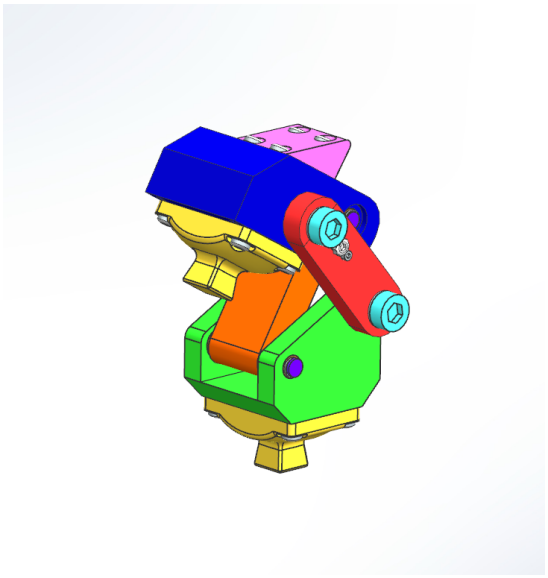

(b) Isometric view of knee in full flexion position.

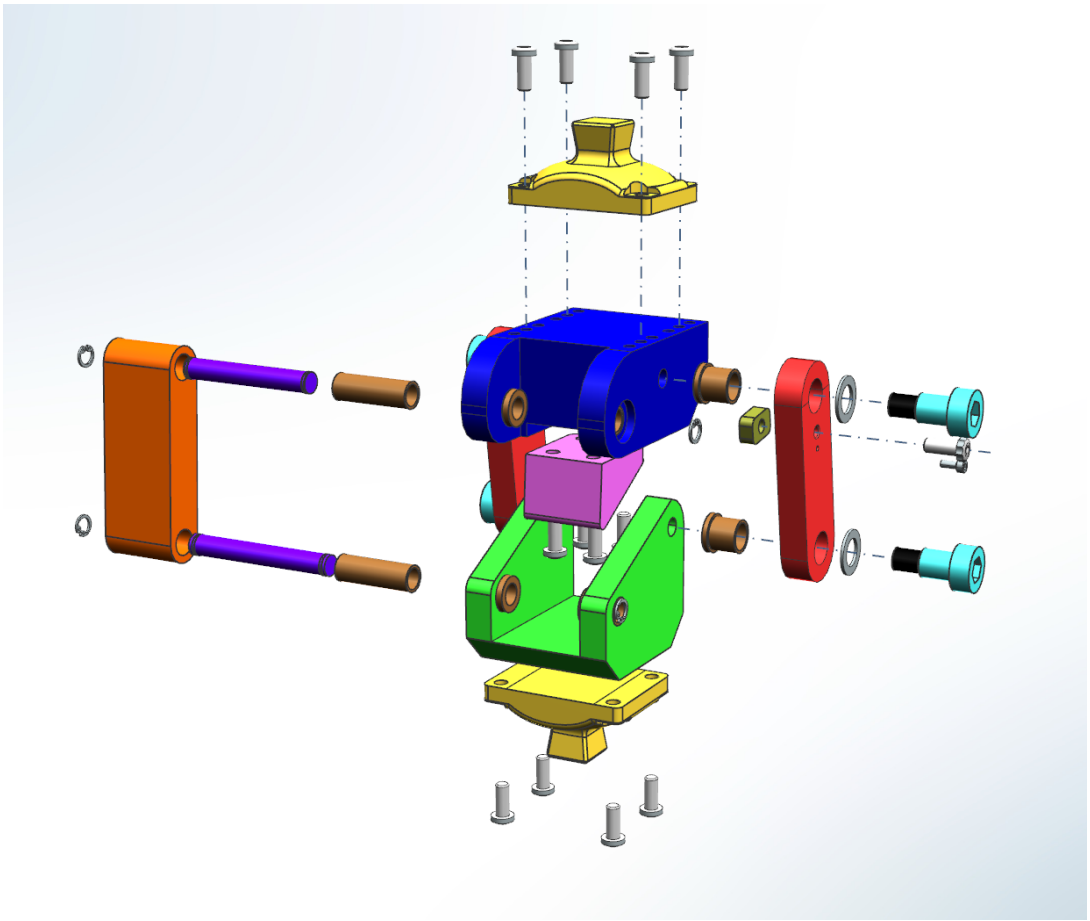

(c) Exploded view of knee showing all components.

Figure 4.7. Final version of the four-bar knee mechanism showing (a) heel strike configuration, (b) maximum flexion configuration, and (c) exploded component layout.

- Provides mounting locations for the anterior and posterior links.

Extension Stop (Pink):

- Attaches to the top link.
- Blocks the motion of the posterior link in the extended position, to prevent overextension.

Posterior shafts (Purple):

- Connect the posterior link to the top (crank) and bottom (ground) links.
- Act as pivot locations for the posterior link.

Bushings (Brown):

- Reduce friction and wear between moving components.
- Provide a low friction interface for rotating shafts.
- Absorb vibrations and ensure proper alignment.
- Serve as spacers between components.

Fasteners (Light blue/grey):

- The M8 shoulder bolts (light blue) fasten the anterior links to the top and bottom links.
- The shoulder bolts act as shafts for the rotation of the anterior links.
- The M5 bolts (grey) secure the pyramid adaptors to the top and bottom links, and secure the extension stop to the top link.
- Circlips used to secure the posterior shafts in place.

4.5.2. Damping mechanism

The damping mechanism takes the form of a variable friction brake. The upper link acts as the brake surface and the brake pads (made of Igus Iglidur J3 [48]) are positioned in cutouts in the anterior links. The cutout can be seen in Fig. 4.8a with the components of the damping mechanism shown in Fig. 4.8b.

The pads are pressed into the top link using an M5 bolt threaded through the anterior links, one on each side. Both the pads and the cutouts are rectangular to prevent the pads from spinning in place. The pads have a blind 5mm hole to accept the bolt. To keep the bolt from loosening over time, it is notched and a M2.5 bolt offset from the M5 hole keeps it from rotating by engaging with the notches. There are 10 notches in total to allow for different damping strengths.

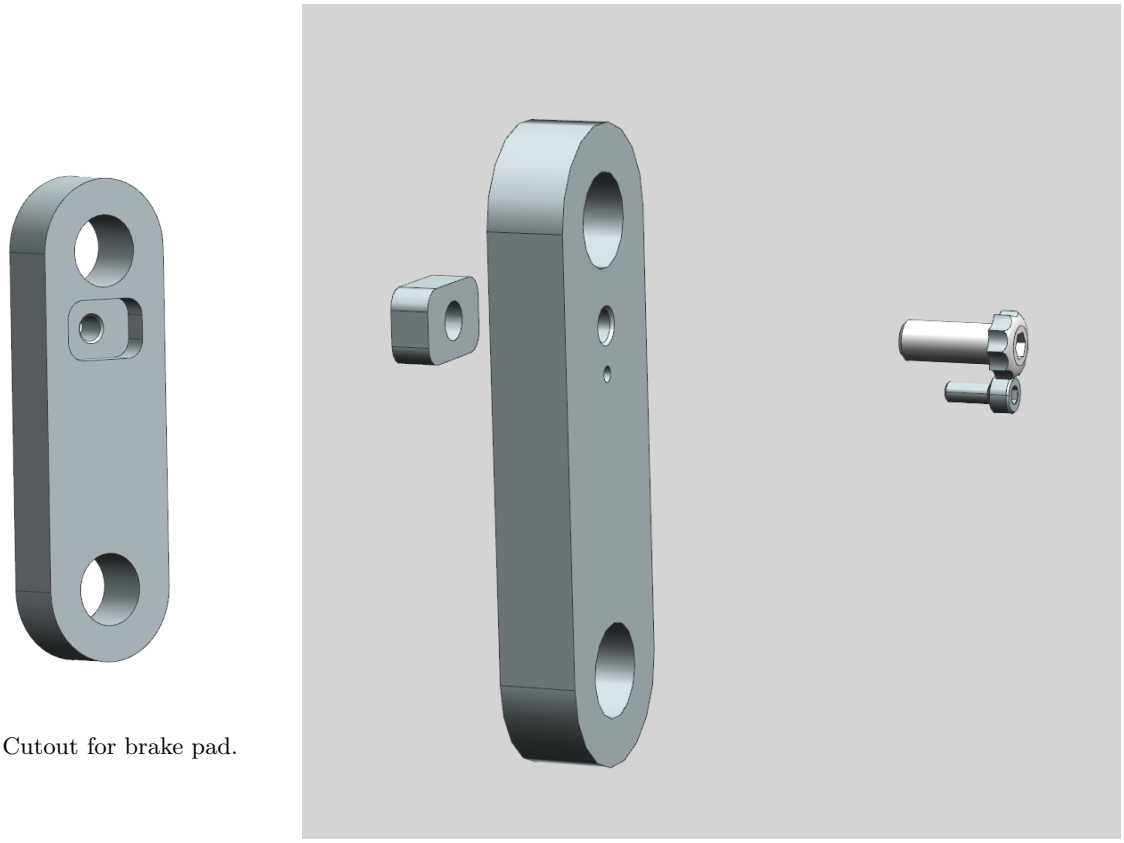

(a) Cutout for brake pad.

(b) Damping Mechanism with set screws.

Figure 4.8. Anterior link showing brake pad cutout and damping mechanism.

4.5.3. Manufacturing Tolerances

The link lengths and, therefore, the relative positions of the pivot centres are of critical importance, as even small deviations can significantly alter the instantaneous centre of rotation (ICR) and affect the overall kinematic behaviour of the mechanism (for example, cause binding during flexion). For this reason, a dimensional tolerance of ± 0.1 mm was specified for all pivot hole locations, the corresponding hole diameters, shaft diameters, and bushing thicknesses, to minimise tolerance stacking across the assembly. Non-critical features, such as surface contours and aesthetic chamfers, were specified with a general tolerance of ± 0.5 mm.

Most components were manufactured using a 5-axis CNC milling machine directly programmed from the CAD models. The positional accuracy of the machine (approximately ± 0.04 mm) ensured that the tolerances for the machined parts were within the design specifications, particularly for the pivot holes and inter-link interfaces. As a result, no significant post-machining alignment or fit adjustment was required during assembly.

4.5.4. Materials

Given the research objective of the project, material selection followed a pragmatic approach. Ready-available stock materials were used to enable easy machining and reduce costs. In a commercial context, alternative alloys or heat-treated variants would be selected to improve durability, reduce mass, and ensure complete compliance with the fatigue requirements of ISO 10328. Table 4.1 summarises the materials used for the prototype and its evaluation of functional performance.

Table 4.1. Materials used for components of prototype

Component	Material	Yield Strength
Pyramid adaptors	304 Stainless steel	276 MPa
Links	6061 Aluminium	240.7 MPa
Extension stop	6061 Aluminium	240.7 MPa
Fasteners	High tensile Steel	Assumed $\geq$ 304 Stainless
Bushings	Vesconite	65 MPa
Friction Pads	igus Igludur J3	Compressive strength 60 MPa

4.6. Shear force on shafts

To evaluate whether the shafts and shoulder bolts were strong enough to support the maximum static load specified by ISO 10328, the average shear stress in the shaft or bolt was calculated as

$$\tau_{\text{ave}} = \frac{F_s}{A} \tag{4.1}$$

where τ_{ave} is the average shear stress, F_s is the shear force transmitted through the shaft or shoulder bolt, and A is the cross-sectional area that resists shear.

Because a bushing separates the components, each shaft is loaded in a single shear plane, so the shear area is

$$A = \pi r^2 \tag{4.2}$$

and

$$\tau_{\text{ave}} = \frac{F_s}{\pi r^2} \tag{4.3}$$

The yield stress of 304 stainless steel is 276 MPa according to the Siemens NX 2312 material library. For a safety factor of 3, the allowable shear force is then 92 MPa. Therefore, if we substitute the allowable shear stress with 92 MPa and 2300N for the shear force (in the event that the knee joint is loaded asymmetrically), we can then solve for the minimum radius that the shaft has to be to support the weight.

$$r_{\text{min}} = \sqrt{\frac{F_s}{\pi \tau_{\text{allow}}}} \tag{4.4}$$

This results in the minimum radius being $\approx$ 3mm, or 6mm in diameter. The shoulder bolts that were chosen are M8 and the posterior shafts have an 8mm diameter; therefore, the shafts exceed the minimum safety factor requirements.

4.7. Finite Element Analysis (FEA)

The FEA conducted in this study served to verify that the structural members could withstand the expected maximum static load safely and to identify potential weak points. A complete assembly analysis was not performed because the objective was to confirm the functional robustness for testing, not to optimise stiffness or fatigue performance. Only the weakest or most critical components were analysed to confirm that their maximum stresses remained below the yield limits and that the safety factors were acceptable for limited use. The simplified approach aligns with the focus of the study on feasibility validation. That being the case, if these parts

were to be optimised for weight, a more rigorous approach needs to be taken with the simulation setup. Because these parts are connected by several pins and bolts, a contact analysis will be necessary to obtain the correct stresses at the junctions.

4.7.1. Simulation Setup

The simulation setup for the anterior link can be seen in Fig. 4.9a. A 3D tetrahedral mesh with element size 4 mm was used, with mesh refinement at expected stress concentrations as can be seen at the central hole of the anterior link. A fixed constraint was added to the location of the bottom pivot and a load of $1150N$ was applied to the bottom half of the top pivot point.

Similar meshes and constraints were used for the posterior link and the bottom (see Fig. 4.9b and Fig. 4.9c). The loads that were applied are consistent with the motion simulation results.

4.7.2. FEA Results

Fig. 4.10a shows the elemental Von Mises stress distribution resulting from the applied load. The maximum stress was 33.37 MPa and the deflection was negligible. According to the NX 2312 material library, the yield stress of 6061 Aluminium at 20°C is 240.7 MPa; therefore the safety factor is 7.2. An additional simulation was performed with the load of 2300 N in case of extreme asymmetric loading and the results can be seen in Fig. 4.10b. This brings the maximum stress to 66.74 MPa and the safety factor to 3.6.

Fig. 4.10c shows the stress distribution for the posterior link with a maximum stress of 7.14 MPa and therefore a safety factor of 33.7.

Fig. 4.10d shows the stress distribution for the bottom component with a maximum stress of 16.51 MPa and therefore a safety factor of 14.6.

4.7.3. Results and Interpretation

Although the scope of the simulation was limited, the results confirmed that the weakest structural components exhibited safety factors above the minimum required for static strength according to the ISO 10328 guidelines. The FEM verification therefore supports the adequacy of the prototype for functional gait analysis within the limits determined by the test protocol.

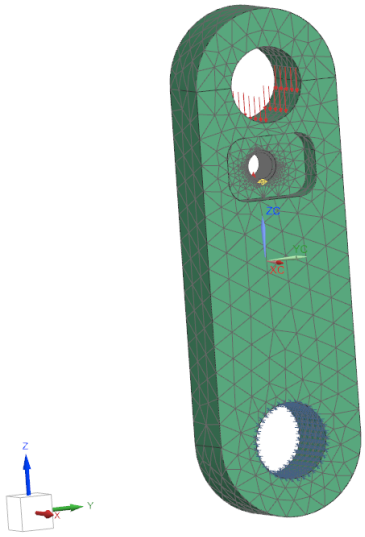

(a) Load and constraint setup for the anterior link.

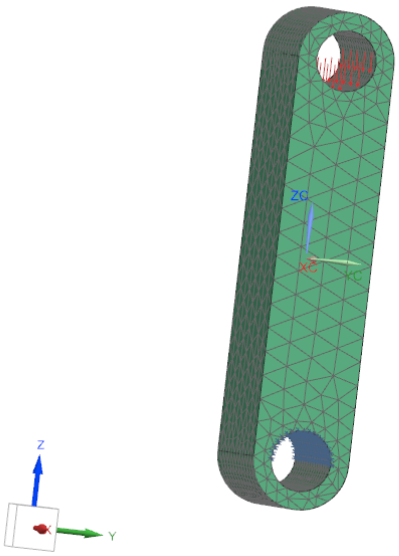

(b) Load and constraint setup for the posterior link.

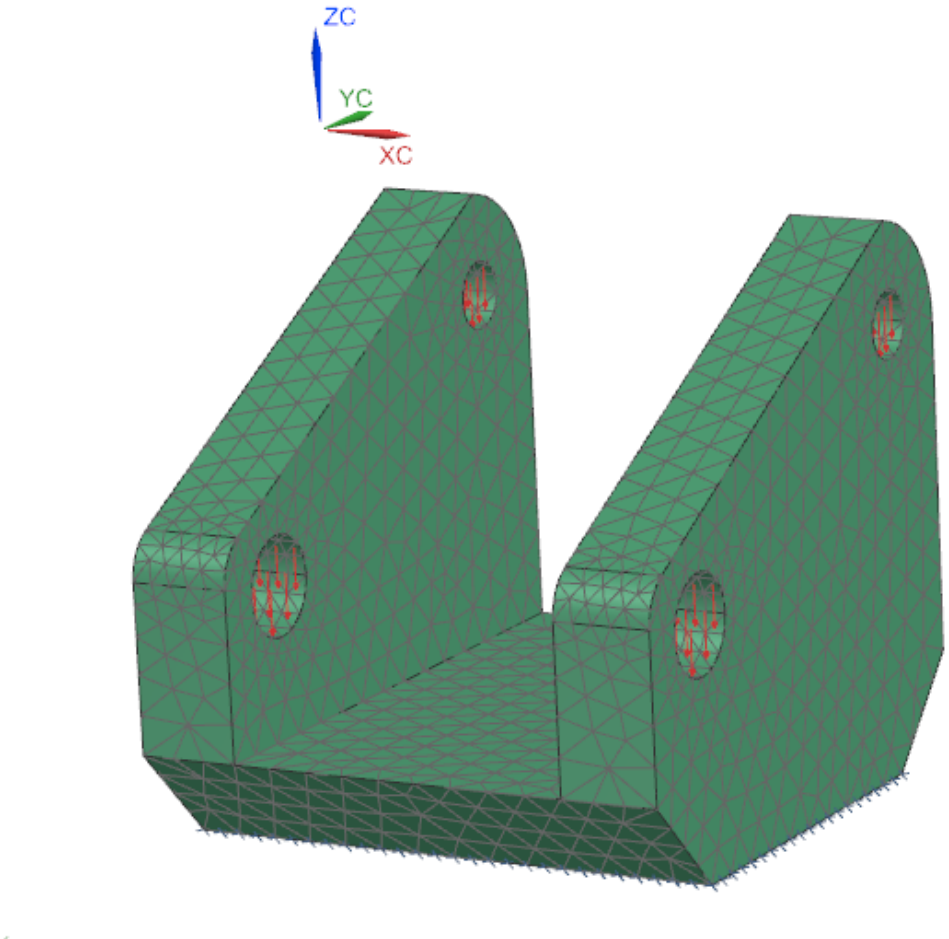

(c) Load and constraint setup for bottom link.

Figure 4.9. FEM setup of critical components.

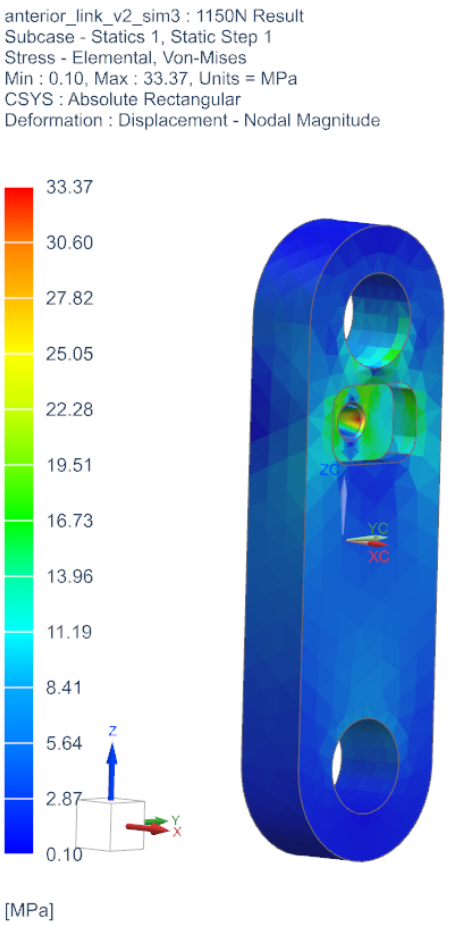

(a) Anterior link stress results for 1150N.

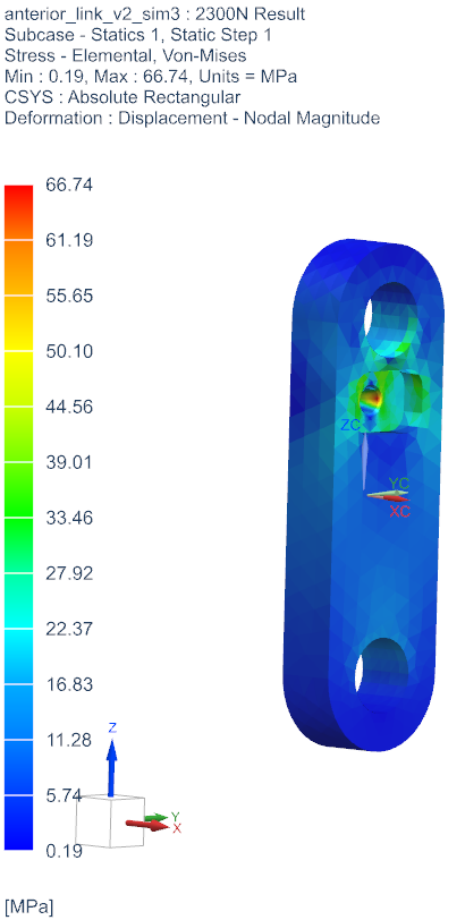

(b) Anterior link stress results for 2300N.

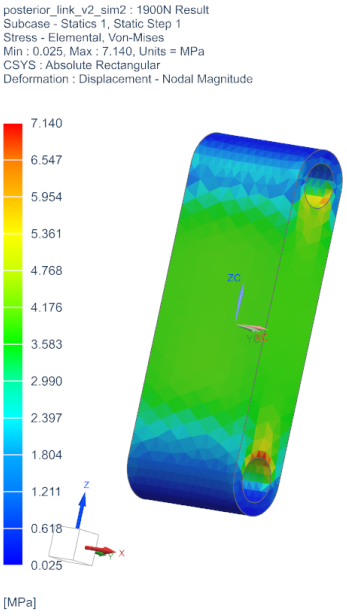

(c) Posterior link stress results for 1900N.

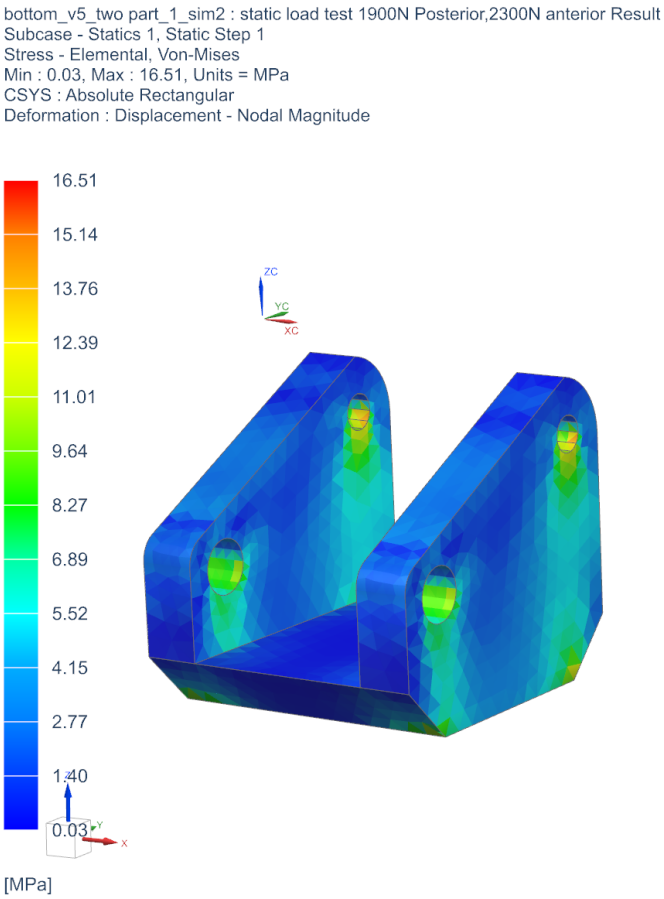

(d) Bottom link stress results.

Figure 4.10: FEM Von Mises stress results for critical components.

4.8. Manufacturing Methods

For the rapid prototyping phase, FDM 3D printed assemblies were used to evaluate fit, form and function. The components were printed with PETG. The prototypes were assembled by hand with basic tools, such as Allen keys. Three iterations of these early prototypes can be seen in Fig. 4.11, showing variations in design choices, such as the placement of components and the different radii used for edge rounds.

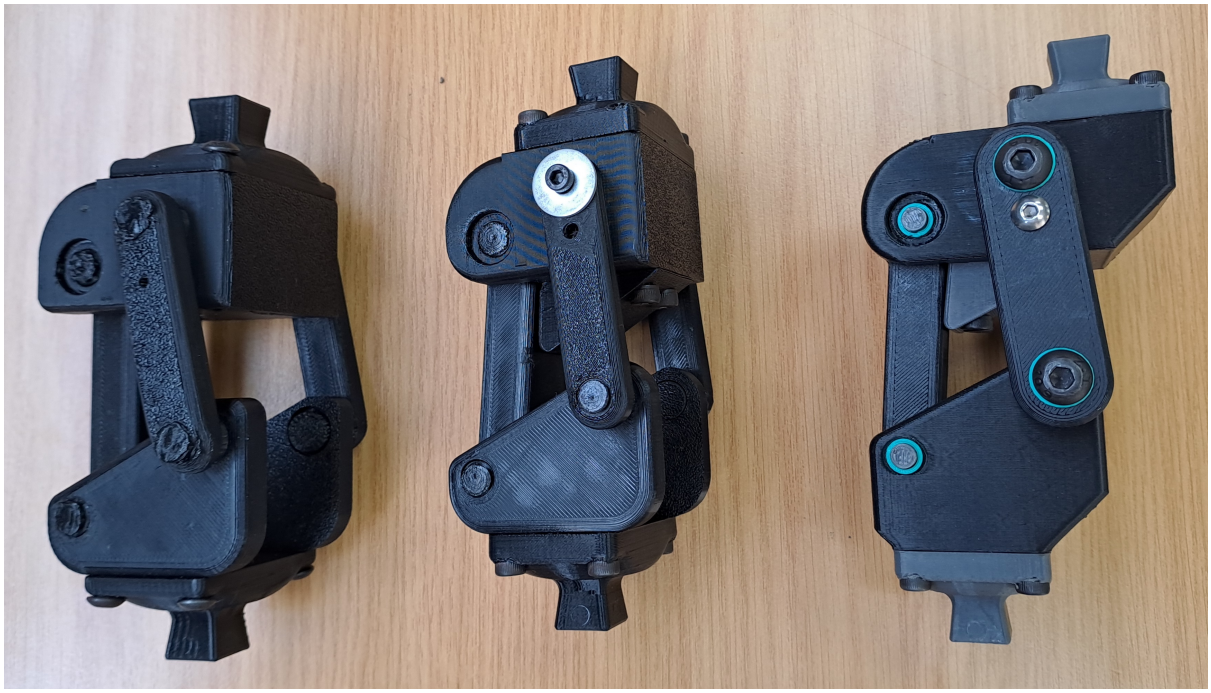

Figure 4.11. 3D printed concepts showing different design choices.

The components for the final prototype used for functional performance evaluation were manufactured using a 5-axis CNC machine for the main components and a lathe for the bushings. The prototype was assembled, similarly to the 3D printed prototypes, by hand using Allen keys.

4.8.1. Alternative Manufacturing Techniques

In the present study, CNC machining was the primary manufacturing technique. However, for the link members, which are predominantly flat components with through-holes, lower-cost profile cutting processes such as laser or water jet cutting followed by finish machining of the critical hole interfaces would be suitable alternatives. Plate bending and welded assemblies could also be used for selected structural components. These also come with drawbacks such as the risk of warping, imprecise fitting, and increased tolerance stacking. The low stress values of the components show that it is not structurally necessary to use billet stock that is machined down to shape, and that near-net-shape manufacturing methods can lower both material usage and production costs.

Polymer based processes such as fibre-reinforced injection moulding may also be viable for mass production , but that would require tooling which is prohibitively expensive in the prototyping phase. The choice of using CNC machining was selected due to various factors, the chief of which was the precision and accuracy that it allowed. It is critical that the geometry of the

prototype is consistent with the mathematical model to ensure that the results of the walking trials will be minimally influenced by manufacturing errors.

4.9. Prototyping and Manufacturing Outcomes

The prototype used for performance testing is shown in Fig. 4.12a, with Fig. 4.12b showing it fully flexed. On the recommendation of expert machinists, the fillets on the outer edges of the components were replaced by edge breaks to reduce machine time and, therefore, cost. The weight of the prototype is 1.33 kg, well below the 2.25 kg threshold specified by Gayley and Gonzales[7]. The fit of the components were satisfactory and there were no interferences between parts throughout the range of motion. Furthermore, the design facilitated easy assembly and disassembly with minimal tools required, ensuring serviceability.

(a) 4BM knee in full extension (i.e. during heel strike).

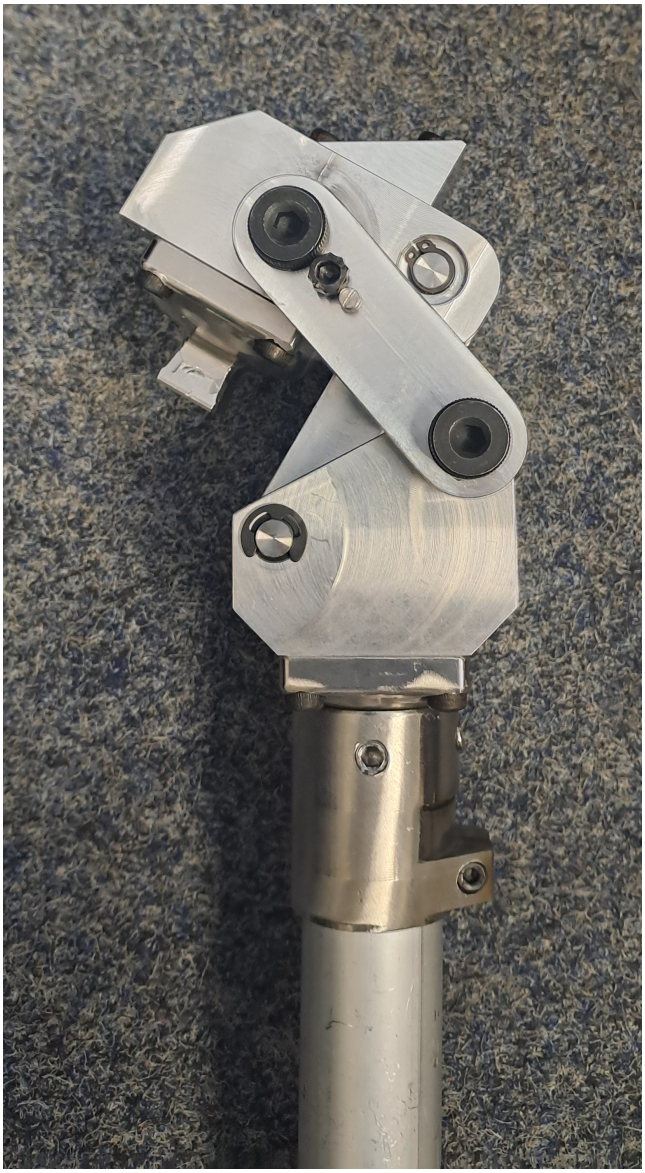

(b) 4BM knee in full flexion (i.e. when sitting).

Figure 4.12. The functional prototype 4BM knee showing full extension and full flexion positions.

4.10. Prototype Scope and Limitations

The prototype described in this chapter was designed to test the functionality of the voluntary-control mechanism, not to serve as a market-ready prosthesis. Finite element analysis was applied only to key components to ensure safety under static loads. Therefore, apart from the static strength test, other tests of the ISO 10328 standard such as cyclic fatigue, torsional, and ultimate failure were not included. The materials and manufacturing techniques used for the prototype development were chosen for their cost-effectiveness and availability. However, despite these considerations, the knee assembly showed structural soundness and reliable mechanical performance in initial tests, validating the design process.

4.11. In summary

At this stage, referring to the list described in Section 3.3.1, the prototype development phase has successfully completed the following requirements, verified against Table 3.2.

3. **Range of motion:** The physical prototype achieved a range of motion greater than 90°.
5. **Mass of prosthesis:** The physical prototype weighed less than 2.27 kg.
6. **Structural strength:** The FEA analysis indicated that the critical components have a safety factor of 3 or greater.
7. **Adjustability:** Features were included to allow the user to adjust the alignment and damping characteristics of the prototype.
8. **Manufacturability and cost:** With design decisions strongly focused on these two metrics, material and machining costs to fabricate the prototype were ≈ R22000.
9. **Serviceability and maintainability:** Standard fasteners and modular components were used to facilitate long term support and maintainability.

The remaining requirements of Table 3.1 depend on functional testing for validation and will be addressed in Chapter 5 where the gait trial case study is described.

5. Experimental Methodology and Results

5.1. Introduction

This chapter focusses on performance evaluation and data processing. Its purpose is to quantify the performance of the prosthetic knee using 3D human gait analysis, in order to validate the outcome of the design process. The gait cycle is an important performance metric and its quality can be determined by an analysis of the symmetry of gait when a healthy leg is compared to a prosthetic device.

In addition, the symmetry of the gait cycles was also compared when using two different prosthetic devices. Functionally, the four-bar knee prototype was compared to the Ottobock Genium X3[61], which is the device that the case study participant normally uses and an example of a premium microprocessor-controlled prosthetic knee. The output measurements obtained were a mixture of joint kinematics and ground reaction force data, as well as spatio-temporal parameters. The experimental protocol, experimental setup, data processing, evaluation criteria, and results are discussed here.

Fig. 5.1 shows the implementation aspects in Chapter 5 that contributed to the various concept solutions for the research challenges RC3 and RC5 (see Section 2.10).

Concept solutions	Four bar Knee	Defined design considerations	Symmetry of Kinematic and Spatio-temporal parameters	Link segment model, CAD,FEA	Gait trial
Chapter 5					
Walking trials			↑		↑
Data analysis			↑		↑
Validation			↑		↑

Figure 5.1. Concept solution implementation in Chapter 5

5.2. Experimental Protocol and Ethical Compliance

Participant information

The participant was a physically active, experienced lower-limb amputee who volunteered for the study. Importantly, he has prior experience testing experimental prosthetic knee joints and is well-informed about the nature of such research. He can also adjust and align the prosthesis to suit his needs. His technical competence and familiarity with the risks and expectations involved

further reduced any potential risk and improved the reliability of the feedback obtained. He weighs 82 kg.

Ethical considerations and safety measures

The ethics number for this study is NWU-00473-24-S3. The participant provided his informed consent. The walking trials were conducted at self-chosen speeds in a controlled lab setting and were supervised by qualified researchers from the Faculty of Engineering and the Faculty of Health (Human Movement Sciences). These trials involved routine physical activities familiar to the participant. Researchers from Human Movement Sciences ensured minimal necessary testing. After each trial, there was a mandatory 10-minute rest, which could be extended on request.

Walking trial Procedure

There were two separate walking trials, one for each type of prosthetic knee and following the same procedure. The participant walked in a straight line for approximately 10 m in one direction, turned around, and walked back to the starting position. The data for each track length was recorded separately. The participant walked the track 10 times with each device, or approximately 200 m in total (100 m for each prosthetic).

5.3. Experimental Equipment Setup

Motion capture system

The 3D motion capture system that was used is called Qualisys[65]. There are 6 infrared Qualisys Oqus 5+ cameras that can track markers placed on the participant as he completes the walking trials (see Fig. 5.3c) and QTM software is used to capture marker movement with a sampling rate of 200Hz. This data represents the limb and joint kinematics, such as joint angles and positions in 3D space.

Marker set and Definitions

The set of markers used is called the Lower Body Marker Set of the Instituti Ortopedici Rizzoli (IOR) [66]. It uses 10mm spherical reflectors paced on key anatomical landmarks[1] of the lower body (see Fig. 5.2, Fig. 5.3a, and Fig. 5.3b). Each joint centre acts as it's own datum coordinate system. The X axis is the flexion/extension axis (sagittal plane) of each joint and will be of primary interest. The Y axis is the adduction/abduction axis, and the Z axis is the internal/external rotation axis. For the purposes of this study, the Y and Z axes will be omitted from the evaluation.

To initialise the locations and angles of the joints, the set of yellow static markers shown in Fig. 5.2 was used. The participant stood still with the limbs extended while the initial measurements were made. This defined 0° flexion for all joints. After initialisation, the yellow markers were replaced with the dynamic marker set that was used for the walking trials.

[1] An enquoteanatomical landmark is a specific, recognisable feature of the body used as a reference point for identification or measurement.

Qualisys PAF package: Istituti Ortopedici Rizzoli (IOR) lower body marker set [1]

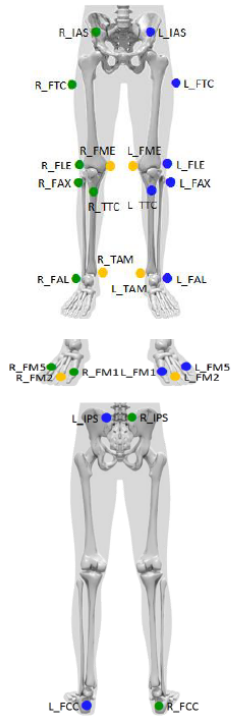

Name	Ref. [2]	Location	Static (26)	Dyn. (20)
L_IAS	IAS	Anterior superior iliac spine	X	X
L_IPS	IPS	Posterior superior iliac spine	X	X
R_IPS	IPS	Posterior superior iliac spine	X	X
R_IAS	IAS	Anterior superior iliac spine	X	X
L_FTC	FTC	Lateral side of greater trochanter, 1/3 from proximal end	X	X
L_FLE	FLE	Femur lateral epicondyle	X	X
L_FME	FME	Femur medial epicondyle	X	
L_FAX	FAX	Proximal tip of the head of the fibula	X	X
L_TTC	TTC	Most anterior border of the tibial tuberosity	X	X
L_FAL	FAL	Lateral prominence of the lateral malleolus	X	X
L_TAM	TAM	Medial prominence of the medial malleolus	X	
L_FCC	FCC	Aspect of the Achilles tendon insertion on the calcaneus	X	X
L_FM1	FM1	Dorsal margin of the first metatarsal head	X	X
L_FM2	FM2	Dorsal margin of the second metatarsal head	X	
L_FM5	FM5	Dorsal margin of the fifth metatarsal head	X	X
R_FTC	FTC	Lateral side of greater trochanter, 1/3 from proximal end	X	X
R_FLE	FLE	Femur lateral epicondyle	X	X
R_FME	FME	Femur medial epicondyle	X	
R_FAX	FAX	Proximal tip of the head of the fibula	X	X
R_TTC	TTC	Most anterior border of the tibial tuberosity	X	X
R_FAL	FAL	Lateral prominence of the lateral malleolus	X	X
R_TAM	TAM	Medial prominence of the medial malleolus	X	
R_FCC	FCC	Aspect of the Achilles tendon insertion on the calcaneus	X	X
R_FM1	FM1	Dorsal margin of the first metatarsal head	X	X
R_FM2	FM2	Dorsal margin of the second metatarsal head	X	
R_FM5	FM5	Dorsal margin of the fifth metatarsal head	X	X

Figure 5.2. IOR lower body marker set definition used in Qualysis

Force plate configuration

There were three force plates in the centre of the walking track, shown in Fig. 5.3d. These measured the ground reaction force of the participant as he walked across them. The sampling rates for the force plates were 2000 Hz. Only gait cycles in which complete force plate data were captured were used for gait analysis. This ensured that only gait cycles that had both kinetic and kinematic data were used for evaluation. Furthermore, the force plates cannot distinguish between multiple load vectors; therefore, only gait cycles in which one foot touched each force plate cleanly were used. (For example: left leg stepped on Force Plate 1 and right leg on Force Plate 3.)

Prosthetic knee Configuration

The participant was responsible for adjusting/aligning the prototype knee to suit his needs and comfort. Markers for each knee were placed as close as possible to the corresponding anatomical landmark locations defined in Fig. 5.2.

Gait comparison between prototype and commercial device

Fig. 5.4 shows photo's from the gait trial of the prototype. Fig. 5.4a shows the prototype during the swing phase while Fig. 5.4b shows the prototype right before heel strike. Fig. 5.5 includes three frames of the gait trial where the participant is walking with the Genium X3. Fig. 5.5a and Fig. 5.5c shows the knee fully extended right before heel strike while Fig. 5.5b shows a rear view of the knee right after the toe-off event.

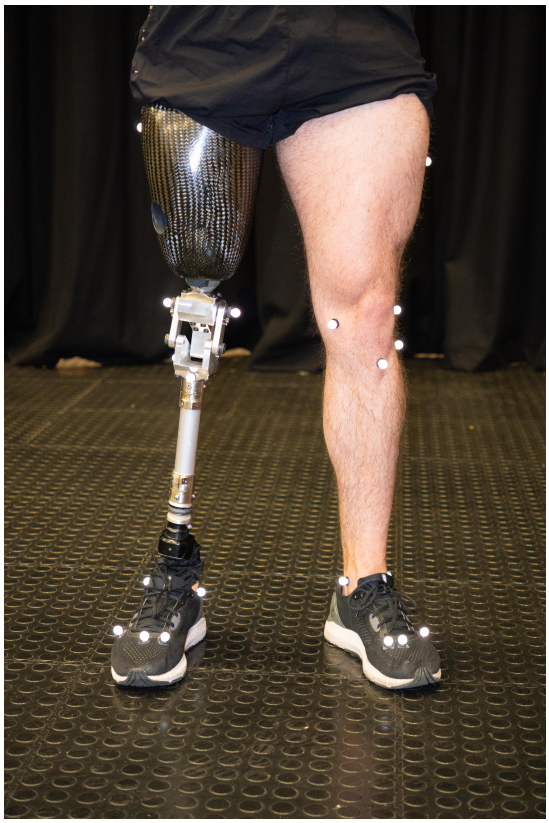

(a) Marker placement for 4BM

(b) Infrared tracking marker

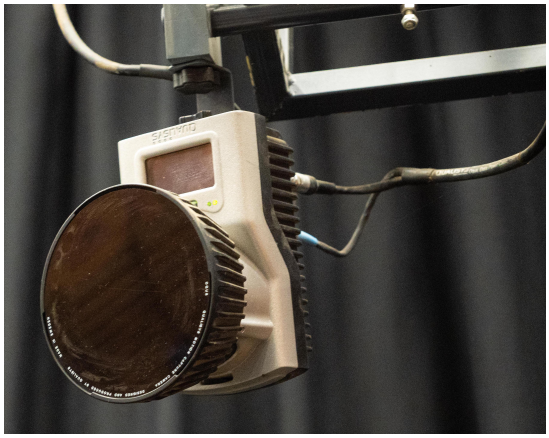

(c) Qualisys infrared camera

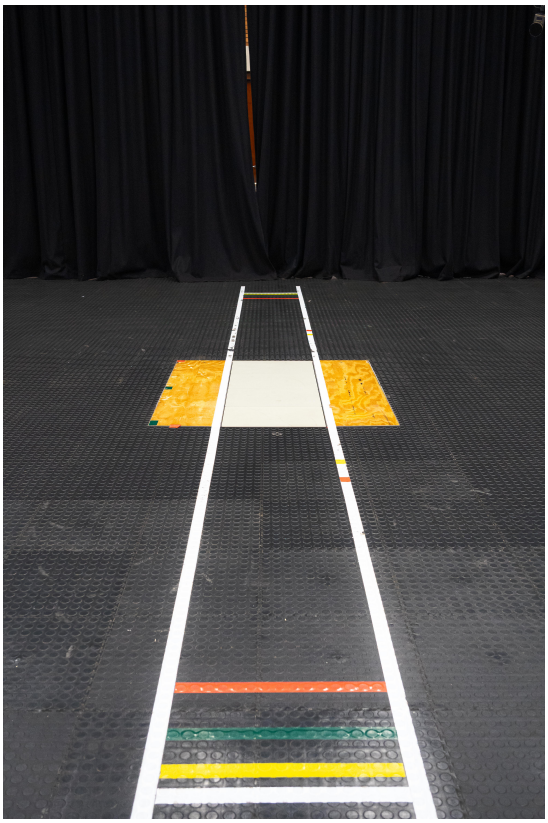

(d) Walking track

Figure 5.3. Gait-trial setup: (a) Marker placement on both legs, (b) Infrared marker with mount, (c) Qualisys camera, (d) Walking track with force plates.

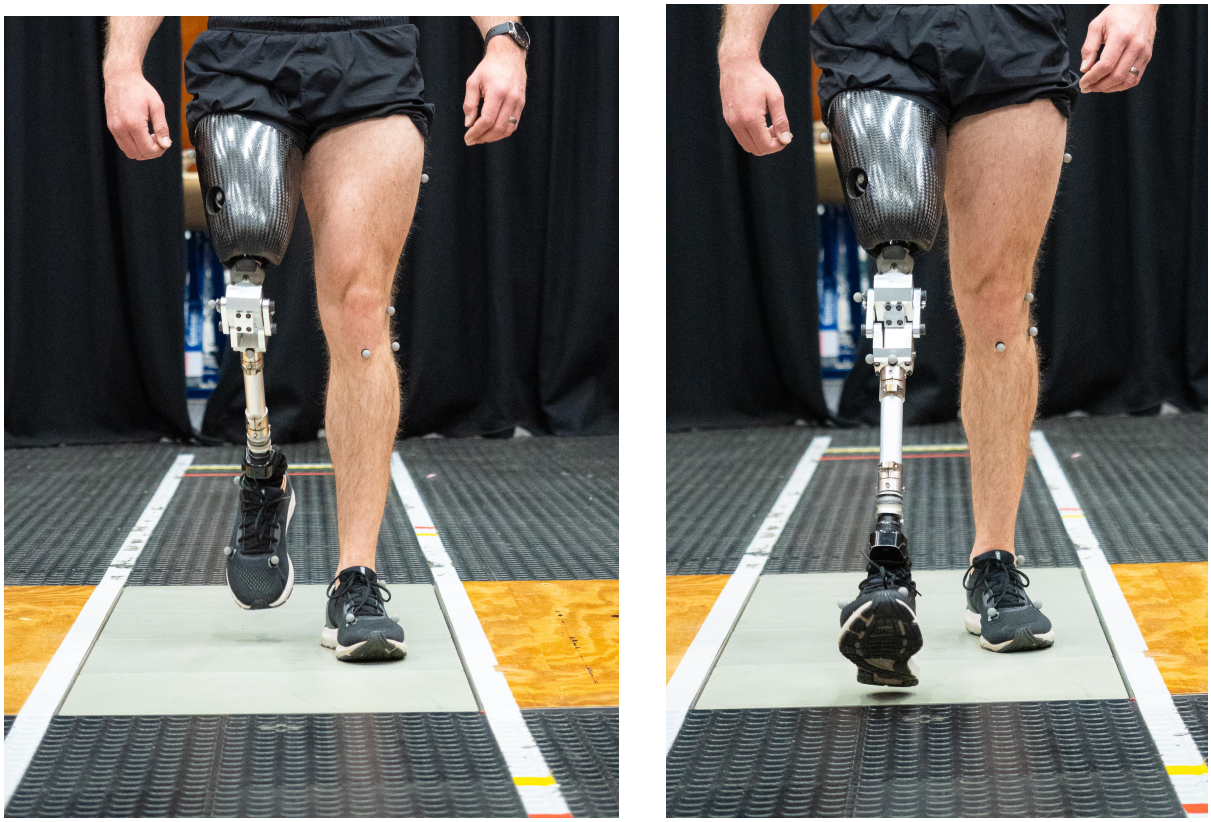

(a) 4BM—front view (frame 1)

(b) 4BM—front view (frame 2)

Figure 5.4. Participant walking with the prototype four-bar mechanism (4BM). Consecutive frames illustrate stance-to-swing progression.

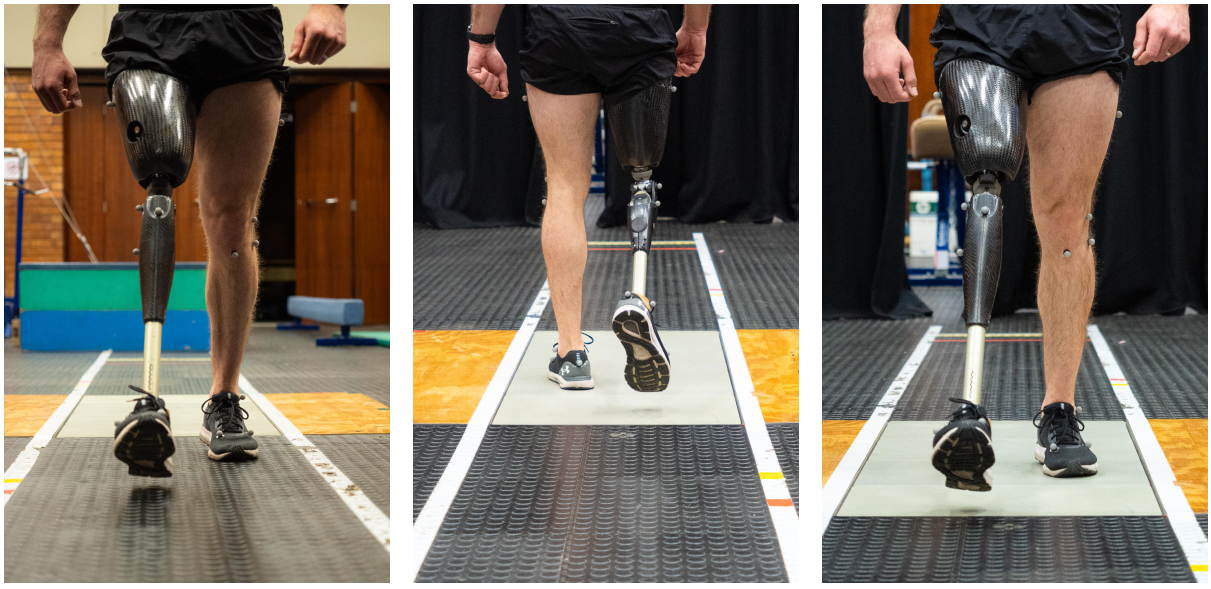

(a) Frame 1

(b) Frame 2

(c) Frame 3

Figure 5.5. Participant walking with the Ottobock Genium X3. Three frames selected from the gait cycle are shown for visual comparison with the 4BM's motion.

5.4. Data Processing Pipeline

5.4.1. Data gathering

The raw data from the QTM software were provided in tab delineated value files. There were files for the 200Hz kinematics files and files for the 2000Hz kinetics files. There were also files that identify the heel strike (HS) and toe off(TO) events. Data processing was performed using custom Python scripts to prepare values for further analysis and plotting.

5.4.2. Filtering and sorting

First, the files for 200Hz and 2000Hz were sorted and merged so that all of the 200Hz data was in one CSV file and the same for the 2000Hz files. The next step was to truncate and split these files according to the event times so that each of the gait cycles for left and right had its own CSV file, starting at HS and ending at the consecutive HS for that leg.

Following these steps, the files were filtered to check if there was a load in the z direction after the heel strike, so that those cycles were included for further evaluation. These files were then used along with the event times to compute the spatio temporal parameters. Furthermore, the joint angles and positions, among other parameters, were normalised and plotted.

5.4.3. Normalisation

In order to visualise the parameters as a function of the percentage of the gait cycle, the values were normalised. That means linear interpolation was used to reduce the raw data to 101 points so that the HS event was at both the beginning and the end of the gait cycle plot.

5.5. Outcome measures

The following outcome measures were selected to evaluate and compare the performance of the prosthetic knee and to calculate symmetry. Although other parameters were also recorded, they were not required for the evaluation of the main outcome measures defined for this study. Nevertheless, the plots for these parameters are included for completeness in Appendix B and Appendix C. Where applicable, parameter changes were reported in relation to the percentage completion of the gait cycle, shown in Fig. 5.6.

5.5.1. Kinetic and Kinematic Outcome Measures

Certain kinetic and kinematic outcome measures were selected to evaluate the function of the knee during a single stride event of the gait cycle (from the 0% HS to the 100% HS):

- Knee flexion angle
- Hip flexion angle
- Toe height
- Vertical ground reaction force
- Hip angular velocity

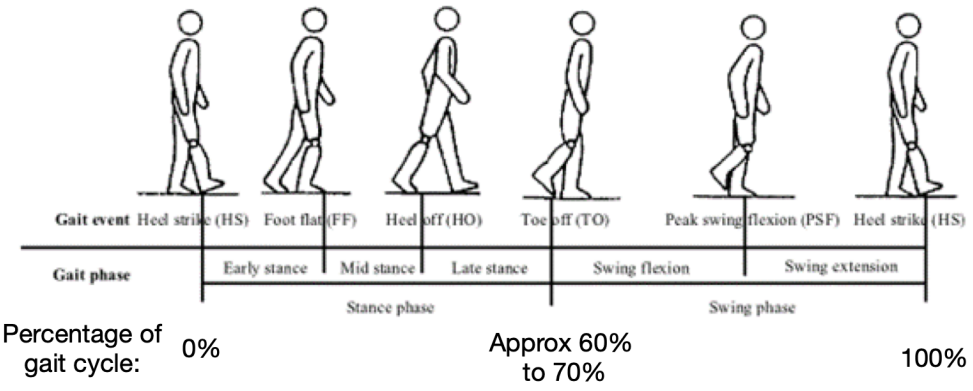

Figure 5.6. Human gait cycle showing percentage completion between subsequent heel strikes, with toe off usually between 60% and 70% depending on the subject (adapted from [23])

5.5.2. Spatio-temporal Outcome Measures

Spatio-temporal outcome measures were calculated for each leg and selected to evaluate the ambulatory function of the knee during sustained walking (thus, for multiple strides):

- Stride time: the time between two consecutive heel strikes of the same foot.
- Speed: foot progression velocity, stride length/ stride time.
- Step length: the distance between the heel strike of one foot and the next heel strike of the opposite foot.
- Step time: the time between the heel strike of one foot and the next heel strike of the opposite foot.
- Steps/minute: cadence, 60 x (number of detected steps/ duration of the trial [s])
- Stride length: the distance between two consecutive heel strikes of the same foot.
- Stance time: time between heel strike and the next toe off of the same foot.
- Swing time: time between toe off and the next heel strike of the same foot.

5.5.3. Evaluation criteria

To evaluate the performance of the knees, the symmetry between the healthy limb and the prosthesis was calculated and compared. The kinetic and kinematic outcome measures used cross correlation while the spatio temporal outcome measures used the symmetry index. The data from the Ottobock Genium X3 device of the participant served as a baseline for the comparison.

5.6. Results

5.6.1. Kinetic and Kinematic Plots

The following plots show the kinematic and kinetic parameters for both legs as a function of the percentage of the gait cycle, for both the 4BM prototype and the Genium X3. The healthy leg side is the left hand side (plotted in blue) and the prosthesis side is the right hand side (plotted

in orange). In the bottom left corner of each plot, it specifies how many gait cycles were used to calculate the distribution of values in the plot. The vertical dotted line of the corresponding colour indicates where the toe off event occurred. The shaded outline of each curve shows its standard deviation.

Fig. 5.7 shows the **knee flexion angle**. Both plots show that the stance phase for the prosthesis side was shorter than for the healthy limb, and this pattern continued for the rest of the parameters as well. It should be noted that the mechanical knee had a greater maximum flexion than the Genium. In contrast, the Genium X3 has early stance flexion (seen around 20°) enabled by the micro-processor controller to improve comfort, while the 4BM prototype does not.

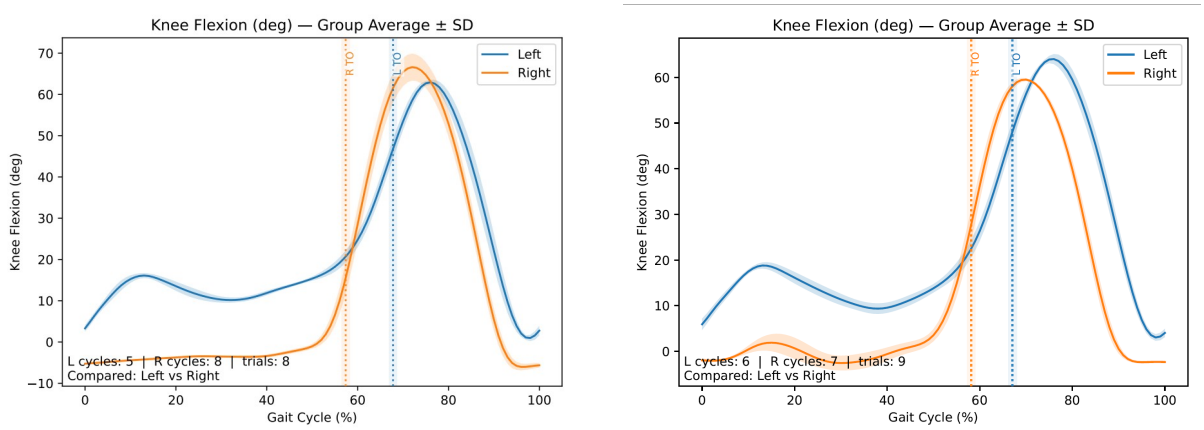

(a) Prototype mechanical knee **(b)** Genium X3

Figure 5.7. Knee flexion angle over the gait cycle for the prototype mechanical knee and the Genium X3 at self-selected walking speed.

Fig. 5.8 shows that the range of motion, as indicated by the **hip flexion angle**, for both prostheses was somewhat greater than that of the healthy limb.

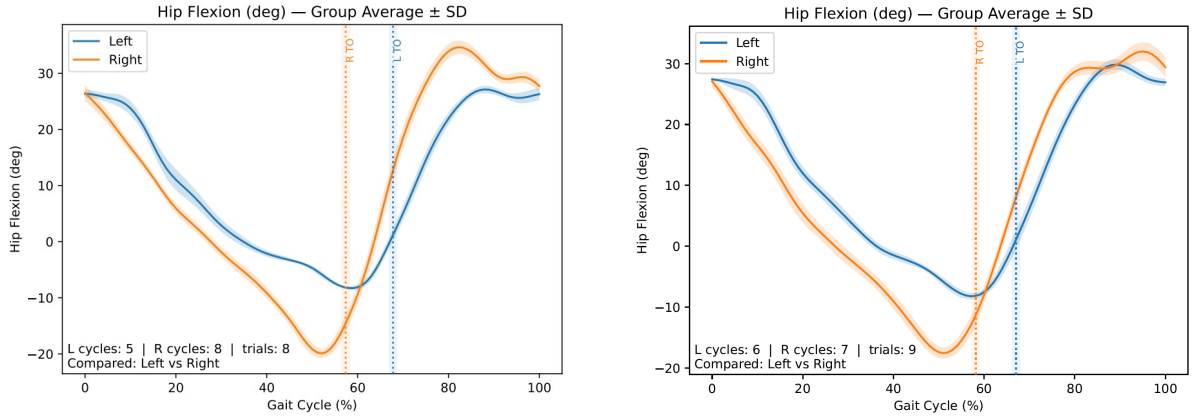

(a) Prototype mechanical knee **(b)** Genium X3

Figure 5.8. Hip flexion angle over the gait cycle for the prototype mechanical knee and the Genium X3 at self-selected walking speed.

Fig. 5.9 clearly shows that the four bar mechanism has **toe height** ground clearance that is comparable with both the Genium X3 and the healthy limb. This is beneficial because it shows that the risk of stumbling is on the same level as with the healthy limb.

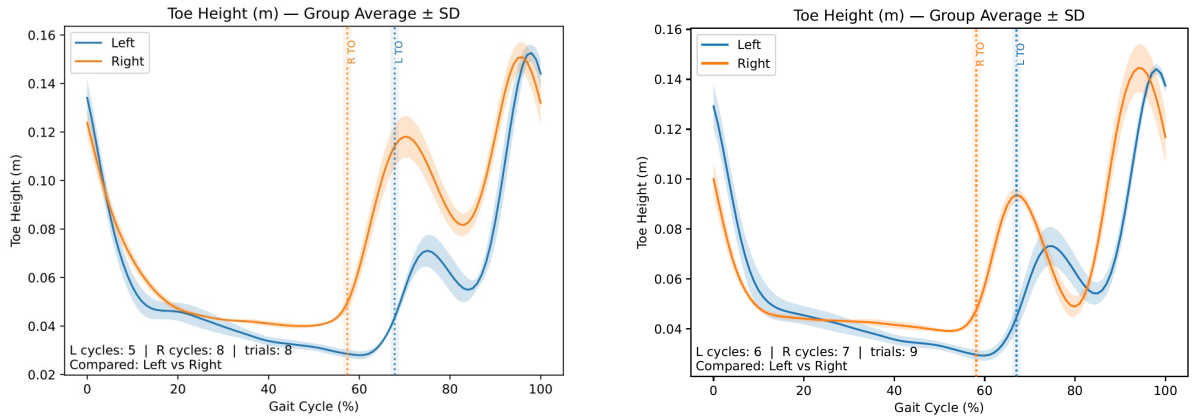

(a) Prototype mechanical knee **(b)** Genium X3

Figure 5.9. Toe height over the gait cycle for the prototype mechanical knee and the Genium X3 at self-selected walking speed.

Fig. 5.10 shows that the dynamic **ground reaction force** for both prostheses peaked slightly above the static body weight of the participant. This is indicative of the trust of the participant in the prostheses to support his weight safely during the stance phase.

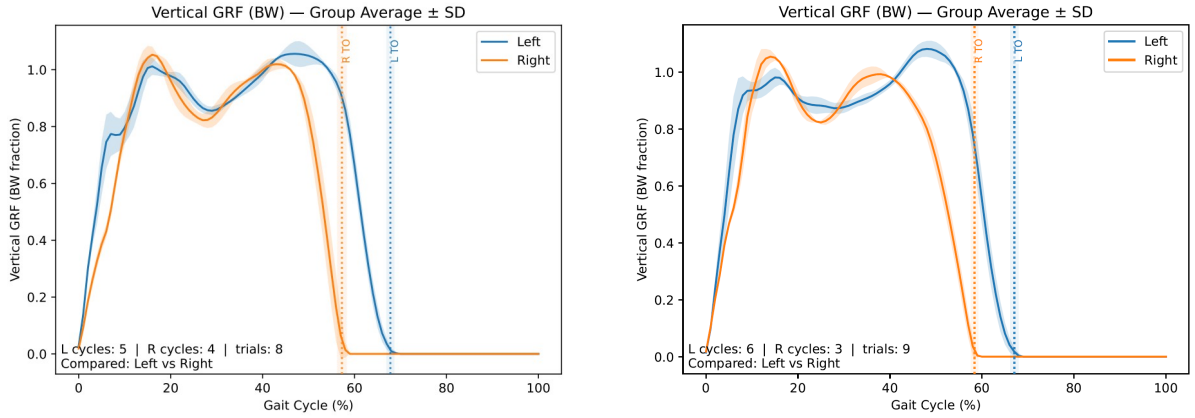

(a) Prototype mechanical knee **(b)** Genium X3

Figure 5.10. Vertical ground reaction force (normalised to body weight) over the gait cycle for the prototype mechanical knee and the Genium X3.

Fig. 5.11 illustrates that the maximum **angular velocity of the hip** was notably higher for the 4BM prosthesis than for the Genium X3. This occurred because the participant naturally needs to engage the hip muscles more with a prosthetic limb than with a healthy limb, but also due to the 4BM's constant damping factor and the lack of an extension assist mechanism.

During the swing phase, the participant exerted additional force to overcome the resistance of the friction pad to ensure full extension of the prototype knee. In comparison, the Genium X3 controller can determine the limb's position within the gait cycle and adjust its forward and backward damping resistance accordingly, reducing the hip moment required from the participant. This highlights the advantage of a knee mechanism with damping settings that can be adjusted depending on how much the knee flexes in the swing or stance phases.

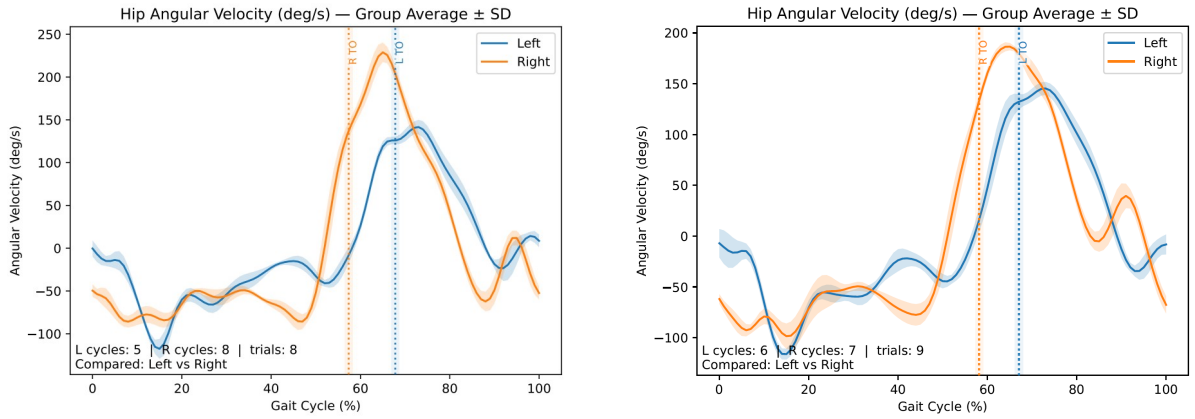

(a) Prototype mechanical knee **(b)** Genium X3

Figure 5.11. Hip angular velocity over the gait cycle for the prototype mechanical knee and the Genium X3.

5.6.2. Cross correlation results

Fig. 5.12 is an example of cross-correlation plots that were made for all kinetic and kinematic parameters. At the bottom of the plot is a summary of the signed lag, phase offset, and maximum r value. The rest of the cross correlation plots can be found in Appendix B and Appendix C.

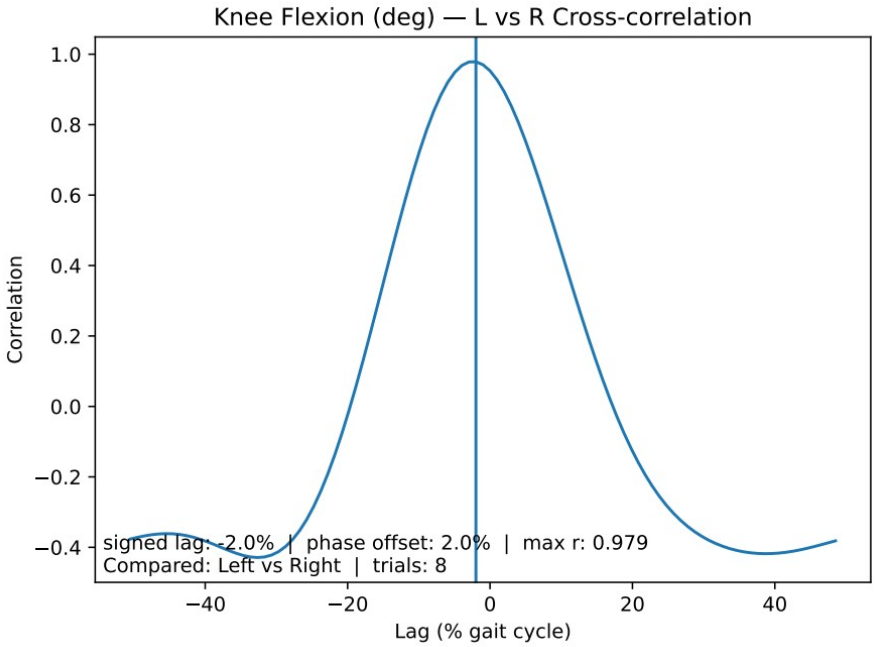

Figure 5.12. Cross correlation of Knee Flexion across gait cycle with 4BM knee prototype

Table 5.1 summarises the cross-correlation analysis between the prosthetic limb and the healthy limb. The average maximum r values for both the prototype and the Genium X3 are very close to 1, indicating that each prosthetic limb replicates the overall waveform shape of the healthy limb with high fidelity.

A perfectly matched signal would yield $r = 1$ with a lag of 0%. As expected, the Genium X3 achieves a slightly higher average correlation coefficient; however, the prototype shows a shorter

temporal lag, with an average of −4% compared to the Genium X3's −5%. This places the prototype approximately one percentage point closer to ideal symmetry.

Table 5.1. Cross-correlation results for the mechanical prototype and Genium X3

	Mechanical Prototype		Genium X3	
Parameter	Max r	Signed lag	Max r	Signed lag
Knee Flexion	0.979	-2%	0.986	-5%
Hip Flexion	0.990	-5.9%	0.994	-5%
Ground Reaction Force	0.929	-4%	0.927	-3%
Hip Angular velocity	0.955	-5.9%	0.956	-6.9%
Toe Height	0.887	-3%	0.959	-5%
Average	0.948	-4%	0.964	-5%

5.7. Spatio-temporal Results

Table 5.2 and Table 5.3 summarise the results of the spatio-temporal parameters. The parameter values for the left- and right hand sides are reported as ***average value, unit, ±standard deviation, (count)***. The Symmetry Index (SI%) for each parameter is in the last column. The perfect left/right symmetry would have an SI of 0%.

The Genium X3 was expected to perform better than the mechanical prototype, and that was indeed the case. With the Genium X3, the participant therefore walked faster and had a longer stance time on the prosthetic. However, what was surprising and encouraging was that the SI indexes for the chosen parameters were very similar between the 4BM prototype knee and Genium X3.

It should be pointed out that the SIs for the stance time and swing time were the largest for both the Genium X3 and the mechanical prototype. This was expected because, as was seen in the kinematics results, the participant consistently favoured his healthy limb in the stance phase, albeit only marginally.

Table 5.2. Spatio-temporal results for the 4BM prototype mechanical knee

Parameter	Units	Left	Right	SI[%]
Stride Time	s	1.36 ± 0.04 (5)	1.34 ± 0.04 (8)	1.34
Speed	m/s	1.09 ± 0.03 (5)	1.10 ± 0.05 (8)	1.68
Step Length	m	0.71 ± 0.02 (8)	0.72 ± 0.03 (13)	10.14
Step Time	s	0.62 ± 0.03 (13)	0.7 ± 0.02 (8)	14.94
Steps/Minute	steps/min	96.49 ± 4.57 (13)	82.96 ± 3.21 (8)	15.08
Stride Length	m	1.48 ± 0.03 (8)	1.48 ± 0.05 (13)	0.32
Stance Time	s	0.92 ± 0.02 (5)	0.77 ± 0.04 (5)	18.10
Swing Time	s	0.44 ± 0.02 (5)	0.57 ± 0.03 (5)	26.36

Table 5.4 compares the stance and swing phases as a percentage of the stride time. For people with both healthy limbs, the normal gait split is that the stance phase is ≈ 60% and the swing phase is ≈ 40% of the stride time. It was evident that the participant in the case study preferred his healthy limb during the stance phase, but both prostheses were remarkably close to the normal gait split, indicating comfortable use of the devices.

Table 5.3. Spatio-temporal results for the Genium X3

Parameter	Units	Left	Right	SI[%]
Stride Time	s	1.28 ± 0.028 (6)	1.26 ± 0.033 (7)	1.83
Speed	m/s	1.11 ± 0.035 (6)	1.14 ± 0.064 (7)	2.19
Step Length	m	0.706 ± 0.025 (8)	0.653 ± 0.028 (13)	10.85
Step Time	s	0.579 ± 0.014 (13)	0.693 ± 0.020 (4)	17.82
Steps/Minute	steps/min	103.648 ± 2.412 (13)	86.710 ± 2.638 (8)	17.80
Stride Length	m	1.429 ± 0.026 (6)	1.434 ± 0.036 (7)	0.34
Stance Time	s	0.861 ± 0.020 (6)	0.731 ± 0.029 (4)	16.28
Swing Time	s	0.422 ± 0.014 (6)	0.526 ± 0.015 (4)	21.87

Table 5.4. Comparison of stride, stance, and swing phase durations for the prototype and Genium X3 knees relative to the contralateral healthy limb (self-selected speed).

	Prototype		Genium X3	
	Healthy	Prosthesis	Healthy	Prosthesis
Stride Time (s)	1.36	1.34	1.28	1.26
Stance Time (s)	0.92 (68%)	0.77 (57%)	0.86 (67%)	0.73 (58%)
Swing Time (s)	0.44 (32%)	0.57 (43%)	0.42 (33%)	0.53 (42%)

5.8. Discussion

The aim of this study was to design and manufacture a cost effective mechanical prosthetic knee that still allowed good gait performance. The experimental evaluation was performed to evaluate the functional performance of the prototype in a controlled setting relative to the participant's daily-use prosthesis and was not intended to be a clinical trial. As the testing of both devices used a "within-subject comparison"[2], it is reasonable to assume that any differences observed in the data are due to differences related to the specific prosthetic knee used.

5.8.1. Kinematic and Kinetic Results

The prototype showed appropriate knee flexion during the swing phase, but not during the stance phase. This was because the prototype lacks an early-stance flexion mechanism. Nevertheless, the overall shape and timing of knee flexion were very similar to those of the healthy limb and did not hinder functional use. This was validated by a correlation coefficient of 0.979 and a phase delay of only -2%.

The hip flexion and angular acceleration graphs showed only modest compensatory hip motion compared to the Genium X3. The usage patterns were very similar to the healthy limb and therefore acceptable.

The toe clearance of the prototype was greater than that of the healthy limb and Genium X3. This is promising because it reduces the risk of tripping on uneven terrain or small obstacles. The toe clearance is greater than that calculated in the link segment model, but can in part be attributed to compensatory hip motion by the participant.

The vertical GRF plot showed the characteristic double-peak pattern and the loading symmetry was acceptable.

[2]Experimental design where the same participant is exposed to all different conditions.

In general, therefore, these results argue for the functional success of the design from a gait biomechanics perspective.

5.8.2. Cross-correlation Results

The total average correlation coefficient for the prototype was 0.948 with an average lag of -4%. This finding suggests that the limb with the 4BM mechanical knee moved in a way very similar to the healthy limb. In some metrics, the lag was even slightly closer to ideal than the Genium X3. However, on average, the Genium X3 still performed better, but similar performance levels between the two prostheses are encouraging.

5.8.3. Spatio-temporal results

The symmetry indices obtained with the prototype closely matched those observed with the Genium X3 across nearly all evaluated parameters. The walking speeds were similar for the participant when using either prosthetic knee. In addition, the swing-to-stance phase ratios approximated those typical of a normal gait. Collectively, these findings indicate that the prototype did not cause any substantial temporal gait deviations. From a functional point of view, the overall gait performance of the prototype is comparable to that of the considerably more advanced commercial prosthetic knee.

5.8.4. Cost-effectiveness Argument

The material and machining cost of the prototype was $\approx$ R22 000 while microprocessor controlled knees can cost upward of R500000 [3]. The purpose of this study's design was not to replicate the advanced control capabilities of a microprocessor knee, but to achieve acceptable functional gait performance at a substantially lower manufacturing cost. Within the limited scope of this evaluation, the prototype demonstrated gait symmetry, phase timing, and waveform similarity that were unexpectedly close to those obtained with a state-of-the-art commercial device.

From a cost to performance perspective, the prototype shows a favourable trade-off. For a radically lower manufacturing cost, it achieved functional level-ground gait patterns that are surprisingly close to those observed with the premium commercial knee. It is important to emphasise that this finding applies specifically to controlled, level-ground walking, and the broader functional benefits of microprocessor knees fall outside the scope of this study.

5.8.5. Limitations

The scope of this experimental evaluation was limited to functional gait performance in a controlled setting. There was only one participant, which limits the generalisability of the results and may also incur bias . The trials were on level ground, in a straight line and at self-selected speeds. Therefore, the performance of the knee in other settings, such as stairs, uneven terrain, or slopes, is not known. No formal qualitative feedback was obtained from the participant on parameters such as comfort, perceived effort, pain experienced, or preference.

Furthermore, the prototype was not robustly tested over a long period of time for fatigue or environmental durability. Additionally, no metabolic or energetics tests were conducted to establish the energy expenditure associated with walking with the prototype. These limitations are important because microprocessor knees provide advanced features, such as adaptive

stance control, stumble recovery, and variable damping, which extend functionality beyond level-ground walking. Therefore, the present study evaluated only a narrow aspect of prosthetic knee performance and its conclusions must be interpreted within that restricted context.

5.9. In summary

The experimental evaluation showed that the prototype satisfied the following requirements as laid out in subsection 3.3.1.

- **1. Stability:** no buckling events were observed during the tests.
- **2. Toe clearance:** the average minimum toe height during the swing phase was greater than that of the healthy limb.
- **4. Gait symmetry:** The prototype demonstrated gait symmetry, phase timing, and waveform similarity that were unexpectedly close to those obtained with a state-of-the-art commercial device.
- **6. Structural strength:** no material or structural failure occurred during the tests.
- **7. Adjustability:** The participant could successfully adjust and align the prosthesis to his satisfaction.

6. Conclusion and Recommendations

6.1. Introduction

This chapter will summarise how each research objective was completed, how the work followed the RVM progression, and what the limitations and recommendations are for future work.

6.2. Restatement of problem, aim and objectives

6.2.1. Problem Statement

The limited functionality of a typical low-cost knee prosthesis results in poor gait performance and subsequently leads to reduced quality of life due to adverse health outcomes. Several concepts and methods are used in premium knees to improve functional performance (e.g. stance-phase locking and swing-phase damping), but due to high costs and specialised maintenance from international suppliers, few patients can be helped with these devices. Therefore, the problem in South Africa is restricted access to cost-effective prosthetic knees with functional gait performance, exacerbated by the lack of expertise in the local design and manufacture of these prostheses.

6.2.2. Aim

This study aims to expand the local knowledge base by designing, manufacturing, and functional testing of a cost-effective mechanical prosthetic knee with swing-phase damping and stance-phase locking that facilitates functional gait performance.

6.2.3. Objectives

Specific objectives that support the aim of this study are as follows.

1. **Review** the relevant literature on prosthetic knees to identify key design challenges, potential solutions, and to select a suitable knee concept.
2. **Design and manufacture** a cost-effective mechanical prosthetic knee prototype using appropriate modelling, simulation, and engineering tools.
3. **Test** the prototype through a controlled case study, using 3D motion capture technology to analyse lower-limb gait kinematics.
4. **Validate** the performance of the prototype against functional outcome measures and compare it with an existing commercial device.

6.3. How each objective was achieved

6.3.1. Completed Research Verification Matrix

Fig. 6.1 shows the completed RVM and illustrates the progression from a research need to a research solution for all five research challenges (RCs), with more detail given in the following sections. The downward arrows indicate the synthesis direction, while the upward arrows indicate the analysis direction.

6.3.2. Objective 1: Literature Review

Review the relevant literature on prosthetic knees to identify key design challenges, potential solutions, and to select a suitable knee concept. This objective formed the analysis phase in the QRM framework. A review of the literature was conducted where research challenges were investigated and concept solutions were formulated. Table 6.1 summarises the research challenges and their corresponding concept solutions. Therefore, Objective 1 was achieved.

6.3.3. Objective 2: Design and Manufacturing

Design and manufacture a cost-effective mechanical prosthetic knee prototype using appropriate modelling, simulation, and engineering tools.

This objective formed part of the synthesis phase of the QRM. The concept solutions for RC1, RC2, and RC4 were used to design and manufacture the physical prototype knee.

A voluntary control, four-bar mechanism was identified as the most appropriate type of knee. A mathematical model was implemented in MATLAB to evaluate the candidate link geometry link configurations for ICR positions, flexion factors, and ground clearance. It was established that the chosen link geometry satisfied the conditions for stability, voluntary control, flexion range, and ground clearance.

This geometry was then used as a starting point to design a physical prototype. The design considerations identified in the concept solution for RC2 were then used as guiding design principles to satisfy the requirements outlined in Section 3.3.1. An iterative design process was followed until the mechanism satisfied the fit, form, and function requirements. Full mechanical optimisation was outside of the scope of this study. Siemens NX 2312 was used for CAD modelling, motion and force study, and limited FEA analysis. The strength, weight and stability requirements were met, and the design was manufactured from suitable materials using a combination of a CNC machine and a precision lathe.

The resulting artefacts of the synthesis phase were the MATLAB-based 4BM Design Tool with which to rapidly evaluate candidate four-bar knee geometries, and a physical prototype knee mechanism that satisfied the requirements and abided by the design considerations identified in the analysis phase. The prototype cost $\approx$ R22000 in material and machining expenses and weighed 1.33 kg. It has stance-phase locking due to the link geometry and an adjustable friction damping mechanism. Features were included to allow adjustment of alignment and stability. Therefore, Objective 2 was achieved.

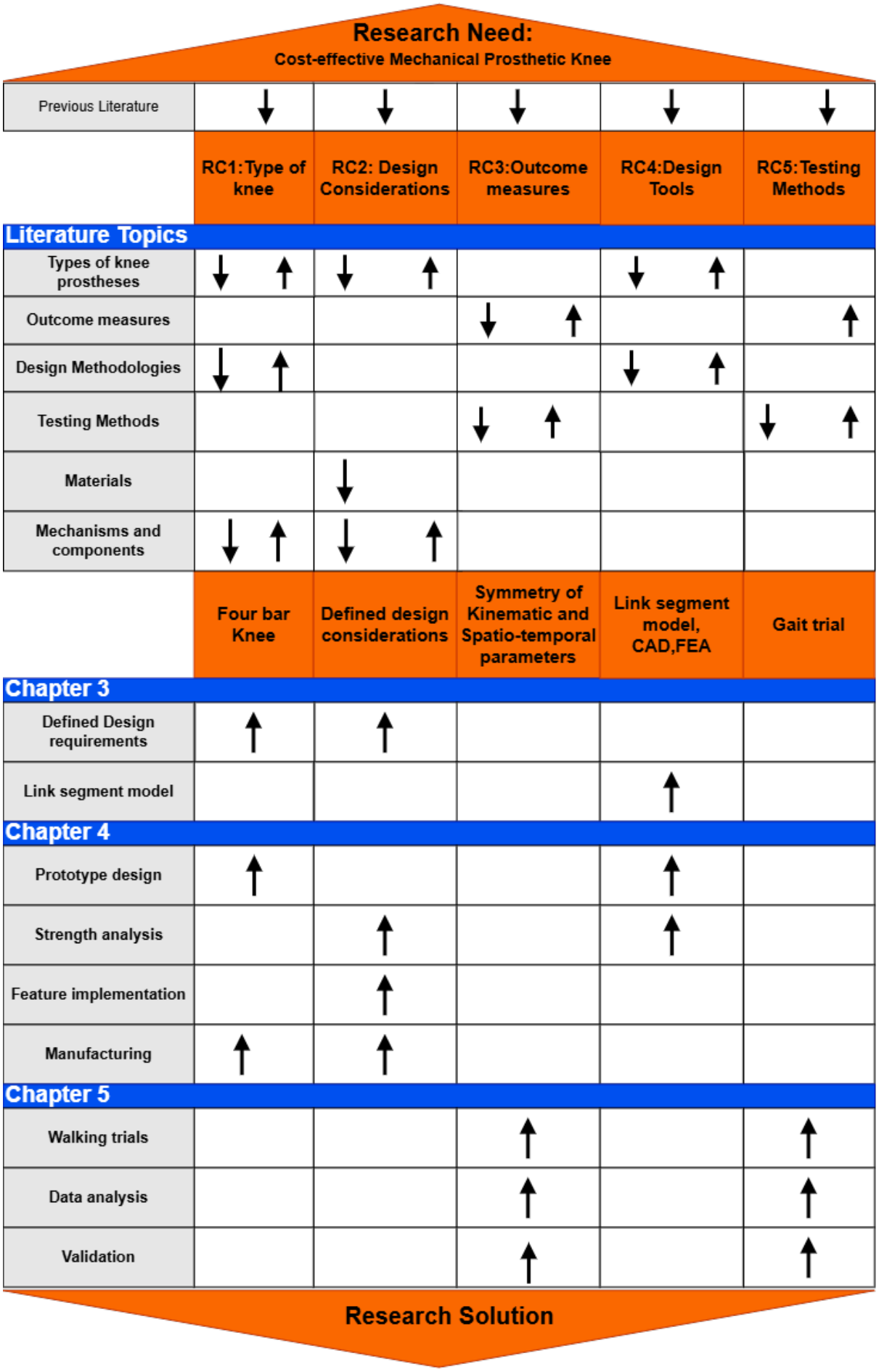

Figure 6.1. Completed Research Verification Matrix for 4BM prosthetic knee development.

Table 6.1. Research Challenges and Corresponding Solutions for Objective 1

RC #	Research Challenge	Solution Applied
RC1: Type of Knee	Identify the most appropriate knee mechanism for a low-cost, functional prosthetic design, considering stance stability, swing-phase behaviour, ground clearance, cost, and maintenance constraints.	Adopted a four-bar mechanism (4BM) knee with frictional damping. This configuration supports voluntary control, provides stance-phase locking, swing-phase damping, and increased toe clearance. Elevated-ICR and hyper-stable variants were considered, but a voluntary-control 4BM was selected as best for this study's objectives.
RC2: Design Considerations	Define the key mechanism-level parameters governing performance (stability features, ROM, toe clearance, damping behaviour, alignment, and manufacturability). Material choices, maintainability, and weight constraints must also be balanced.	Integrated stance-phase locking, frictional swing damping, and favourable ground clearance into the 4BM geometry. Used cost-effective materials, simple manufacturable geometry, standard fasteners, low mass envelope, and adjustable alignment and damping features to ensure practicality and maintainability.
RC3: Outcome Measures	Select clinically meaningful and feasible metrics to evaluate functional gait performance of the prototype relative to a benchmark device.	Used gait symmetry as the core performance construct. Applied the Symmetry Index (SI) for spatio-temporal metrics (stride time, speed, cadence, stance time, swing time, step length) and cross-correlation for comparing waveform similarity (joint angles, hip angular velocity, vertical GRF, toe height).
RC4: Design Tools	Identify modelling and simulation tools capable of supporting rapid iteration, design-space exploration, and structural verification within resource constraints.	Developed a MATLAB link-segment model (from [1]) for geometry screening. Used Siemens NX 2312 for parametric CAD, motion study, and mechanism simulation. Applied FEA to verify structural integrity under expected static force loadings.
RC5: Testing Methods	Determine an evidence-generating testing approach that is feasible, ethical, and able to validate whether the prototype achieves functional gait performance.	Conducted a controlled gait-trial case study with a single experienced prosthesis user. Collected full gait data using both the user's microprocessor knee (baseline) and the prototype. Used this comparison to assess functional performance and identify areas for improvement.

6.3.4. Objective 3: Test and Evaluation

Evaluate the functional performance of the prototype knee using a controlled human gait trial, with 3D motion capture technology to analyse lower-limb gait kinematics. This is part of the testing and evaluation phase of the QRM framework. The RC5 concept solution was used to test the prototype. The outcome measures identified From RC3 were used to evaluate the performance.

A controlled human gait trial with one participant was conducted to test the prototype. Qualysis motion capture technology and software were used to capture lower body gait kinematics using the IOR marker set. The test consisted of level ground walking at self selected speeds in a controlled laboratory setting. A combination of kinematic, kinetic, and spatio-temporal parameters was recorded. The gait symmetry was quantified with cross-correlation for kinetic and kinematic parameters and symmetry index for spatio-temporal parameters. Thus, achieving Objective 3.

6.3.5. Objective 4

Evaluate the performance of the prototype against functional outcome measures and compare it with an existing device.

Similarly to Objective 3, this is part of the testing and evaluation phase of the QRM framework. Data for the participant's standard prosthetic knee (an Ottobock Genium X3 microprocessor knee) were collected using exactly the same testing procedure that had been applied to evaluate the prototype, ensuring direct comparability between the two devices and testing conditions.

Although the participant walked marginally faster and had better overall gait symmetry while walking with the Genium X3, both the cross-correlation and SI results of the prototype were surprisingly similar to those of the much more advanced microprocessor-controlled knee.

The average correlation coefficient (r) for the prototype was 0.948 and 0.964 for the Genium X3 and was very close to ideal symmetry. For the 4BM prototype, the SI values of the spatio-temporal parameters varied from 0.32% for stride length to 26.36% for swing time. For the Genium X3, the corresponding SI values for stride length and swing time were 0.34% and 21.87%, respectively. The participant consistently spent more time on his healthy limb during the stance phase, explaining the swing time asymmetry. Additionally, the swing/stance ratio for the prototype and Genium X3 was closer to the ideal 40%/60% split of a normal gait cycle than the healthy limb. Furthermore, the toe clearance for the 4BM prototype was higher than that of the healthy limb and the Genium X3. Taking into account all the evidence, Objective 4 can also be deemed successfully completed.

6.4. Contribution to Knowledge and Practice

Academic Contributions

This study proposes a validated design framework and testing methodology that can be used in future studies on the design of a cost-effective mechanical prosthetic knee. Furthermore, it adds experimental evidence of the performance of a voluntary control four bar knee under controlled circumstances.

Practical contributions

The MATLAB design tool developed in this study can be used for future design developments of four bar knees. The physical prototype is also an artefact that can be used in future studies for research. In addition, the study gave insight to engineers designing mechanical prosthetic knees for the South African context.

6.5. Limitations

Although the limitations listed here fall mostly outside the formal scope of the study, it is still important to mention them.

- Limited mechanical and structural optimisation of the design. Further refinements could reduce weight and cost and improve manufacturability.
- A top-down approach was used with the 4BM Design Tool, where literature values were adopted instead of a bottom up approach, where parameters were optimised. Consequently, there may be alternative parameter combinations that facilitate improved performance.
- Single participant case study, which limits the generalisability of results.
- Level ground gait trials only mean that performance is unknown for other conditions.
- The scope of prototype development was restricted to achieving and demonstrating functional gait performance, but not necessarily long term durability.
- The prototype was not tested for structural design compliance with ISO 10328.

6.6. Recommendations for Future Work

In light of the limitations listed above, the following recommendations are for future work.

- Perform complete mechanical and structural optimisation to reduce weight and cost and improve manufacturability and ease of maintenance.
- Investigate the applicability of using the 4BM Design Tool for the development of other mechanical knees with different control strategies, for use by amputees with a broader variety in their activity level requirements.
- Conduct gait trials with multiple participants.
- Conduct gait trials over uneven terrain or climbing stairs.
- Conduct complete ISO 10328 structural compliance testing.

6.7. Conclusion

Overall, the 4BM mechanical knee prototype achieved the aim set at the beginning of this study. It expanded the local knowledge base by designing, manufacturing and testing a cost effective mechanical prosthetic knee with swing phase damping and stance phase locking that facilitated functionally acceptable gait patterns.

The prototype demonstrated consistent and physiologically appropriate gait behaviour at a substantially lower cost than that of a high-end microprocessor-controlled knee. Therefore, the findings of this research study fully support the feasibility of locally manufactured, affordable knee prostheses for transfemoral amputees, while adhering to "Appropriate Technology Use" as defined by the World Health Organisation.

Bibliography

[1] T. Anand and S. Sujatha, "A method for performance comparison of polycentric knees and its application to the design of a knee for developing countries," *Prosthetics & Orthotics International*, vol. 41, no. 4, pp. 402–411, Aug. 2017, ISSN: 0309-3646. DOI: 10.1177/0309364616652017. (visited on 05/24/2023).

[2] B. E. Lawson, J. Mitchell, D. Truex, A. Shultz, E. Ledoux, and M. Goldfarb, "A Robotic Leg Prosthesis: Design, Control, and Implementation," *IEEE Robotics & Automation Magazine*, vol. 21, no. 4, pp. 70–81, Dec. 2014, ISSN: 1558-223X. DOI: 10.1109/MRA.2014.2360303.

[3] Grant McGimpsey and Terry C. Bradford, *Limb Prosthetics Services and Devices Critical Unmet Need: Market Analysis White Paper*, 2017.

[4] W. Liang, Z. Qian, W. Chen, *et al.*, "Mechanisms and component design of prosthetic knees: A review from a biomechanical function perspective," *Frontiers in Bioengineering and Biotechnology*, vol. 10, p. 950 110, Sep. 2022. DOI: 10.3389/fbioe.2022.950110.

[5] G. F. Vintimilla Leon, S. Ferrandiz Bou, C. M. Cobos Maldonado, and F. V. Pintado Albarracin, "Mechanical Design of a Knee Prosthesis for Transfemoral Amputation," in *2020 IEEE ANDESCON*, Oct. 2020, pp. 1–6. DOI: 10.1109/ANDESCON50619.2020.9271991.

[6] Z. Zhang, H. Yu, W. Cao, *et al.*, "Design of a Semi-Active Prosthetic Knee for Transfemoral Amputees: Gait Symmetry Research by Simulation," *Applied Sciences*, vol. 11, no. 12, p. 5328, 2021. DOI: 10.3390/app11125328. (visited on 04/13/2023).

[7] L. Galey and R. V. Gonzalez, "Design and Initial Evaluation of a Low-Cost Microprocessor-Controlled Above-Knee Prosthesis: A Case Report of 2 Patients," *Prosthesis*, vol. 4, no. 1, pp. 60–72, Mar. 2022, ISSN: 2673-1592. DOI: 10.3390/prosthesis4010007. (visited on 04/19/2023).

[8] V. N. M. Arelekatti, "Frameworks for the design of passive prosthetic knee components using user-centered methods and biomechanics of level-ground walking," Thesis, Massachusetts Institute of Technology, 2019. (visited on 11/26/2024).

[9] S. Pfeifer, A. Pagel, R. Riener, and H. Vallery, "Actuator With Angle-Dependent Elasticity for Biomimetic Transfemoral Prostheses," *IEEE/ASME Transactions on Mechatronics*, vol. 20, no. 3, pp. 1384–1394, Jun. 2015, ISSN: 1941-014X. DOI: 10.1109/TMECH.2014.2337514.

[10] H. Sun, C. He, and I. Vujaklija, "Design trends in actuated lower-limb prosthetic systems: A narrative review," *Expert Review of Medical Devices*, vol. 20, no. 12, pp. 1157–1172, Dec. 2023, ISSN: 1743-4440, 1745-2422. DOI: 10.1080/17434440.2023.2279999. (visited on 05/28/2025).

[11] X. Wang, Q. Meng, Z. Zhang, J. Sun, J. Yang, and H. Yu, "Design and evaluation of a hybrid passive–active knee prosthesis on energy consumption," *Mechanical Sciences*, vol. 11, no. 2, pp. 425–436, Nov. 2020, ISSN: 2191-916X. DOI: 10.5194/ms-11-425-2020. (visited on 05/16/2023).

[12] M. Jochan, S. Dharshini, and K. Ravikumar, "A REVIEW ON PROSTHETICS AND ORTHOTICS FOR AMPUTEES AND DISABLED," *Journal of Critical Reviews*, vol. 7, pp. 2175–2189, Jul. 2020.

[13] E. M. Balk, A. Gazula, G. Markozannes, *et al.*, *Table 1, Lower limb extremity prosthesis Medicare Functional Classification Levels (K levels)*, https://www.ncbi.nlm.nih.gov/books/NBK531517/t Text, Sep. 2018. (visited on 05/22/2023).

[14] J. Uchytil, D. Jandacka, D. Zahradnik, R. Farana, and M. Janura, "Temporal–spatial parameters of gait in transfemoral amputees: Comparison of bionic and mechanically passive knee joints," *Prosthetics and Orthotics International*, vol. 38, no. 3, pp. 199–203, Jun. 2014, ISSN: 0309-3646. DOI: 10.1177/0309364613492789. (visited on 01/18/2023).

[15] F. Rasheed, S. Martin, and K. M. Tse, "Design, Kinematics and Gait Analysis, of Prosthetic Knee Joints: A Systematic Review," *Bioengineering*, vol. 10, no. 7, p. 773, Jun. 2023, ISSN: 2306-5354. DOI: 10.3390/bioengineering10070773. (visited on 11/27/2025).

[16] J. W. Michael, "Modern Prosthetic Knee Mechanisms," *Clinical Orthopaedics and Related Research®*, vol. 361, p. 39, Apr. 1999, ISSN: 0009-921X. (visited on 01/16/2023).

[17] S. Viteckova, P. Kutilek, Z. Svoboda, R. Krupicka, J. Kauler, and Z. Szabo, "Gait symmetry measures: A review of current and prospective methods," *Biomedical Signal Processing and Control*, vol. 42, pp. 89–100, Apr. 2018, ISSN: 17468094. DOI: 10.1016/j.bspc.2018.01.013. (visited on 11/27/2025).

[18] J. Aviles, J. Castleberry, and M. L. Madigan, "Effects of a low-cost prosthetic knee on amputee gait over uneven and even terrains," *Prosthetics & Orthotics International*, vol. 49, no. 1, pp. 47–50, Feb. 2025, ISSN: 1746-1553. DOI: 10.1097/PXR.0000000000000400. (visited on 11/27/2025).

[19] J. E. W. Holm and G. P. Van Der Merwe, "QUALITY RESEARCH MANAGEMENT IMPROVES DESIGN RESEARCH EFFECTIVENESS," *South African Journal of Industrial Engineering*, vol. 30, no. 3, Nov. 2019, ISSN: 22247890. DOI: 10.7166/30-3-2246. (visited on 10/28/2024).

[20] T. Lenzi, M. Cempini, L. Hargrove, and T. Kuiken, "Design, development, and testing of a lightweight hybrid robotic knee prosthesis," *The International Journal of Robotics Research*, vol. 37, no. 8, pp. 953–976, Jul. 2018, ISSN: 0278-3649. DOI: 10.1177/0278364918785993. (visited on 01/18/2023).

[21] T. Schmalz, S. Blumentritt, and R. Jarasch, "Energy expenditure and biomechanical characteristics of lower limb amputee gait:: The influence of prosthetic alignment and different prosthetic components," *Gait & Posture*, vol. 16, no. 3, pp. 255–263, Dec. 2002, ISSN: 0966-6362. DOI: 10.1016/S0966-6362(02)00008-5. (visited on 10/28/2024).

[22] L. Guercini, F. Tessari, J. Driessen, *et al.*, "An Over-Actuated Bionic Knee Prosthesis: Modeling, Design and Preliminary Experimental Characterization," in *2022 International Conference on Robotics and Automation (ICRA)*, May 2022, pp. 5467–5473. DOI: 10.1109/ICRA46639.2022.9812197.

[23] W. Cao, H. Yu, W. Chen, Q. Meng, and C. Chen, "Design and Evaluation of a Novel Microprocessor-Controlled Prosthetic Knee," *IEEE Access*, vol. 7, pp. 178 553–178 562, 2019, ISSN: 2169-3536. DOI: 10.1109/ACCESS.2019.2957823.

[24] J. Perry and J. Burnfield, *Gait Analysis: Normal and Pathological Function*, 2nd ed. Boca Raton: CRC Press, Jun. 2024, ISBN: 978-1-003-52559-2. DOI: 10.1201/9781003525592. (visited on 09/18/2025).

[25] T. Varrecchia, M. Serrao, M. Rinaldi, *et al.*, "Common and specific gait patterns in people with varying anatomical levels of lower limb amputation and different prosthetic components," *Human Movement Science*, vol. 66, pp. 9–21, Aug. 2019, ISSN: 1872-7646. DOI: 10.1016/j.humov.2019.03.008.

[26] L. Van Tuan, "Evaluation of Trans-femoral Prosthesis Function Using Finite Element Analysis," Thesis, Shibuara Institute of Technology, Sep. 2017.

[27] World Health Organization and International Society for Prosthetics and Orthotics, "GUIDELINES FOR TRAINING PERSONNEL IN DEVELOPING COUNTRIES FOR PROSTHETICS AND ORTHOTICS SERVICES," World Health Organization, Geneva, Switzerland, Technical Report, 2004. (visited on 02/19/2025).

[28] C. W. Radcliffe, "Four-bar linkage prosthetic knee mechanisms: Kinematics, alignment and prescription criteria," *Prosthetics and Orthotics International*, vol. 18, no. 3, pp. 159–173, Dec. 1994, ISSN: 0309-3646. DOI: 10.3109/03093649409164401.

[29] P. Marisami and R. Venkatachalam, "Design and experimental validation of a high-performance polycentric prosthetic knee joint for transfemoral amputees in developing countries," *Journal of the Brazilian Society of Mechanical Sciences and Engineering*, vol. 45, no. 3, p. 146, Feb. 2023, ISSN: 1806-3691. DOI: 10.1007/s40430-023-04072-6. (visited on 07/09/2024).

[30] M. Koçak and E. Gezgin, "Unified Design Methodology for a Polycentric Transfemoral Knee Prosthesis Using Kinematic Synthesis," *Machines*, vol. 13, no. 1, p. 20, Jan. 2025, ISSN: 2075-1702. DOI: 10.3390/machines13010020. (visited on 05/28/2025).

[31] Y. Sun, W. Ge, J. Zheng, and D. Dong, "Design and Evaluation of a Prosthetic Knee Joint Using the Geared Five-Bar Mechanism," *IEEE Transactions on Neural Systems and Rehabilitation Engineering*, vol. 23, no. 6, pp. 1031–1038, Nov. 2015, ISSN: 1558-0210. DOI: 10.1109/TNSRE.2015.2401042.

[32] E. J. Rouse, L. M. Mooney, and H. M. Herr, "Clutchable series-elastic actuator: Implications for prosthetic knee design," *The International Journal of Robotics Research*, vol. 33, no. 13, pp. 1611–1625, Nov. 2014, ISSN: 0278-3649. DOI: 10.1177/0278364914545673. (visited on 01/18/2023).

[33] D. Wyss, "Evaluation and Design of a Globally Applicable Rear-locking Prosthetic Knee Mechanism," Thesis, Nov. 2012. (visited on 01/19/2023).

[34] J. Andrysek, "Lower-Limb Prosthetic Technologies in the Developing World: A Review of Literature from 1994–2010," *Prosthetics and Orthotics International*, vol. 34, no. 4, pp. 378–398, Dec. 2010, ISSN: 0309-3646. DOI: 10.3109/03093646.2010.520060. (visited on 10/24/2024).

[35] F. Mohanad, J. Chiad, and M. Enad, "Evaluation and Analysis of Different Types of Prosthetic Knee Joint Used by above Knee Amputee," *Defect and Diffusion Forum*, vol. 398, pp. 34–40, Jan. 2020. DOI: 10.4028/www.scientific.net/DDF.398.34.

[36] K. R. Kaufman, J. A. Levine, R. H. Brey, *et al.*, "Gait and balance of transfemoral amputees using passive mechanical and microprocessor-controlled prosthetic knees," *Gait & Posture*, vol. 26, no. 4, pp. 489–493, Oct. 2007, ISSN: 0966-6362. DOI: 10.1016/j.gaitpost.2007.07.011. (visited on 05/28/2025).

[37] S. Keeratihattayakorn, C. Virulsri, C. Ophaswongse, and P. Tangpornprasert, "Design and evaluation of a hydraulic mechanism with available components for passive knee prostheses," *Disability and Rehabilitation: Assistive Technology*, vol. 16, no. 2, pp. 144–151, Feb. 2021, ISSN: 1748-3107, 1748-3115. DOI: 10.1080/17483107.2019.1642396. (visited on 02/16/2023).

[38] H.-L. Xie, Z.-Z. Liang, F. Li, and L.-X. Guo, "The knee joint design and control of above-knee intelligent bionic leg based on magneto-rheological damper," *International Journal of Automation and Computing*, vol. 7, no. 3, pp. 277–282, Aug. 2010, ISSN: 1751-8520. DOI: 10.1007/s11633-010-0503-y. (visited on 01/18/2023).

[39] C. W. Radcliffe, *Biomechanics of Knee Stability Control with Four-Bar Prosthetic Knees*, Presentation, Melbourne, Austrailia, Nov. 2003.

[40] M. G. Bernal-Torres, H. I. Medellín-Castillo, and J. C. Arellano-González, "Design and Control of a New Biomimetic Transfemoral Knee Prosthesis Using an Echo-Control Scheme," *Journal of Healthcare Engineering*, vol. 2018, e8783642, Apr. 2018, ISSN: 2040-2295. DOI: 10.1155/2018/8783642. (visited on 01/17/2023).

[41] G. Waycaster, S.-K. Wu, and X. Shen, "Design and Control of a Pneumatic Artificial Muscle Actuated Above-Knee Prosthesis," *Journal of Medical Devices*, vol. 5, no. 3, p. 031 003, Sep. 2011, ISSN: 1932-6181, 1932-619X. DOI: 10.1115/1.4004417. (visited on 05/28/2025).

[42] J. Andrysek and G. Chau, "An Electromechanical Swing-Phase-Controlled Prosthetic Knee Joint for Conversion of Physiological Energy to Electrical Energy: Feasibility Study," *IEEE Transactions on Biomedical Engineering*, vol. 54, no. 12, pp. 2276–2283, Dec. 2007, ISSN: 1558-2531. DOI: 10.1109/TBME.2007.908309. (visited on 05/28/2025).

[43] S. Blumentritt, H. W. Scherer, J. W. Michael, and T. Schmalz, "Transfemoral Amputees Walking on a Rotary Hydraulic Prosthetic Knee Mechanism: A Preliminary Report:" *JPO Journal of Prosthetics and Orthotics*, vol. 10, no. 3, pp. 61–70, 1998, ISSN: 1040-8800. DOI: 10.1097/00008526-199801030-00005. (visited on 01/16/2023).

[44] Callister, William D. and Rethwisch, David G., *Materials Science and Engineering AN INTRODUCTION*, 10th ed. Hoboken, NJ: Wiley, 2020, ISBN: ISBN 9781119405436.

[45] R. K. Mohanty, R. C. Mohanty, and S. K. Sabut, "Design and analysis of polycentric prosthetic knee with enhanced kinematics and stability," *Physical and Engineering Sciences in Medicine*, vol. 46, no. 1, pp. 209–226, Mar. 2023, ISSN: 2662-4737. DOI: 10.1007/s13246-022-01211-6. (visited on 11/05/2025).

[46] M. F. Ashby, *Materials Selection in Mechanical Design*, 3rd ed. Amsterdam ; Boston: Butterworth-Heinemann, 2005, ISBN: 978-0-7506-6168-3.

[47] *Vesconite and Vesconite Hilube specifications and chemical resistance data*, https://vesconite.com/charts/s (visited on 11/05/2025).

[48] *Iglidur® J3, bar stock round bar*, https://www.igus.co.za/product/barstock_round_rod_J3?artnr=SFRJ3-1000. (visited on 11/05/2025).

[49] R. K. Mohanty, R. C. Mohanty, and S. K. Sabut, "A systematic review on design technology and application of polycentric prosthetic knee in amputee rehabilitation," *Physical and Engineering Sciences in Medicine*, vol. 43, no. 3, pp. 781–798, Sep. 2020, ISSN: 2662-4737. DOI: 10.1007/s13246-020-00882-3. (visited on 05/28/2025).

[50] V. G. M. Kooiman, E. S. van Staveren, R. A. Leijendekkers, *et al.*, "Testing and evaluation of lower limb prosthesis prototypes in people with a transfemoral amputation: A scoping review on research protocols," *Journal of NeuroEngineering and Rehabilitation*, vol. 20, no. 1, p. 1, Jan. 2023, ISSN: 1743-0003. DOI: 10.1186/s12984-023-01125-8. (visited on 02/22/2023).

[51] H. Richter, D. Simon, W. A. Smith, and S. Samorezov, "Dynamic modeling, parameter estimation and control of a leg prosthesis test robot," *Applied Mathematical Modelling*, vol. 39, no. 2, pp. 559–573, Jan. 2015, ISSN: 0307-904X. DOI: 10.1016/j.apm.2014.06.006. (visited on 10/28/2024).

[52] T. Seel, J. Raisch, and T. Schauer, "IMU-Based Joint Angle Measurement for Gait Analysis," *Sensors*, vol. 14, no. 4, pp. 6891–6909, Apr. 2014, ISSN: 1424-8220. DOI: 10.3390/s140406891. (visited on 06/24/2024).

[53] S. Manz, D. Seifert, B. Altenburg, T. Schmalz, S. Dosen, and J. Gonzalez-Vargas, "Using embedded prosthesis sensors for clinical gait analyses in people with lower limb amputation: A feasibility study," *Clinical Biomechanics*, vol. 106, p. 105 988, Jun. 2023, ISSN: 0268-0033. DOI: 10.1016/j.clinbiomech.2023.105988. (visited on 07/21/2023).

[54] M. Riveras, E. Ravera, A. F. Shaheen, D. Ewins, and P. C. Formento, "Spatio Temporal Parameters and Symmetry Index in Transtibial Amputees Wearing Prosthetic Feet with and without Adaptive Ankles," in *2019 Global Medical Engineering Physics Exchanges/ Pan American Health Care Exchanges (GMEPE/PAHCE)*, Mar. 2019, pp. 1–6. DOI: 10.1109/GMEPE-PAHCE.2019.8717362. (visited on 09/30/2025).

[55] D. H. K. Chow, A. D. Holmes, C. K. L. Lee, and S. W. Sin, "The Effect of Prosthesis Alignment on the Symmetry of Gait in Subjects with Unilateral Transtibial Amputation," *Prosthetics & Orthotics International*, vol. 30, no. 2, pp. 114–128, Aug. 2006, ISSN: 0309-3646. DOI: 10.1080/03093640600568617. (visited on 09/30/2025).

[56] V. Agrawal, R. Gailey, C. O'Toole, I. Gaunaurd, and T. Dowell, "Symmetry in External Work (SEW): A Novel Method of Quantifying Gait Differences Between Prosthetic Feet," *Prosthetics & Orthotics International*, vol. 33, no. 2, pp. 148–156, Jun. 2009, ISSN: 0309-3646. DOI: 10.1080/03093640902777254. (visited on 09/30/2025).

[57] D. Gouwanda and S. Arosha Senanayake, "Identifying gait asymmetry using gyroscopes—A cross-correlation and Normalized Symmetry Index approach," *Journal of Biomechanics*, vol. 44, no. 5, pp. 972–978, Mar. 2011, ISSN: 00219290. DOI: 10.1016/j.jbiomech.2010.12.013. (visited on 11/27/2025).

[58] *MATLAB*, Mathworks, Natick, Massachusetts, United States of America, 2025.

[59] *SiemensNX 2312*, Siemens, Germany, 2023.

[60] I. Thomson, *Design considerations for prosthtic knees*, Ongoing conversation, consultations, 2024,2025.

[61] Ottobock, *Genium X3 — Choose powerful versatility*, https://www.ottobock.com/en-hk/product/3B5-3-61070. (visited on 11/27/2025).

[62] Raise3D, *Raise3D Pro3 Dual Extruder 3D printer*, https://www.raise3d.com/pro3-series/. (visited on 11/27/2025).

[63] *ISO10328:2016 Prosthetics — Structural testing of lower-limb prostheses — Requirements and test methods*, Standard, Geneva, Switzerland, Jun. 2016.

[64] T. Taljaard and T. Van Niekerk, *Machinist input*, Consultations, 2025.

[65] Qualisys, *QualisysMotion capture*, https://www.qualisys.com/, Sep. 2013. (visited on 11/27/2025).

[66] A. Leardini, Z. Sawacha, G. Paolini, S. Ingrosso, R. Nativo, and M. G. Benedetti, "A new anatomically based protocol for gait analysis in children," *Gait & Posture*, vol. 26, no. 4, pp. 560–571, Oct. 2007, ISSN: 0966-6362. DOI: 10.1016/j.gaitpost.2006.12.018. (visited on 11/18/2025).

A. Four-bar Mechanism Design Tool Scripts

The following MATLAB script is an implementation of the calculations in Chapter 3. This design tool allows the user to iterate on the lengths and angles of the links and calculate the ICR, the flexion factor, the hip moment, and the leg length variability in the specified flexion range.

```
% Main script

% Lengths of the links
a = 66; % Length of link OA
b = 30;% Length of link AB
c = 56; % Length of link BC
d = 45; % Length of link OC

P = 1200; % 1.2 * bodyweight Load in N

CP_heelstrike = [-50, -500]; % Centre of pressure at heelstrike
CP_toe_off = [100, -500]; % Centre of pressure at toe off
toe_coordinates = [200,-500];

% Initial angle in radians
theta1 = deg2rad(26); % Initial angle of link OC and the x-axis in radians

% User-specified initial value and range for theta3
initial_theta3 = deg2rad(18); % Specify the initial value for theta3 in degrees
    and convert to radians
theta3_range_start = initial_theta3; % Start of theta3 range in degrees and
    convert to radians
theta3_range = deg2rad(140);
theta3_range_end = initial_theta3 + theta3_range; % End of theta3 range in
    degrees and convert to radians

% Time steps for simulation
t = linspace(theta3_range_start, theta3_range_end, 100); % Example time steps
    based on theta3 range
%knee_flexion_angle = linspace(0,theta3_range,50);

% Initialize arrays to store positions, ICRs,
x_heelstrike = zeros(1, length(t));
y_heelstrike = zeros(1, length(t));
x_toe_off = zeros(1, length(t));
y_toe_off = zeros(1, length(t));

L_heelstrike = zeros(1, length(t)); % Length from hip to centre of pressure in
    mm
L_toe_off = zeros(1, length(t));

L_overall = zeros(1,length(t)); %length from hip to toe to measure ground
    clrearance

A_toe_off = zeros(1, length(t));
B_toe_off = zeros(1, length(t));
C_toe_off = zeros(1, length(t));

```

```
A_heelstrike = zeros(1, length(t));
B_heelstrike = zeros(1, length(t));
C_heelstrike = zeros(1, length(t));

flexionfactor_heelstrike = zeros(1, length(t));
flexionfactor_toe_off = zeros(1, length(t));

X_icr_AB = zeros(1, length(t));
Y_icr_AB = zeros(1, length(t));
theta2_values = zeros(1, length(t));
theta3_values = zeros(1, length(t));
theta4_values = zeros(1, length(t));

M_h_heelstrike = zeros(1, length(t));
M_h_toe_off = zeros(1, length(t));


% Initial calculations to determine the y offset
theta3 = initial_theta3;
[theta2_1, theta2_2] = solve_theta2(a, b, c, d, theta1, theta3);
[theta4_1, theta4_2] = solve_theta4(a, b, c, d, theta1, theta3);

% Choose the real solutions (if any)
if isreal(theta2_1) && isreal(theta4_1)
    theta2 = theta2_1;
    theta4 = theta4_1;
elseif isreal(theta2_2) && isreal(theta4_2)
    theta2 = theta2_2;
    theta4 = theta4_2;
else
    theta2 = NaN;
    theta4 = NaN;
end

% Calculate initial positions of joints
O = [0, 0]; % Point O (fixed)
A = O + [a*cos(theta2), a*sin(theta2)];
B = A + [b*cos(theta3), b*sin(theta3)];
C = O + [d*cos(theta1), d*sin(theta1)];

%knee centre of all links

K_x = (O(1) + A(1) + B(1) + C(1)) / 4;
K_y = (O(2) + A(2) + B(2) + C(2)) / 4;

% Calculate the initial y offset to place B on the x-axis
y_offset = -B(2);
x_offset = - (O(1) + C(1)) / 2;


% Create figure for animation
figure;
hold on;
axis equal;
grid on;

% Plot placeholders for links
link_a = plot([0, 0], [0, 0], 'b', 'LineWidth', 2);
link_b = plot([0, 0], [0, 0], 'g', 'LineWidth', 2);
link_c = plot([0, 0], [0, 0], 'r', 'LineWidth', 2);
link_d = plot([0, 0], [0, 0], 'm', 'LineWidth', 2);
foot = plot([-50, 200], [-500, -500], 'b', 'LineWidth', 2);

```

```
106
107 % Plot placeholders for ICR trajectories
108 icr_plot_AB = plot(NaN, NaN, 'ko');
109
110 % Plot placeholders for joint labels
111 label_O = text(0, 0, 'O', 'HorizontalAlignment', 'center', 'VerticalAlignment',
        'bottom');
112 label_A = text(0, 0, 'A', 'HorizontalAlignment', 'center', 'VerticalAlignment',
        'bottom');
113 label_B = text(0, 0, 'B', 'HorizontalAlignment', 'center', 'VerticalAlignment',
        'bottom');
114 label_C = text(0, 0, 'C', 'HorizontalAlignment', 'center', 'VerticalAlignment',
        'bottom');
115
116 % Plot placeholder for the hip joint
117 hip_joint = plot(NaN, NaN, 'bo', 'MarkerSize', 8, 'MarkerFaceColor', 'b');
118
119 for i = 1:length(t)
120     % Use specified range for theta3
121     theta3 = t(i);
122
123     % Solve for theta2 and theta4
124     [theta2_1, theta2_2] = solve_theta2(a, b, c, d, theta1, theta3);
125     [theta4_1, theta4_2] = solve_theta4(a, b, c, d, theta1, theta3);
126
127     % Choose the real solutions (if any)
128     if isreal(theta2_1) && isreal(theta4_1)
129         theta2 = theta2_1;
130         theta4 = theta4_1;
131     elseif isreal(theta2_2) && isreal(theta4_2)
132         theta2 = theta2_2;
133         theta4 = theta4_2;
134     else
135         % Handle the case where no real solutions are found
136         theta2 = NaN;
137         theta4 = NaN;
138     end
139
140     % Store the angles
141     theta2_values(i) = theta2;
142     theta3_values(i) = theta3;
143     theta4_values(i) = theta4;
144
145     % Calculate positions of joints
146     O = [0, 0]; % Point O (fixed)
147     A = O + [a*cos(theta2), a*sin(theta2)];
148     B = A + [b*cos(theta3), b*sin(theta3)];
149     C = O + [d*cos(theta1), d*sin(theta1)];
150
151     % Apply offsets to positions
152     O = O + [x_offset, y_offset];
153     A = A + [x_offset, y_offset];
154     B = B + [x_offset, y_offset];
155     C = C + [x_offset, y_offset];
156
157     shin = plot([(O(1) + C(1)) / 2, 0], [(O(2) + C(2)) / 2, -500], 'b', '
        LineWidth', 2);
158
159     % Calculate the ICRs if the angles are real
160     if isreal(theta2) && isreal(theta4)
161         [X_icr_AB(i), Y_icr_AB(i)] = calculate_ICR_AB(O, A, B, C);
162     else
163         X_icr_AB(i) = NaN;
```

```
        Y_icr_AB(i) = NaN;
    end

    % Calculate the position of the hip joint
    phi = pi / 2 - theta3_values(1); % phi = 90 degrees - theta3
    alpha = phi + theta3;


    hip_x= (x_offset + 450)*cos(alpha);
    hip_y =(y_offset+ 450)*sin(alpha);


    % L is the distance from hip joint to centre of pressure
    L_heelstrike(i) = sqrt((hip_x - CP_heelstrike(1))^2 + (hip_y -
        CP_heelstrike(2))^2);
    L_toe_off(i) = sqrt((hip_x - CP_toe_off(1))^2 + (hip_y - CP_toe_off(2))^2);

    L_overall(i) = sqrt((hip_x - toe_coordinates(1))^2 + (hip_y -
        toe_coordinates(2))^2);

    % y is distance from knee ICR to centre of pressure
    y_heelstrike(i) = sqrt((X_icr_AB(i) - CP_heelstrike(1))^2 + (Y_icr_AB(i) -
        CP_heelstrike(2))^2);
    y_toe_off(i) = sqrt((X_icr_AB(i) - CP_toe_off(1))^2 + (Y_icr_AB(i) -
        CP_toe_off(2))^2);

    % Line equations for the different L's
    %L_toe_off
A_toe_off(i) = Y_icr_AB(i) - CP_toe_off(2);
B_toe_off(i) = X_icr_AB(i) - CP_toe_off(1);
C_toe_off(i) = (Y_icr_AB(i) * (CP_toe_off(1) - X_icr_AB(i))) - ((CP_toe_off(2)
    - Y_icr_AB(i)) * X_icr_AB(i));

%L_heelstrike
A_heelstrike(i) = Y_icr_AB(i) - CP_heelstrike(2);
B_heelstrike(i) = X_icr_AB(i) - CP_heelstrike(1);
C_heelstrike(i) = (Y_icr_AB(i) * (CP_heelstrike(1) - X_icr_AB(i))) - ((
    CP_heelstrike(2) - Y_icr_AB(i)) * X_icr_AB(i));




% x is perpendicular distance from ICR to L (signed distance)
x_toe_off(i) = ((A_toe_off(i) * X_icr_AB(i)) + (B_toe_off(i) * Y_icr_AB(i)) +
    C_toe_off(i)) / sqrt(A_toe_off(i)^2 + B_toe_off(i)^2);
x_heelstrike(i) = ((A_heelstrike(i) * X_icr_AB(i)) + (B_heelstrike(i) *
    Y_icr_AB(i)) + C_heelstrike(i)) / sqrt(A_heelstrike(i)^2 + B_heelstrike(i)
    ^2);


    % Calculate flexion factors
    flexionfactor_toe_off(i) = x_toe_off(i) / y_toe_off(i);
    flexionfactor_heelstrike(i) = x_heelstrike(i) / y_heelstrike(i);

    % Calculate Hip moment required
    M_h_toe_off(i) = (P * L_toe_off(i)/1000) * flexionfactor_toe_off(i);
    M_h_heelstrike(i) = (P * L_heelstrike(i)/1000) * flexionfactor_heelstrike(i
        );


    % Update plot data
    set(link_a, 'XData', [O(1), A(1)], 'YData', [O(2), A(2)]);
    set(link_b, 'XData', [A(1), B(1)], 'YData', [A(2), B(2)]);
```

```
    set(link_c, 'XData', [B(1), C(1)], 'YData', [B(2), C(2)]);
    set(link_d, 'XData', [C(1), O(1)], 'YData', [C(2), O(2)]);
   % set(hip_line, 'XData', [hip_x, B(1)], 'YData', [hip_y, B(2)]); % Line from
       hip to AB

    % Update joint labels
    set(label_O, 'Position', O);
    set(label_A, 'Position', A);
    set(label_B, 'Position', B);
    set(label_C, 'Position', C);

    % Update ICR plot data
    set(icr_plot_AB, 'XData', X_icr_AB, 'YData', Y_icr_AB);

    % Update hip joint plot data
    set(hip_joint, 'XData', hip_x, 'YData', hip_y);

    % Pause for animation effect
    %pause(0.1);
end

% Plot flexion factors
figure;
plot(rad2deg(t-theta3_range_start), flexionfactor_toe_off, 'r-', 'LineWidth',
    2);
hold on;
plot(rad2deg(t-theta3_range_start), flexionfactor_heelstrike, 'b--', 'LineWidth
    ', 2);
xlabel('Knee Flexion angle (degrees)');
ylabel('Flexion Factor');
legend('Toe Off', 'Heel Strike');
title('Flexion Factors vs Knee Flexion angle');
grid on;

% Plot hip moments
figure;
plot(rad2deg(t-theta3_range_start), M_h_toe_off, 'r-', 'LineWidth', 2);
hold on;
plot(rad2deg(t-theta3_range_start), M_h_heelstrike, 'b--', 'LineWidth', 2);
xlabel('Knee Flexion angle (degrees)');
ylabel('Hip Moment (Nm)');
legend('Toe Off', 'Heel Strike');
title('Hip Moments vs Knee Flexion angle');
grid on;

%Plot L_overall against knee flexion to see toe clearance
figure;
plot(rad2deg(t-theta3_range_start), L_overall, 'r-', 'LineWidth', 2);
hold on;
xlabel('Knee Flexion angle (degrees)');
ylabel('Leg length (mm)');
title('Leg legnth vs Knee Flexion angle');
grid on;

% Function definitions

% Function to solve for theta2
function [theta2_1, theta2_2] = solve_theta2(a, b, c, d, theta1, theta3)
    A = (a^2 + b^2 - c^2 + d^2)/(2*a*b) - d*(cos(theta1)*cos(theta3)+sin(theta1
        )*sin(theta3))/a-cos(theta3)+d*cos(theta1)/b;
    B = 2 * (sin(theta3) - d*sin(theta1)/b);
    C = (a^2 + b^2 - c^2 + d^2)/(2*a*b) - d*(cos(theta1)*cos(theta3)+sin(theta1
        )*sin(theta3))/a+ cos(theta3)-d*cos(theta1)/b;
```

```
    theta2_1 = 2*atan((-B + sqrt(B^2 - 4*A*C))/(2*A));
    theta2_2 = 2*atan((-B - sqrt(B^2 - 4*A*C))/(2*A));
end

% Function to solve for theta4
function [theta4_1, theta4_2] = solve_theta4(a, b, c, d, theta1, theta3)
    D = (b^2 - a^2 + c^2 + d^2)/(2*b*c) - d*(cos(theta1)*cos(theta3) + sin(
        theta1)*sin(theta3))/c -d*cos(theta1)+b*cos(theta3);
    E = 2 * (d * sin(theta1)/b - sin(theta3));
    F = (b^2 - a^2 + c^2 + d^2)/(2*b*c) - d*(cos(theta1)*cos(theta3) + sin(
        theta1)*sin(theta3))/c + d*cos(theta1)/b-cos(theta3);
    theta4_1 = 2*atan((-E + sqrt(E^2 - 4*D*F))/(2*D));
    theta4_2 = 2*atan((-E - sqrt(E^2 - 4*D*F))/(2*D));
end

% Function to calculate ICR of link AB by extending lines OA and CB
function [X_icr, Y_icr] = calculate_ICR_AB(O, A, B, C)
    % Directions of links OA and CB
    direction_OA = [A(1)-O(1), A(2)-O(2)];
    direction_CB = [B(1) - C(1), B(2) - C(2)];

    % Slopes of the extended lines
    m_OA = direction_OA(2) / direction_OA(1);
    m_CB = direction_CB(2) / direction_CB(1);

    % Intercepts of the lines
    c_OA = O(2) - m_OA * O(1);
    c_CB = C(2) - m_CB * C(1);

    % Solve the system of linear equations to find the intersection
    if m_OA ~= m_CB
        X_icr = (c_CB - c_OA) / (m_OA - m_CB);
        Y_icr = m_OA * X_icr + c_OA;
    else
        X_icr = NaN;
        Y_icr = NaN;
    end
end
```

Listing A.1 Four-bar mechanism design tool

The following MATLAB script takes the initial positions of the links calculated in the design tool and calculates the socket centrode for the mechanism. This is used for a more accurate ground clearance calculation as well as to obtain the maximum knee flexion.

```
% === SOCKET CENTRODE + TOE CLEARANCE + socket SPHERE COLLISION ===
% Ground rotated about hip, offset preserved. Sphere at to simulate socket.

clear; close all; clc;

% ---------------------------
% Link lengths
% ---------------------------
a = 66;
b = 30;
c = 56;
d = 45;

% ---------------------------
% Fixed thigh link AB
% ---------------------------
theta3 = deg2rad(18);                   % Angle of link AB
```

```
B = [12.232790758158707, 0];          % Knee joint coordinates from FBM design tool
A = B - b * [cos(theta3), sin(theta3)];  % Hip-end of AB

% ---------------------------
% OC coordinates from shank-centrode start (relative to knee B)
% ---------------------------
O_orig = [-20.22, -75.15];
C_orig = [ 20.22, -55.43];

% ---------------------------
% Hip, toe, ankle positions
% ---------------------------
H  = [0, 374.85];        % Fixed hip joint (global)
T0 = [200, -500];        % Initial toe position (just for visualisation)
A0_ankle = [0, -500];    % Initial ankle position (to build shank line)

% ---------------------------
% Original flat ground
% ---------------------------
Floor_line_y = -500;
d0 = H(2) - Floor_line_y;   % perpendicular distance hip->ground before rotation

% ---------------------------
% Rotated ground (tilted "floor") definition
% ---------------------------
hip_flex_deg = 23;
phi = deg2rad(hip_flex_deg);

% Direction of ground, sloping downward in +x
ground_dir = [cos(phi), -sin(phi)];

% Choose upward normal (toward hip) and normalize
cand1 = [ ground_dir(2), -ground_dir(1) ];
cand2 = [-ground_dir(2),  ground_dir(1) ];
if cand1(2) >= 0
    ground_normal = cand1;
else
    ground_normal = cand2;
end
ground_normal = ground_normal / norm(ground_normal);

% Offset ground so perpendicular distance from hip to ground = d0
ground_ref_point = H - ground_normal * d0;

% Build ground line for plotting
ground_span_x = -800:20:800;
t_vals = (ground_span_x - ground_ref_point(1)) ./ ground_dir(1);
ground_line_y = ground_ref_point(2) + t_vals .* ground_dir(2);

% ---------------------------
% Socket sphere (for clearance)
% ---------------------------
sphere_radius = 60; % mm (diameter 120)
sphere_center = B + [20, 80]; % 20 mm forward (x), 80 mm up (y) from knee

% parametric circle for plotting
theta_circ = linspace(0, 2*pi, 200);
circle_x = sphere_center(1) + sphere_radius * cos(theta_circ);
circle_y = sphere_center(2) + sphere_radius * sin(theta_circ);

% ---------------------------
```

```
% Rotation steps (knee flexion sweep)
% ---------------------------
n_steps = 100;
theta_range = deg2rad(127.85);              % total flexion range to simulate
theta_vals = linspace(0, -theta_range, n_steps);  % clockwise

% ---------------------------
% Storage arrays
% ---------------------------
X_icr = zeros(1, n_steps);
Y_icr = zeros(1, n_steps);
toe_clearance    = zeros(1, n_steps);  % hip-to-toe distance
ground_clearance = zeros(1, n_steps);  % toe perp distance to tilted ground
sphere_clearance = zeros(1, n_steps);  % min perp distance to sphere surface

% ---------------------------
% Setup figure for geometry / animation
% ---------------------------
figure;
axis equal;
grid on;
xlabel('X (mm)');
ylabel('Y (mm)');
title('Socket Centrode, Toe Clearance, and Socket Clearance');
hold on;

% Plot rotated / offset ground line
%plot(ground_span_x, ground_line_y, 'k--', 'LineWidth', 1.5);

% Plot socket sphere
plot(circle_x, circle_y, 'm-', 'LineWidth', 1.5);

% Mark hip and sphere center
plot(H(1), H(2), 'bo', 'MarkerSize', 8, 'MarkerFaceColor', 'b');
plot(sphere_center(1), sphere_center(2), 'mo', 'MarkerSize', 6, '
    MarkerFaceColor', 'm');

% Initialize plot handles for mechanism + shank line + toe
link_oa = plot([0, 0], [0, 0], 'b', 'LineWidth', 2);  % O -> A
link_cb = plot([0, 0], [0, 0], 'r', 'LineWidth', 2);  % C -> B
link_ab = plot([0, 0], [0, 0], 'g', 'LineWidth', 2);  % A -> B (thigh)
link_oc = plot([0, 0], [0, 0], 'k', 'LineWidth', 2);  % O -> C
toe_marker   = plot(NaN, NaN, 'ro', 'MarkerSize', 6, 'MarkerFaceColor', 'r');
icr_path     = plot(NaN, NaN, 'ko');
shank_line_h = plot([0,0],[0,0],'c-','LineWidth',2); % midpoint(OC) -> ankle

% Annotation
% text(H(1)+30, H(2)-30, ...
%      sprintf('Ground rotated %d^\\circ about hip,\nkept %.1f mm below hip',
    ...
%              hip_flex_deg, d0), ...
%      'Color','k','FontSize',8,'BackgroundColor','w');
text(sphere_center(1)+20, sphere_center(2), ...
     sprintf('Socket sphere D=120 mm'), ...
     'Color','m','FontSize',8,'BackgroundColor','w');

% ---------------------------
% Helper to get shortest dist from point P to segment [S1,S2]
% ---------------------------
segment_point_dist = @(P,S1,S2) ...
    segmentDistance2D(P,S1,S2);  % defined later in file

% ---------------------------
```

```
% Main simulation loop
% --------------------------
for i = 1:n_steps
    theta = theta_vals(i);

    % Rotate OC, ankle, toe about knee B
    OC_center = B;
    O_rel = O_orig      - OC_center;
    C_rel = C_orig      - OC_center;
    T_rel = T0          - OC_center;
    Ank_rel = A0_ankle  - OC_center;

    R = [cos(theta), -sin(theta);
         sin(theta),  cos(theta)];

    O_rot   = (R * O_rel')'   + OC_center;
    C_rot   = (R * C_rel')'   + OC_center;
    T_rot   = (R * T_rel')'   + OC_center;
    Ank_rot = (R * Ank_rel')' + OC_center;

    % Midpoint of OC (to represent shank centerline start)
    mid_OC = 0.5*(O_rot + C_rot);

    % --- Instantaneous Center of Rotation (ICR) ---
    [x_icr, y_icr] = calculate_ICR_AB(O_rot, A, B, C_rot);
    X_icr(i) = x_icr;
    Y_icr(i) = y_icr;

    % --- Hip-to-toe distance (leg length proxy) ---
    toe_clearance(i) = norm(T_rot - H);

    % --- Toe clearance from rotated+offset ground ---
    toe_vec = T_rot - ground_ref_point;
    perp_dist_ground = abs( toe_vec(1)*ground_dir(2) - toe_vec(2)*ground_dir(1)
        ) / norm(ground_dir);
    ground_clearance(i) = perp_dist_ground;

    % --- Sphere collision / clearance ---
    % We check several relevant segments against the sphere:
    %   1) O_rot -> C_rot  (link OC)
    %   2) O_rot -> A      (link OA)
    %   3) C_rot -> B      (link CB)
    %   4) A     -> B      (thigh AB)
    %   5) mid_OC -> Ank_rot (shank line)
    % Distance from sphere center to each segment, minus radius.

    d1 = segment_point_dist(sphere_center, O_rot,   C_rot);
    d2 = segment_point_dist(sphere_center, O_rot,   A);
    d3 = segment_point_dist(sphere_center, C_rot,   B);
    d4 = segment_point_dist(sphere_center, A,       B);
    d5 = segment_point_dist(sphere_center, mid_OC,  Ank_rot);

    d_min = min([d1,d2,d3,d4,d5]);
    sphere_clearance(i) = d_min - sphere_radius;
    % sphere_clearance < 0 means penetration/contact

    % --- Update plot / animation ---
    set(link_oa, 'XData', [O_rot(1), A(1)], 'YData', [O_rot(2), A(2)]);
    set(link_cb, 'XData', [C_rot(1), B(1)], 'YData', [C_rot(2), B(2)]);
    set(link_oc, 'XData', [O_rot(1), C_rot(1)], 'YData', [O_rot(2), C_rot(2)]);
    set(link_ab, 'XData', [A(1), B(1)], 'YData', [A(2), B(2)]);
    set(toe_marker, 'XData', T_rot(1), 'YData', T_rot(2));
   % set(icr_path, 'XData', X_icr(1:i), 'YData', Y_icr(1:i));
```

```
    set(shank_line_h,'XData',[mid_OC(1), Ank_rot(1)],...
                     'YData',[mid_OC(2), Ank_rot(2)]);

    drawnow;
end

% ---------------------------
% Plot leg length vs knee flexion
% ---------------------------
figure;
plot(rad2deg(-theta_vals), toe_clearance, 'b-', 'LineWidth', 2);
xlabel('Knee Flexion Angle (deg)');
ylabel('Hip-Toe Distance (mm)');
title('Leg Length vs Knee Flexion');
grid on;

% ---------------------------
% Plot toe-floor clearance vs knee flexion
% ---------------------------
figure;
plot(rad2deg(-theta_vals), ground_clearance, 'r-', 'LineWidth', 2);
xlabel('Knee Flexion Angle (deg)');
ylabel('Toe Clearance from Rotated Floor (mm)');
title('Toe Clearance vs Knee Flexion (Floor Rotated, Offset Preserved)');
grid on;

% ---------------------------
% Plot sphere clearance vs knee flexion
% ---------------------------
figure;
plot(rad2deg(-theta_vals), sphere_clearance, 'm-', 'LineWidth', 2);
xlabel('Knee Flexion Angle (deg)');
ylabel('Min Clearance to Socket Sphere (mm)');
title('Socket Clearance vs Knee Flexion');
yline(0,'k--','Contact');
grid on;


% === Helper: Instantaneous Center of Rotation ===
function [X_icr, Y_icr] = calculate_ICR_AB(O, A, B, C)
    direction_OA = A - O;
    direction_CB = B - C;

    m_OA = direction_OA(2) / direction_OA(1);
    m_CB = direction_CB(2) / direction_CB(1);

    c_OA = A(2) - m_OA * A(1);
    c_CB = B(2) - m_CB * B(1);

    if abs(m_OA - m_CB) < 1e-6
        X_icr = NaN;
        Y_icr = NaN;
    else
        X_icr = (c_CB - c_OA) / (m_OA - m_CB);
        Y_icr = m_OA * X_icr + c_OA;
    end
end

% === Helper: distance from a point P to a segment [S1,S2] in 2D ===
function d = segmentDistance2D(P, S1, S2)
    % Vector along segment
    v = S2 - S1;
    % Vector from S1 to point
```

```
    w = P - S1;

    v_norm2 = dot(v,v);
    if v_norm2 < 1e-12
        % Segment is effectively a point
        d = norm(P - S1);
        return;
    end

    % Projection parameter t of w onto v
    t = dot(w,v) / v_norm2;

    % Clamp t to [0,1] so we stay on the segment
    t = max(0, min(1, t));

    % Closest point on the segment
    closest = S1 + t * v;

    % Distance from P to closest point
    d = norm(P - closest);
end
```

Listing A.2 Socket Centrode Script

B. Gait Trial Results — 4BM Prototype

This appendix includes the complete gait-trial report generated for the four-bar mechanism (4BM). Table B.1 lists the kinematic and cross-correlation plots that the report contains.

Table B.1. Overview of 4BM gait-trial plots included in this appendix. Each variable includes both group-average and left–right cross-correlation plots.

Parameter	Plot Type	Page
Hip Flexion	Group Average	100
	L vs R Cross-correlation	101
Knee Flexion	Group Average	102
	L vs R Cross-correlation	103
Ankle Flexion	Group Average	104
	L vs R Cross-correlation	105
Hip Moment	Group Average	106
	L vs R Cross-correlation	107
Knee Moment	Group Average	108
	L vs R Cross-correlation	109
Ankle Moment	Group Average	110
	L vs R Cross-correlation	111
Hip Power	Group Average	112
	L vs R Cross-correlation	113
Knee Power	Group Average	114
	L vs R Cross-correlation	115
Ankle Power	Group Average	116
	L vs R Cross-correlation	117
Vertical GRF	Group Average	118
	L vs R Cross-correlation	119
Toe Height	Group Average	120
	L vs R Cross-correlation	121
Ankle Angular Velocity	Group Average	122
	L vs R Cross-correlation	123
Knee Angular Velocity	Group Average	124
	L vs R Cross-correlation	125
Hip Angular Velocity	Group Average	126
	L vs R Cross-correlation	127
Ankle Angular Acceleration	Group Average	128
	L vs R Cross-correlation	129
Knee Angular Acceleration	Group Average	130
	L vs R Cross-correlation	131
Hip Angular Acceleration	Group Average	132
	L vs R Cross-correlation	133

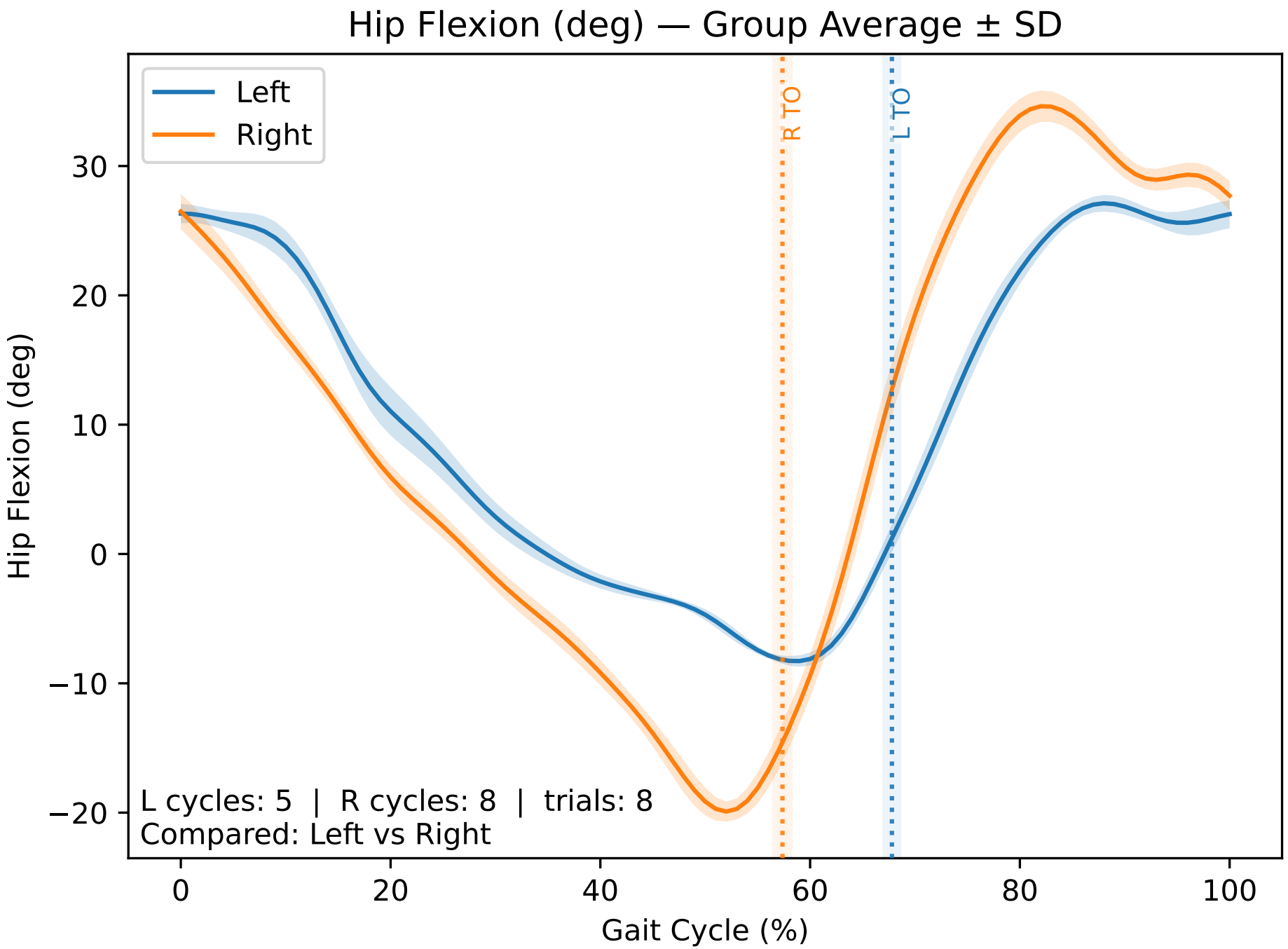
Hip Flexion (deg) — Group Average ± SD
Left
Right
R TO
L TO
Hip Flexion (deg)
30
20
10
0
−10
−20
0
20
40
60
80
100
Gait Cycle (%)
L cycles: 5 | R cycles: 8 | trials: 8
Compared: Left vs Right

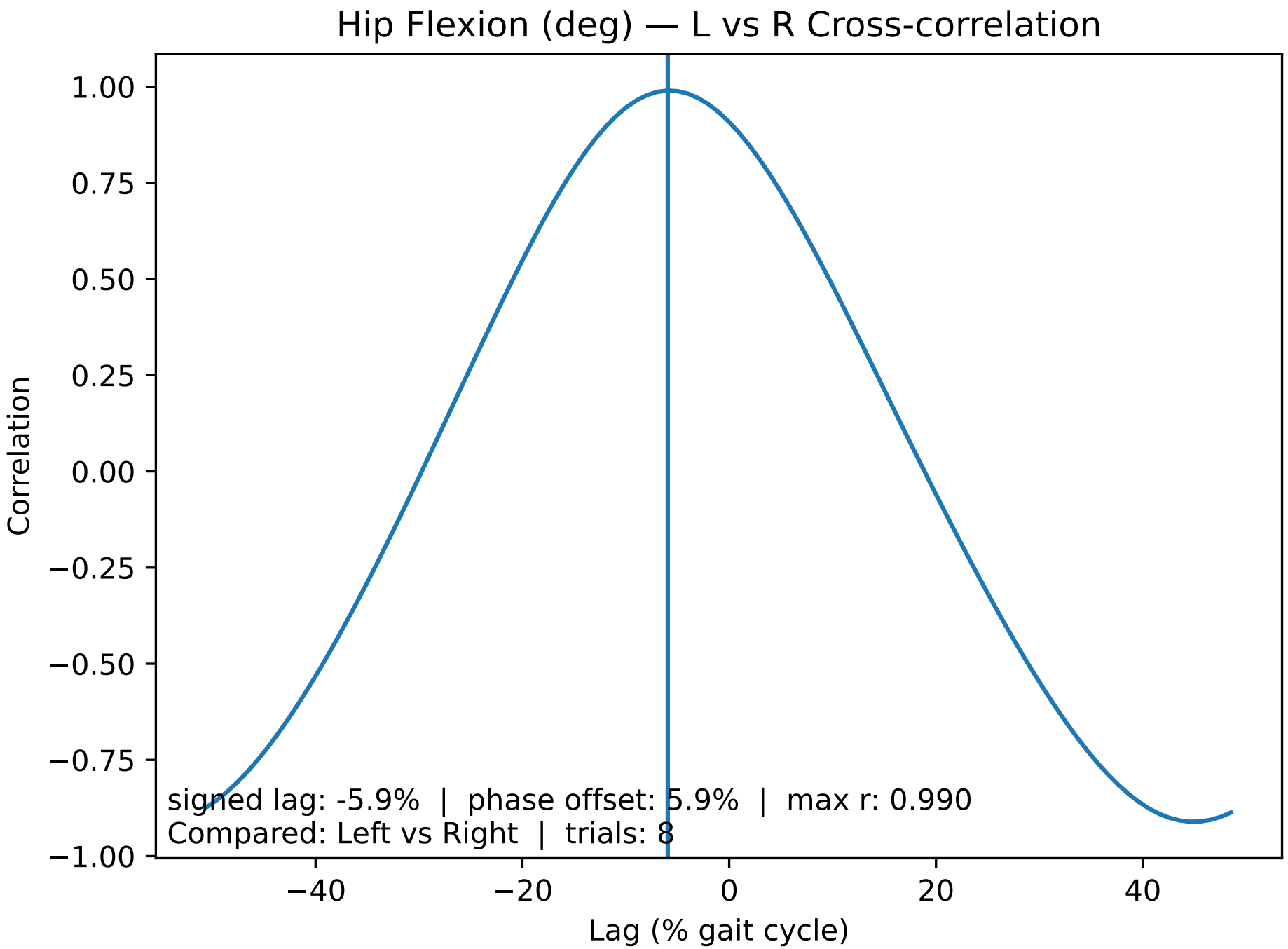
Hip Flexion (deg) — L vs R Cross-correlation
Correlation
1.00
0.75
0.50
0.25
0.00
−0.25
−0.50
−0.75
−1.00
−40
−20
0
20
40
Lag (% gait cycle)
signed lag: -5.9% | phase offset: 5.9% | max r: 0.990
Compared: Left vs Right | trials: 8

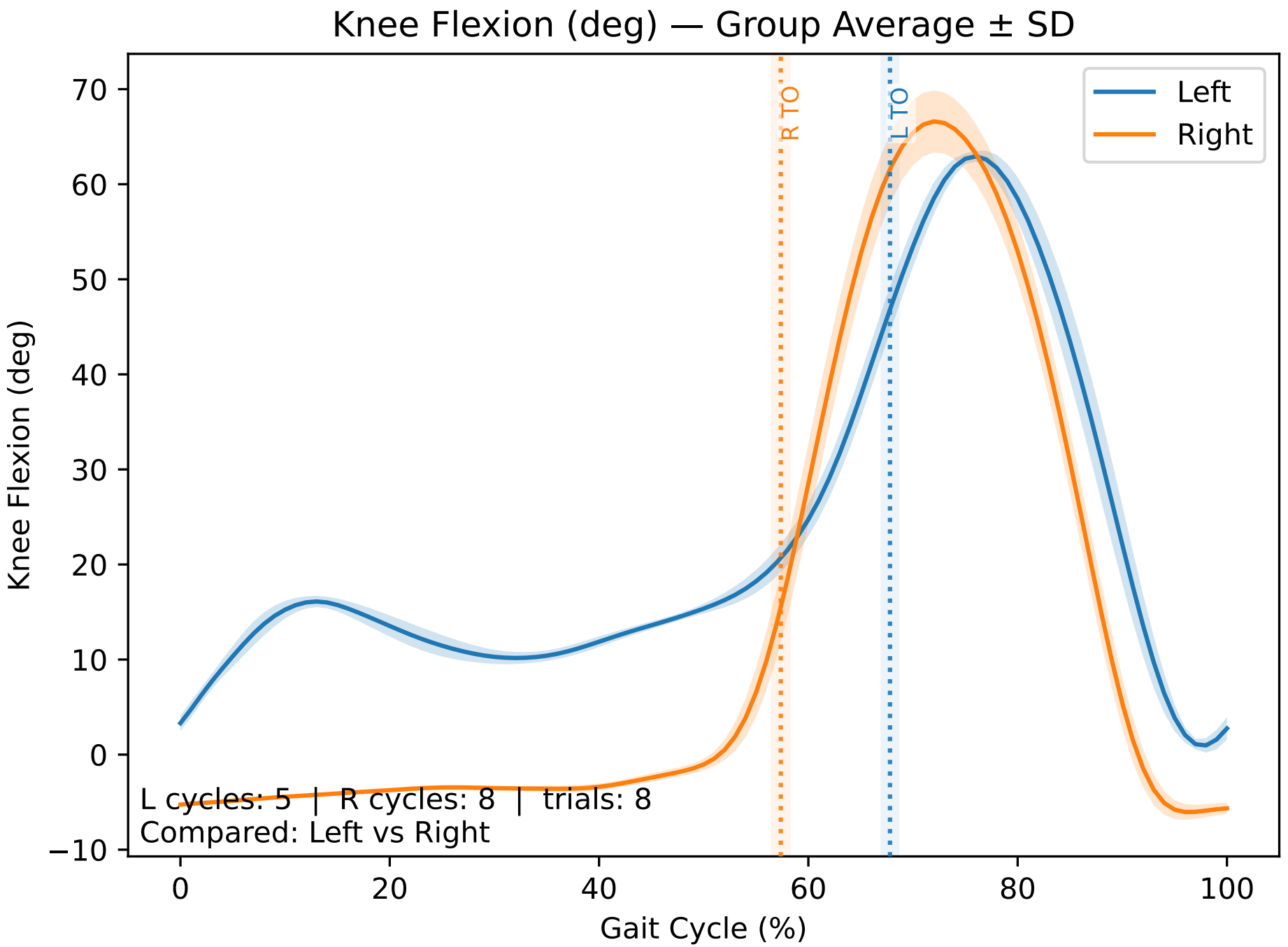
Knee Flexion (deg) — Group Average ± SD
Knee Flexion (deg)
Gait Cycle (%)
Left
Right
R TO
L TO
L cycles: 5 | R cycles: 8 | trials: 8
Compared: Left vs Right
70
60
50
40
30
20
10
0
−10
0
20
40
60
80
100

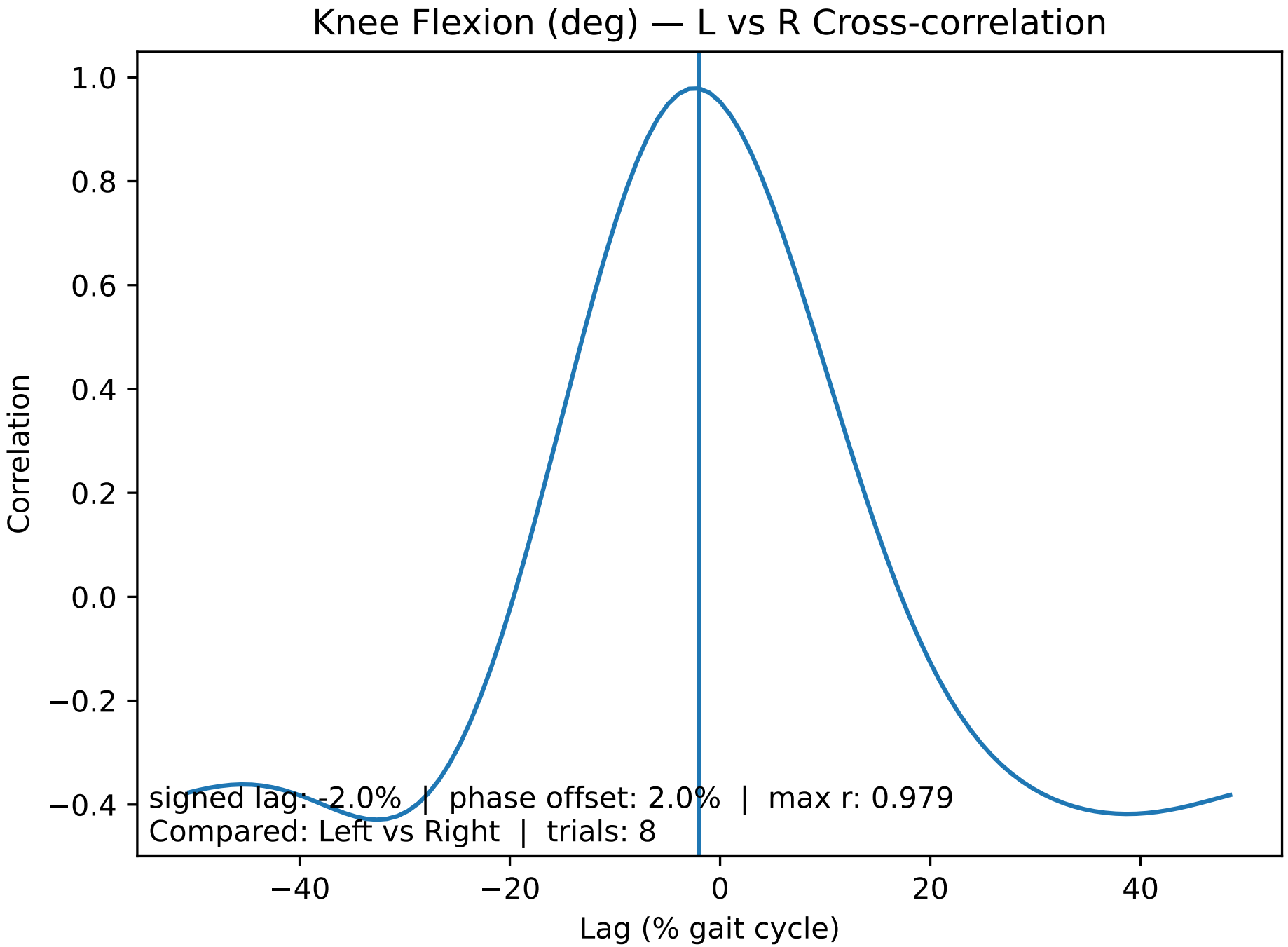
Knee Flexion (deg) — L vs R Cross-correlation
Correlation
1.0
0.8
0.6
0.4
0.2
0.0
−0.2
−0.4
−40
−20
0
20
40
Lag (% gait cycle)
signed lag: -2.0% | phase offset: 2.0% | max r: 0.979
Compared: Left vs Right | trials: 8

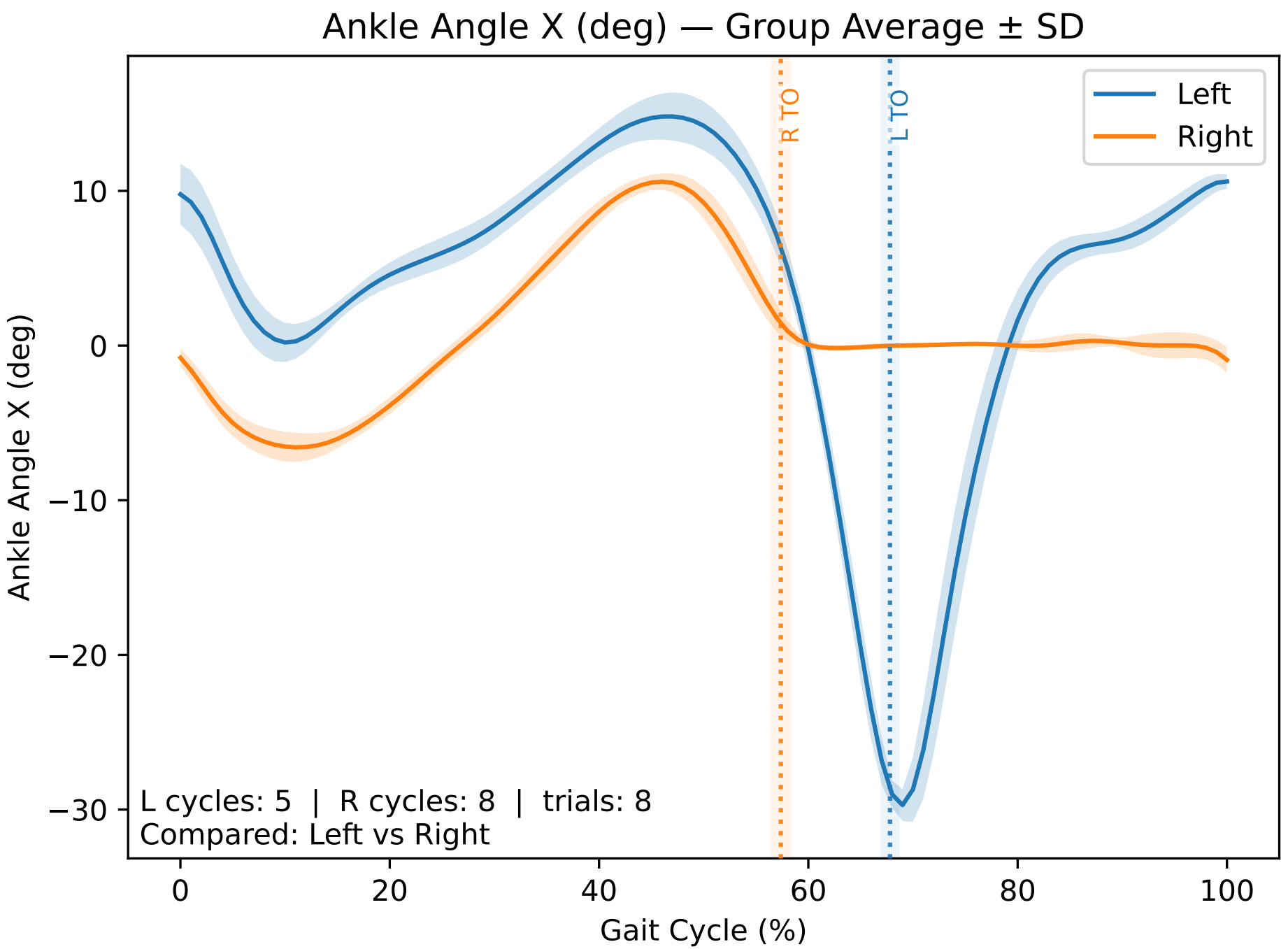
Ankle Angle X (deg) — Group Average ± SD
Left
Right
R TO
L TO
Ankle Angle X (deg)
10
0
−10
−20
−30
0
20
40
60
80
100
Gait Cycle (%)
L cycles: 5 | R cycles: 8 | trials: 8
Compared: Left vs Right

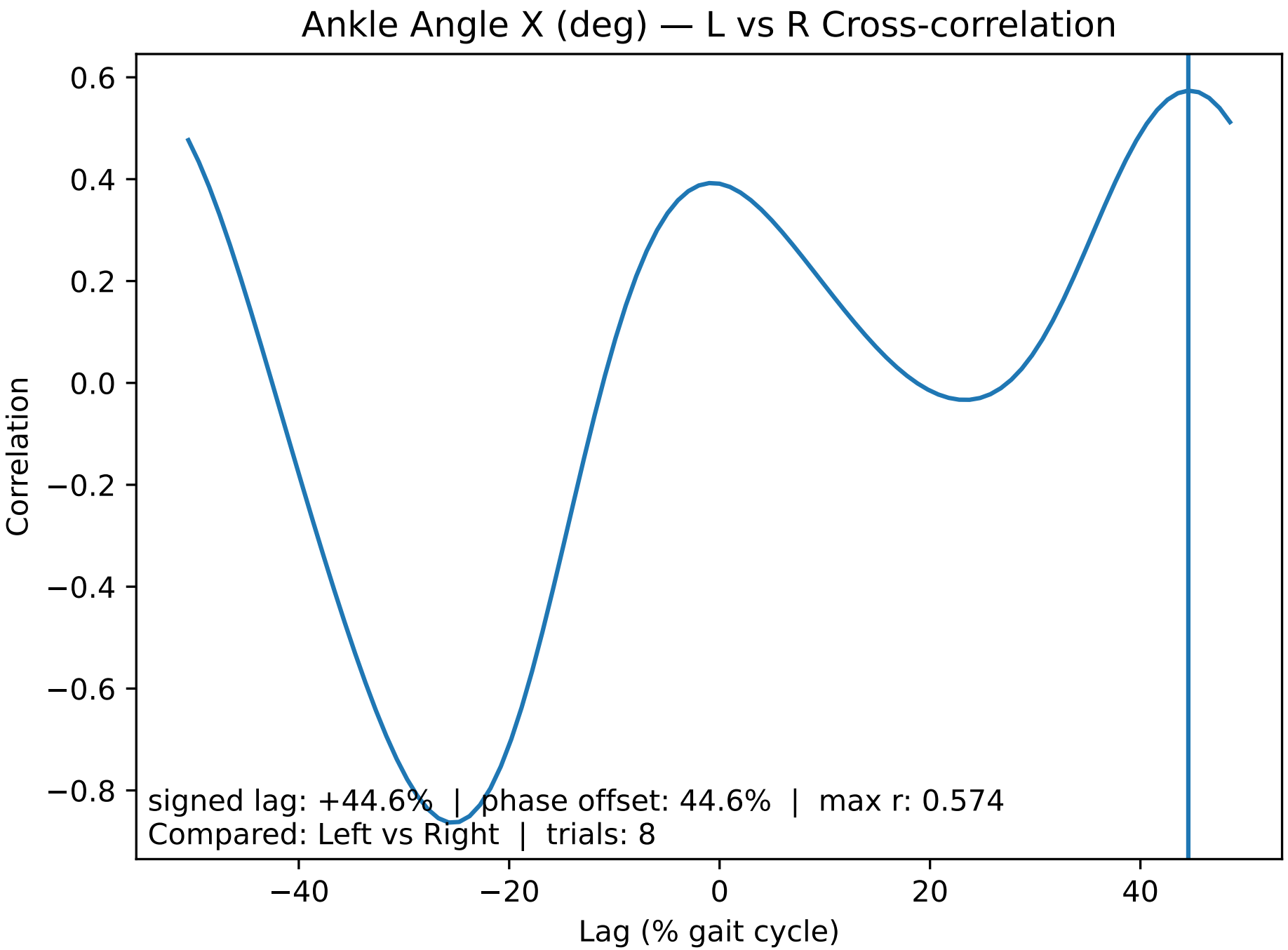
Ankle Angle X (deg) — L vs R Cross-correlation
Correlation
0.6
0.4
0.2
0.0
−0.2
−0.4
−0.6
−0.8
signed lag: +44.6% | phase offset: 44.6% | max r: 0.574
Compared: Left vs Right | trials: 8
−40
−20
0
20
40
Lag (% gait cycle)

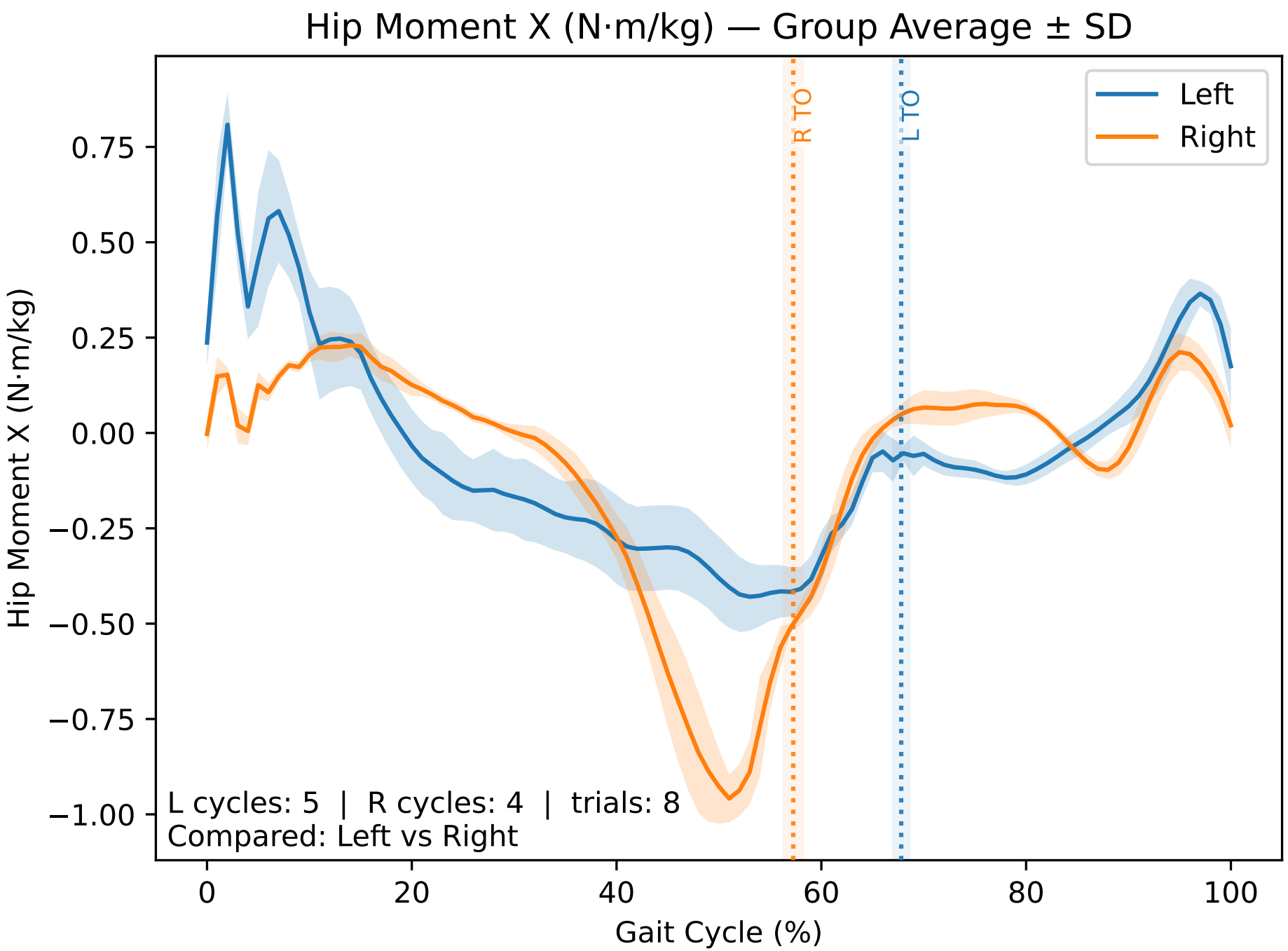
Hip Moment X (N·m/kg) — Group Average ± SD
Left
Right
R TO
L TO
Hip Moment X (N·m/kg)
0.75
0.50
0.25
0.00
−0.25
−0.50
−0.75
−1.00
0
20
40
60
80
100
Gait Cycle (%)
L cycles: 5 | R cycles: 4 | trials: 8
Compared: Left vs Right

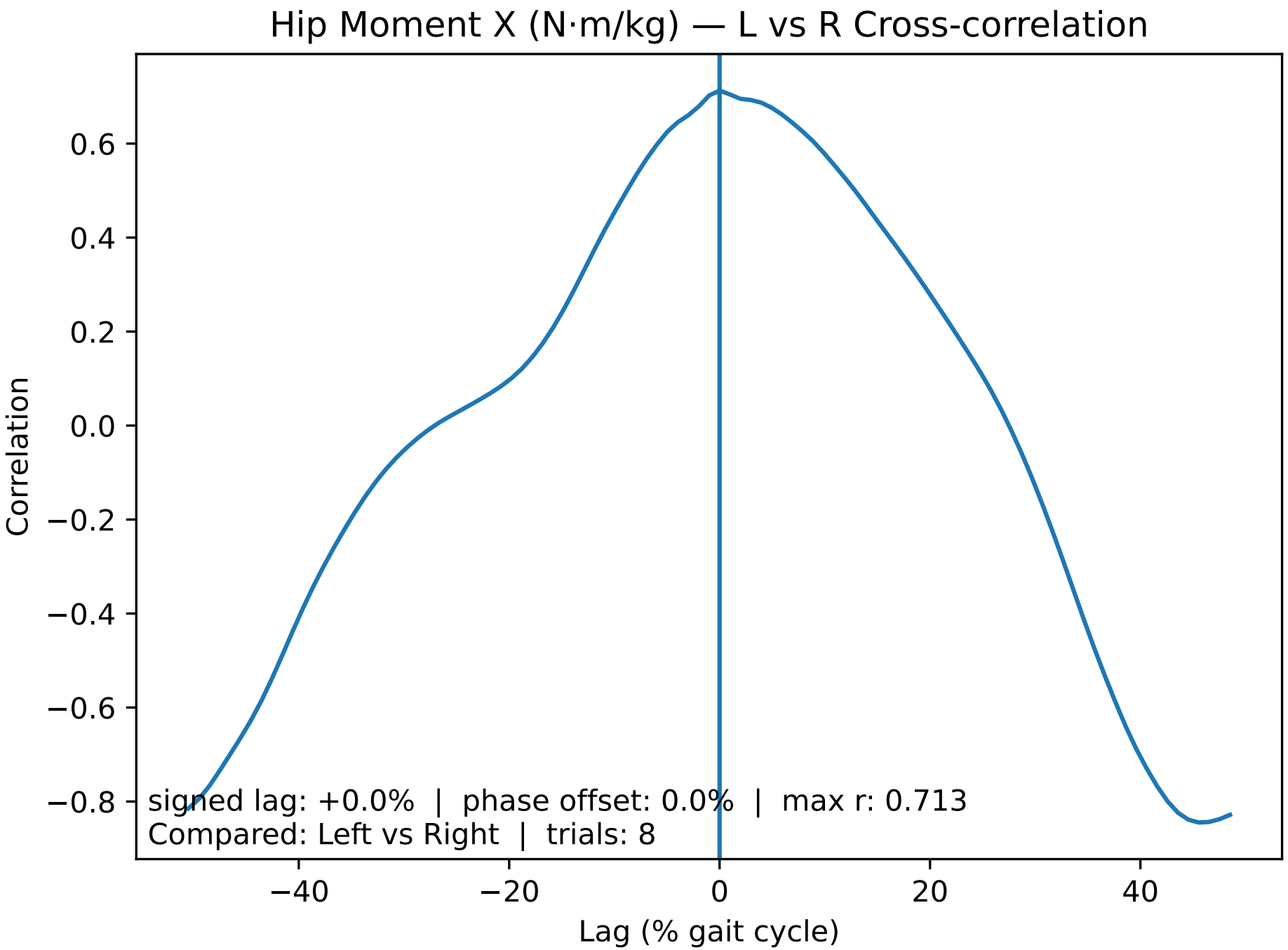
Hip Moment X (N·m/kg) — L vs R Cross-correlation
Correlation
0.6
0.4
0.2
0.0
−0.2
−0.4
−0.6
−0.8
signed lag: +0.0% | phase offset: 0.0% | max r: 0.713
Compared: Left vs Right | trials: 8
−40
−20
0
20
40
Lag (% gait cycle)

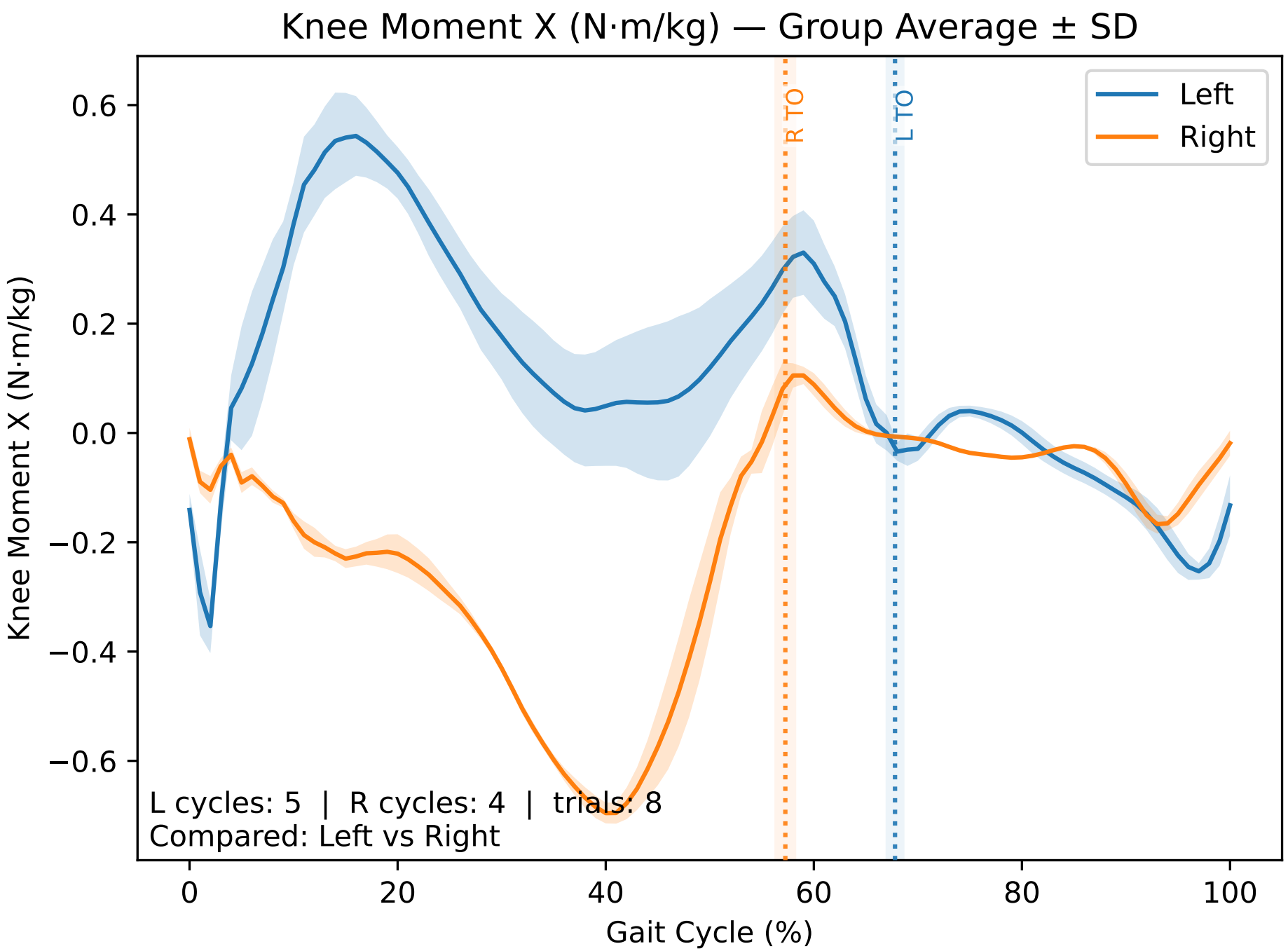
Knee Moment X (N·m/kg) — Group Average ± SD
Knee Moment X (N·m/kg)
0.6
0.4
0.2
0.0
−0.2
−0.4
−0.6
R TO
L TO
Left
Right
L cycles: 5 | R cycles: 4 | trials: 8
Compared: Left vs Right
0
20
40
60
80
100
Gait Cycle (%)

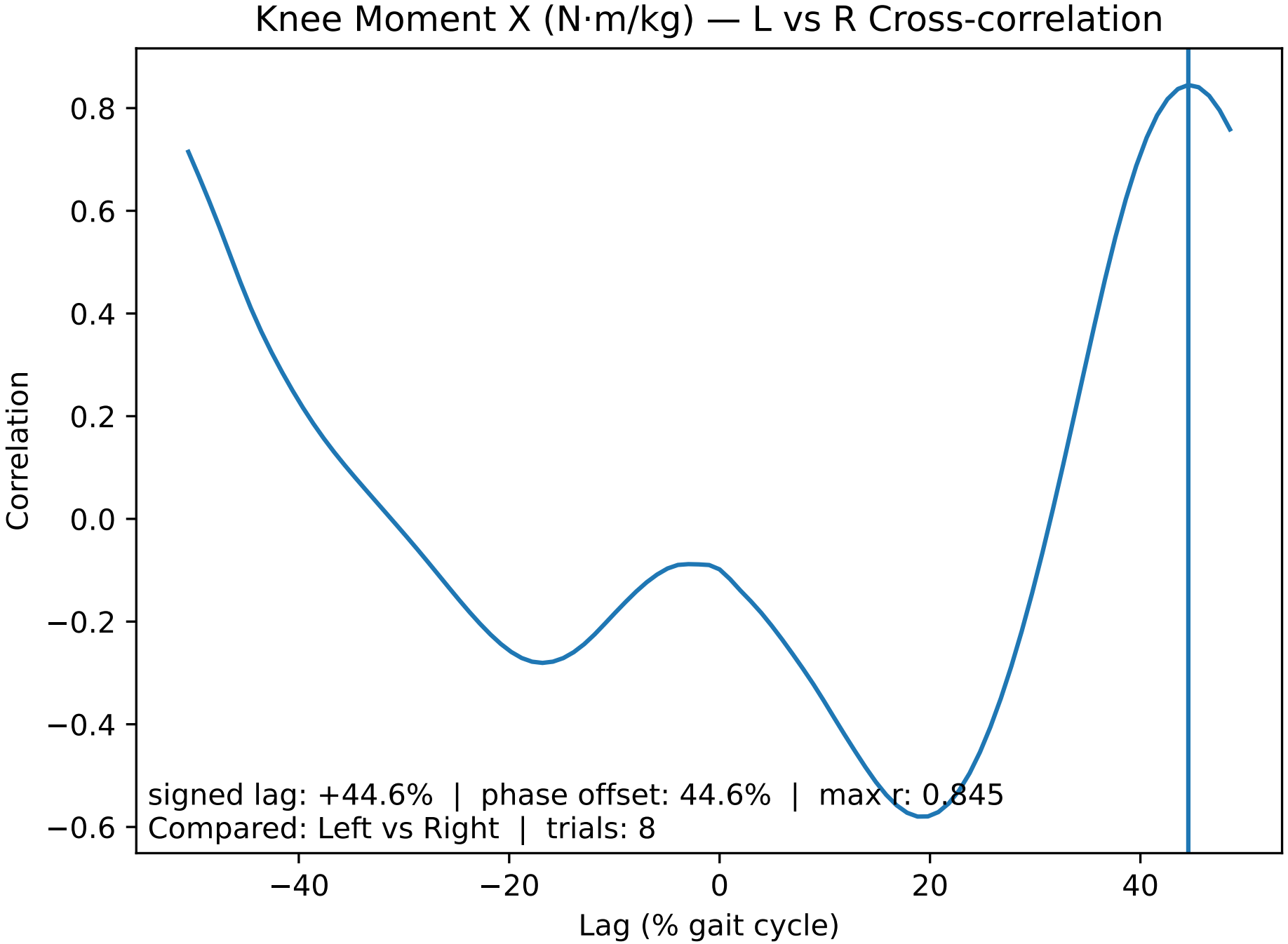
Knee Moment X (N·m/kg) — L vs R Cross-correlation
Correlation
0.8
0.6
0.4
0.2
0.0
−0.2
−0.4
−0.6
−40
−20
0
20
40
Lag (% gait cycle)
signed lag: +44.6% | phase offset: 44.6% | max r: 0.845
Compared: Left vs Right | trials: 8

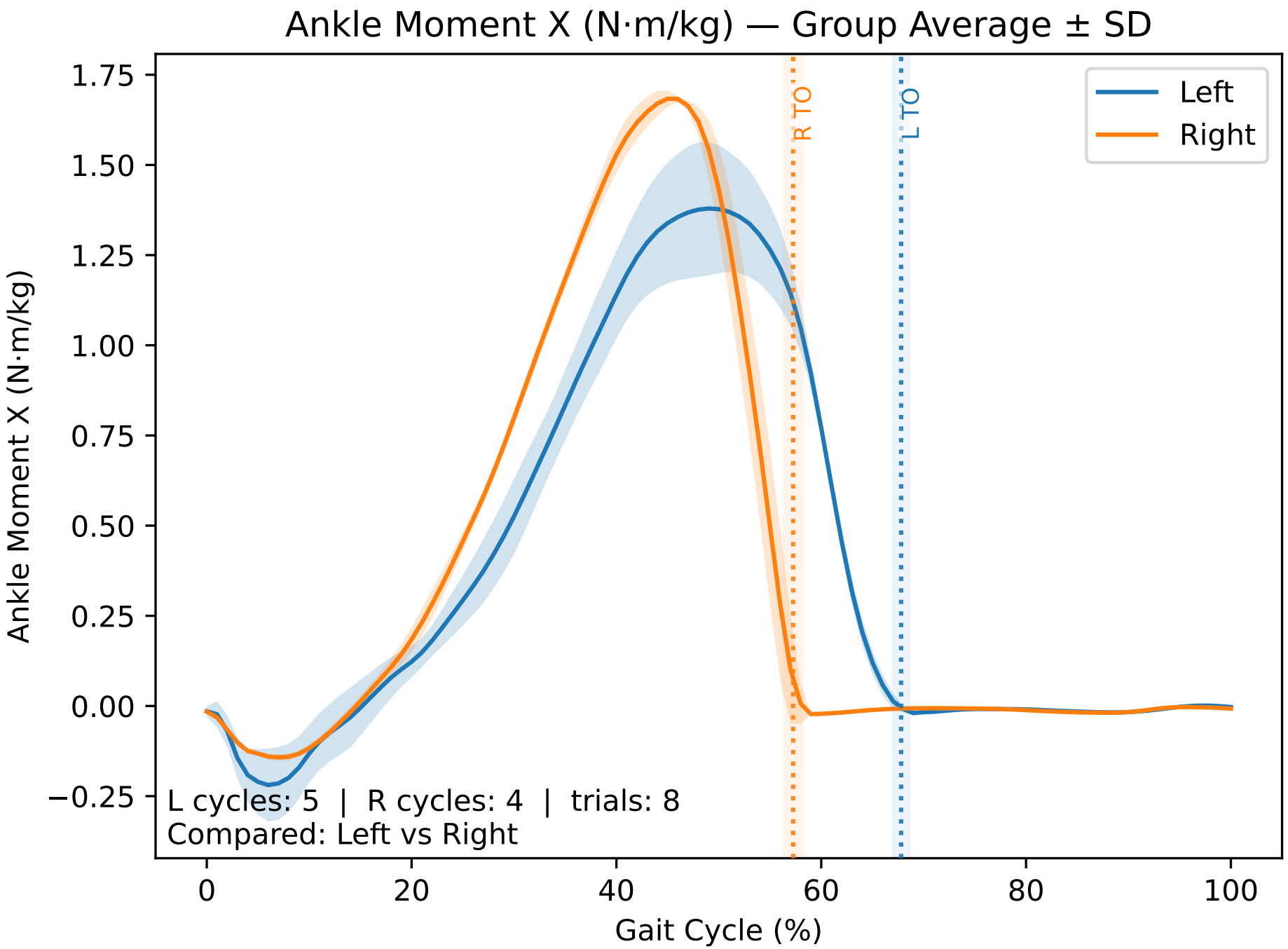
Ankle Moment X (N·m/kg) — Group Average ± SD
Ankle Moment X (N·m/kg)
1.75
1.50
1.25
1.00
0.75
0.50
0.25
0.00
−0.25
0
20
40
60
80
100
Gait Cycle (%)
R TO
L TO
Left
Right
L cycles: 5 | R cycles: 4 | trials: 8
Compared: Left vs Right

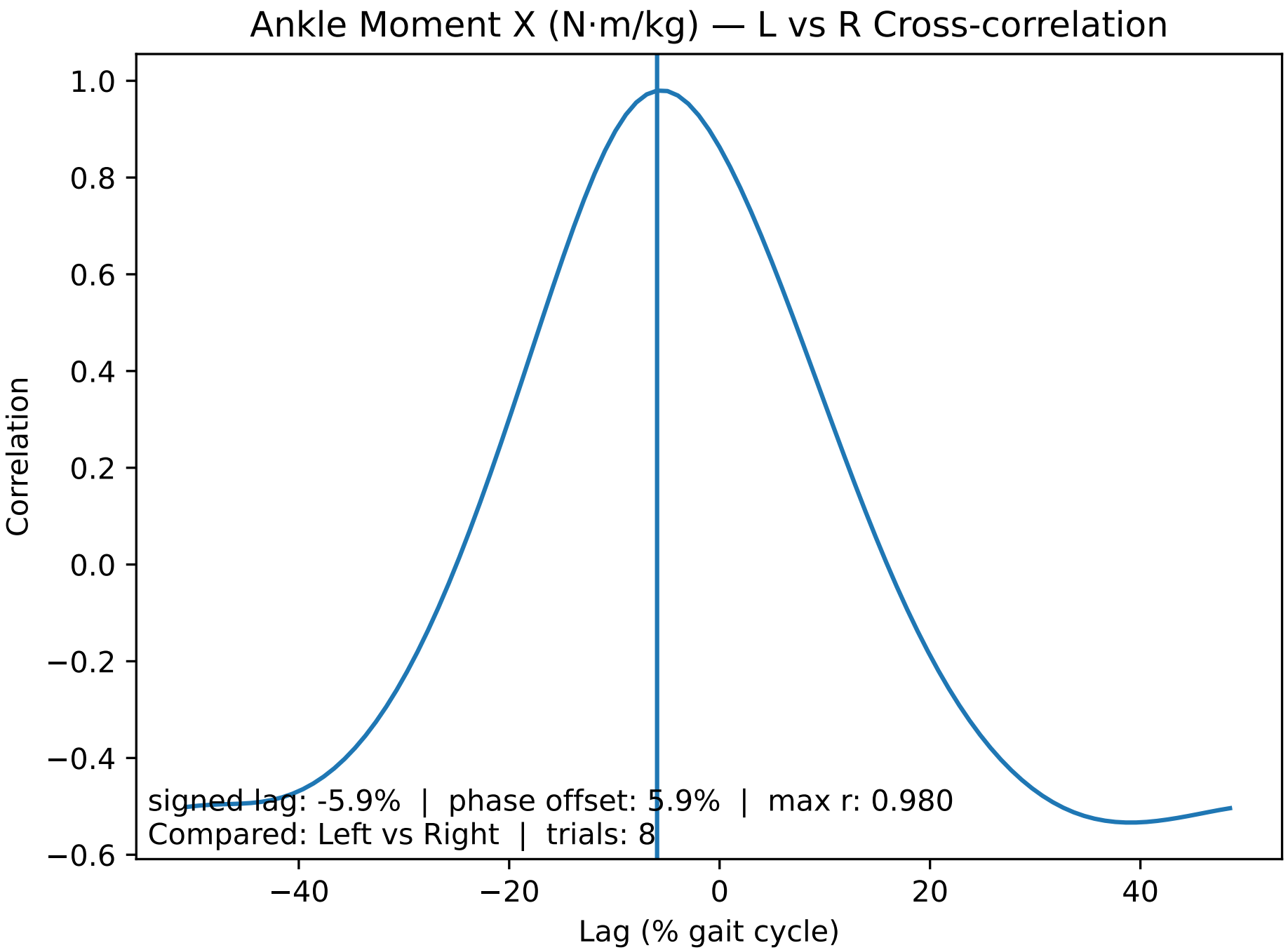
Ankle Moment X (N·m/kg) — L vs R Cross-correlation
Correlation
1.0
0.8
0.6
0.4
0.2
0.0
−0.2
−0.4
−0.6
−40
−20
0
20
40
Lag (% gait cycle)
signed lag: -5.9% | phase offset: 5.9% | max r: 0.980
Compared: Left vs Right | trials: 8

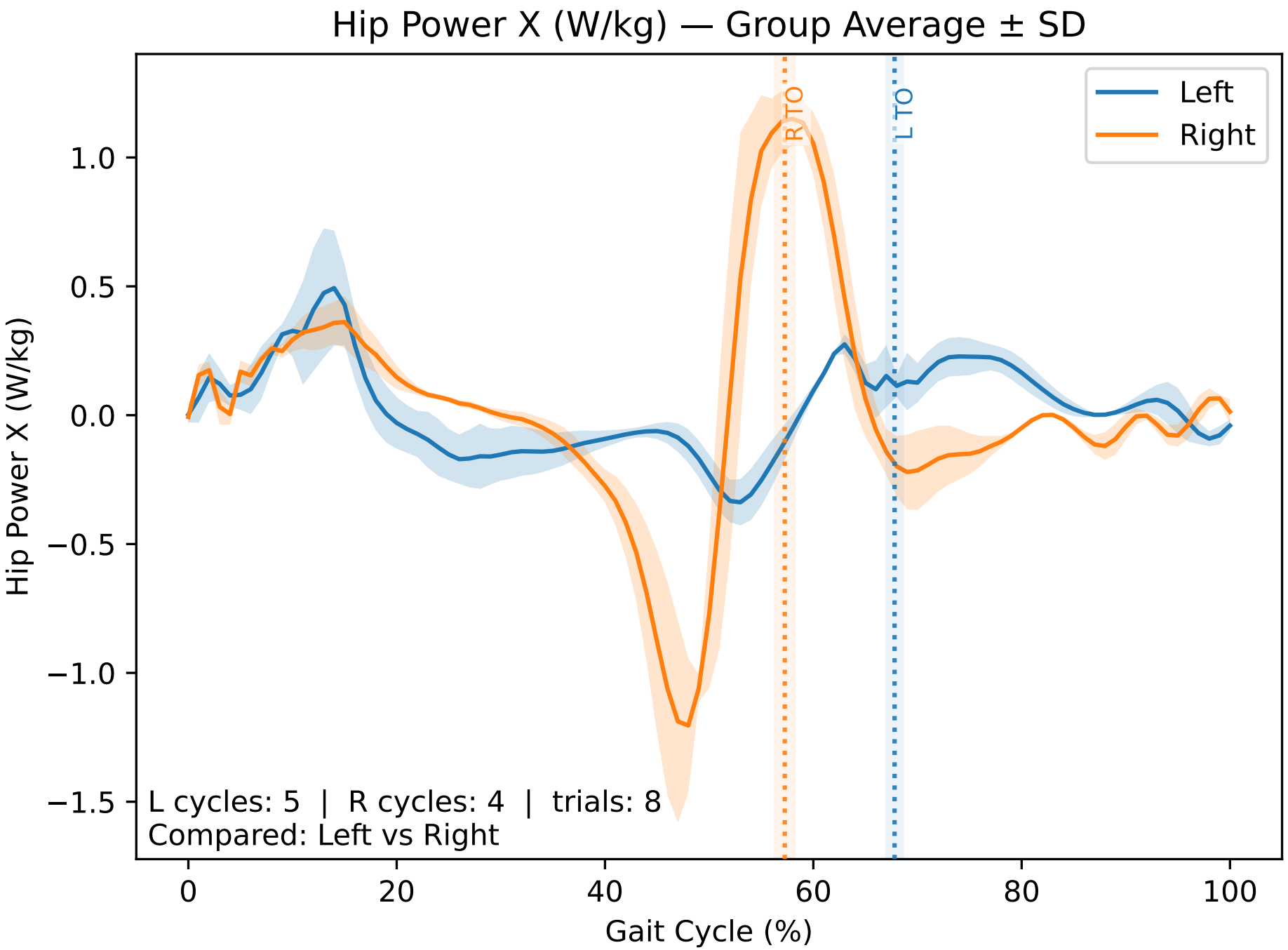
Hip Power X (W/kg) — Group Average ± SD
Left
Right
R TO
L TO
Hip Power X (W/kg)
1.0
0.5
0.0
−0.5
−1.0
−1.5
0
20
40
60
80
100
Gait Cycle (%)
L cycles: 5 | R cycles: 4 | trials: 8
Compared: Left vs Right

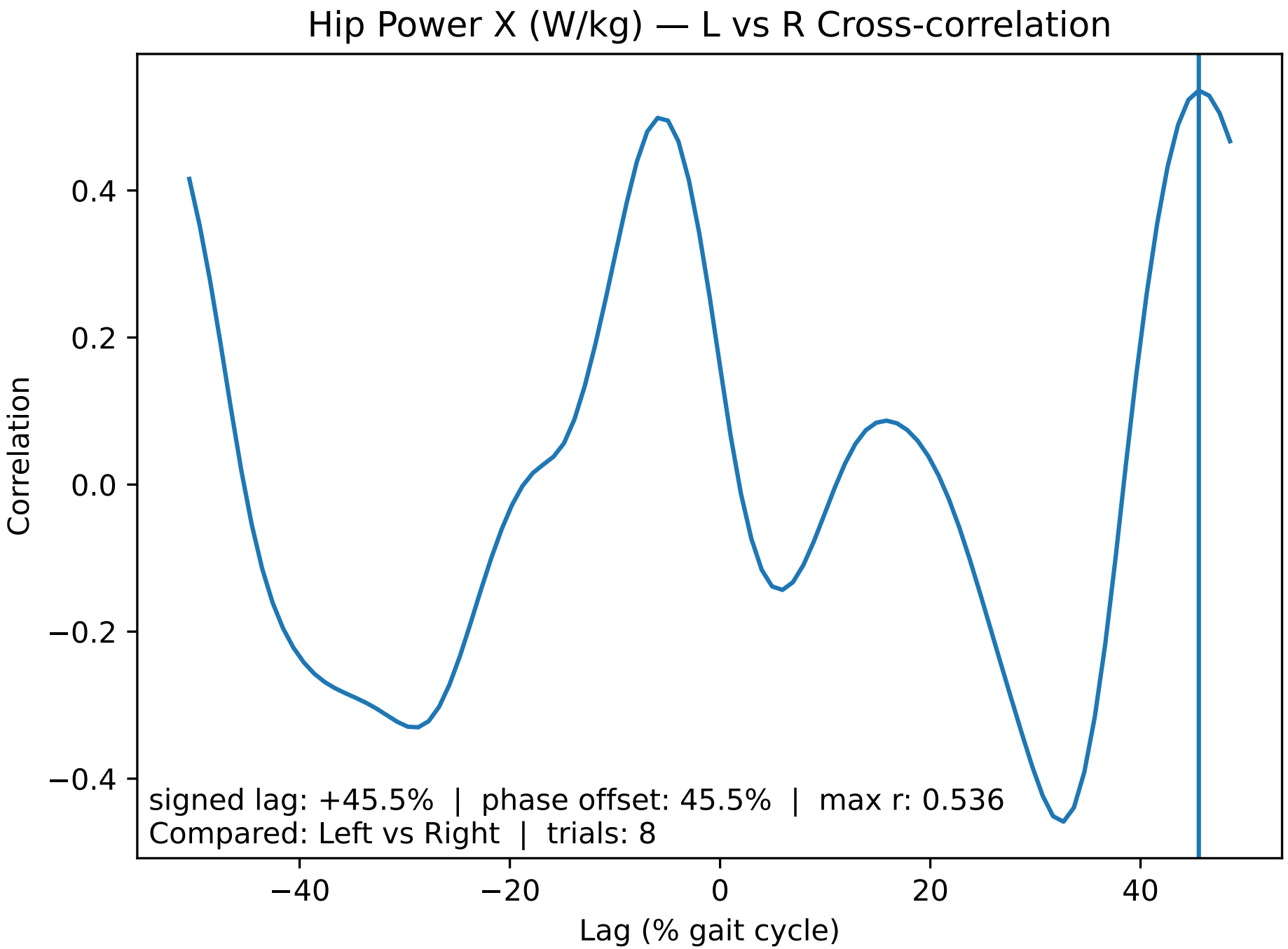
Hip Power X (W/kg) — L vs R Cross-correlation
Correlation
0.4
0.2
0.0
−0.2
−0.4
signed lag: +45.5% | phase offset: 45.5% | max r: 0.536
Compared: Left vs Right | trials: 8
−40
−20
0
20
40
Lag (% gait cycle)

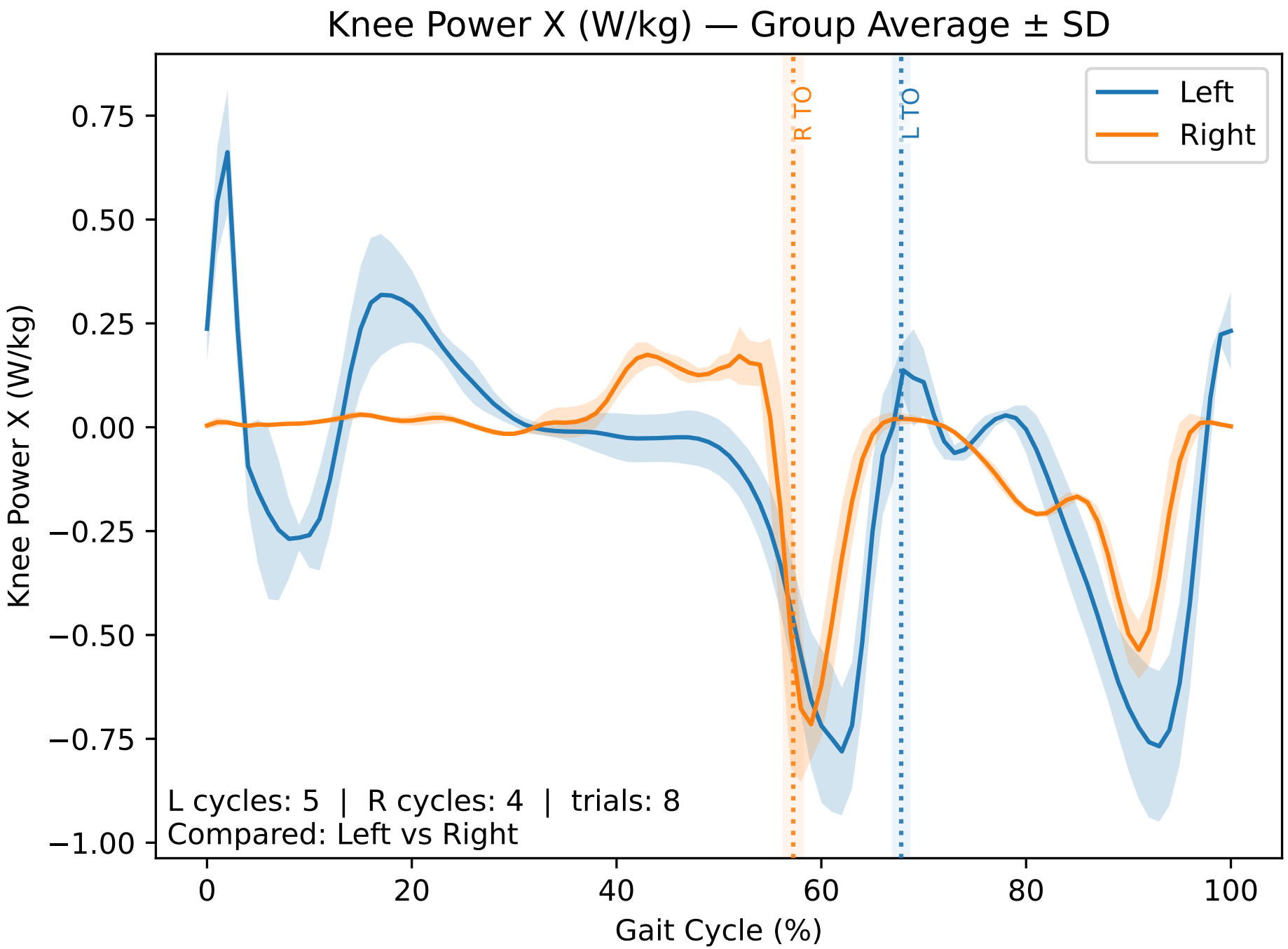
Knee Power X (W/kg) — Group Average ± SD
Knee Power X (W/kg)
Gait Cycle (%)
Left
Right
R TO
L TO
L cycles: 5 | R cycles: 4 | trials: 8
Compared: Left vs Right
0.75
0.50
0.25
0.00
−0.25
−0.50
−0.75
−1.00
0
20
40
60
80
100

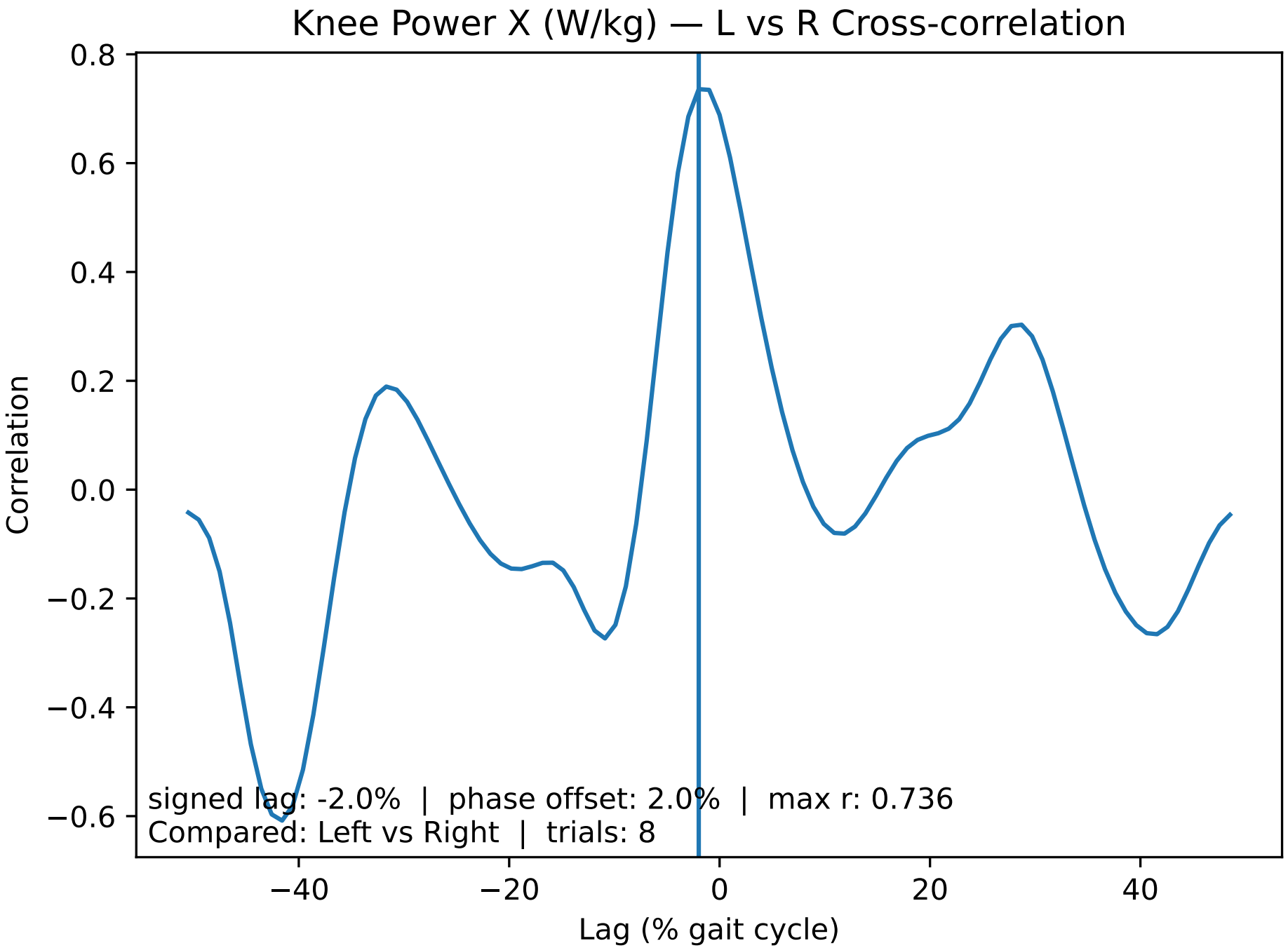
Knee Power X (W/kg) — L vs R Cross-correlation
Correlation
0.8
0.6
0.4
0.2
0.0
−0.2
−0.4
−0.6
−40
−20
0
20
40
Lag (% gait cycle)
signed lag: -2.0% | phase offset: 2.0% | max r: 0.736
Compared: Left vs Right | trials: 8

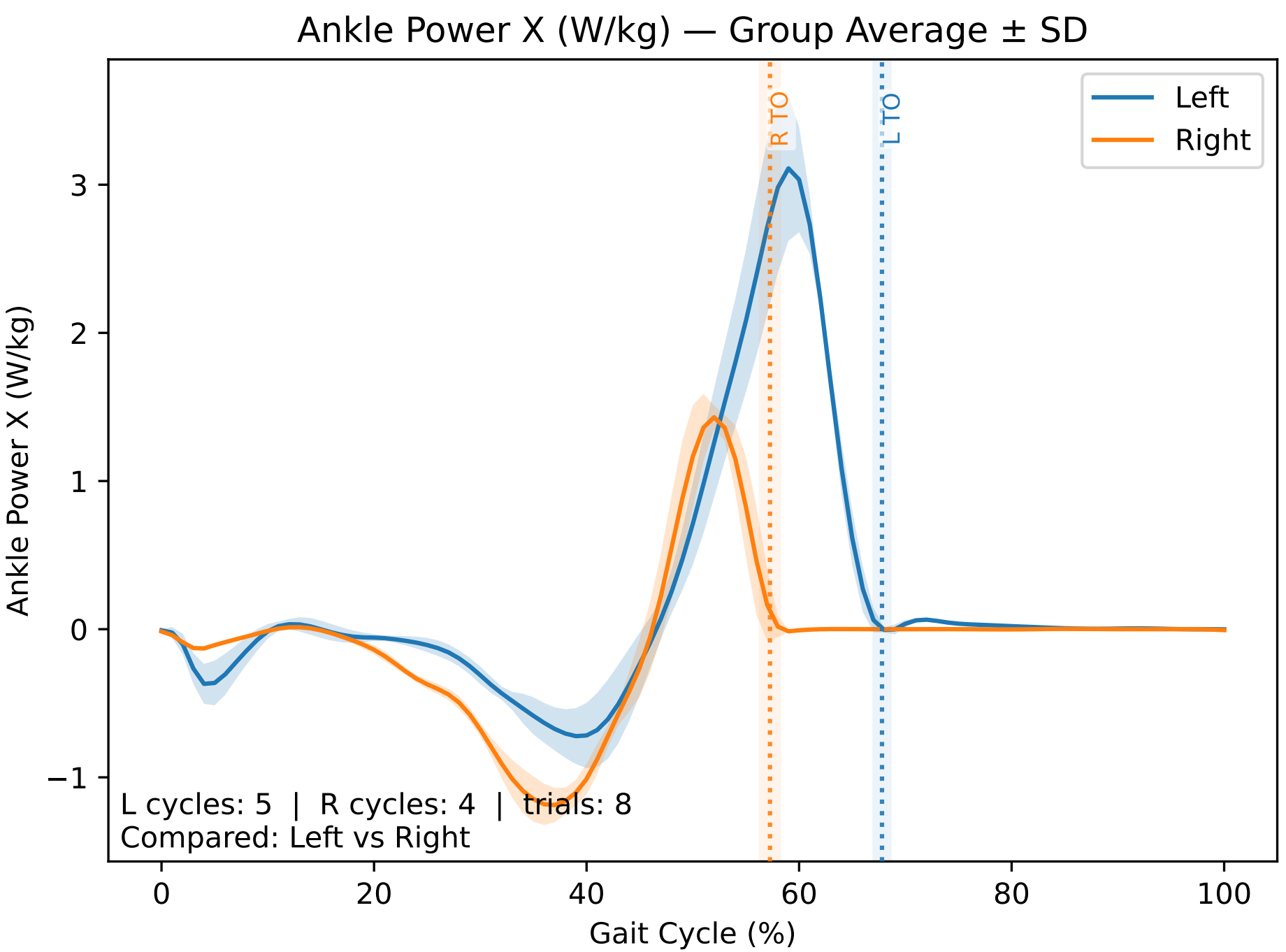
Ankle Power X (W/kg) — Group Average ± SD
Left
Right
R TO
L TO
Ankle Power X (W/kg)
Gait Cycle (%)
L cycles: 5 | R cycles: 4 | trials: 8
Compared: Left vs Right

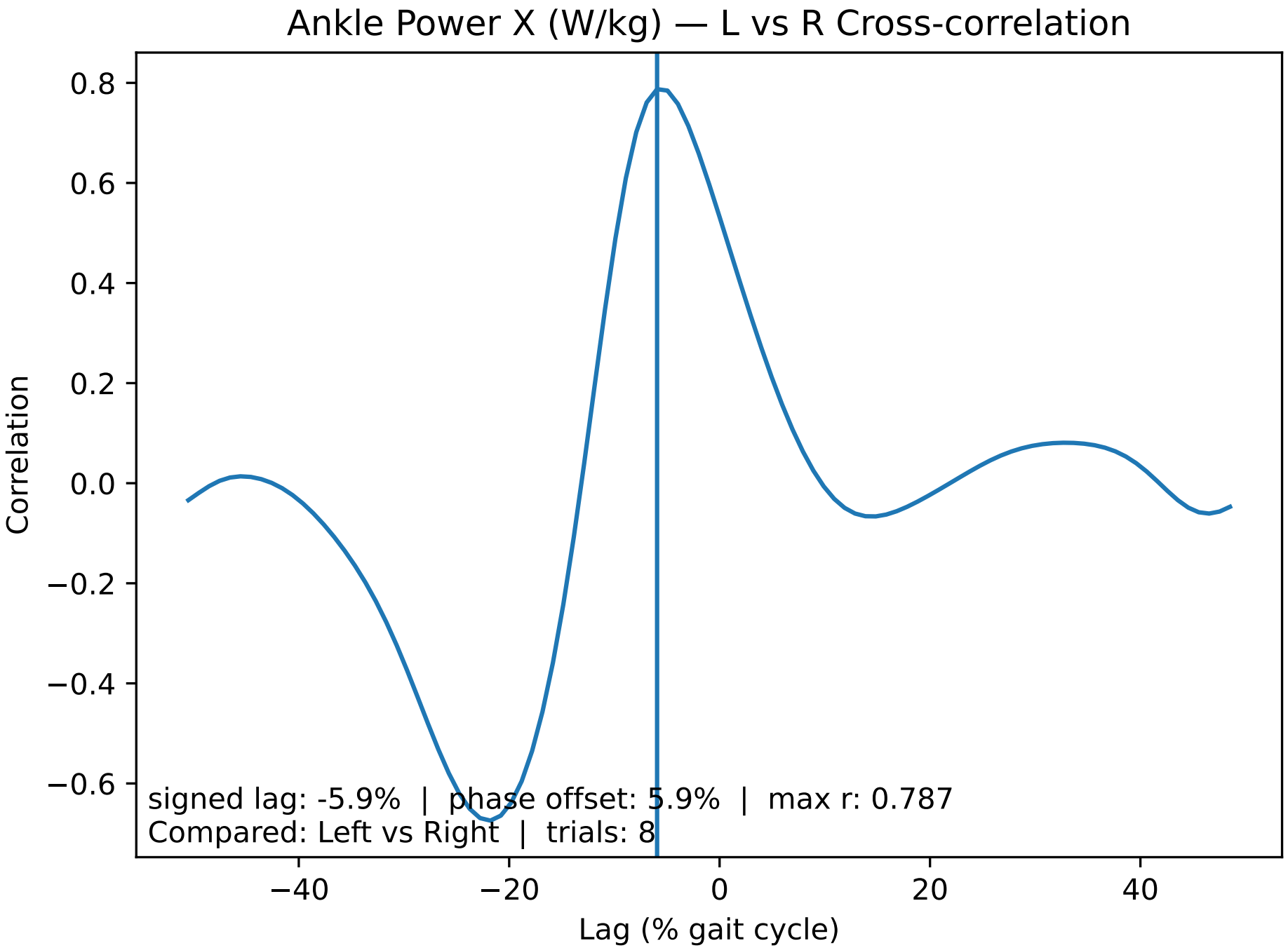
Ankle Power X (W/kg) — L vs R Cross-correlation
Correlation
0.8
0.6
0.4
0.2
0.0
−0.2
−0.4
−0.6
signed lag: -5.9% | phase offset: 5.9% | max r: 0.787
Compared: Left vs Right | trials: 8
−40
−20
0
20
40
Lag (% gait cycle)

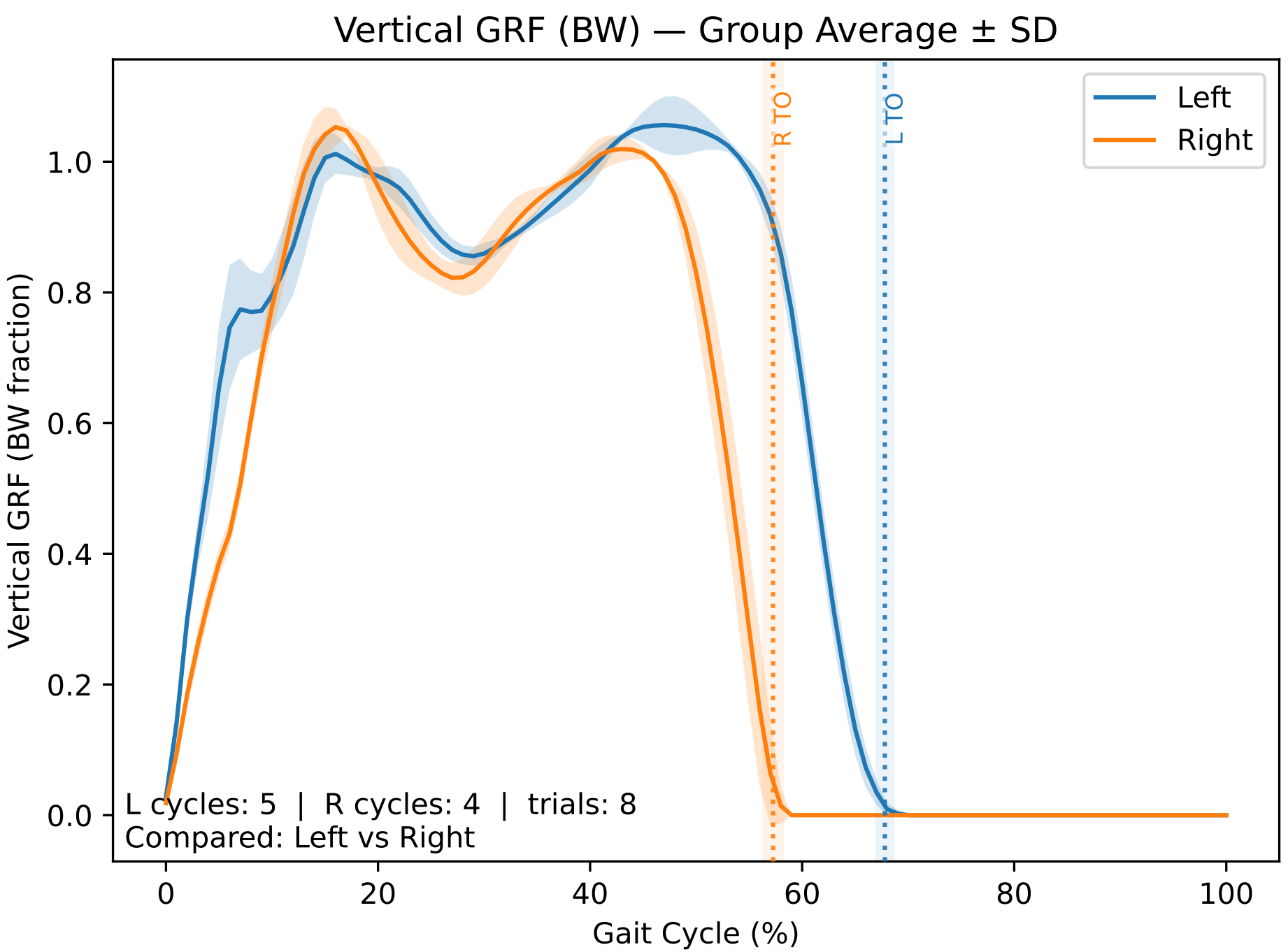
Vertical GRF (BW) — Group Average ± SD
Left
Right
R TO
L TO
Vertical GRF (BW fraction)
Gait Cycle (%)
0.0
0.2
0.4
0.6
0.8
1.0
0
20
40
60
80
100
L cycles: 5 | R cycles: 4 | trials: 8
Compared: Left vs Right

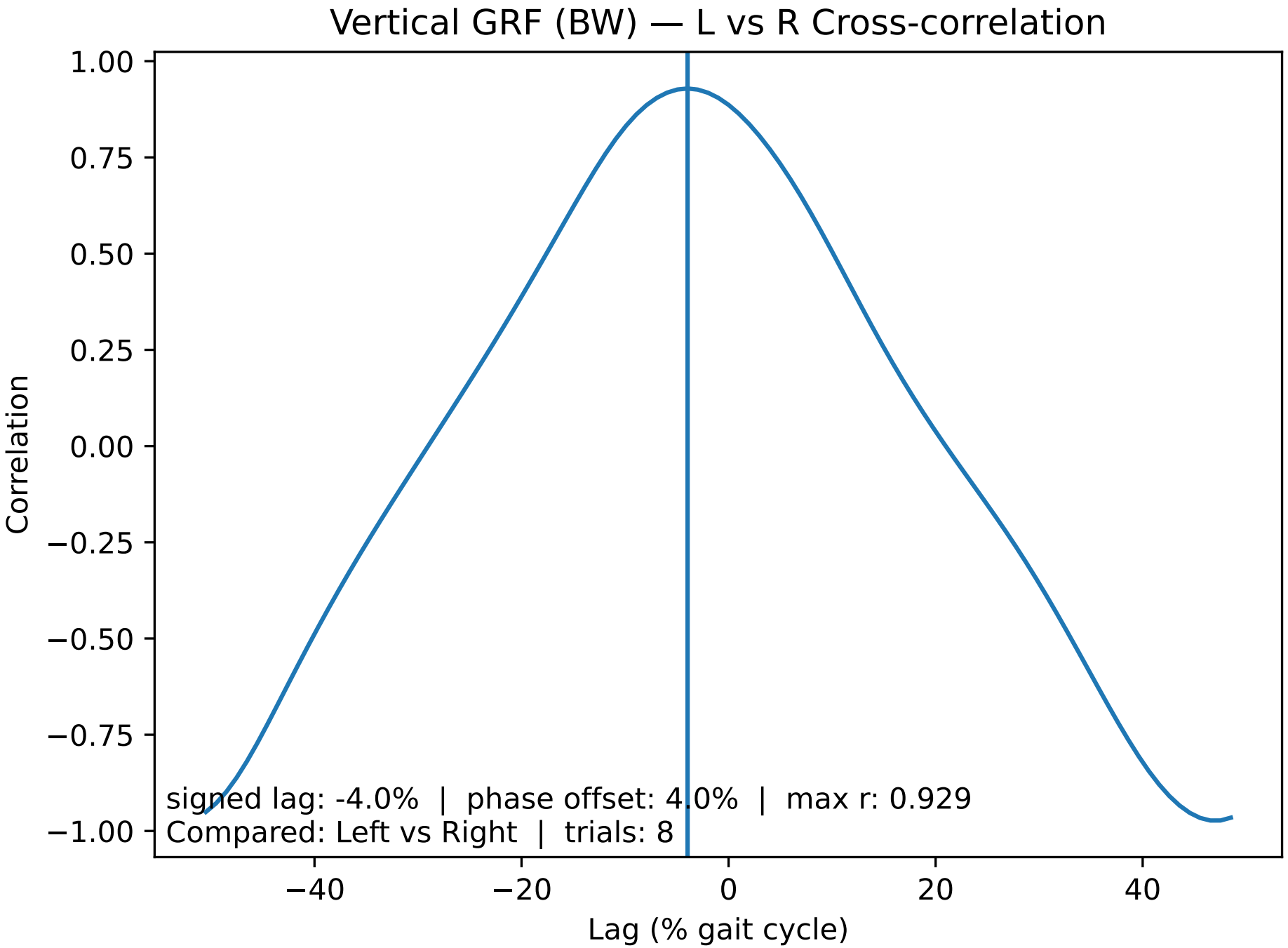
Vertical GRF (BW) — L vs R Cross-correlation
Correlation
1.00
0.75
0.50
0.25
0.00
−0.25
−0.50
−0.75
−1.00
−40
−20
0
20
40
Lag (% gait cycle)
signed lag: -4.0% | phase offset: 4.0% | max r: 0.929
Compared: Left vs Right | trials: 8

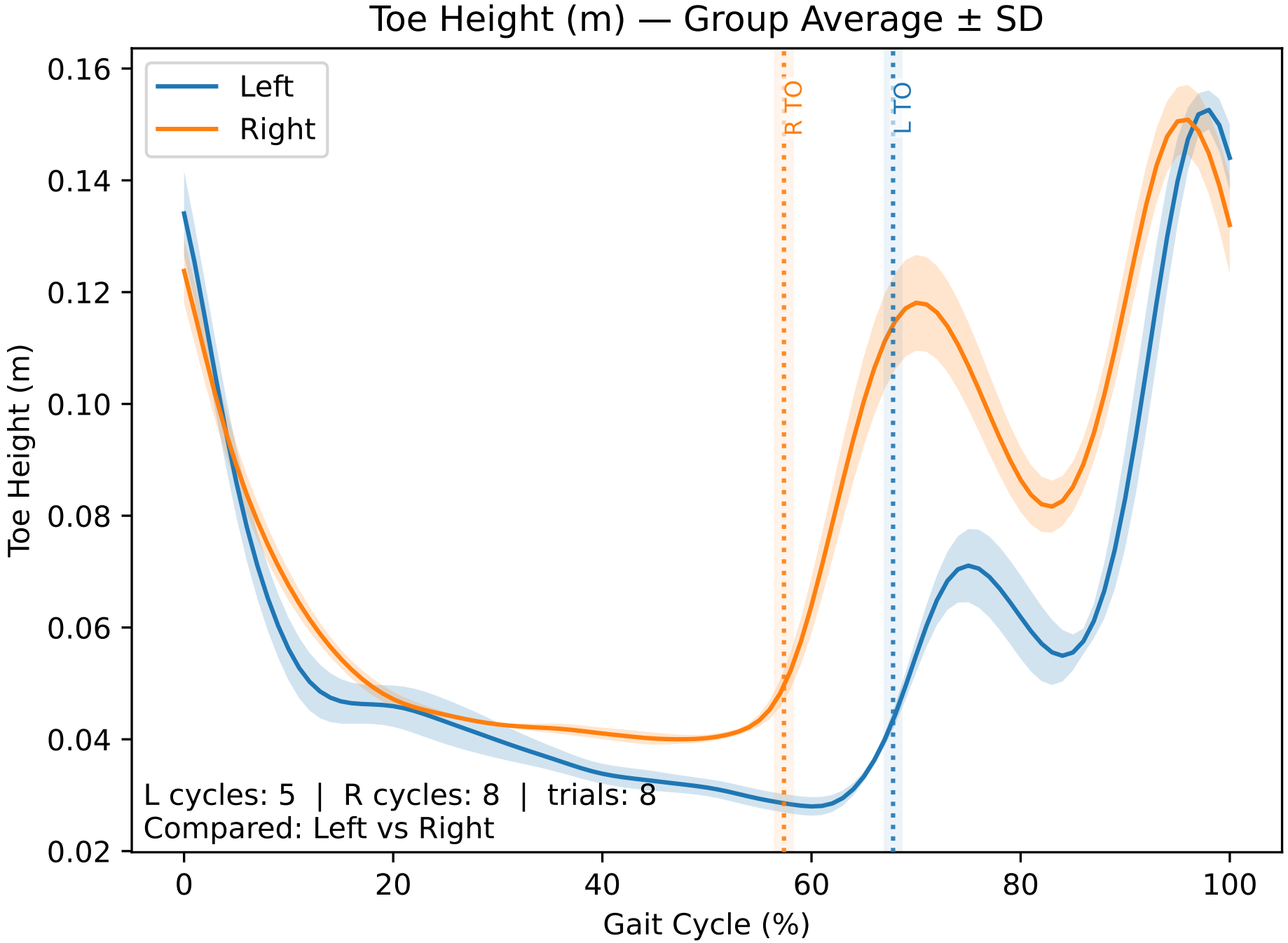
Toe Height (m) — Group Average ± SD
Left
Right
R TO
L TO
Toe Height (m)
0.16
0.14
0.12
0.10
0.08
0.06
0.04
0.02
0
20
40
60
80
100
Gait Cycle (%)
L cycles: 5 | R cycles: 8 | trials: 8
Compared: Left vs Right

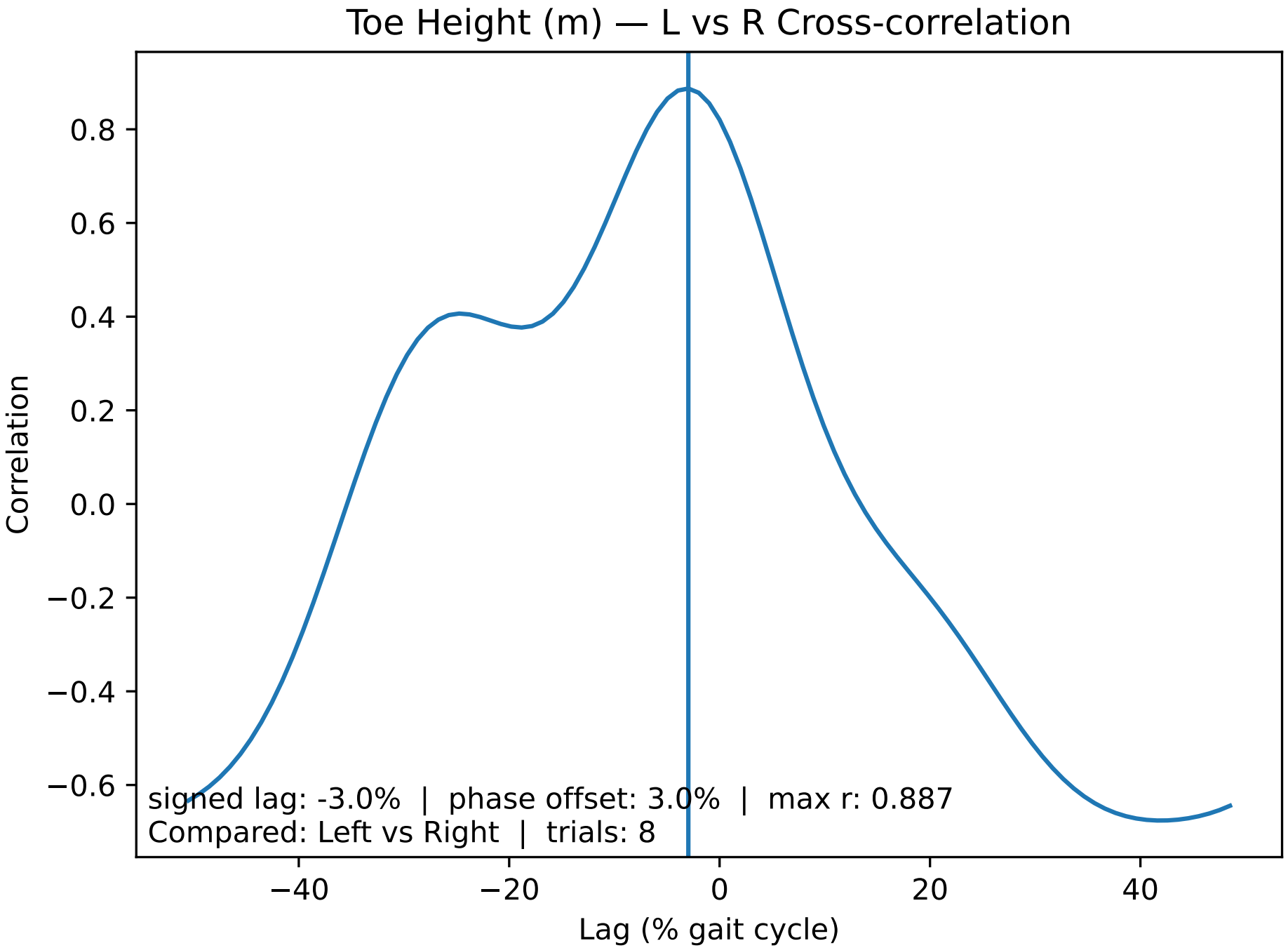
Toe Height (m) — L vs R Cross-correlation
Correlation
0.8
0.6
0.4
0.2
0.0
−0.2
−0.4
−0.6
signed lag: -3.0% | phase offset: 3.0% | max r: 0.887
Compared: Left vs Right | trials: 8
−40
−20
0
20
40
Lag (% gait cycle)

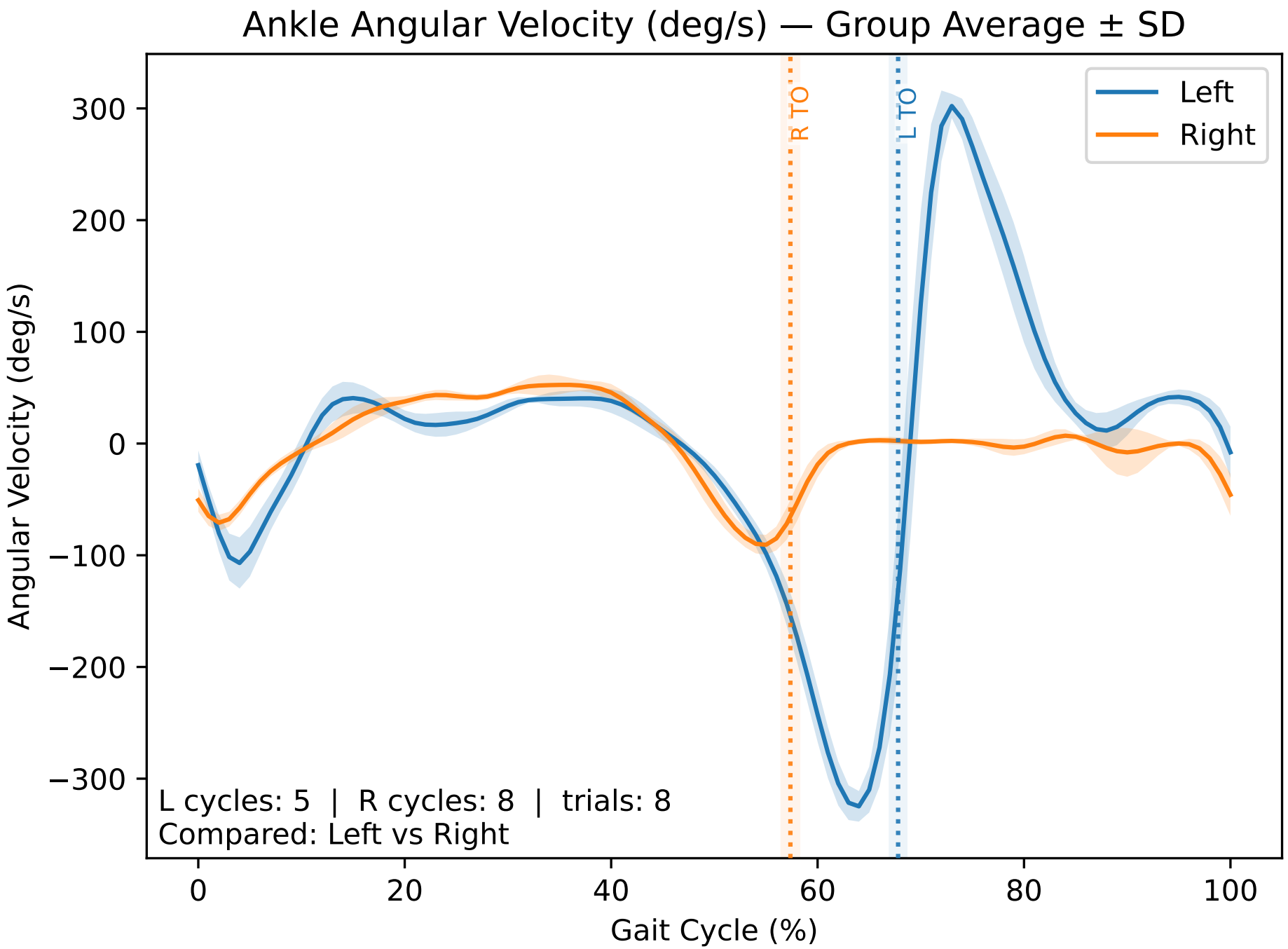
Ankle Angular Velocity (deg/s) — Group Average ± SD
Angular Velocity (deg/s)
Gait Cycle (%)
Left
Right
R TO
L TO
L cycles: 5 | R cycles: 8 | trials: 8
Compared: Left vs Right
300
200
100
0
−100
−200
−300
0
20
40
60
80
100

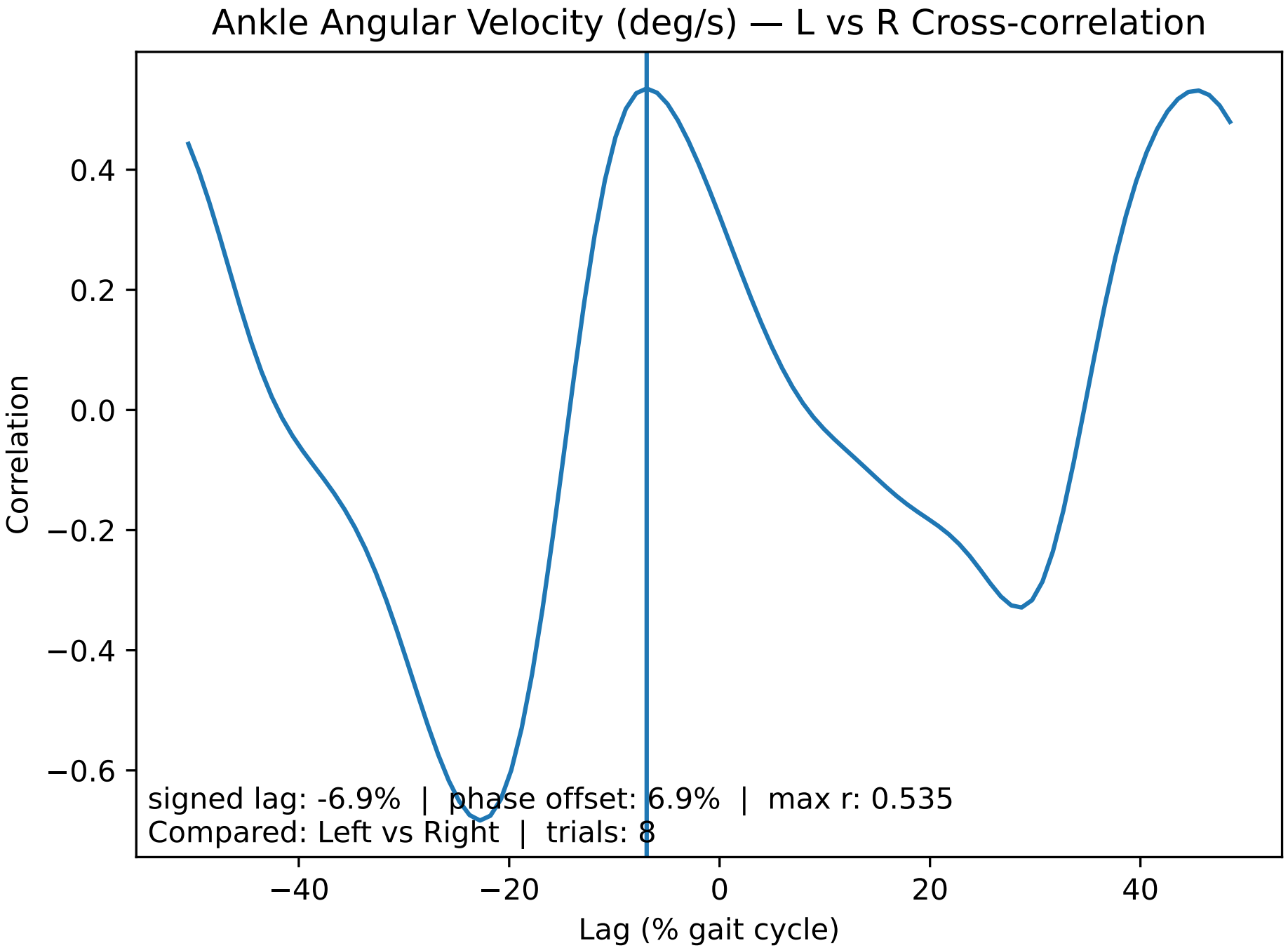
Ankle Angular Velocity (deg/s) — L vs R Cross-correlation
Correlation
0.4
0.2
0.0
−0.2
−0.4
−0.6
signed lag: -6.9% | phase offset: 6.9% | max r: 0.535
Compared: Left vs Right | trials: 8
−40
−20
0
20
40
Lag (% gait cycle)

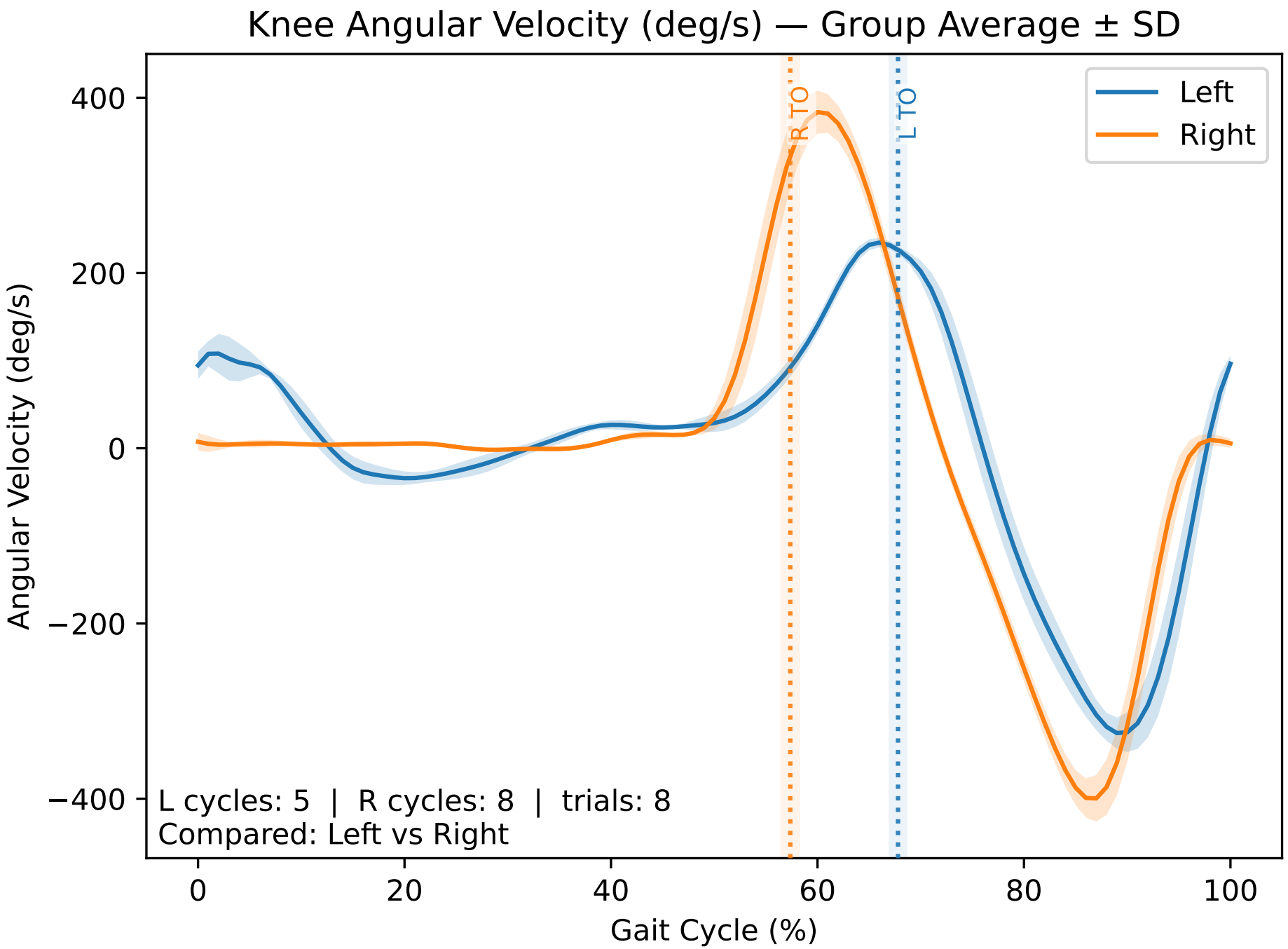
Knee Angular Velocity (deg/s) — Group Average ± SD
Angular Velocity (deg/s)
400
200
0
−200
−400
0
20
40
60
80
100
Gait Cycle (%)
R TO
L TO
Left
Right
L cycles: 5 | R cycles: 8 | trials: 8
Compared: Left vs Right

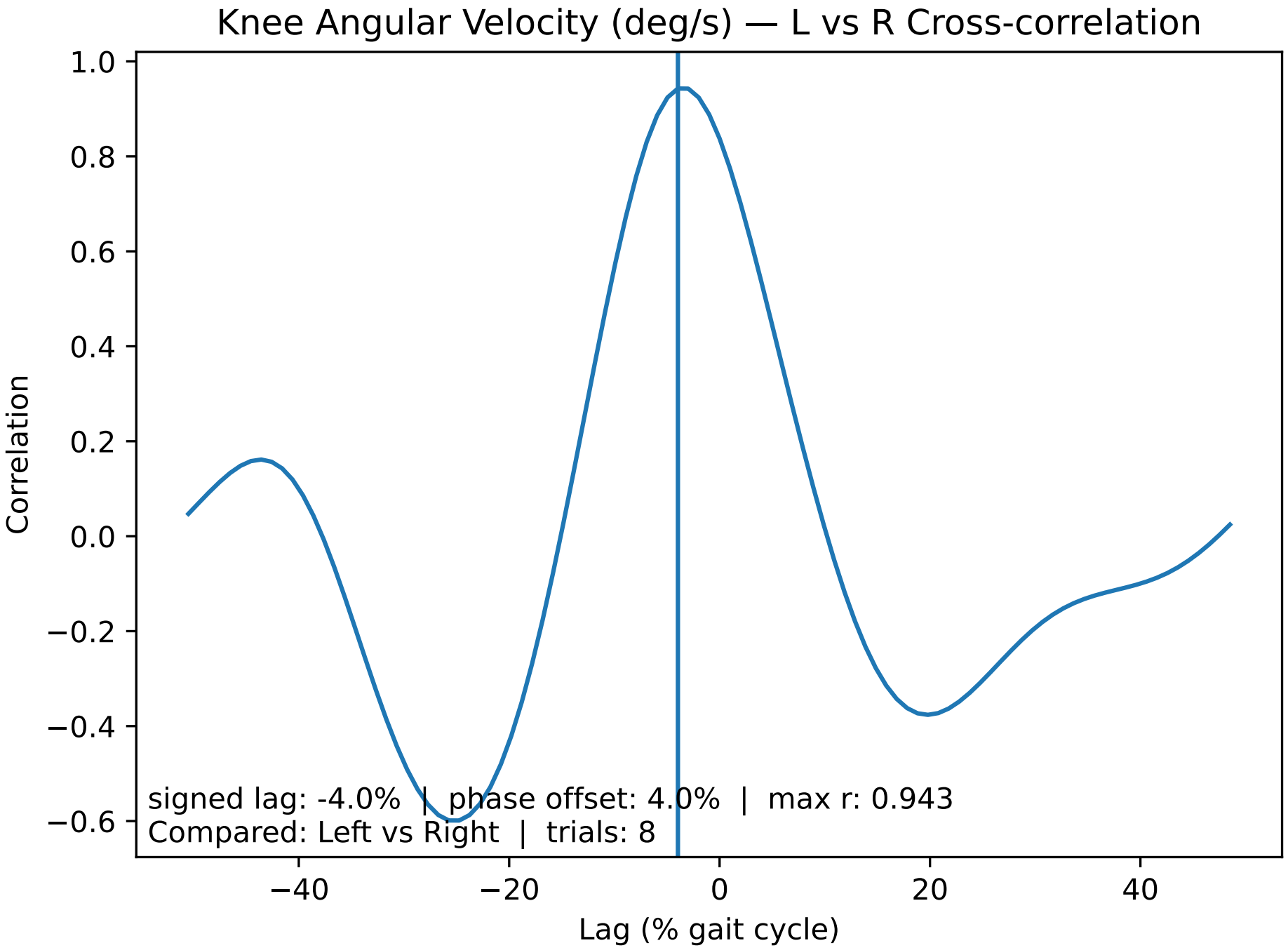
Knee Angular Velocity (deg/s) — L vs R Cross-correlation
Correlation
1.0
0.8
0.6
0.4
0.2
0.0
−0.2
−0.4
−0.6
−40
−20
0
20
40
Lag (% gait cycle)
signed lag: -4.0% | phase offset: 4.0% | max r: 0.943
Compared: Left vs Right | trials: 8

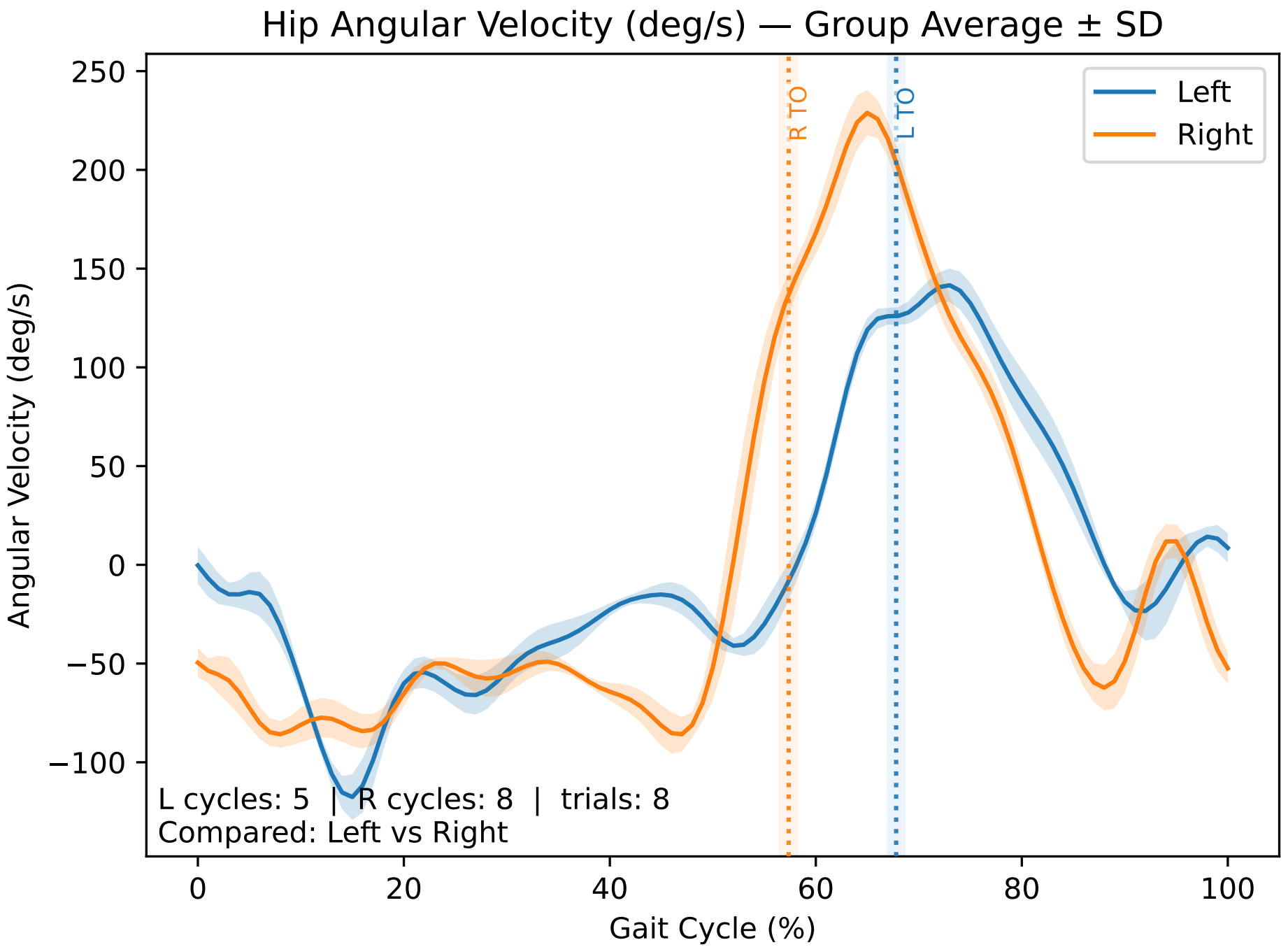
Hip Angular Velocity (deg/s) — Group Average ± SD
Angular Velocity (deg/s)
Gait Cycle (%)
Left
Right
R TO
L TO
L cycles: 5 | R cycles: 8 | trials: 8
Compared: Left vs Right
250
200
150
100
50
0
−50
−100
0
20
40
60
80
100

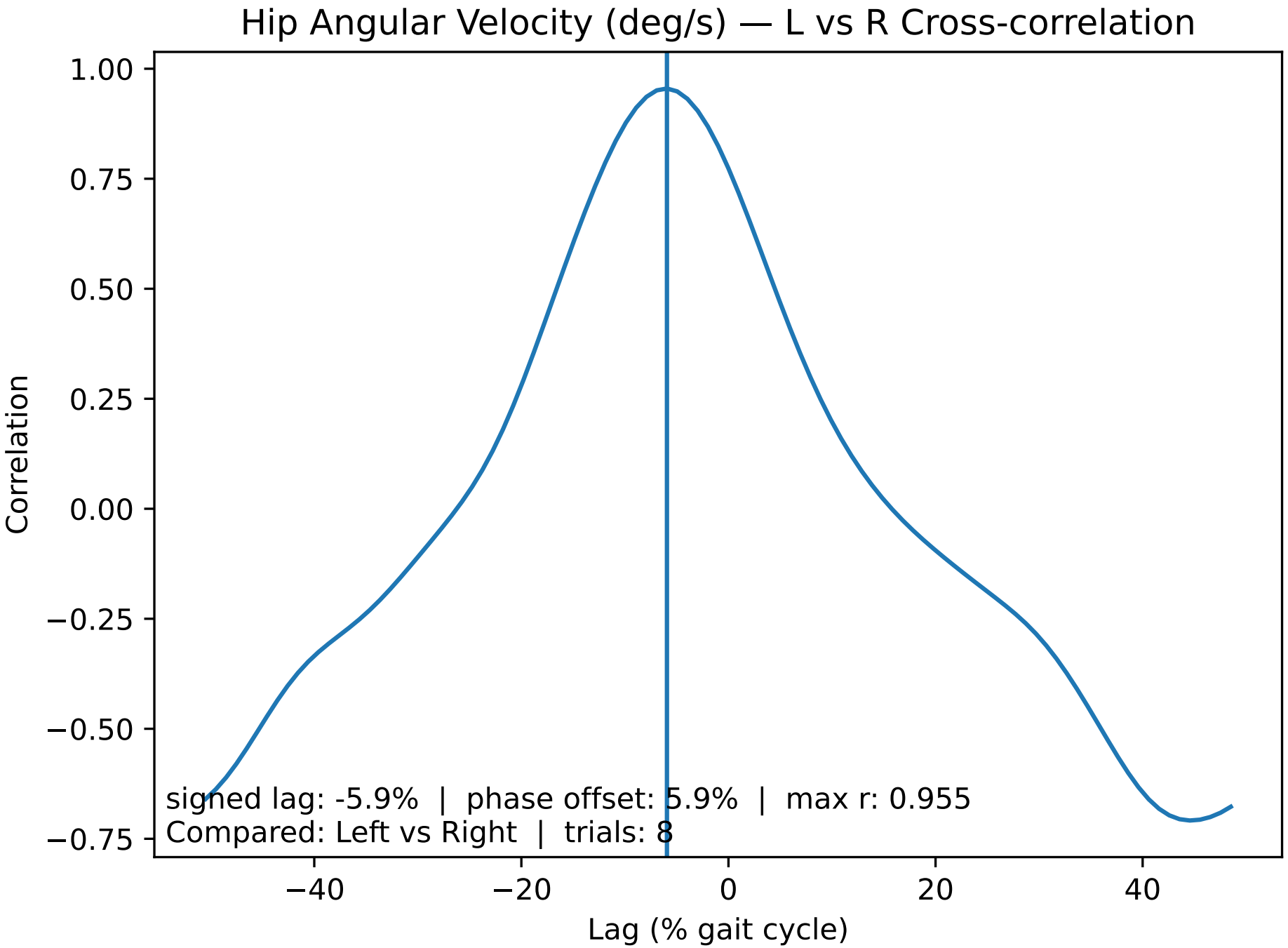
Hip Angular Velocity (deg/s) — L vs R Cross-correlation
Correlation
1.00
0.75
0.50
0.25
0.00
−0.25
−0.50
−0.75
−40
−20
0
20
40
Lag (% gait cycle)
signed lag: -5.9% | phase offset: 5.9% | max r: 0.955
Compared: Left vs Right | trials: 8

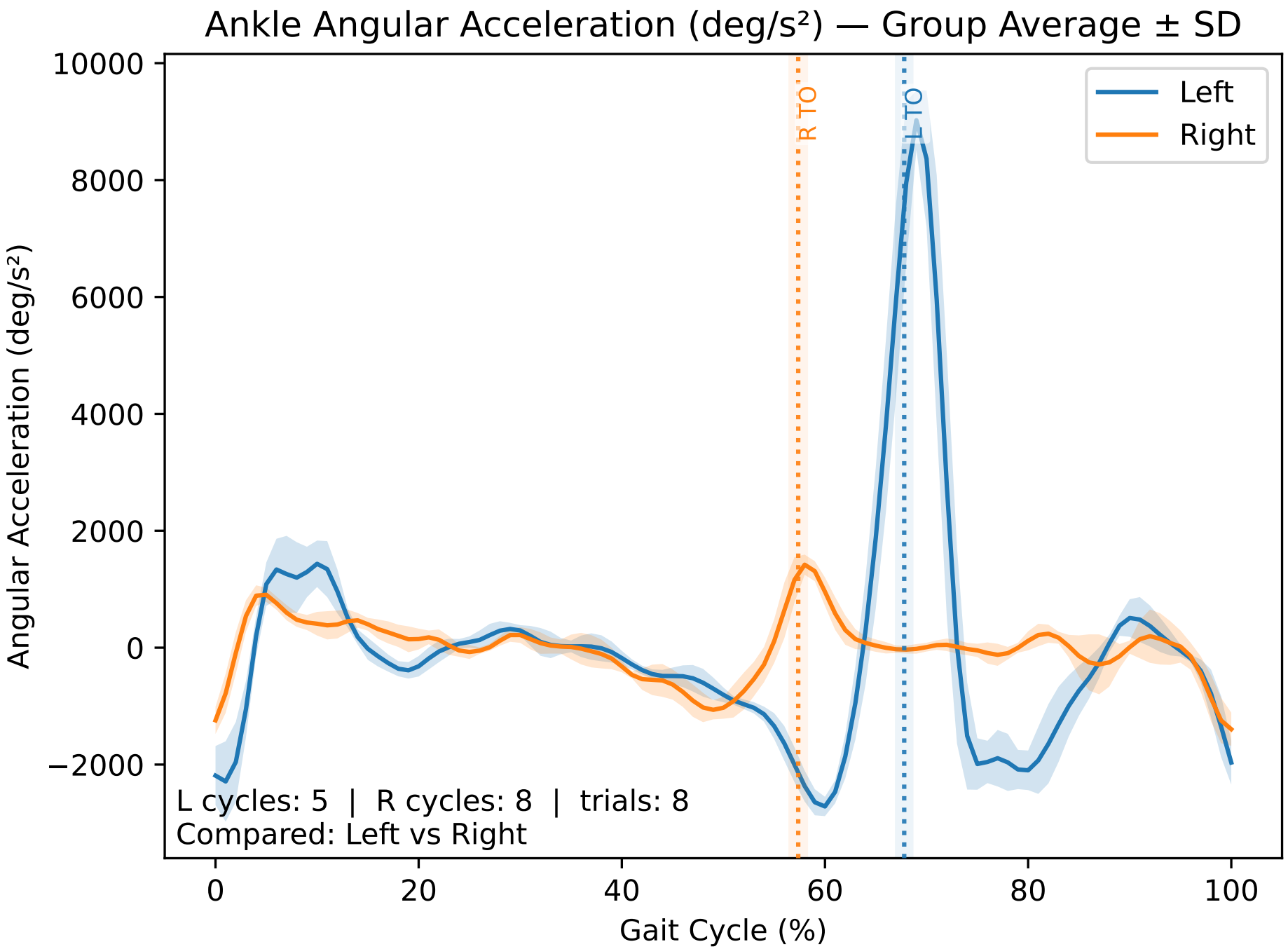
Ankle Angular Acceleration (deg/s²) — Group Average ± SD
Angular Acceleration (deg/s²)
10000
8000
6000
4000
2000
0
−2000
0
20
40
60
80
100
Gait Cycle (%)
R TO
L TO
Left
Right
L cycles: 5 | R cycles: 8 | trials: 8
Compared: Left vs Right

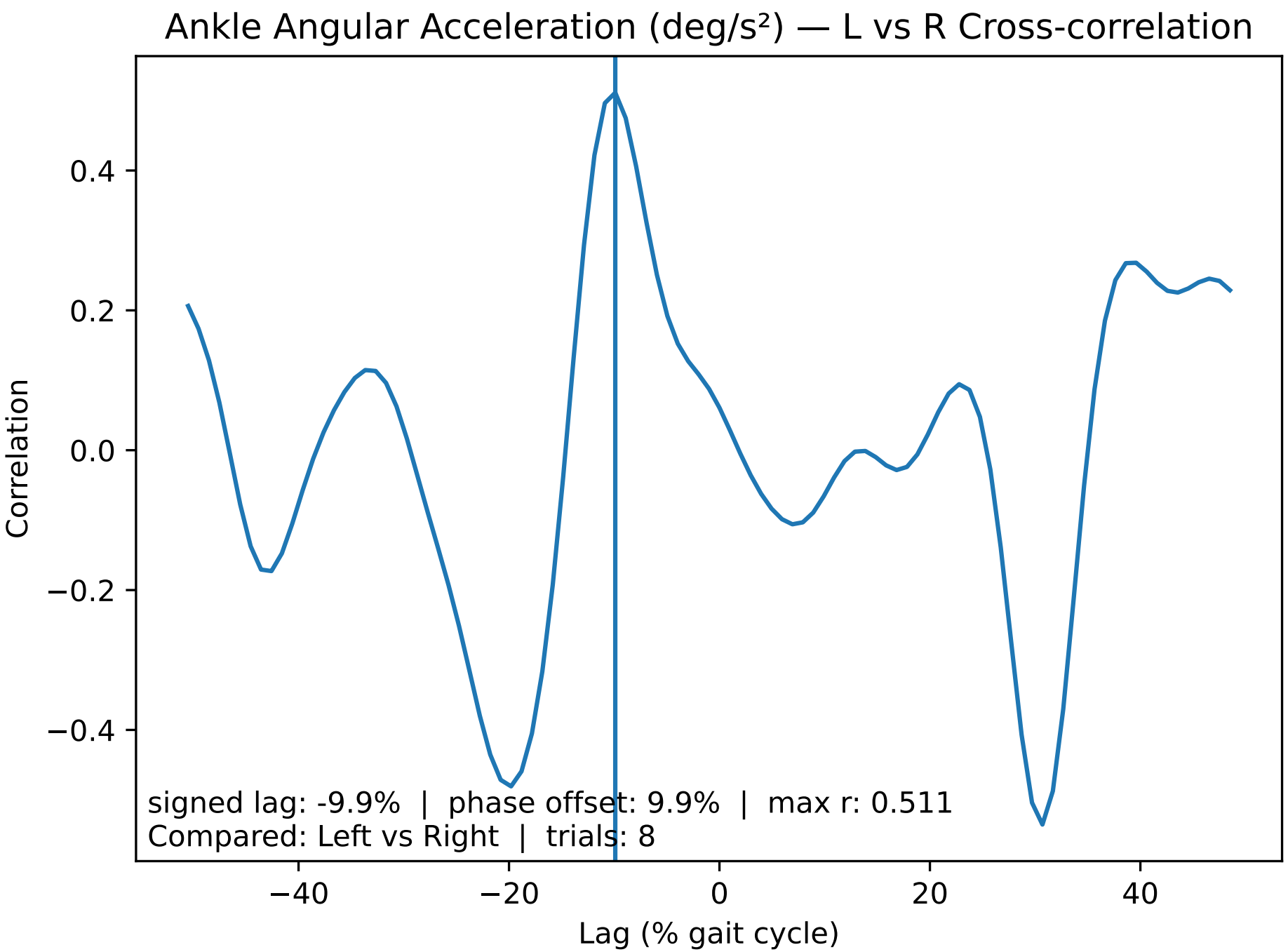
Ankle Angular Acceleration (deg/s²) — L vs R Cross-correlation
Correlation
0.4
0.2
0.0
−0.2
−0.4
signed lag: -9.9% | phase offset: 9.9% | max r: 0.511
Compared: Left vs Right | trials: 8
−40
−20
0
20
40
Lag (% gait cycle)

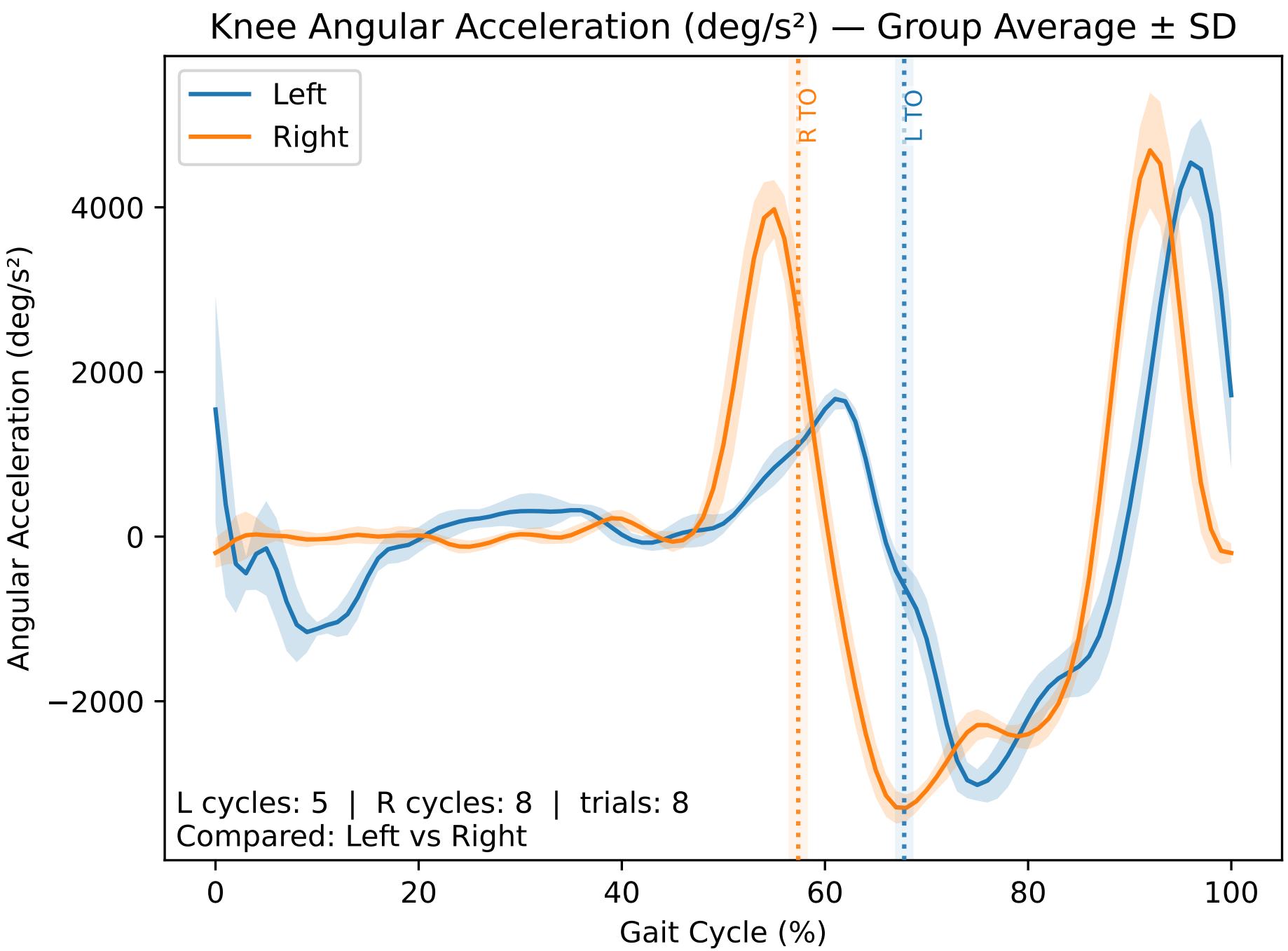
Knee Angular Acceleration (deg/s²) — Group Average ± SD
Left
Right
R TO
L TO
4000
2000
0
−2000
Angular Acceleration (deg/s²)
0
20
40
60
80
100
Gait Cycle (%)
L cycles: 5 | R cycles: 8 | trials: 8
Compared: Left vs Right

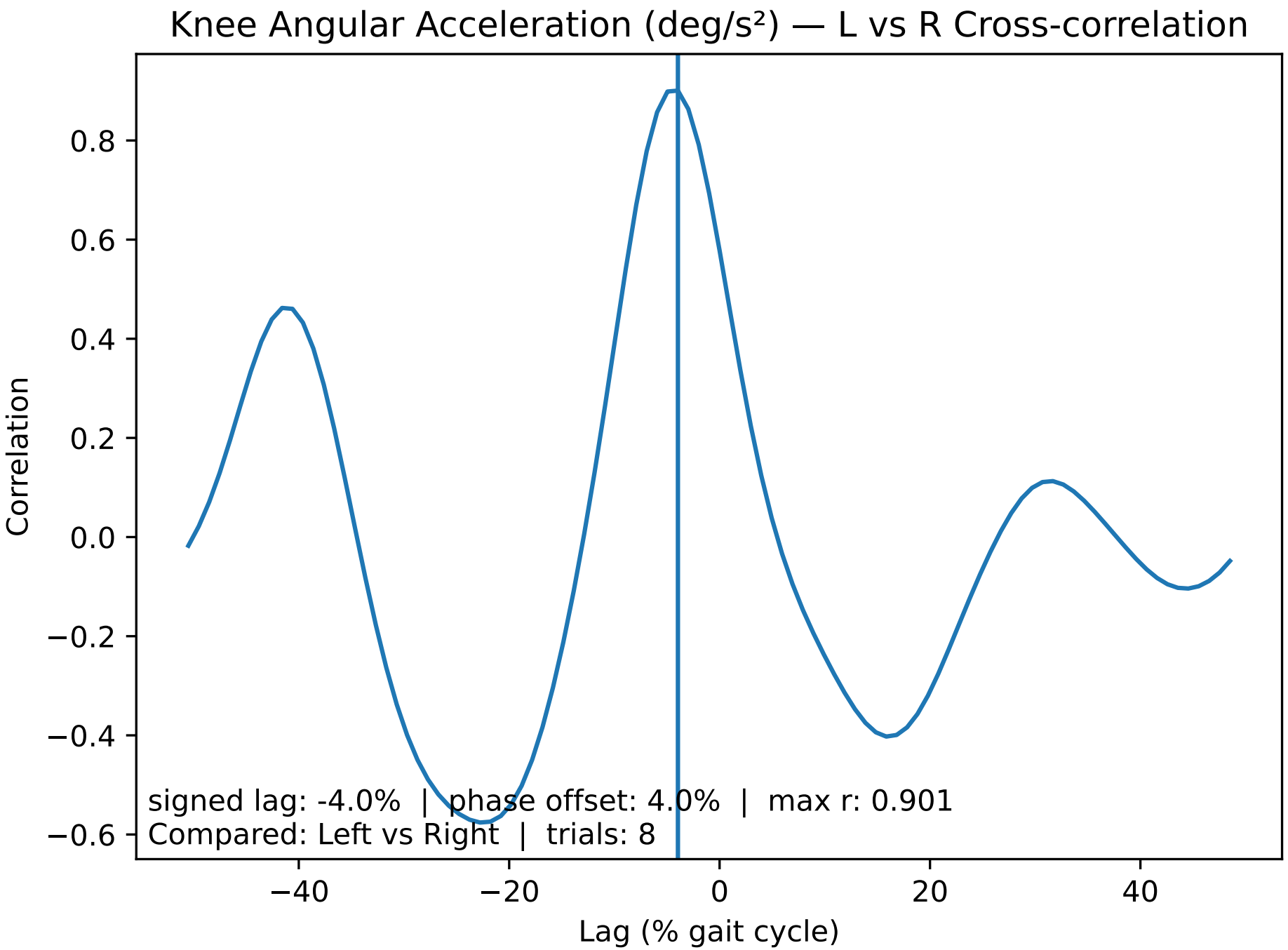
Knee Angular Acceleration (deg/s²) — L vs R Cross-correlation
Correlation
0.8
0.6
0.4
0.2
0.0
−0.2
−0.4
−0.6
−40
−20
0
20
40
Lag (% gait cycle)
signed lag: -4.0% | phase offset: 4.0% | max r: 0.901
Compared: Left vs Right | trials: 8

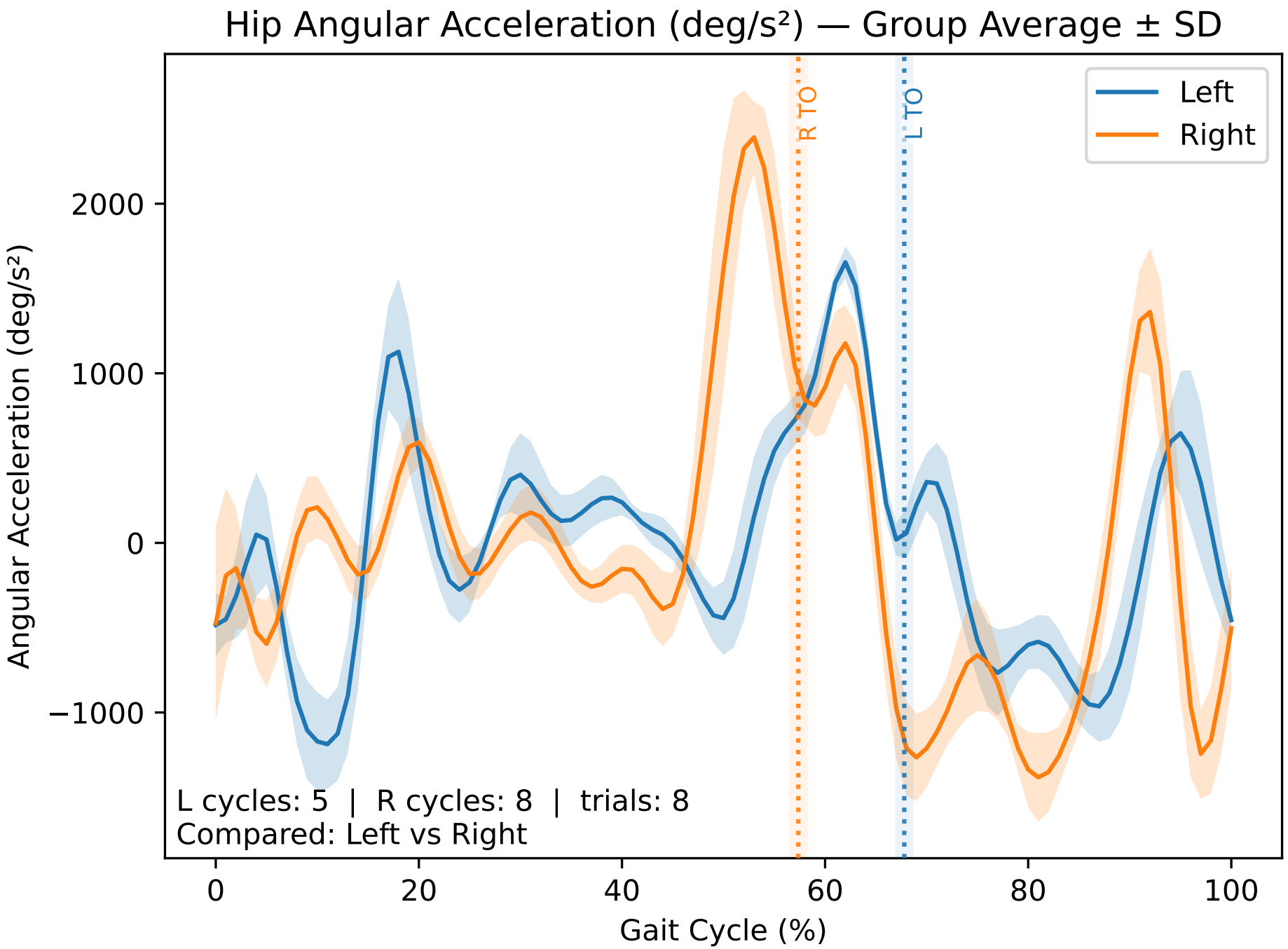
Hip Angular Acceleration (deg/s²) — Group Average ± SD
Left
Right
R TO
L TO
Angular Acceleration (deg/s²)
2000
1000
0
−1000
0
20
40
60
80
100
Gait Cycle (%)
L cycles: 5 | R cycles: 8 | trials: 8
Compared: Left vs Right

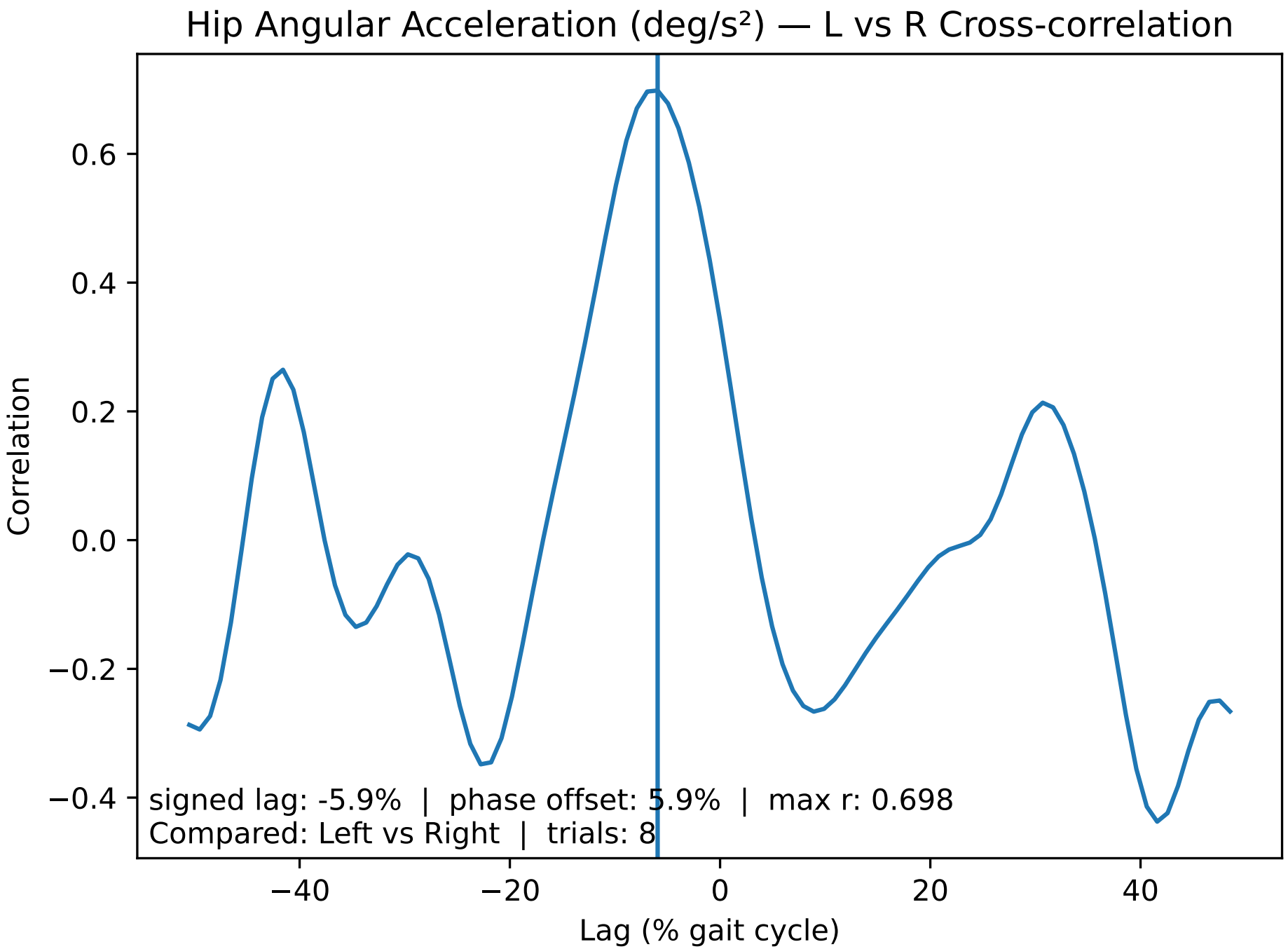
Hip Angular Acceleration (deg/s²) — L vs R Cross-correlation
Correlation
0.6
0.4
0.2
0.0
−0.2
−0.4
signed lag: -5.9% | phase offset: 5.9% | max r: 0.698
Compared: Left vs Right | trials: 8
−40
−20
0
20
40
Lag (% gait cycle)

C. Gait Trial Results — Ottobock Genium X3

This appendix presents the corresponding gait-trial results for the Ottobock Genium X3. Table C.1 lists the kinematic and cross-correlation plots that the report contains.The data serve as a reference for comparison with the 4BM prototype in Chapter 5.

Table C.1. Overview of Genium X3 gait-trial plots included in this appendix. Each variable includes both group-average and left–right cross-correlation plots.

Parameter	Plot Type	Page
Hip Flexion	Group Average	135
	L vs R Cross-correlation	136
Knee Flexion	Group Average	137
	L vs R Cross-correlation	138
Ankle Flexion	Group Average	139
	L vs R Cross-correlation	140
Hip Moment	Group Average	141
	L vs R Cross-correlation	142
Knee Moment	Group Average	143
	L vs R Cross-correlation	144
Ankle Moment	Group Average	145
	L vs R Cross-correlation	146
Hip Power	Group Average	147
	L vs R Cross-correlation	148
Knee Power	Group Average	149
	L vs R Cross-correlation	150
Ankle Power	Group Average	151
	L vs R Cross-correlation	152
Vertical GRF	Group Average	153
	L vs R Cross-correlation	154
Toe Height	Group Average	155
	L vs R Cross-correlation	156
Ankle Angular Velocity	Group Average	157
	L vs R Cross-correlation	158
Knee Angular Velocity	Group Average	159
	L vs R Cross-correlation	160
Hip Angular Velocity	Group Average	161
	L vs R Cross-correlation	162
Ankle Angular Acceleration	Group Average	163
	L vs R Cross-correlation	164
Knee Angular Acceleration	Group Average	165
	L vs R Cross-correlation	166
Hip Angular Acceleration	Group Average	167
	L vs R Cross-correlation	168

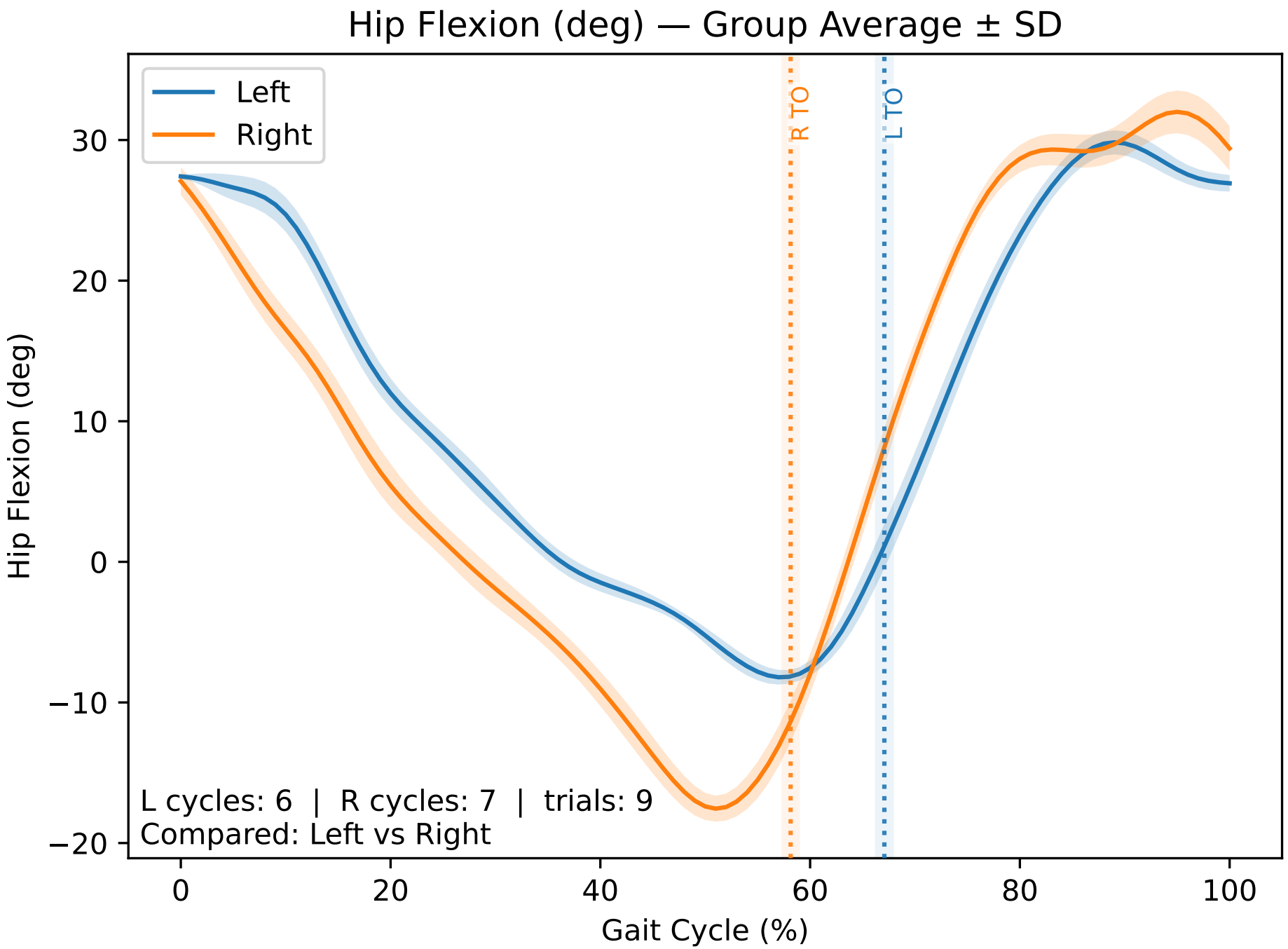
Hip Flexion (deg) — Group Average ± SD
Left
Right
R TO
L TO
Hip Flexion (deg)
30
20
10
0
−10
−20
0
20
40
60
80
100
Gait Cycle (%)
L cycles: 6 | R cycles: 7 | trials: 9
Compared: Left vs Right

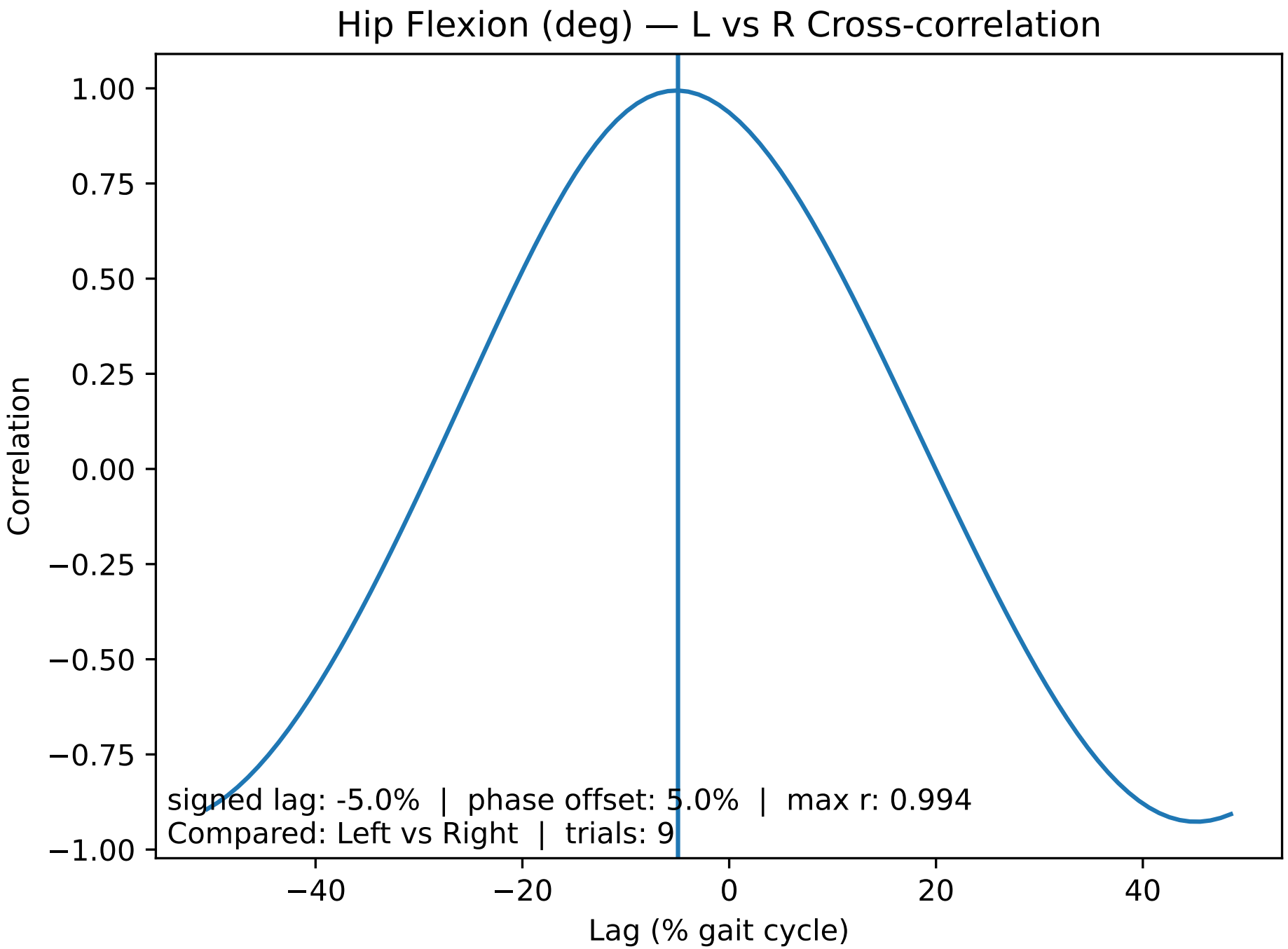
Hip Flexion (deg) — L vs R Cross-correlation
Correlation
1.00
0.75
0.50
0.25
0.00
−0.25
−0.50
−0.75
−1.00
−40
−20
0
20
40
Lag (% gait cycle)
signed lag: -5.0% | phase offset: 5.0% | max r: 0.994
Compared: Left vs Right | trials: 9

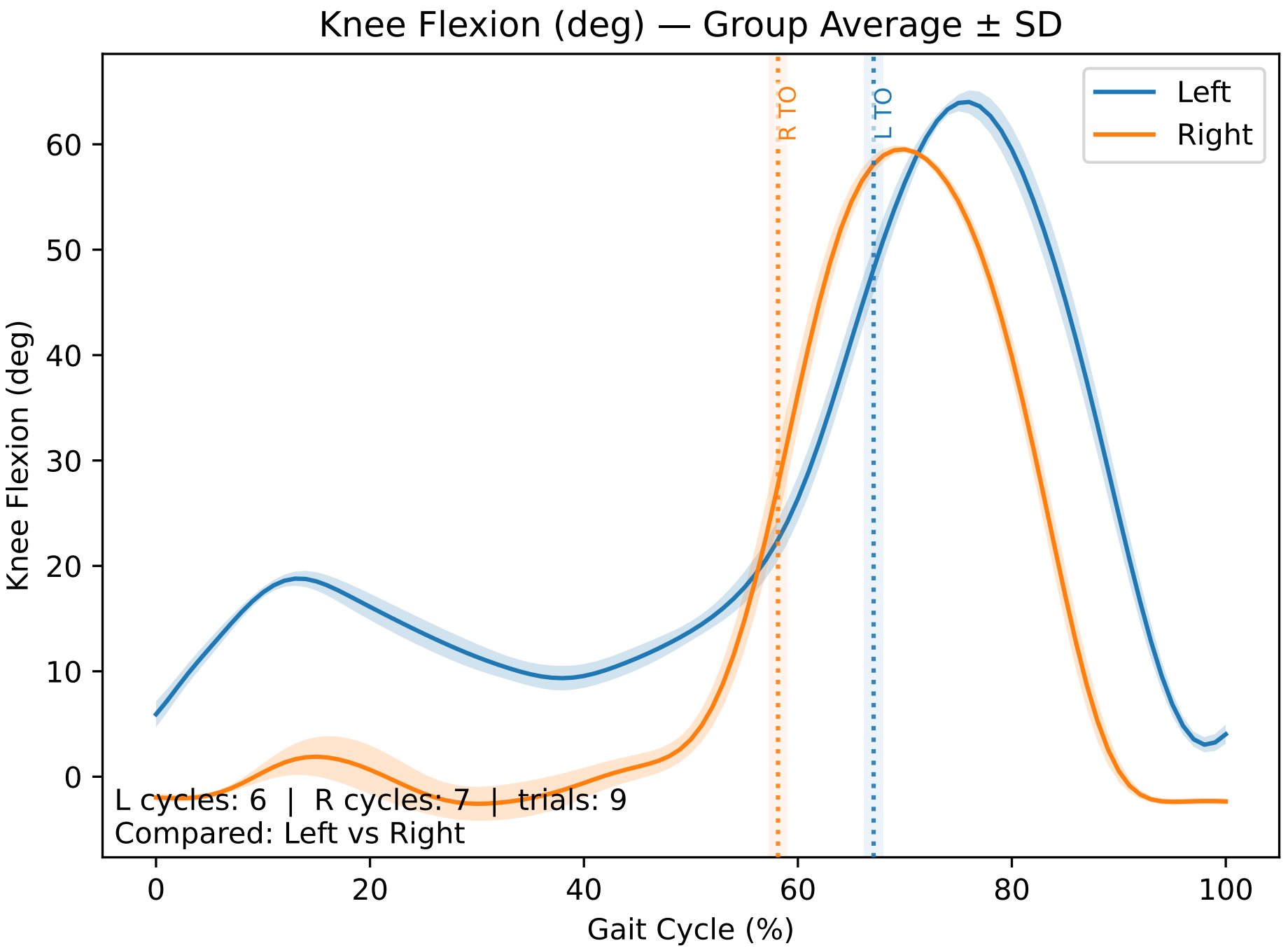
Knee Flexion (deg) — Group Average ± SD
Left
Right
R TO
L TO
Knee Flexion (deg)
Gait Cycle (%)
0
10
20
30
40
50
60
0
20
40
60
80
100
L cycles: 6 | R cycles: 7 | trials: 9
Compared: Left vs Right

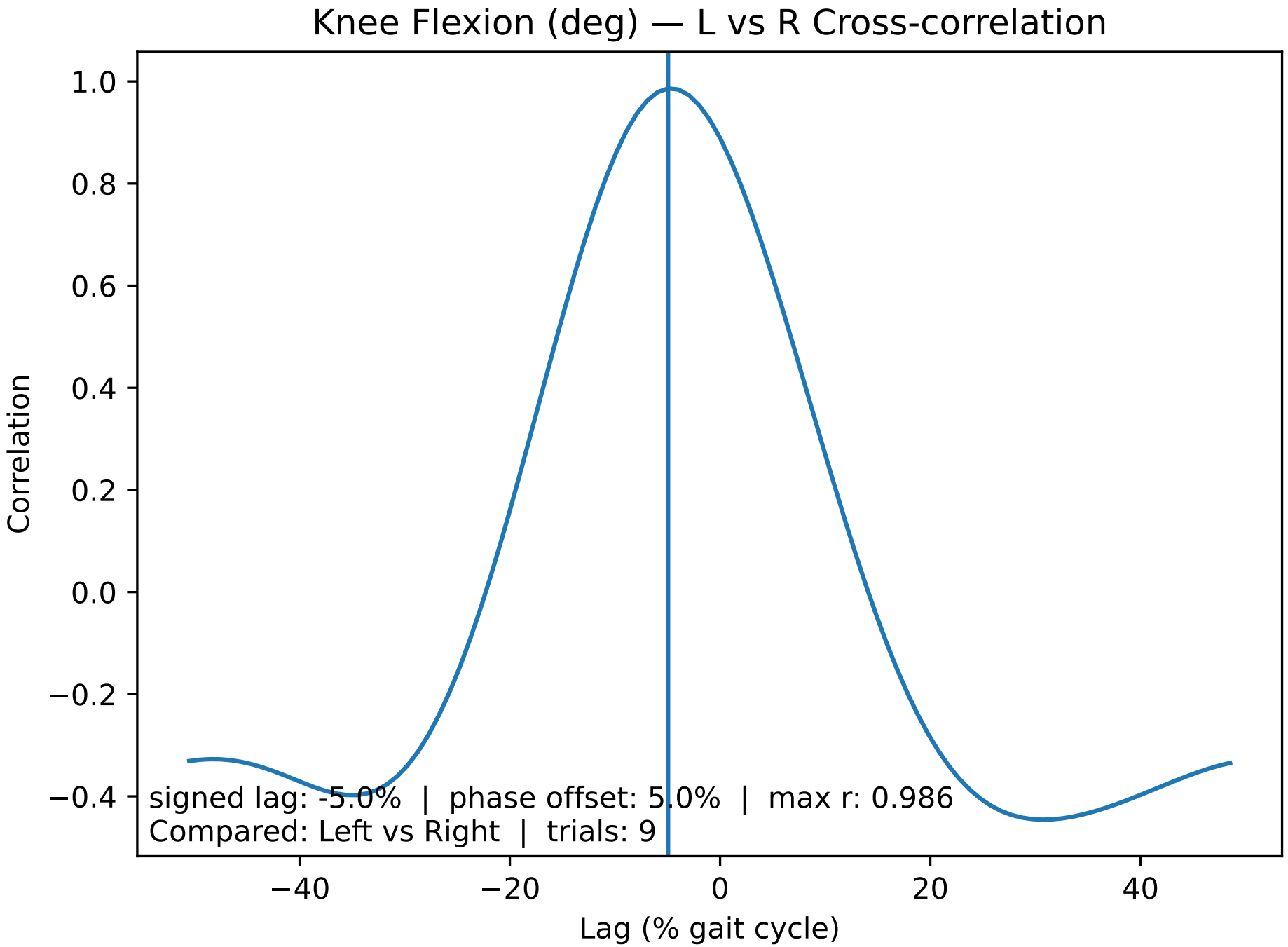
Knee Flexion (deg) — L vs R Cross-correlation
Correlation
1.0
0.8
0.6
0.4
0.2
0.0
−0.2
−0.4
signed lag: -5.0% | phase offset: 5.0% | max r: 0.986
Compared: Left vs Right | trials: 9
−40
−20
0
20
40
Lag (% gait cycle)

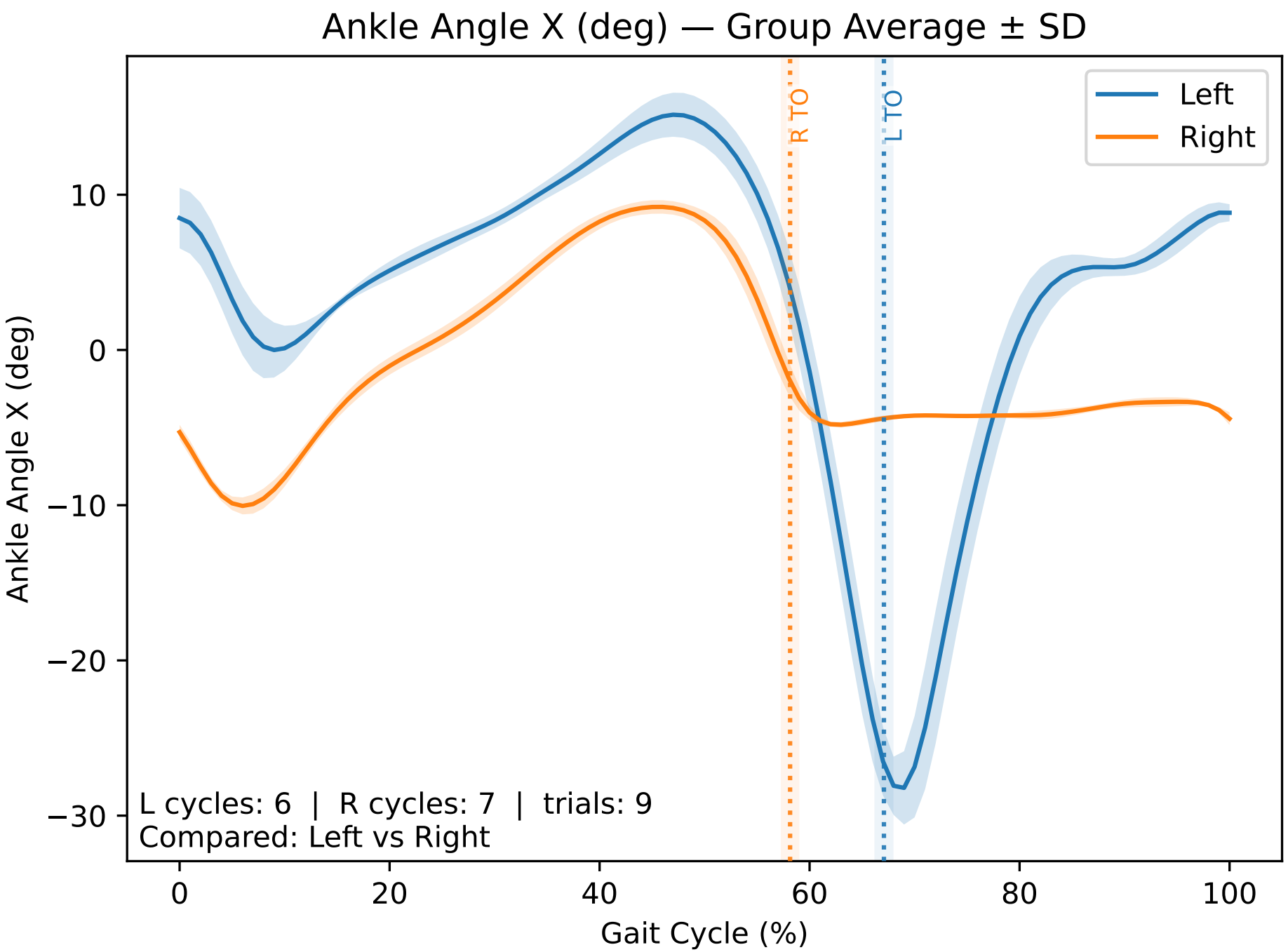
Ankle Angle X (deg) — Group Average ± SD
Left
Right
R TO
L TO
Ankle Angle X (deg)
10
0
−10
−20
−30
0
20
40
60
80
100
Gait Cycle (%)
L cycles: 6 | R cycles: 7 | trials: 9
Compared: Left vs Right

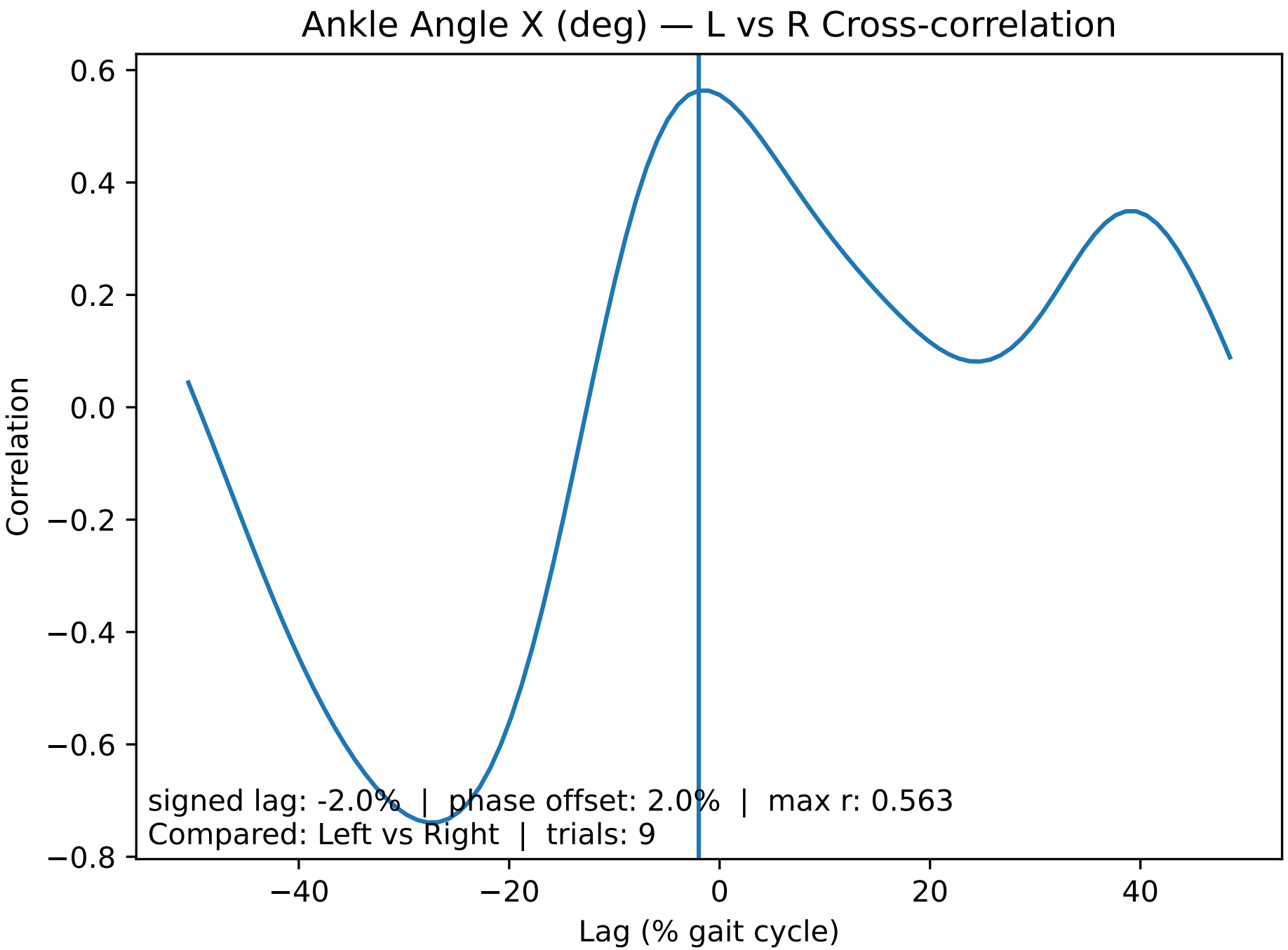
Ankle Angle X (deg) — L vs R Cross-correlation
Correlation
0.6
0.4
0.2
0.0
−0.2
−0.4
−0.6
−0.8
−40
−20
0
20
40
Lag (% gait cycle)
signed lag: -2.0% | phase offset: 2.0% | max r: 0.563
Compared: Left vs Right | trials: 9

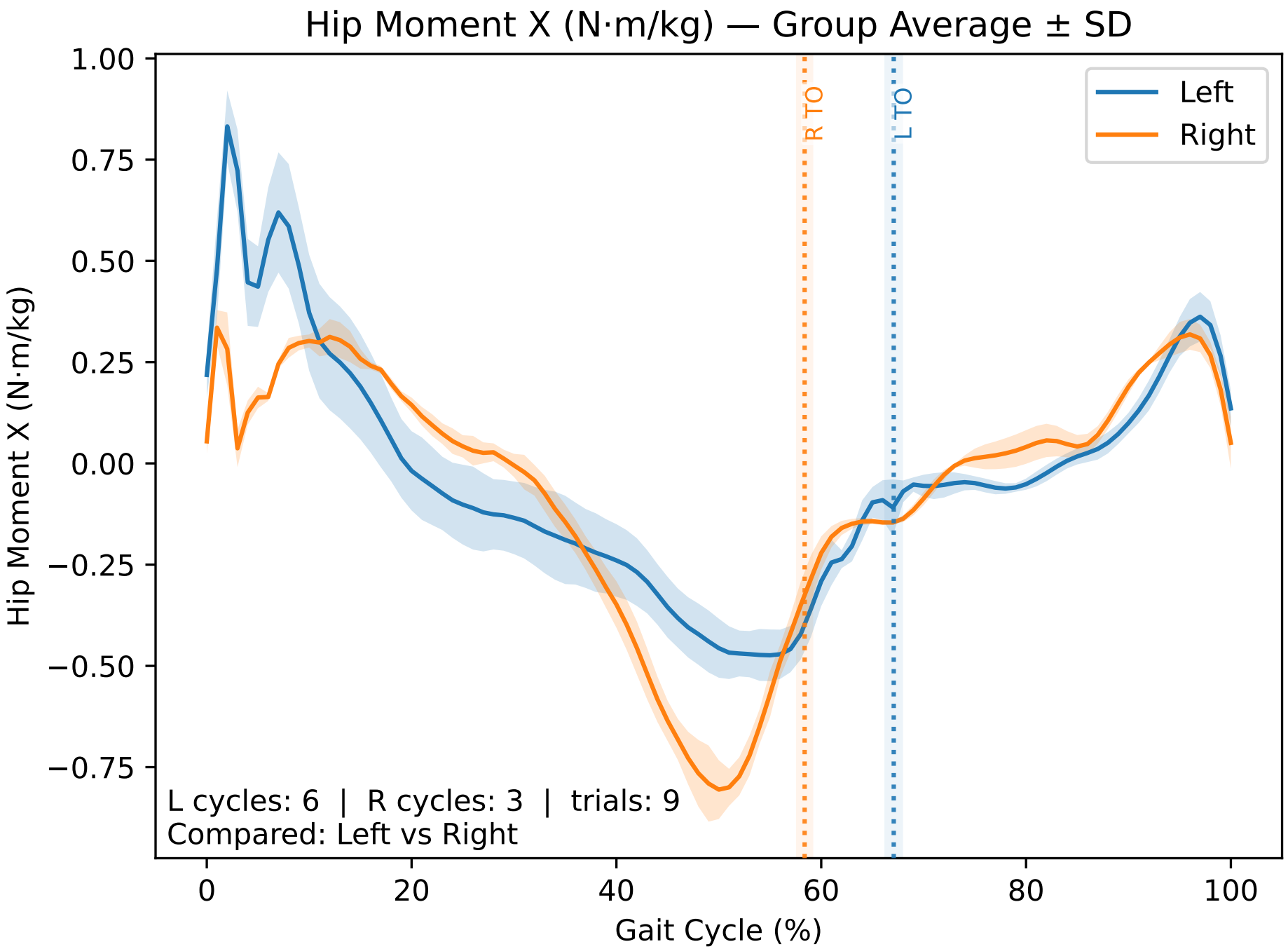
Hip Moment X (N·m/kg) — Group Average ± SD
Hip Moment X (N·m/kg)
Gait Cycle (%)
Left
Right
R TO
L TO
L cycles: 6 | R cycles: 3 | trials: 9
Compared: Left vs Right
1.00
0.75
0.50
0.25
0.00
−0.25
−0.50
−0.75
0
20
40
60
80
100

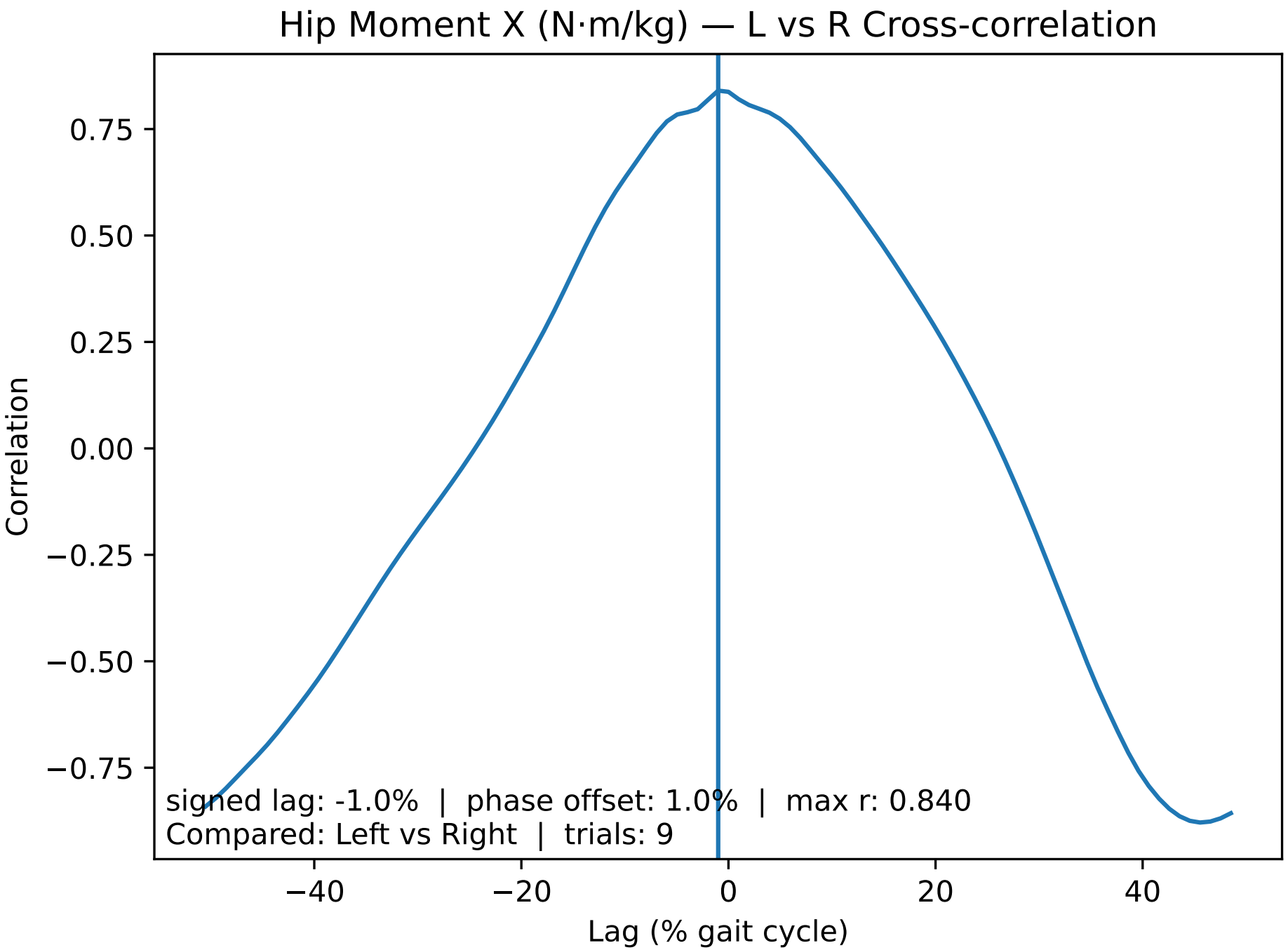
Hip Moment X (N·m/kg) — L vs R Cross-correlation
Correlation
0.75
0.50
0.25
0.00
−0.25
−0.50
−0.75
−40
−20
0
20
40
Lag (% gait cycle)
signed lag: -1.0% | phase offset: 1.0% | max r: 0.840
Compared: Left vs Right | trials: 9

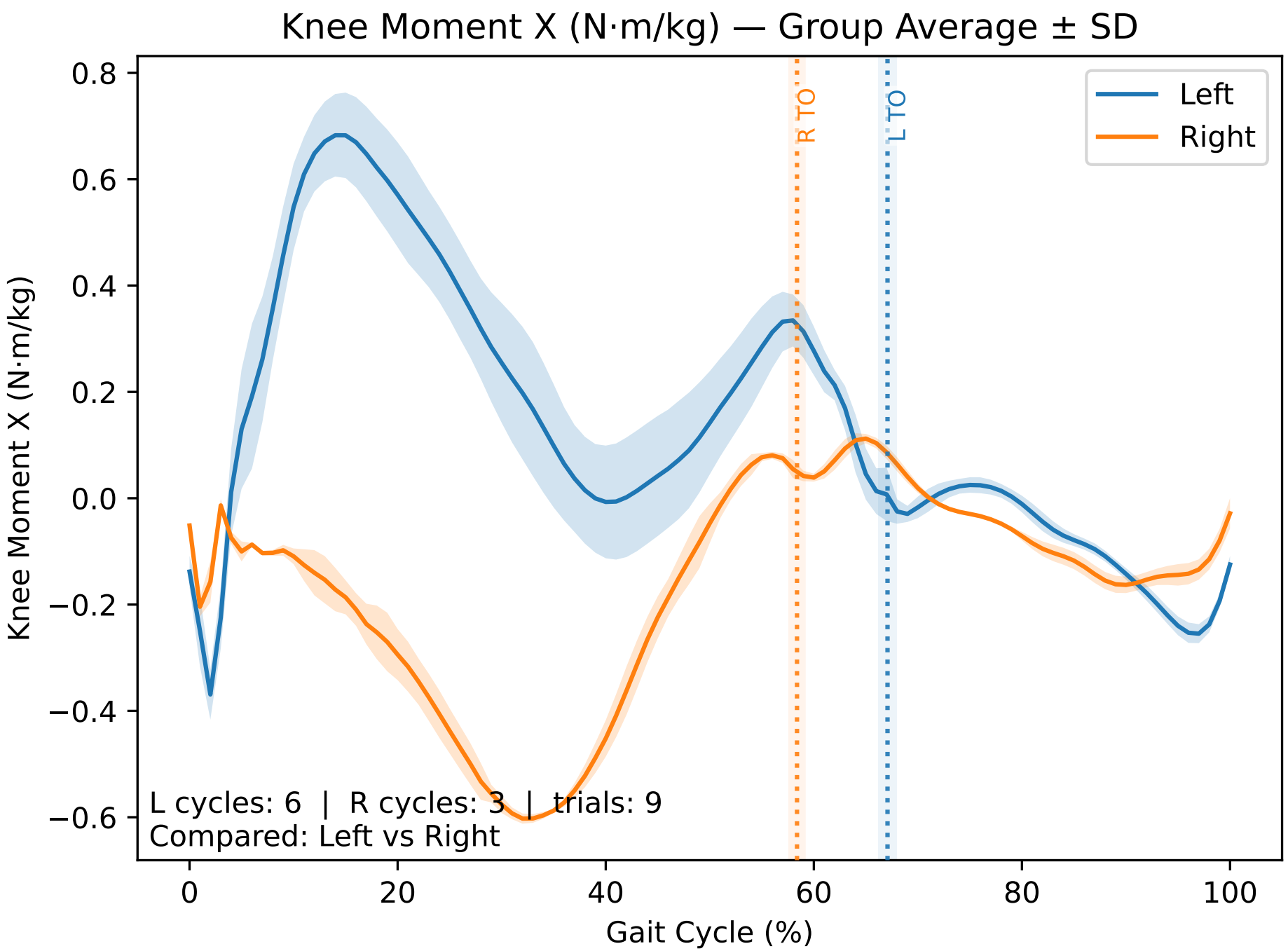
Knee Moment X (N·m/kg) — Group Average ± SD
Knee Moment X (N·m/kg)
0.8
0.6
0.4
0.2
0.0
−0.2
−0.4
−0.6
0
20
40
60
80
100
Gait Cycle (%)
R TO
L TO
Left
Right
L cycles: 6 | R cycles: 3 | trials: 9
Compared: Left vs Right

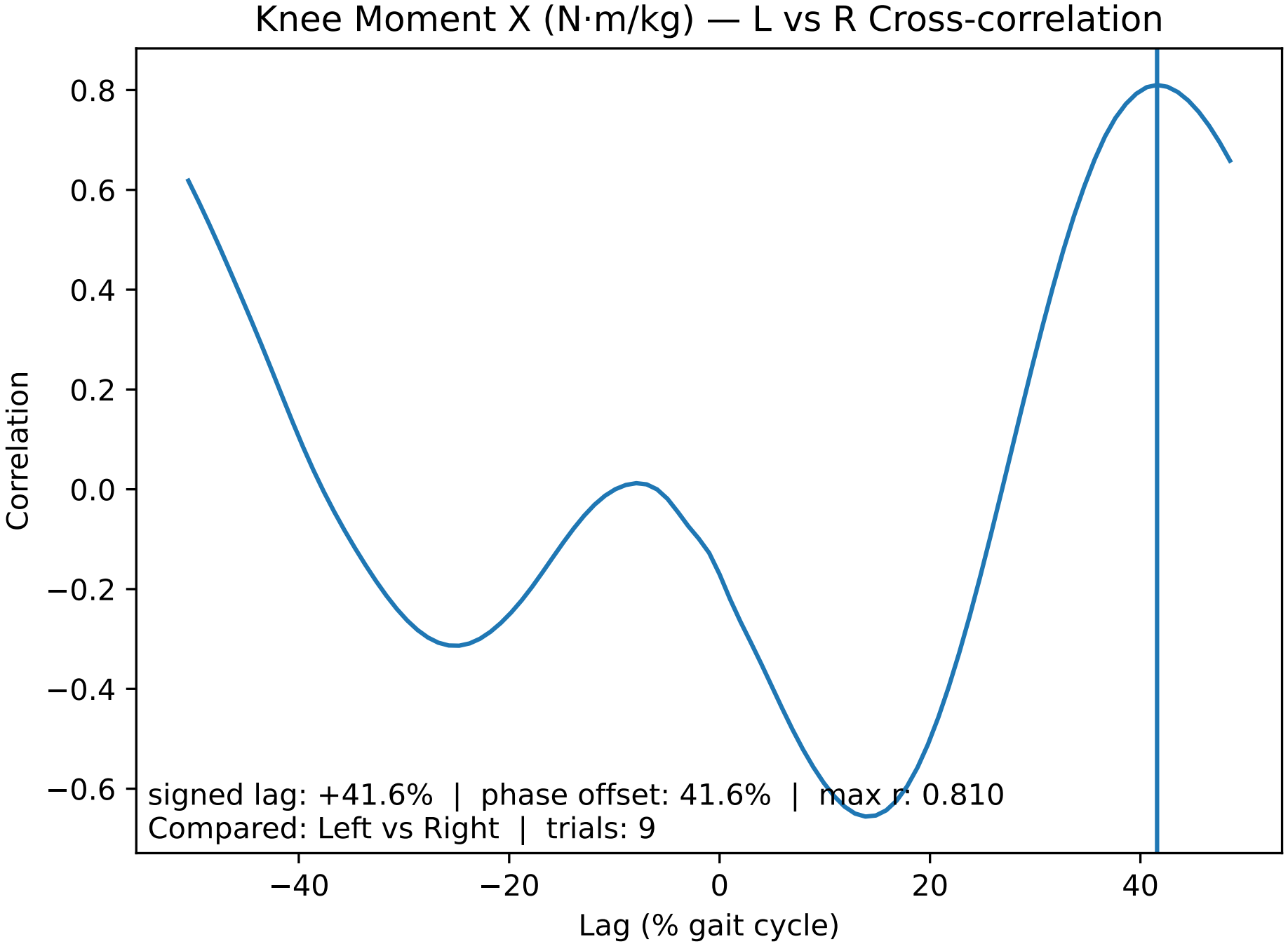
Knee Moment X (N·m/kg) — L vs R Cross-correlation
Correlation
0.8
0.6
0.4
0.2
0.0
−0.2
−0.4
−0.6
signed lag: +41.6% | phase offset: 41.6% | max r: 0.810
Compared: Left vs Right | trials: 9
−40
−20
0
20
40
Lag (% gait cycle)

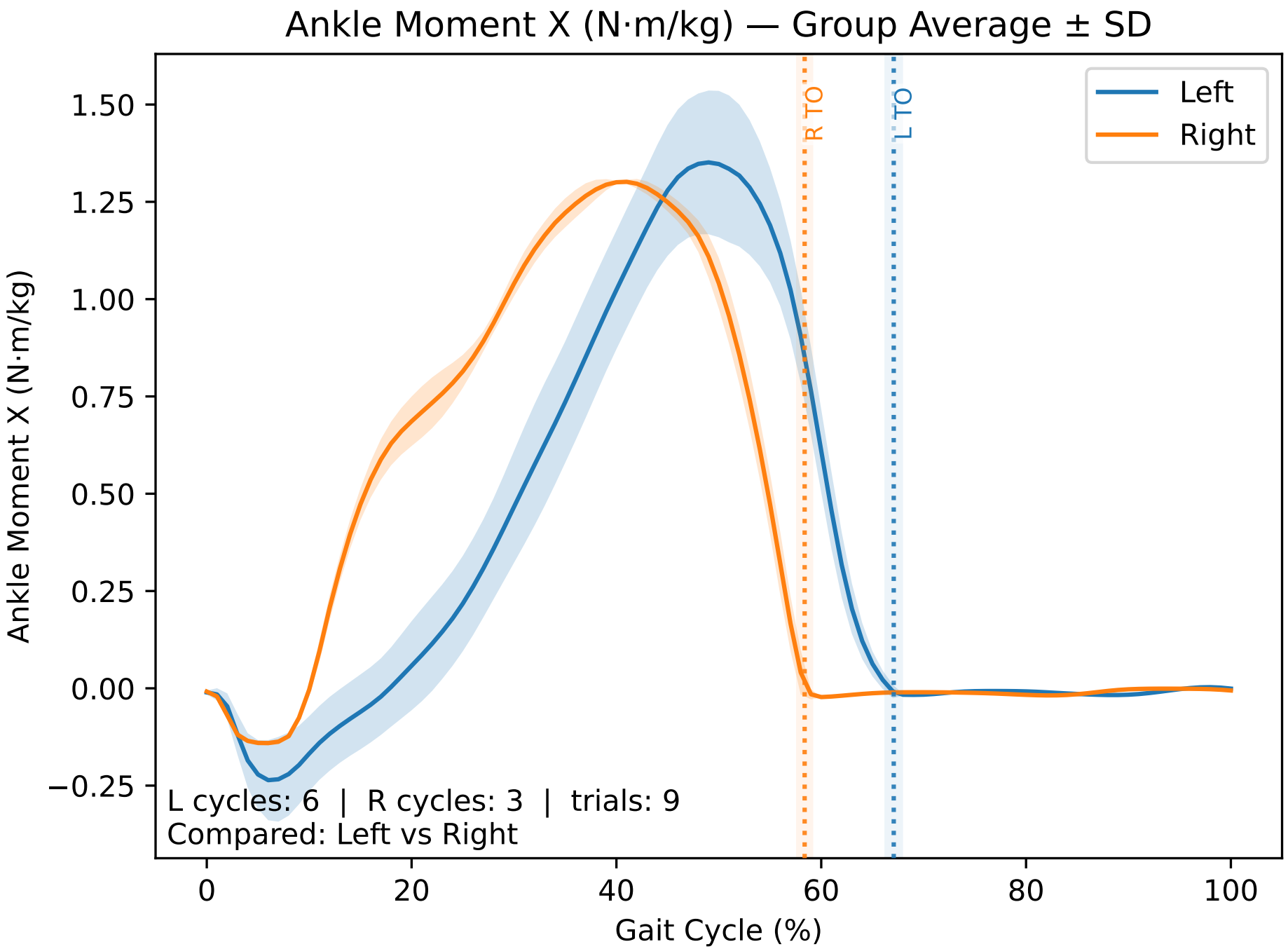
Ankle Moment X (N·m/kg) — Group Average ± SD
Ankle Moment X (N·m/kg)
1.50
1.25
1.00
0.75
0.50
0.25
0.00
−0.25
0
20
40
60
80
100
Gait Cycle (%)
R TO
L TO
Left
Right
L cycles: 6 | R cycles: 3 | trials: 9
Compared: Left vs Right

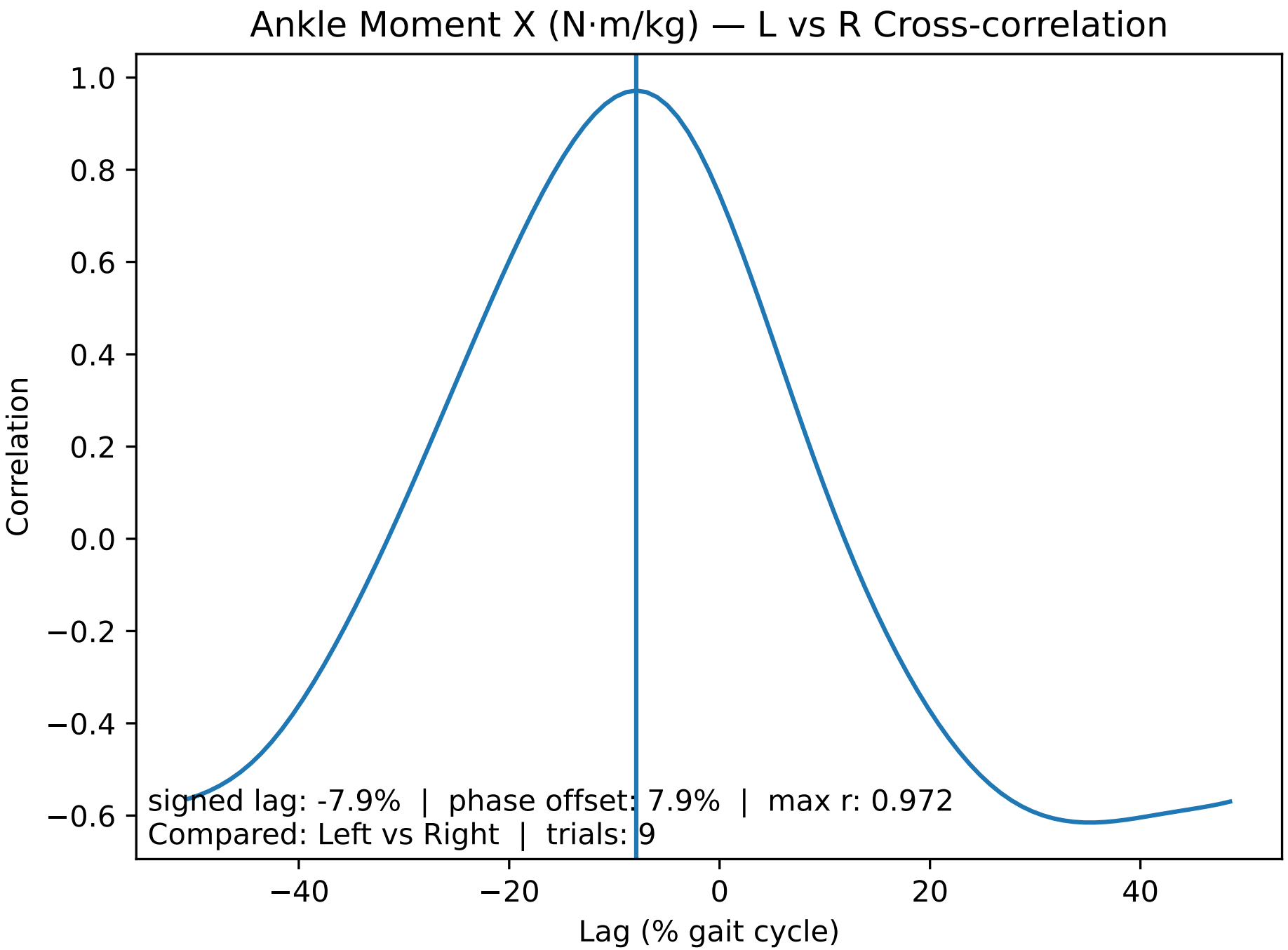
Ankle Moment X (N·m/kg) — L vs R Cross-correlation
Correlation
1.0
0.8
0.6
0.4
0.2
0.0
−0.2
−0.4
−0.6
−40
−20
0
20
40
Lag (% gait cycle)
signed lag: -7.9% | phase offset: 7.9% | max r: 0.972
Compared: Left vs Right | trials: 9

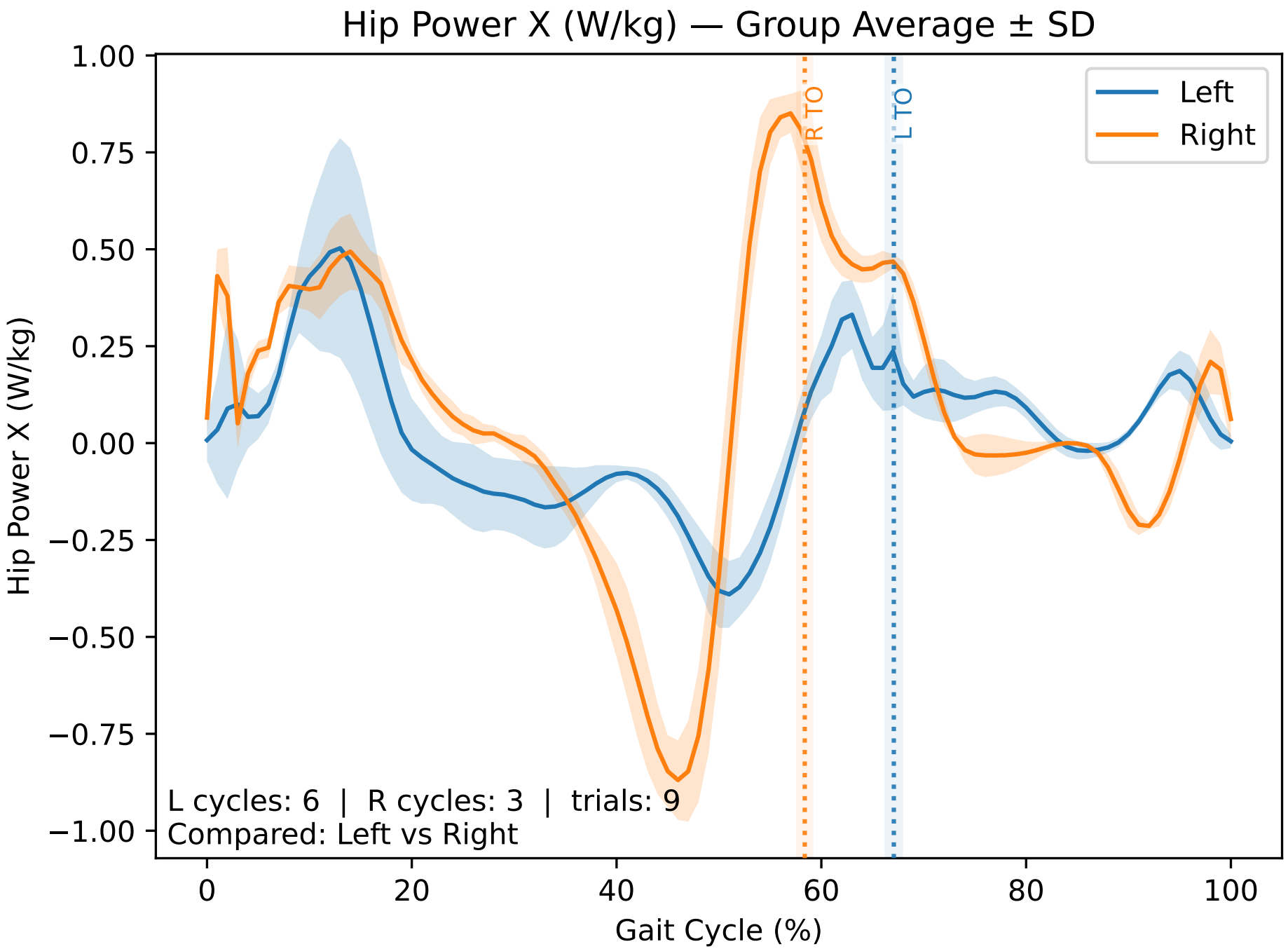
Hip Power X (W/kg) — Group Average ± SD
Hip Power X (W/kg)
Gait Cycle (%)
Left
Right
R TO
L TO
L cycles: 6 | R cycles: 3 | trials: 9
Compared: Left vs Right
1.00
0.75
0.50
0.25
0.00
−0.25
−0.50
−0.75
−1.00
0
20
40
60
80
100

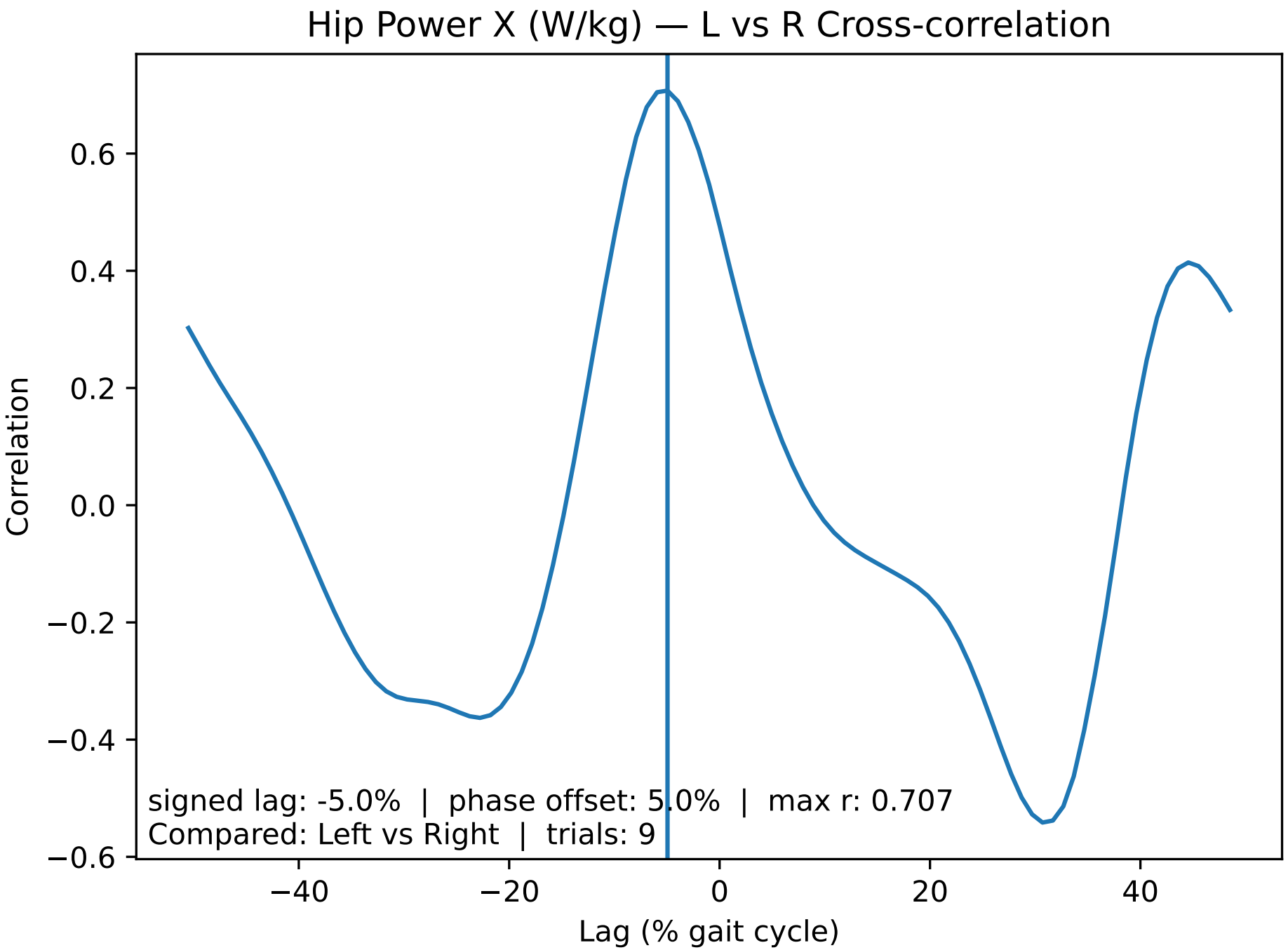
Hip Power X (W/kg) — L vs R Cross-correlation
Correlation
0.6
0.4
0.2
0.0
−0.2
−0.4
−0.6
−40
−20
0
20
40
Lag (% gait cycle)
signed lag: -5.0% | phase offset: 5.0% | max r: 0.707
Compared: Left vs Right | trials: 9

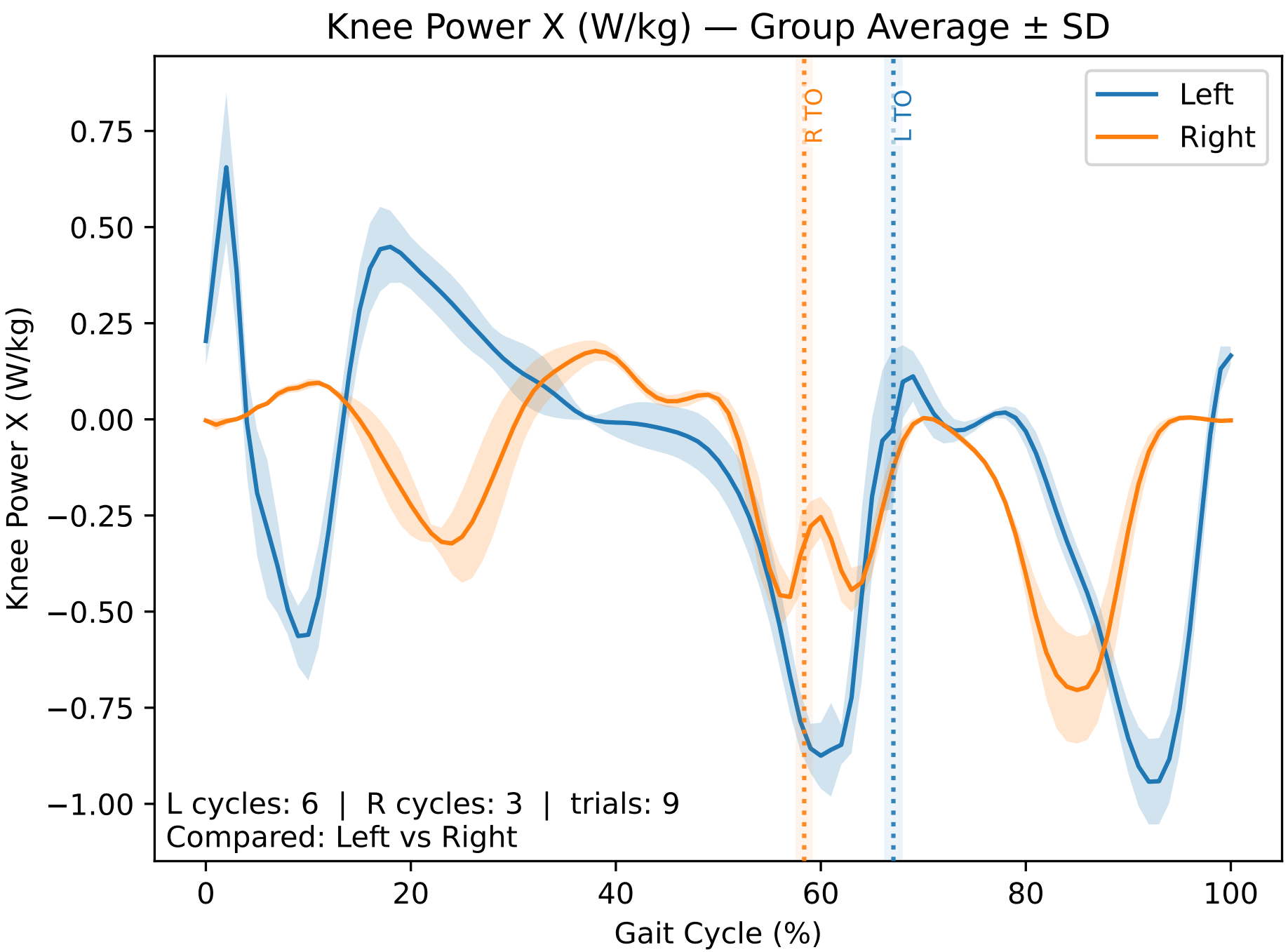
Knee Power X (W/kg) — Group Average ± SD
Left
Right
R TO
L TO
Knee Power X (W/kg)
0.75
0.50
0.25
0.00
−0.25
−0.50
−0.75
−1.00
L cycles: 6 | R cycles: 3 | trials: 9
Compared: Left vs Right
0
20
40
60
80
100
Gait Cycle (%)

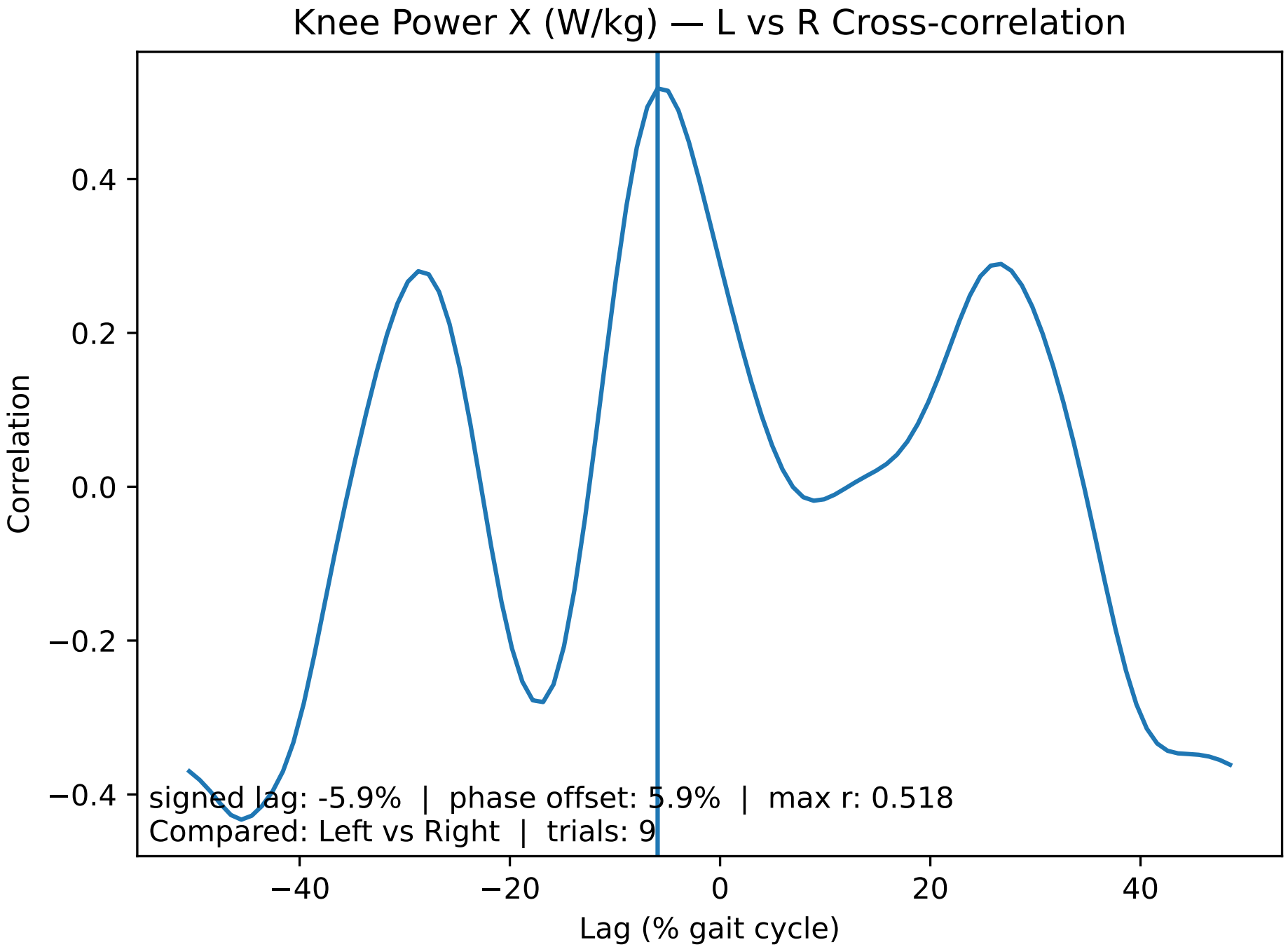
Knee Power X (W/kg) — L vs R Cross-correlation
Correlation
0.4
0.2
0.0
−0.2
−0.4
signed lag: -5.9% | phase offset: 5.9% | max r: 0.518
Compared: Left vs Right | trials: 9
−40
−20
0
20
40
Lag (% gait cycle)

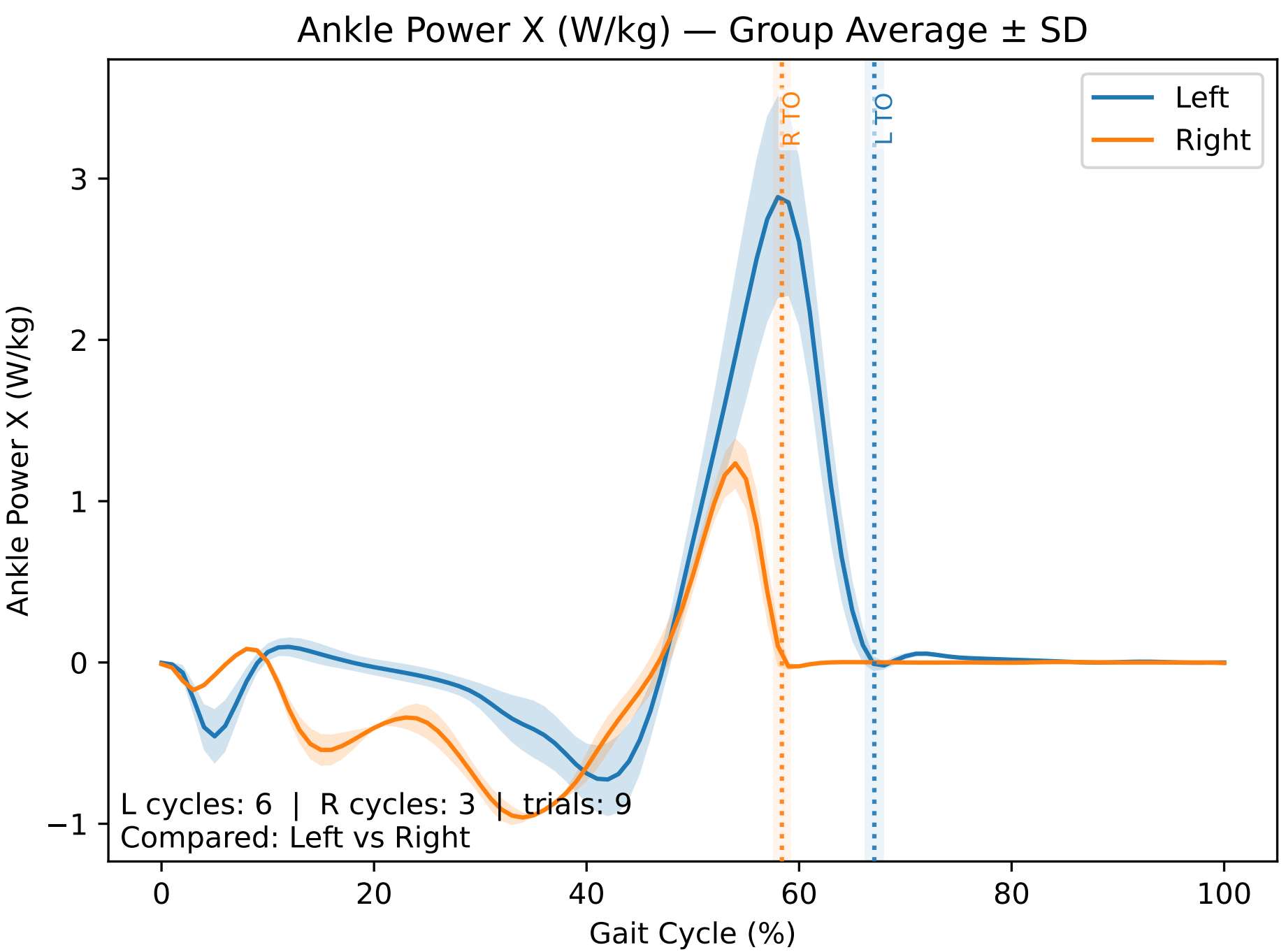
Ankle Power X (W/kg) — Group Average ± SD
Left
Right
R TO
L TO
Ankle Power X (W/kg)
Gait Cycle (%)
L cycles: 6 | R cycles: 3 | trials: 9
Compared: Left vs Right

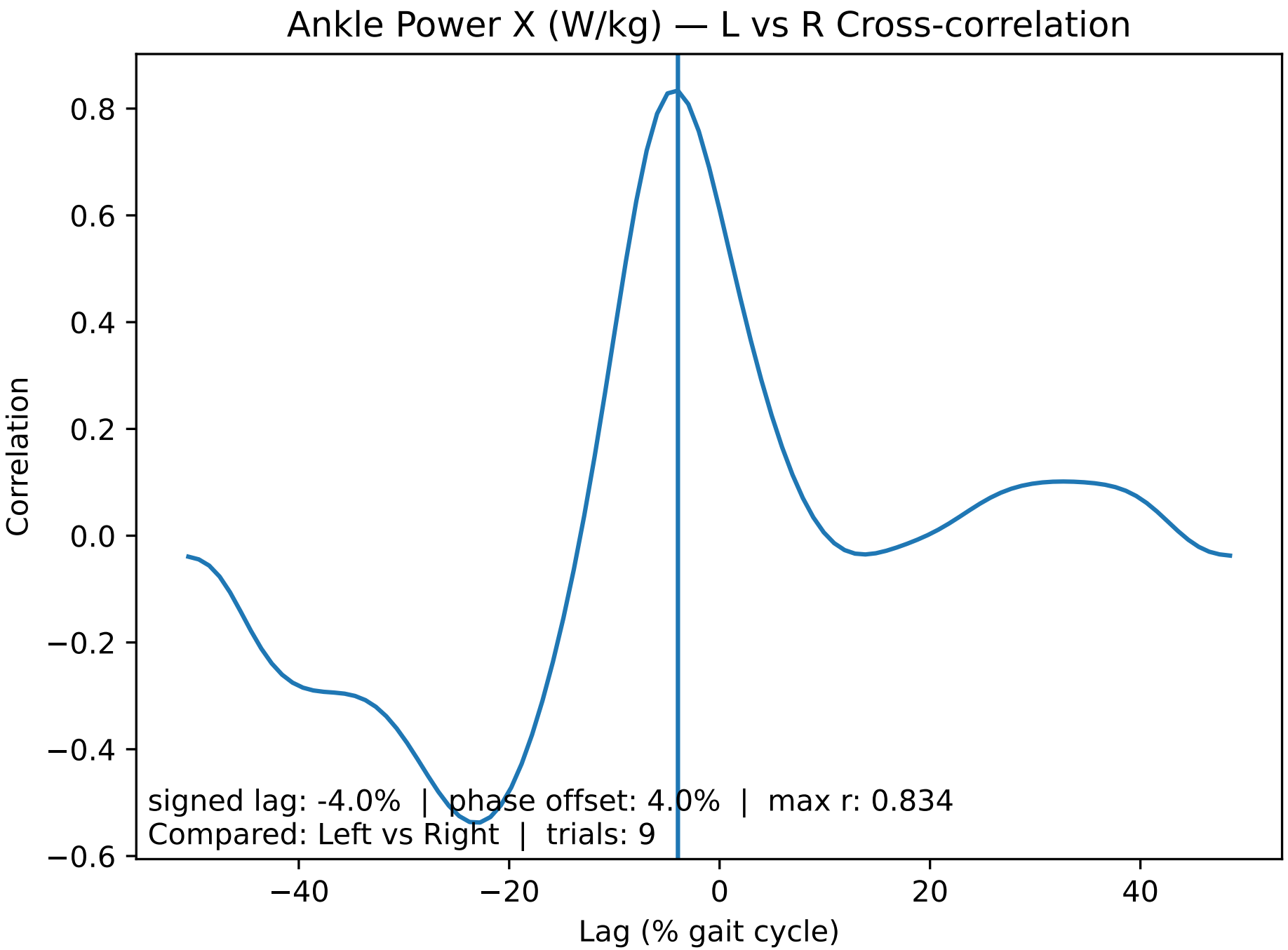
Ankle Power X (W/kg) — L vs R Cross-correlation
Correlation
0.8
0.6
0.4
0.2
0.0
−0.2
−0.4
−0.6
−40
−20
0
20
40
Lag (% gait cycle)
signed lag: -4.0% | phase offset: 4.0% | max r: 0.834
Compared: Left vs Right | trials: 9

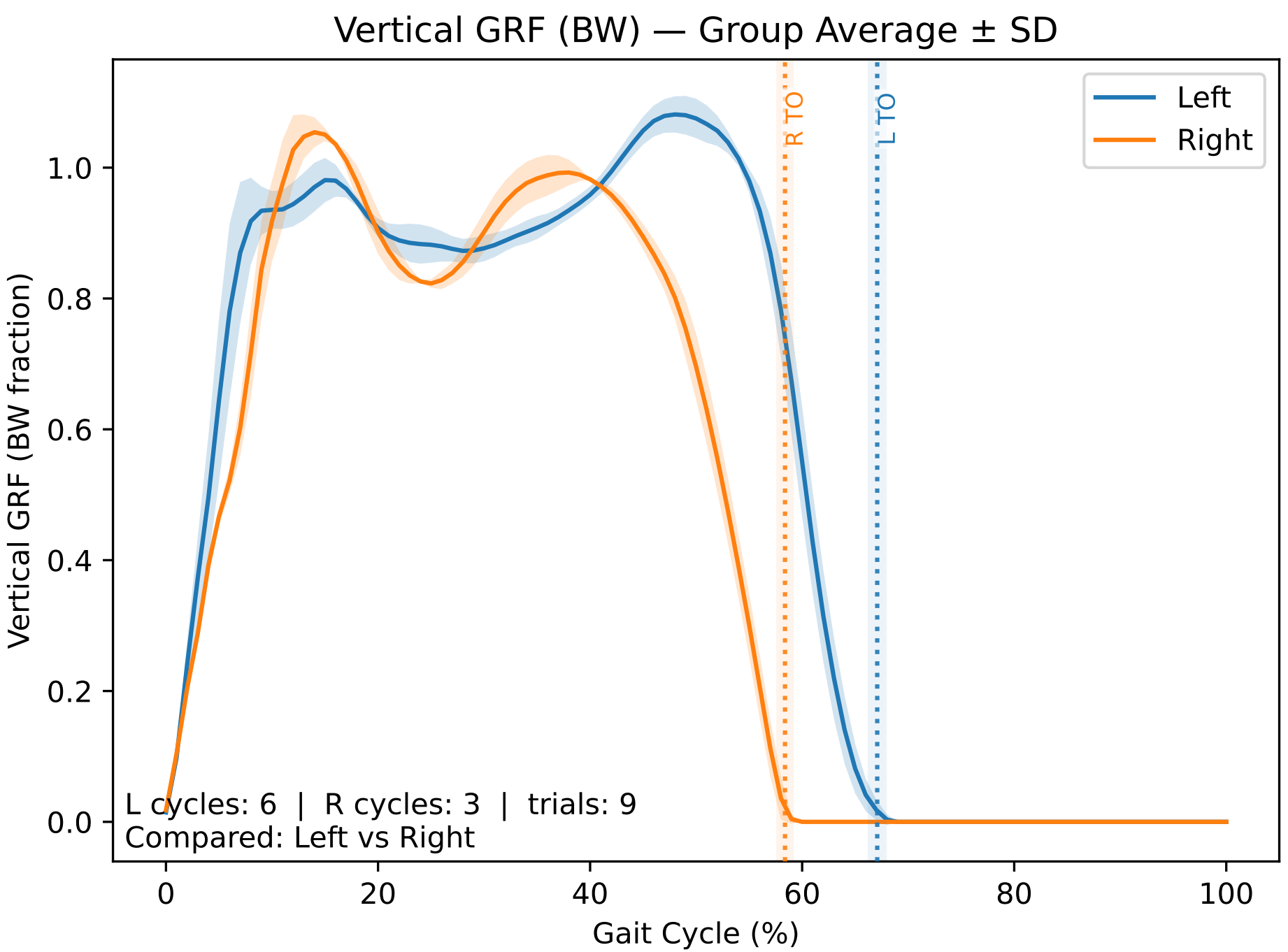
Vertical GRF (BW) — Group Average ± SD
Left
Right
R TO
L TO
Vertical GRF (BW fraction)
Gait Cycle (%)
0.0
0.2
0.4
0.6
0.8
1.0
0
20
40
60
80
100
L cycles: 6 | R cycles: 3 | trials: 9
Compared: Left vs Right

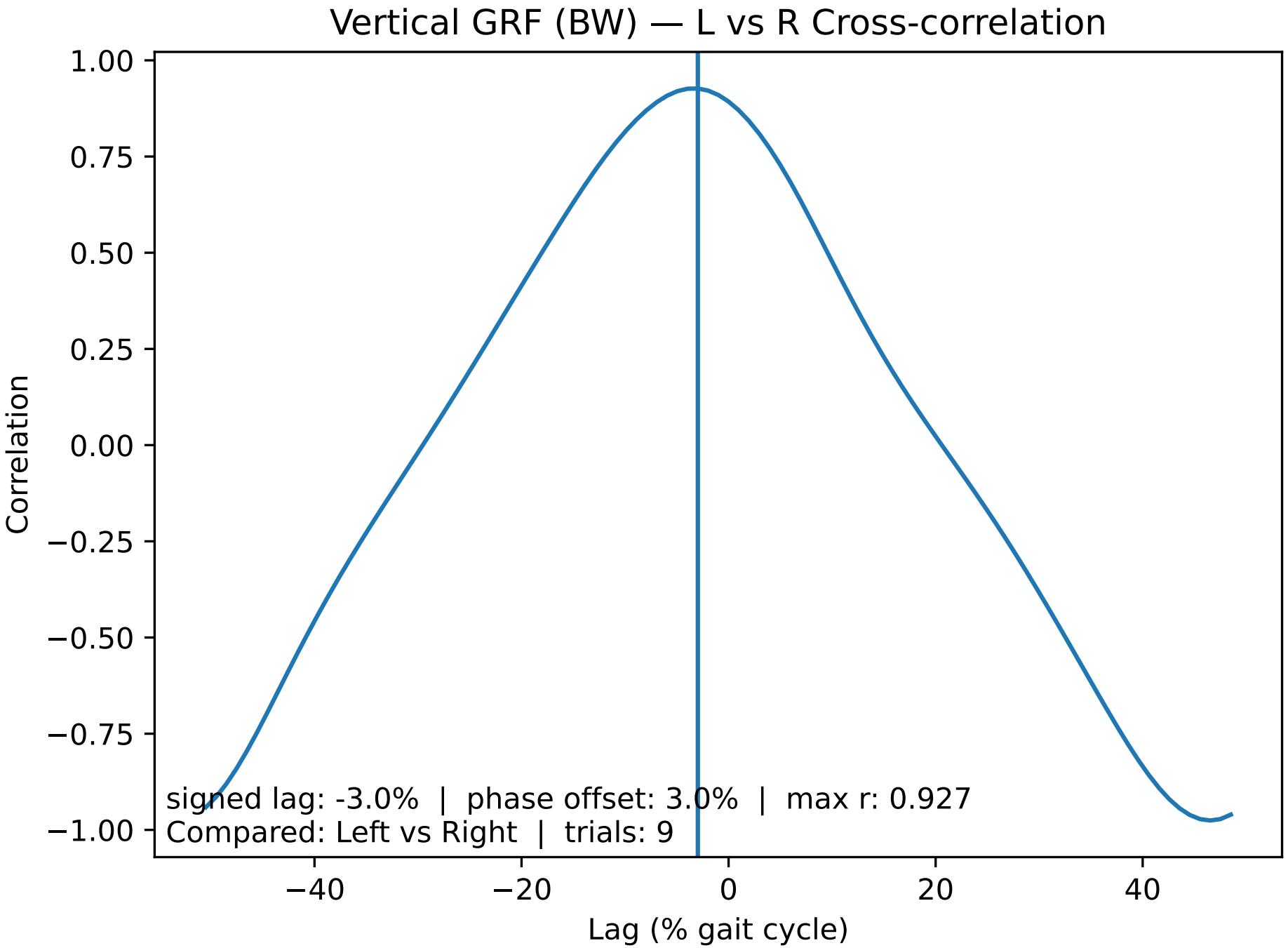
Vertical GRF (BW) — L vs R Cross-correlation
Correlation
1.00
0.75
0.50
0.25
0.00
−0.25
−0.50
−0.75
−1.00
−40
−20
0
20
40
Lag (% gait cycle)
signed lag: -3.0% | phase offset: 3.0% | max r: 0.927
Compared: Left vs Right | trials: 9

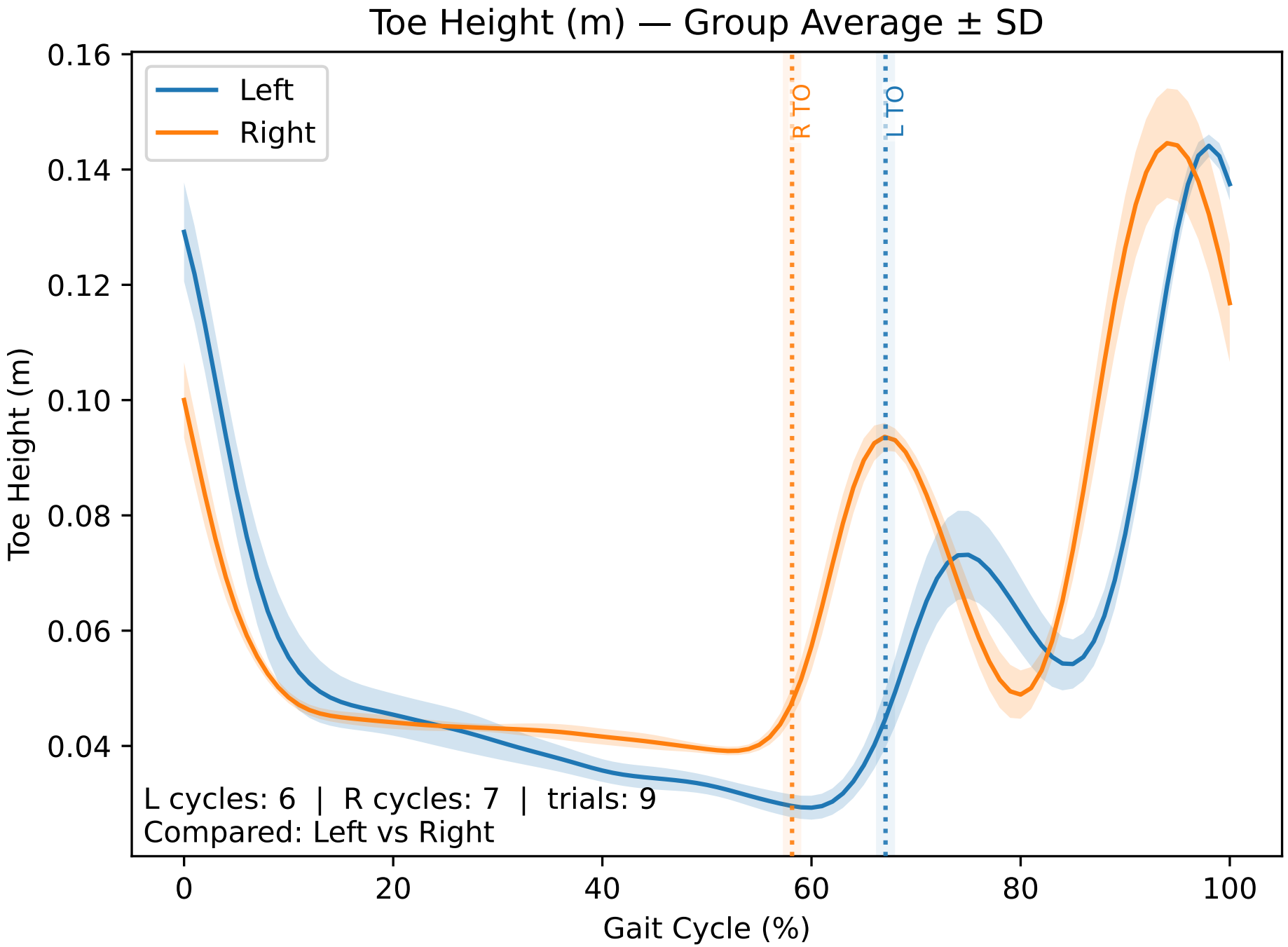
Toe Height (m) — Group Average ± SD
Left
Right
R TO
L TO
Toe Height (m)
0.16
0.14
0.12
0.10
0.08
0.06
0.04
L cycles: 6 | R cycles: 7 | trials: 9
Compared: Left vs Right
0
20
40
60
80
100
Gait Cycle (%)

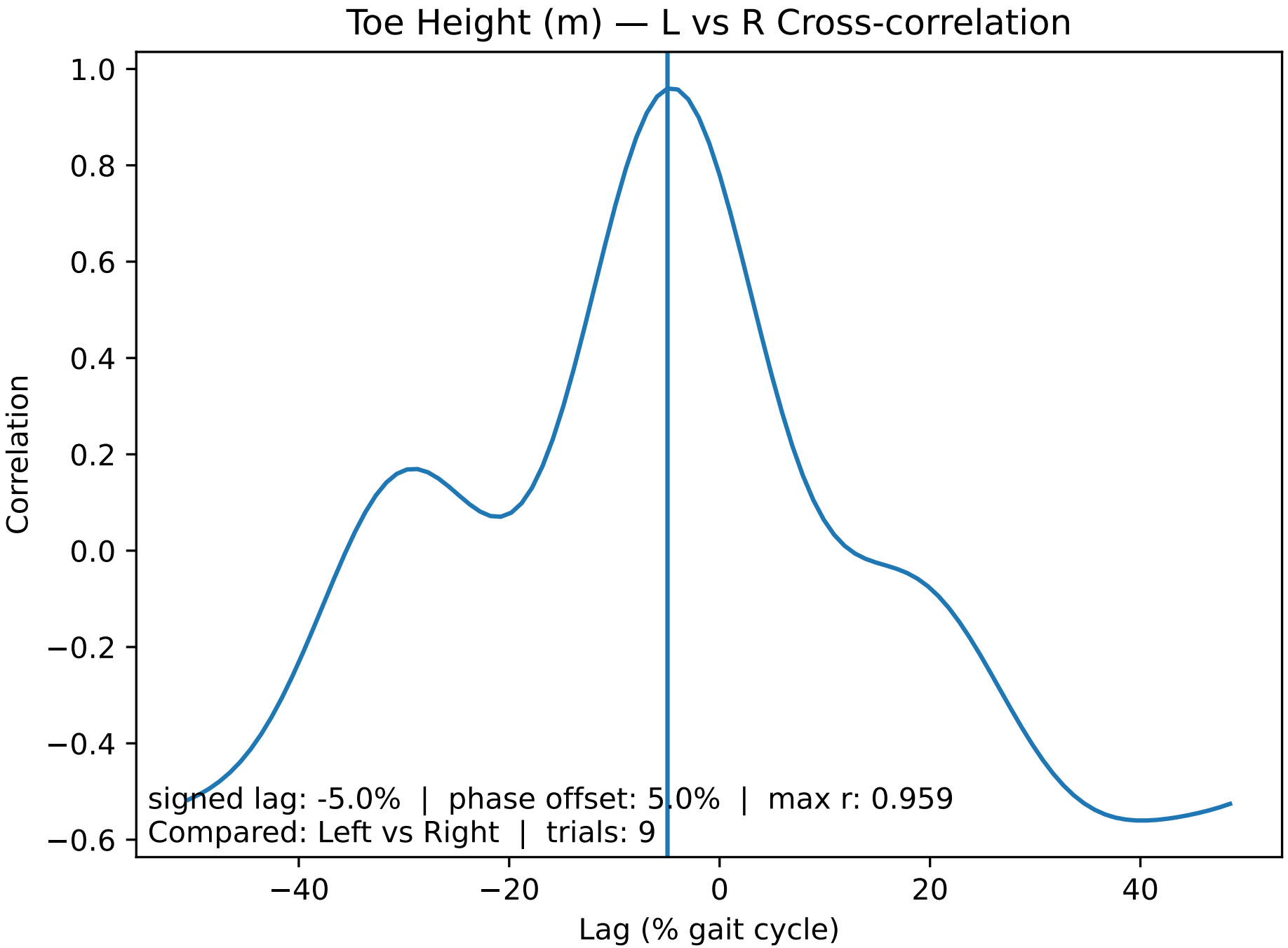
Toe Height (m) — L vs R Cross-correlation
Correlation
1.0
0.8
0.6
0.4
0.2
0.0
−0.2
−0.4
−0.6
−40
−20
0
20
40
Lag (% gait cycle)
signed lag: -5.0% | phase offset: 5.0% | max r: 0.959
Compared: Left vs Right | trials: 9

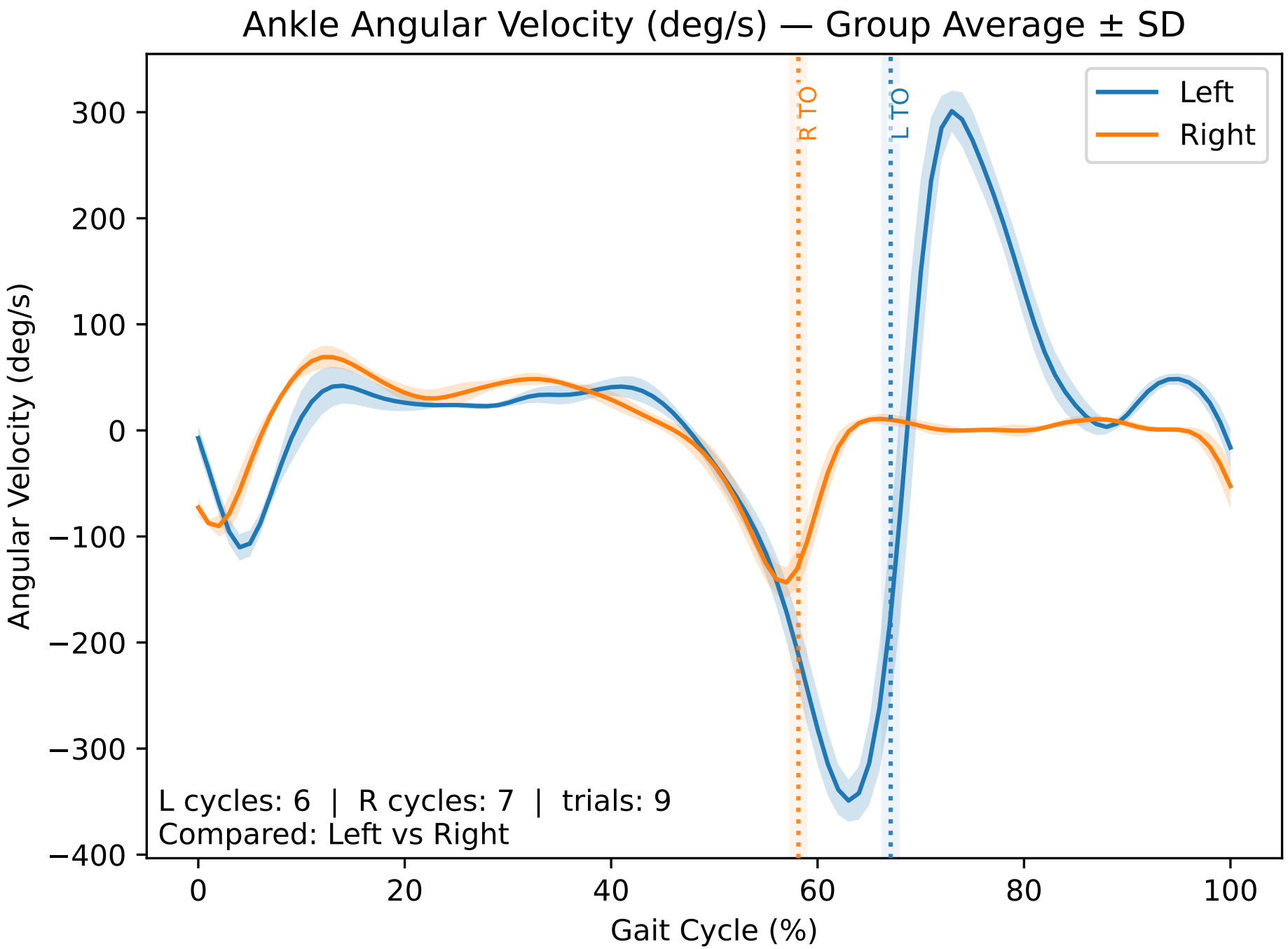
Ankle Angular Velocity (deg/s) — Group Average ± SD
Angular Velocity (deg/s)
Gait Cycle (%)
Left
Right
R TO
L TO
L cycles: 6 | R cycles: 7 | trials: 9
Compared: Left vs Right
300
200
100
0
−100
−200
−300
−400
0
20
40
60
80
100

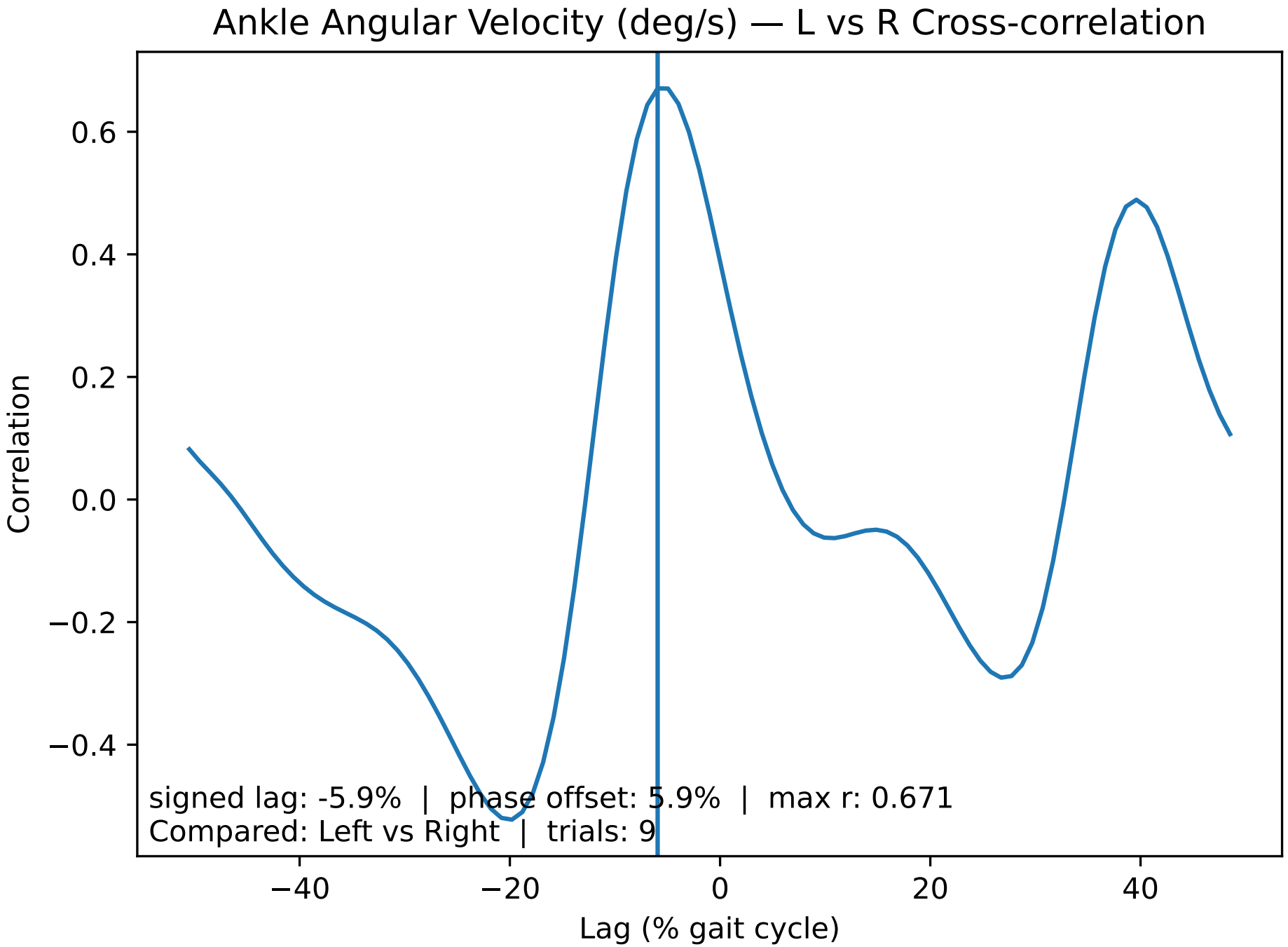
Ankle Angular Velocity (deg/s) — L vs R Cross-correlation
Correlation
0.6
0.4
0.2
0.0
−0.2
−0.4
signed lag: -5.9% | phase offset: 5.9% | max r: 0.671
Compared: Left vs Right | trials: 9
−40
−20
0
20
40
Lag (% gait cycle)

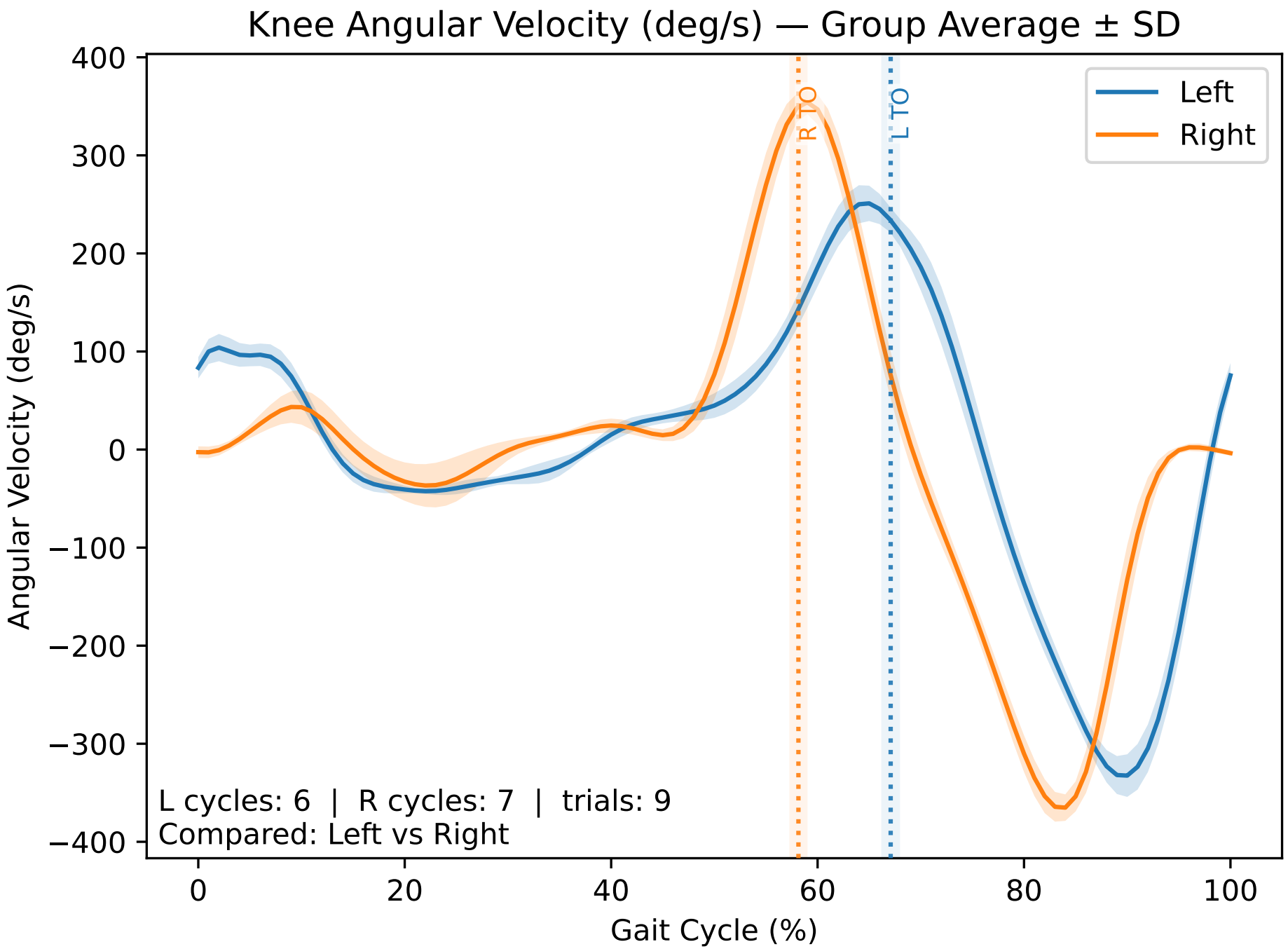
Knee Angular Velocity (deg/s) — Group Average ± SD
Angular Velocity (deg/s)
Gait Cycle (%)
Left
Right
R TO
L TO
L cycles: 6 | R cycles: 7 | trials: 9
Compared: Left vs Right
400
300
200
100
0
−100
−200
−300
−400
0
20
40
60
80
100

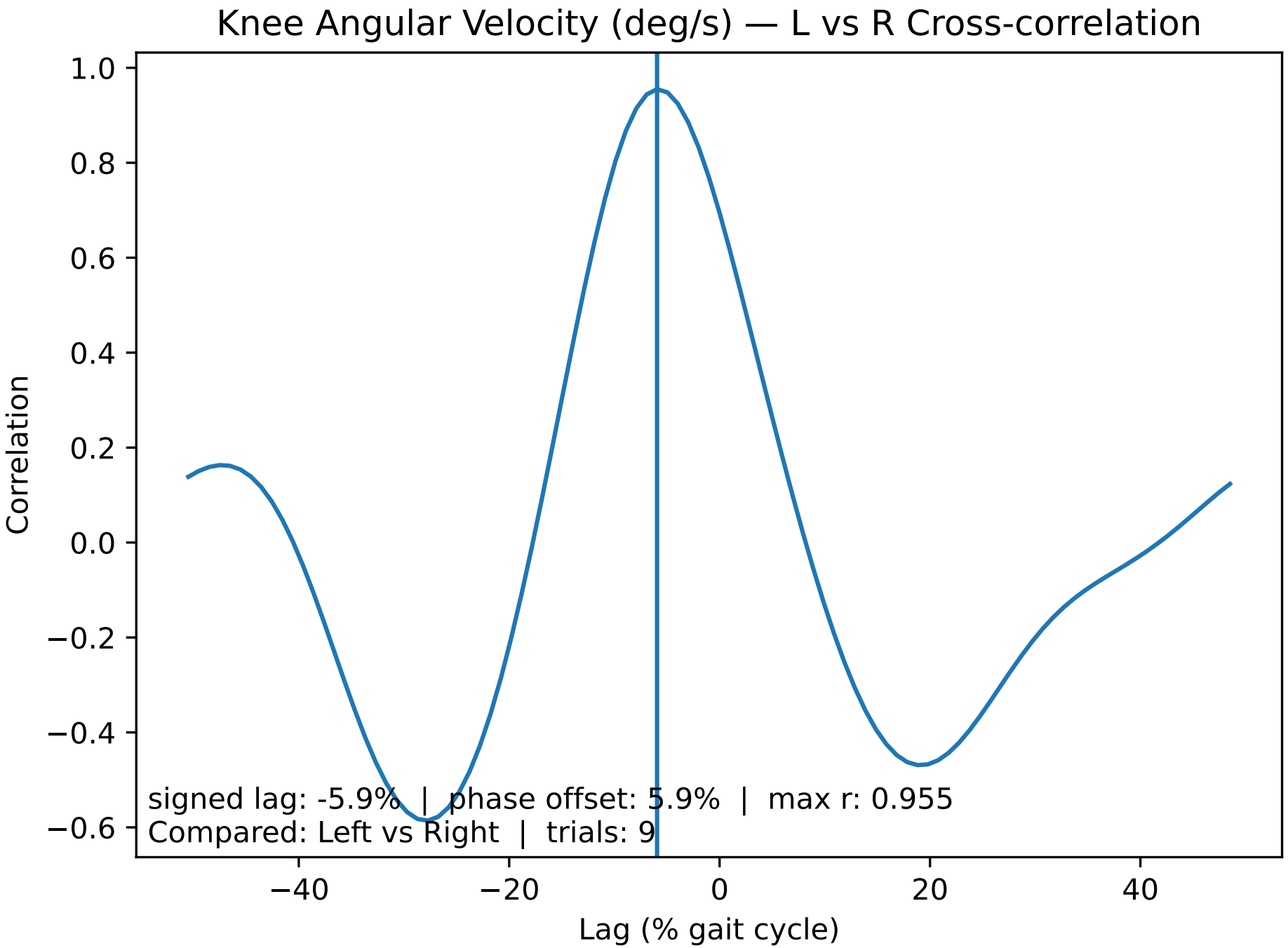
Knee Angular Velocity (deg/s) — L vs R Cross-correlation
Correlation
1.0
0.8
0.6
0.4
0.2
0.0
−0.2
−0.4
−0.6
−40
−20
0
20
40
Lag (% gait cycle)
signed lag: -5.9% | phase offset: 5.9% | max r: 0.955
Compared: Left vs Right | trials: 9

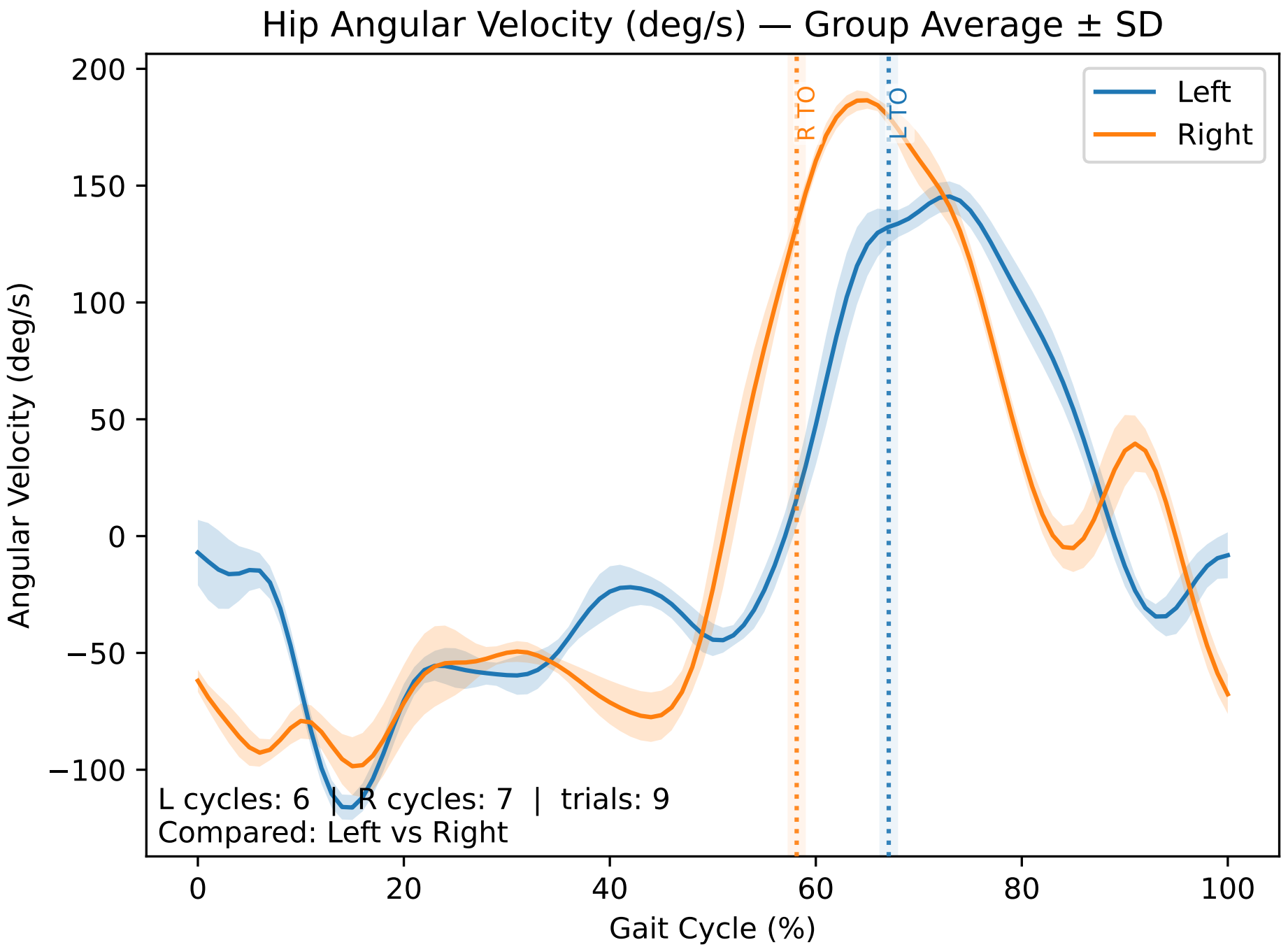
Hip Angular Velocity (deg/s) — Group Average ± SD
Angular Velocity (deg/s)
Gait Cycle (%)
Left
Right
R TO
L TO
L cycles: 6 | R cycles: 7 | trials: 9
Compared: Left vs Right
200
150
100
50
0
−50
−100
0
20
40
60
80
100

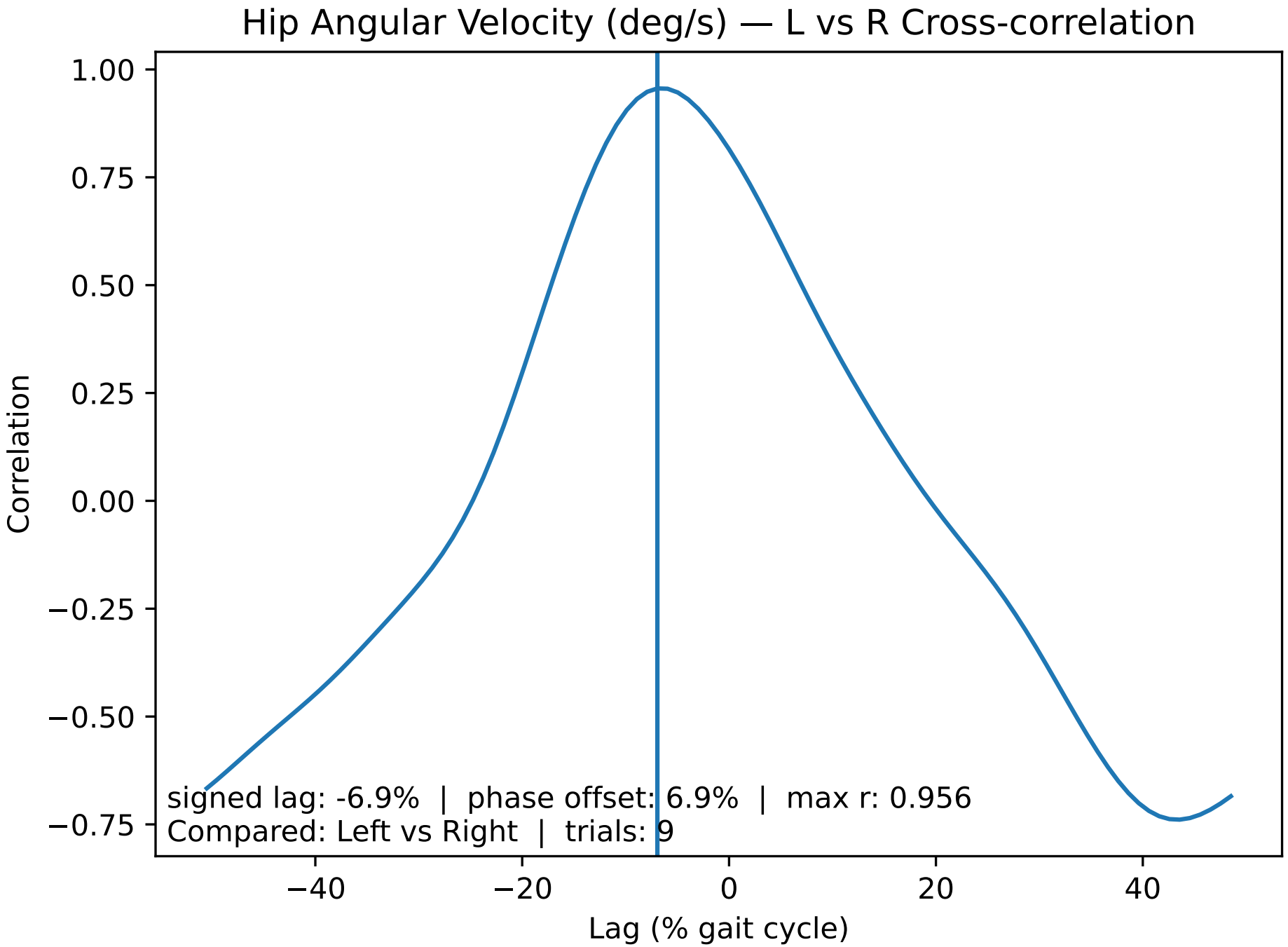
Hip Angular Velocity (deg/s) — L vs R Cross-correlation
Correlation
1.00
0.75
0.50
0.25
0.00
−0.25
−0.50
−0.75
−40
−20
0
20
40
Lag (% gait cycle)
signed lag: -6.9% | phase offset: 6.9% | max r: 0.956
Compared: Left vs Right | trials: 9

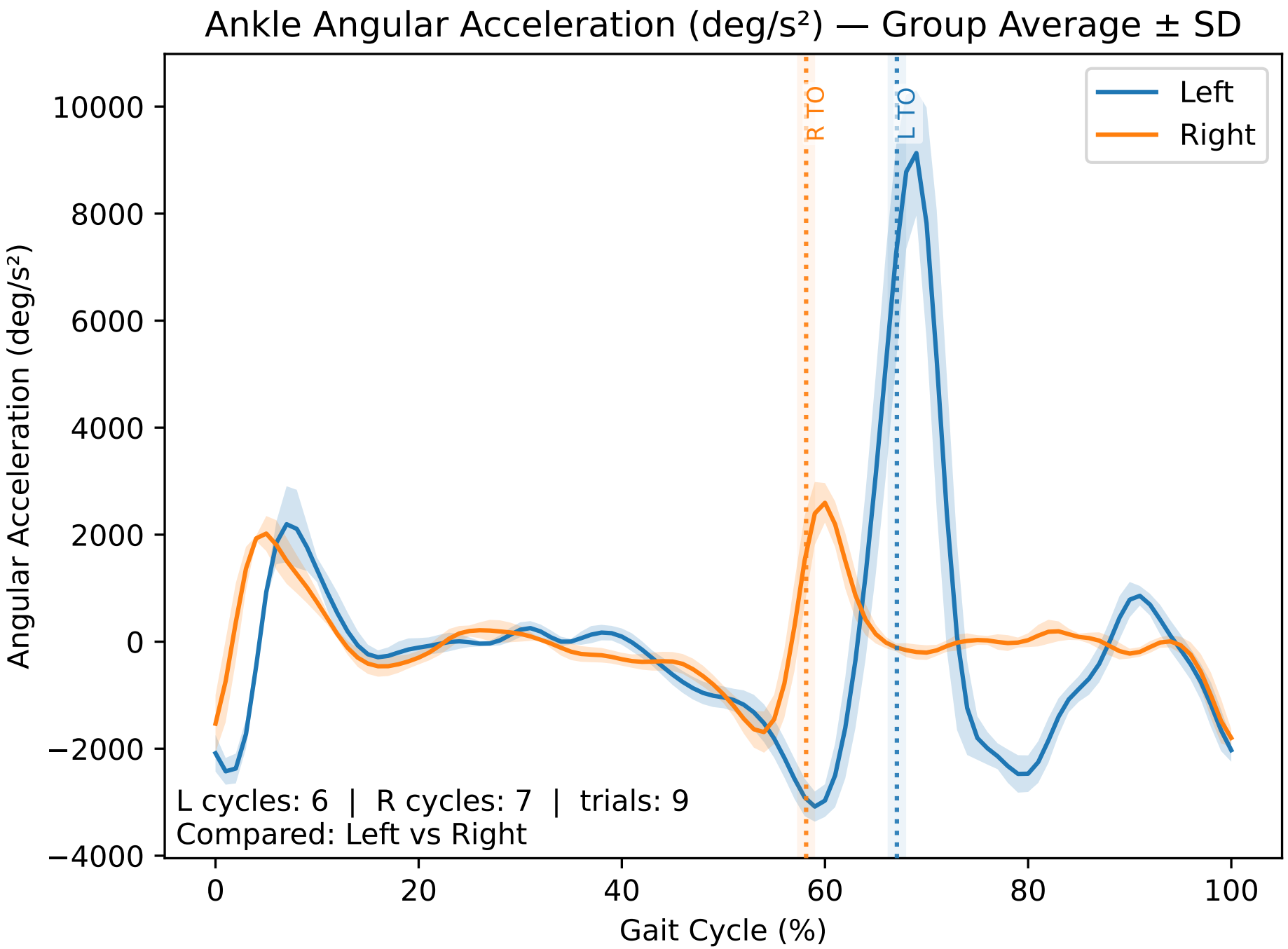
Ankle Angular Acceleration (deg/s²) — Group Average ± SD
Left
Right
R TO
L TO
Angular Acceleration (deg/s²)
10000
8000
6000
4000
2000
0
−2000
−4000
0
20
40
60
80
100
Gait Cycle (%)
L cycles: 6 | R cycles: 7 | trials: 9
Compared: Left vs Right

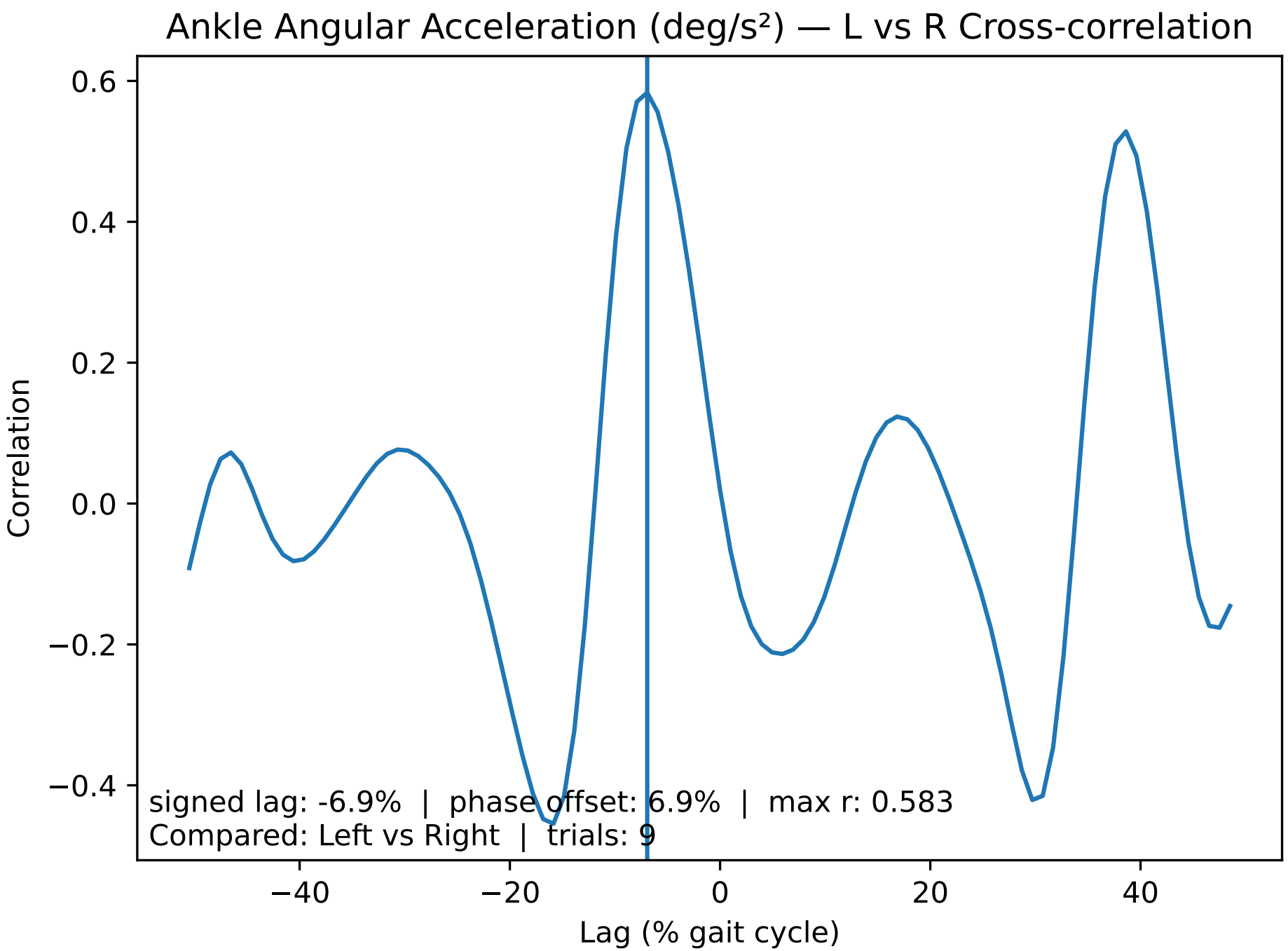
Ankle Angular Acceleration (deg/s²) — L vs R Cross-correlation
Correlation
0.6
0.4
0.2
0.0
−0.2
−0.4
signed lag: -6.9% | phase offset: 6.9% | max r: 0.583
Compared: Left vs Right | trials: 9
−40
−20
0
20
40
Lag (% gait cycle)

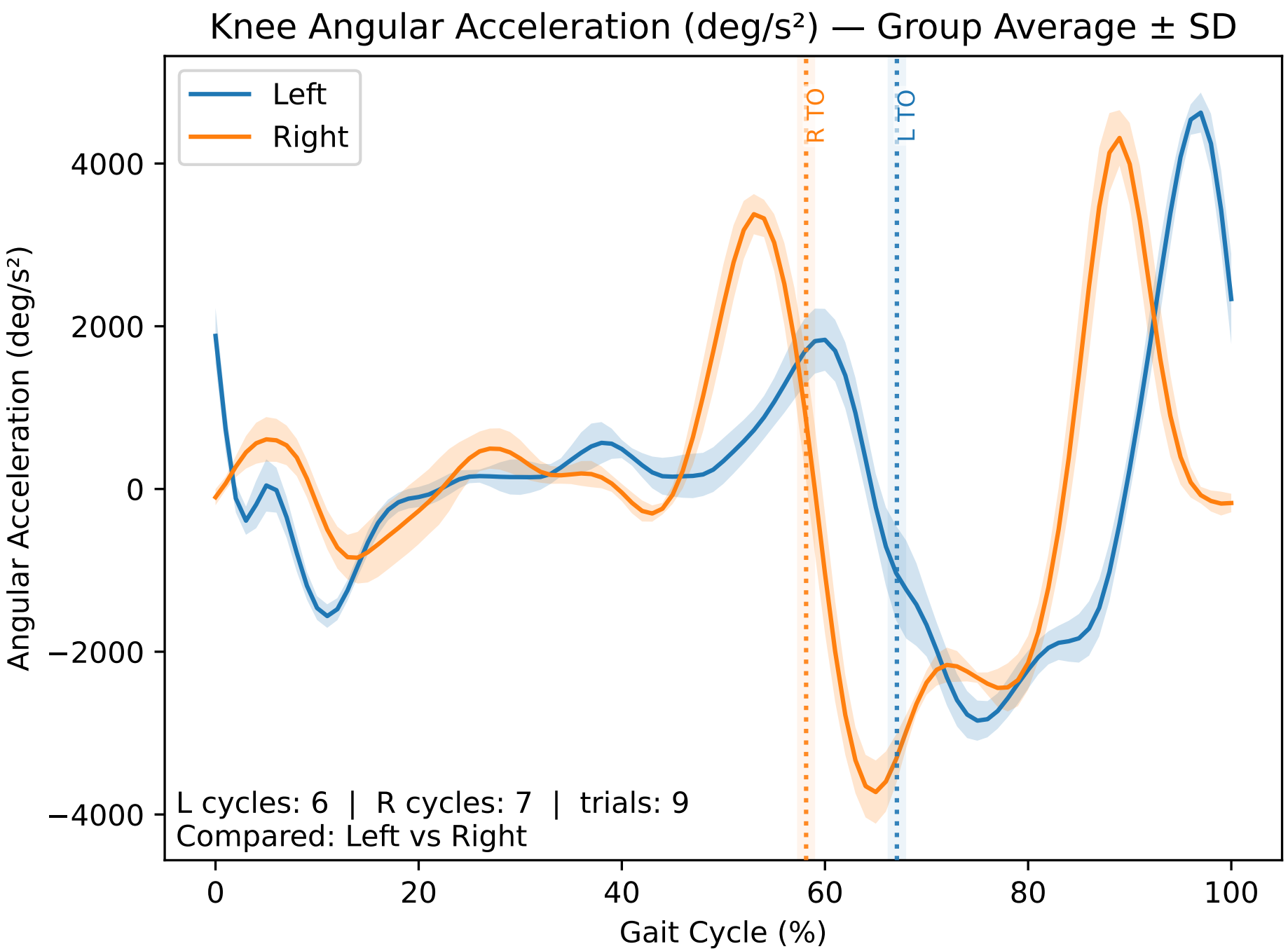
Knee Angular Acceleration (deg/s²) — Group Average ± SD
Left
Right
R TO
L TO
4000
2000
0
−2000
−4000
Angular Acceleration (deg/s²)
0
20
40
60
80
100
Gait Cycle (%)
L cycles: 6 | R cycles: 7 | trials: 9
Compared: Left vs Right

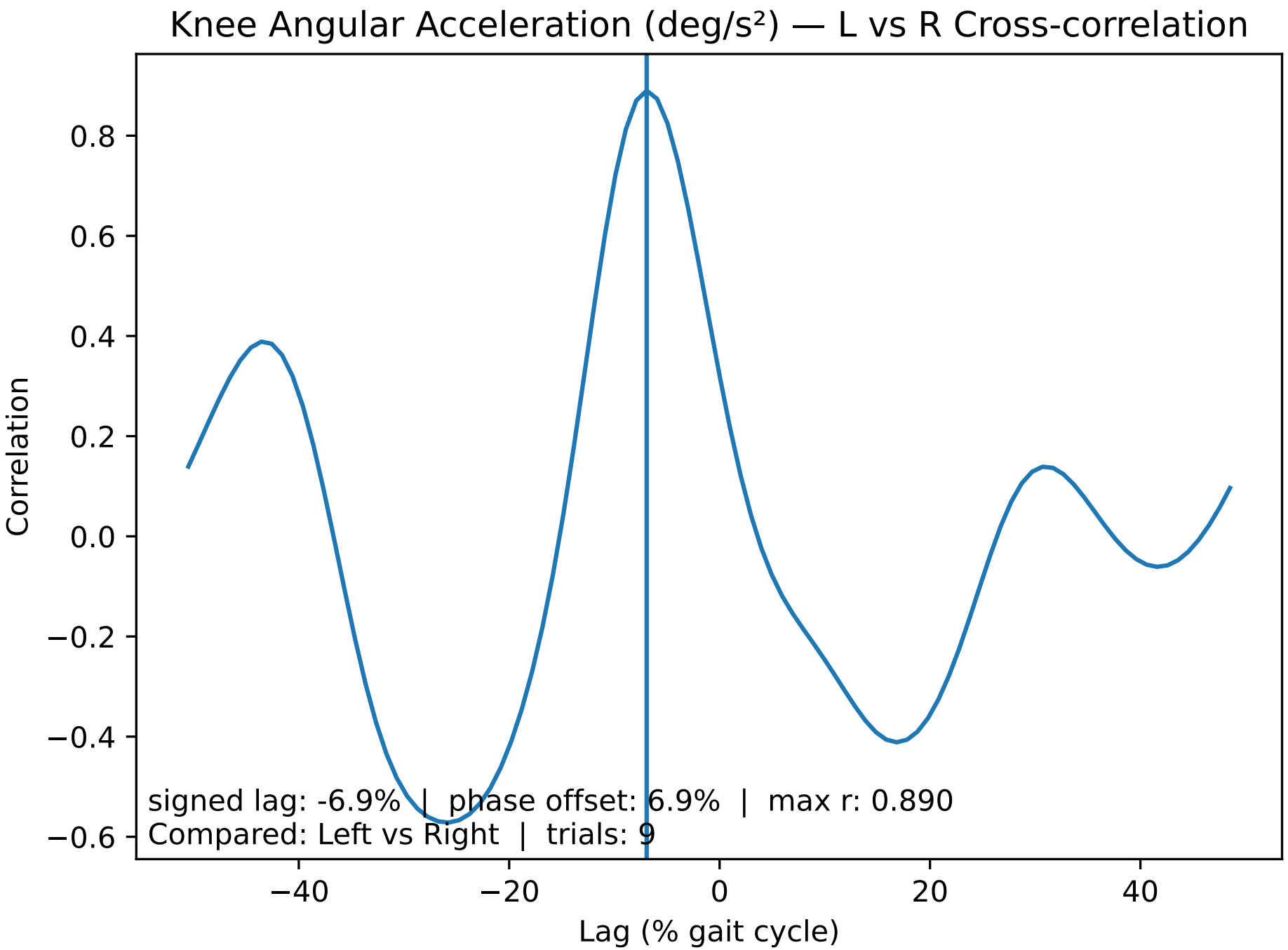
Knee Angular Acceleration (deg/s²) — L vs R Cross-correlation
Correlation
0.8
0.6
0.4
0.2
0.0
−0.2
−0.4
−0.6
−40
−20
0
20
40
Lag (% gait cycle)
signed lag: -6.9% | phase offset: 6.9% | max r: 0.890
Compared: Left vs Right | trials: 9

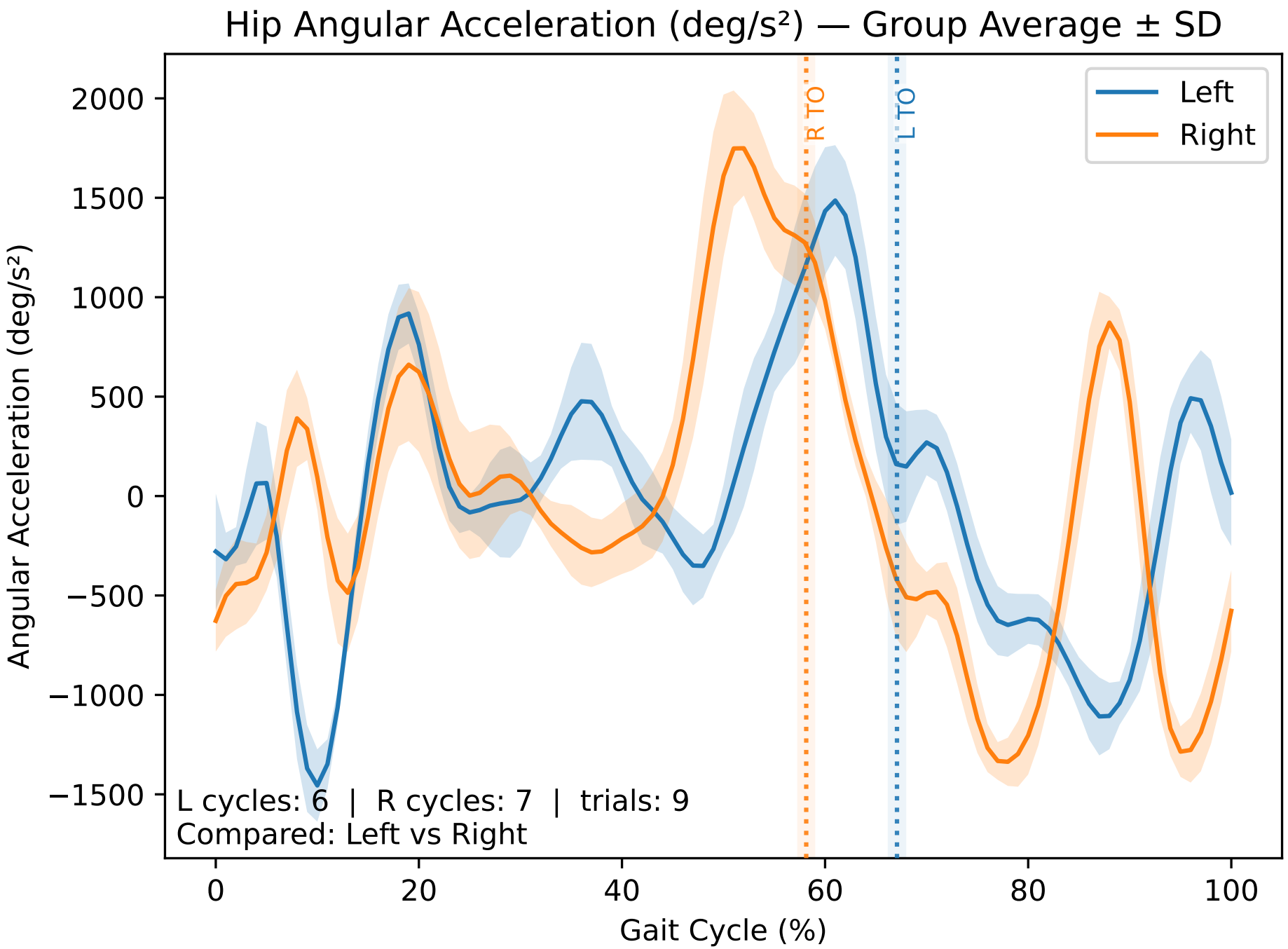
Hip Angular Acceleration (deg/s²) — Group Average ± SD
Angular Acceleration (deg/s²)
2000
1500
1000
500
0
−500
−1000
−1500
0
20
40
60
80
100
Gait Cycle (%)
R TO
L TO
Left
Right
L cycles: 6 | R cycles: 7 | trials: 9
Compared: Left vs Right

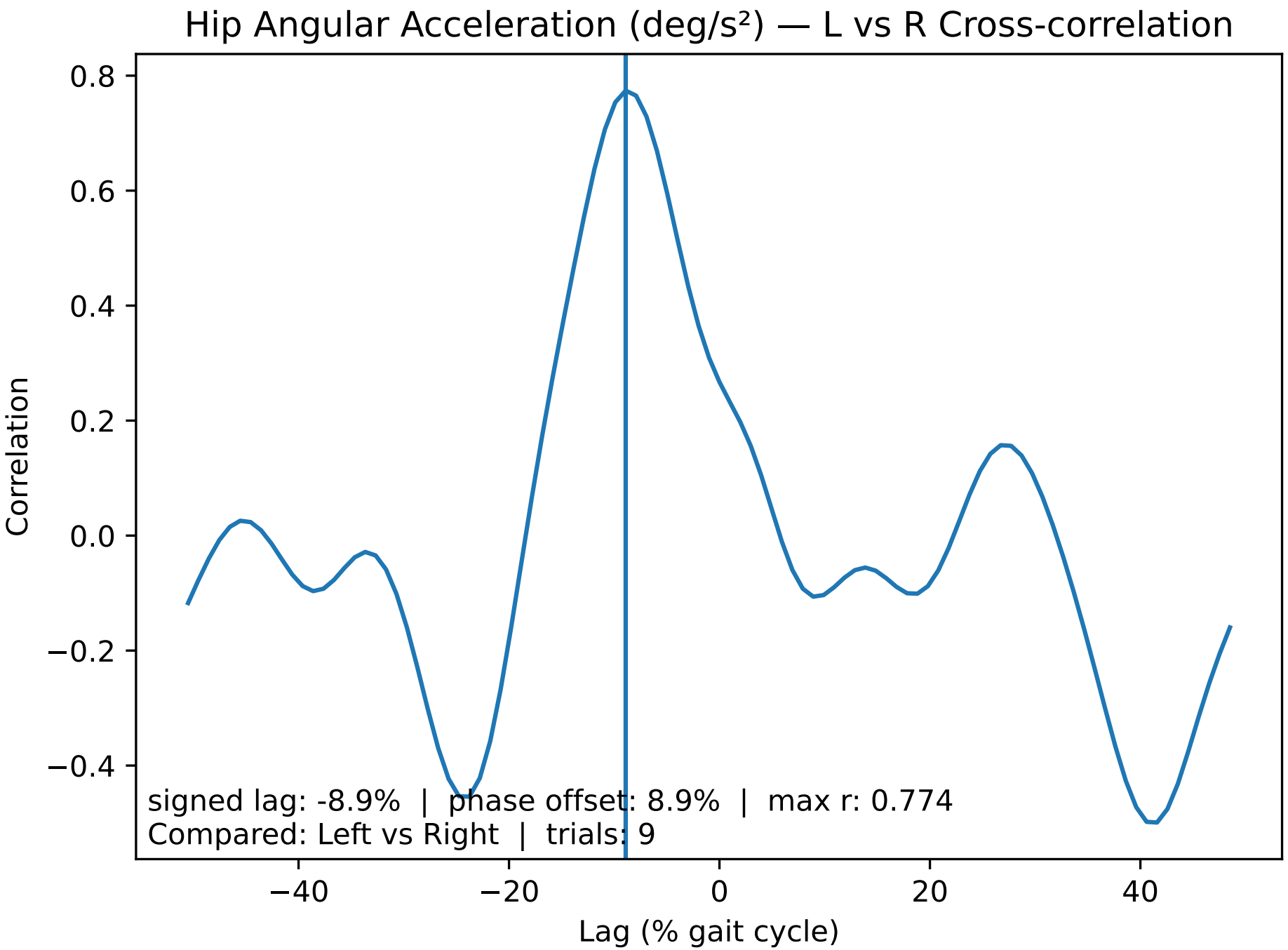
Hip Angular Acceleration (deg/s²) — L vs R Cross-correlation
Correlation
0.8
0.6
0.4
0.2
0.0
−0.2
−0.4
−40
−20
0
20
40
Lag (% gait cycle)
signed lag: -8.9% | phase offset: 8.9% | max r: 0.774
Compared: Left vs Right | trials: 9